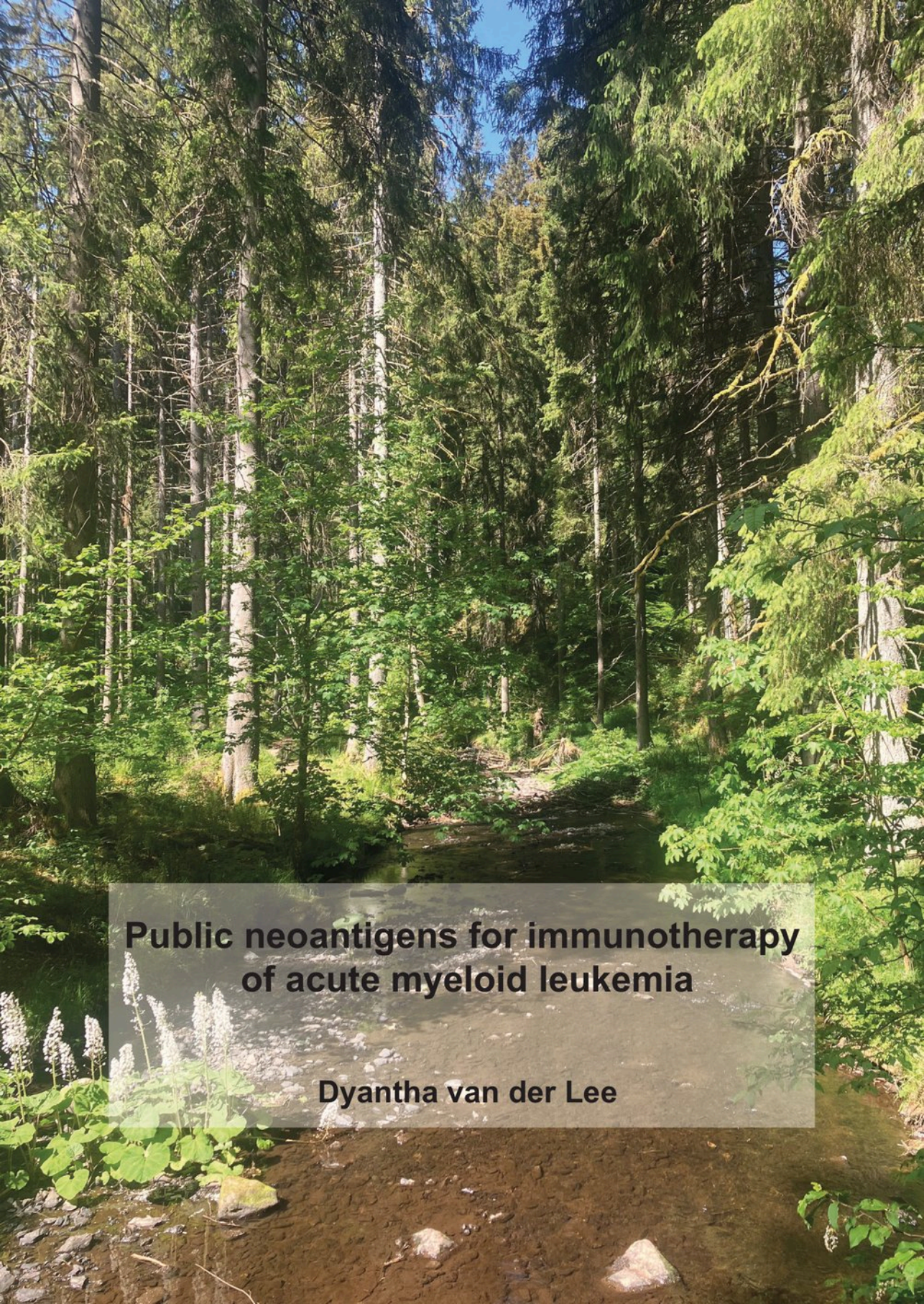

Public neoantigens for immunotherapy of acute myeloid leukemia

Dyantha van der Lee

Public neoantigens for immunotherapy of acute myeloid leukemia

Dyantha van der Lee

ISBN: 978-94-6537-704-9

Cover: Schwarzwald, Germany. Photo by Dyantha van der Lee.
Layout: Dyantha van der Lee
Printed by: Ridderprint, www.ridderprint.nl

The research described in this thesis was performed at the Department of Hematology of the Leiden University Medical Center (LUMC), the Netherlands, and was financially supported by the Dutch Cancer Society (project numbers 10222/2016 and 11867/2018-2). The mass spectrometry work was part of the Investment Grant NWO (Dutch Research Council) Medium Programme (project number 91116004), which was partly financed by ZonMw (the Dutch Organisation for knowledge and innovation in health, healthcare and well-being). D.I. van der Lee was supported by the MD/PhD-programme of the LUMC and by Doelfonds Leukemie of the Bontius Stichting | LUMC Research Foundation.

Public neoantigens for immunotherapy of acute myeloid leukemia

Public neoantigens for immunotherapy of acute myeloid leukemia

Proefschrift

ter verkrijging van
de graad van doctor aan de Universiteit Leiden,
op gezag van rector magnificus prof.dr. S. de Rijcke,
volgens besluit van het college voor promoties
te verdedigen op vrijdag 18 september 2026
klokke 13.00 uur

door

Dyantha van der Lee

Promotor
Prof. dr. J.H.F. Falkenburg

Copromotor
Dr. M. Griffioen

Promotiecommissie
Prof. dr. N.F.C.C. de Miranda
Prof. dr. R. Arens
Prof. dr. J.E.M.A. Debets (Erasmus Medical Center)
Prof. dr. I.J.M. de Vries (Radboud University Medical Center)

Table of contents

Chapter 1

General introduction and aim of the thesis

1

General introduction

T-cell immunobiology

T cells have diverse functions

T cells are highly specific immune cells that can discern self- from non-self-antigens with their T-cell receptor (TCR). Self-antigens are expressed in healthy cells, whereas pathogens and malignant cells can give rise to non-self or foreign antigens. After their development in the thymus, naive CD8 and CD4 T cells continuously surveil the body for the presence of foreign antigens. In the lymphatic system, naive T cells interact with professional antigen-presenting cells (APCs) that are designed to present foreign antigens to T cells (1). Naive T cells that recognize a foreign antigen on a professional APC are activated (primed) and start to proliferate and differentiate into effector T cells. The main function of effector or cytotoxic CD8 T cells is direct lysis of cells expressing their target antigen. Effector CD4 T cells are more versatile. Helper T cells provide help to other immune cells to initiate and promote immune responses, while regulatory T cells modulate and dampen immune responses by suppressing other immune cells (1). In addition, a small subset of CD4 T cells is cytotoxic and can directly kill target cells (2). After activation, CD8 and CD4 T cells give rise to memory T cells (3). The resulting immunological memory will lead to faster and stronger immune responses upon rechallenge with the same antigen.

The TCR is highly variable and specific

The TCR is a cell surface receptor that binds to peptide ligands presented on cells by membrane-bound proteins called human leukocyte antigen (HLA) molecules (4). The TCRs of CD8 and CD4 T cells are structurally similar and are composed of an α and β chain, each folded into a constant and a variable domain. The variable domains make up the antigen-binding site. Within each variable domain are three hypervariable regions, termed complementarity-determining regions (CDR) 1, 2 and 3 (5). CDR1 and CDR2 mainly interact with the presenting HLA molecule, whereas CDR3 interacts with the peptide ligand in the context of the presenting HLA molecule. Only the combination of a peptide with a specific HLA molecule is recognized by a T cell. Each T cell carries a single unique TCR that is capable of recognizing only one or a limited number of antigens. To cover the vast range of potential antigens, millions of TCRs with different specificities are present within the naive T-cell repertoire (6). This TCR diversity and specificity is created by a stochastic process termed V(D)J recombination, in which functional exons encoding the variable regions of the TCR α and β chain are generated by gene rearrangement of numerous variable (V), diversity (D) and joining (J) segments of non-functional germline genes (7). The variable region of the α chain is encoded by one V and one J segment, whereas the

variable region of the β chain also requires a D segment. The vast number of different V, D and J combinations contributes to TCR diversity, which is further increased by insertion or deletion of random nucleotides at the VDJ junctions. After V(D)J recombination, the genes for the α and β chain can be transcribed and translated. The TCR is assembled in the endoplasmic reticulum (ER) and associates with the CD3 protein complex, which is necessary for expression of the TCR on the cell surface (8) and responsible for intracellular signal transduction after the TCR binds to its ligand (9).

Functional and safe T cells are selected in the thymus

V(D)J recombination takes place during T-cell development in the thymus and creates TCRs specific for a vast number of unknown antigens. These TCRs include non-functional receptors that are unable to recognize peptides in the context of HLA as well as autoreactive receptors that recognize self-peptides in self-HLA. T cells with non-functional or autoreactive TCRs are deleted from the T-cell repertoire by the process of thymic selection (10). The first step is positive selection and leads to selection of T cells that can recognize peptides in the context of HLA molecules. These peptide-HLA complexes are presented on cortical thymic epithelial cells and only T cells with TCRs that bind to these complexes are signaled to survive. The second step is negative selection and results in the elimination of autoreactive T cells. Medullary thymic epithelial cells and other APC subsets present self-peptides in the context of self-HLA molecules and T cells with TCRs that bind to these complexes are triggered to undergo apoptosis, a process called clonal deletion. Only self-tolerant T cells that do not recognize self-antigens in self-HLA survive thymic selection, leading to a state of immunological tolerance.

Two types of HLA molecules present distinct and large sets of peptides

Two classes of HLA molecules exist, HLA class I and HLA class II. HLA class I molecules present peptides derived from intracellular proteins to CD8 T cells, while HLA class II molecules mainly present peptides from extracellular and membrane-bound proteins to CD4 T cells (4). Almost all nucleated cells express HLA class I. Expression of HLA class II is restricted to specialized APCs of hematopoietic origin, but can be induced on non-hematopoietic cells under inflammatory conditions. HLA class I molecules consist of a variable α heavy chain that gives rise to the peptide-binding site and a supporting invariant β_2-microglobulin light chain. The heavy chain also contains a binding site for the CD8 coreceptor. HLA class II molecules are composed of an α and β chain which both constitute the peptide-binding site. The β chain also has a binding site for the CD4 coreceptor. The peptide-binding site in both HLA classes is shaped like a groove and fits one peptide at a time (11). In HLA class I, this groove is closed at both ends, thereby allowing the binding of peptides with a limited length of approximately 8-11 amino acids. The peptide-binding groove in HLA

class II is open-ended and accommodates peptides of 13-25 residues in length. Each HLA molecule is capable of presenting a large repertoire of different peptides (12). The biochemical properties of the amino acids in the peptide-binding groove determine which amino acids are favored at which positions within a peptide in order for it to bind to HLA (12-14). This 'preferred' peptide sequence is called the peptide-binding motif. Not all residues within a peptide contribute equally to the peptide-binding motif. For some positions, the identity of the amino acid has little or no effect on the peptide-HLA interaction. Substitutions of the preferred amino acids at other positions, however, can lead to a substantial reduction or abrogation of peptide-HLA binding, or to a less pronounced but still relevant reduction in peptide-HLA binding. The residues at these positions are called primary and secondary anchor residues, respectively (12-14). For most HLA class I molecules, the second and last residue of a peptide function as primary anchors (12-14), whereas anchor residues in peptides binding to HLA class II molecules are more heterogeneous (12, 13).

HLA molecules are highly polymorphic

HLA class I and II molecules are encoded by a complex of genes on chromosome 6 (15). The heavy chains of HLA class I are encoded by three functional genes, *HLA-A*, *HLA-B* or *HLA-C*, whereas β_2-microglobulin is encoded by a single gene on chromosome 15. The α and β chains of HLA class II are each encoded by three functional genes, *HLA-DRA*, *HLA-DPA1* or *HLA-DQA1*, and *HLA-DRB1*, *HLA-DPB1* or *HLA-DQB1*, respectively. Some individuals also possess a functional *HLA-DRB3*, *-DRB4* or *-DRB5* gene. Classical HLA genes are highly polymorphic, with HLA class I being more polymorphic than HLA class II and, within HLA class II, the β chain being more polymorphic than the α chain (16). The sequence diversity between HLA alleles is mainly located in regions encoding the peptide-binding site, thereby influencing the peptide specificity of the different HLA allotypes (17). As a result, each HLA allotype presents a large and distinct set of peptides. These peptide repertoires can, however, overlap between allotypes (17, 18). For instance, HLA-A*03:01 and HLA-A*11:01 have a similar peptide-binding groove to which similar peptides bind (19). Due to the large diversity of HLA alleles, most individuals are heterozygous for each HLA locus, leading to an HLA type of 6 different HLA class I alleles and 6-8 different HLA class II alleles (dependent on the presence of *HLA-DRB3*, *-DRB4* or *-DRB5*). The chance that two unrelated individuals have the same HLA type is very low. However, HLA allotypes are not evenly distributed within the human population, as specific allotypes can be more common or rare in populations from different geographical regions (20) and certain combinations of allotypes are frequently inherited together (4). The likelihood that two individuals share one or more HLA allotypes is therefore much higher.

Different antigen processing pathways generate HLA-binding peptides

Peptides presented by the two classes of HLA molecules are differentially processed within the cell (21). HLA class I-binding peptides are derived from cytosolic proteins that are cleaved into peptides by a large proteolytic protein complex, the proteasome. The proteasome can be converted into an alternative form, the immunoproteasome, which more efficiently produces peptides that are likely to bind to HLA class I (21, 22). The immunoproteasome is constitutively expressed in hematopoietic cells, in particular in professional APCs, and produced under the influence of IFN-γ in non-hematopoietic cells (22, 23). Peptides formed in the cytosol are translocated into the ER by a heterodimeric membrane transporter termed transporter associated with antigen processing (TAP) (21). TAP facilitates the transport of peptides with appropriate size and biochemical properties for HLA class I binding. Peptides may be further trimmed by ER aminopeptidases ERAP1 and ERAP2. The peptides are then sampled by HLA class I molecules. This process is catalyzed by a protein complex associated with the HLA molecules, the peptide-loading complex. After binding of a suitable peptide, the HLA class I molecule is released from this complex and transported from the ER through the Golgi apparatus to the cell surface. HLA class II-binding peptides are derived from exogenous and membrane-bound proteins that are internalized by cells through endocytosis and phagocytosis. The resulting endosomes are acidified to support protein unfolding. Proteolysis occurs after acidified endosomes fuse with lysosomes and is mediated by lysosomal proteases that become activated in the acidic environment. The resulting peptides remain in the endolysosomal compartment for sampling by HLA class II molecules. HLA class II molecules assemble in the ER and associate with the invariant chain (Ii) protein to prevent premature binding of peptides. The Ii also coordinates the transport of the HLA molecules to the endolysosomal compartment. Within the endolysosomes, the Ii is cleaved into the class II-associated invariant chain peptide (CLIP), a small remaining fragment that occupies the peptide-binding site. CLIP is removed by HLA-DM, a chaperone protein that catalyzes successive loading of peptides onto the HLA class II molecule. When a stable peptide-HLA complex is formed, HLA-DM dissociates and the complex is transported to the cell surface. In addition to peptides from exogenous proteins, HLA class II molecules can also present peptides derived from endogenous proteins (24). This occurs mainly through autophagy, a process in which autophagosomes containing cytosolic and nuclear content are formed. These autophagosomes then fuse with endosomes or lysosomes to deliver their cargo to the HLA class II antigen processing pathway.

Peptide-HLA binding can be measured or predicted

Peptides that are recognized by T cells need to be properly processed and presented on the cell surface by HLA molecules. HLA-binding peptides, also called HLA ligands, can be identified by three approaches, i.e. peptide-HLA binding assays,

mass spectrometry and T-cell assays (25). Peptide-HLA binding assays quantify the ability of peptides to bind to specific HLA alleles. This is often tested by competition with a labelled known ligand of the specific HLA allotype, resulting in IC50 values that denote peptide-HLA binding affinities (26). Peptide-HLA binding assays, however, do not provide information about endogenous processing and immunogenicity. HLA ligands that are naturally processed and presented on cells and tissues can be identified by mass spectrometry. These natural HLA ligands are part of the HLA ligandome, which is the collection of all HLA-bound peptides in a given cell type or tissue. To identify these ligands, peptide-HLA complexes are isolated from cells, and peptides are eluted from HLA molecules and separated by chromatography (27, 28). Peptides are then measured by a mass spectrometer to determine their amino acid sequences. Using this technique, thousands of natural HLA ligands can be identified. Similar to peptide-HLA binding assays, the immunogenicity of HLA ligands needs to be validated. T-cell assays provide the ultimate validation of HLA binding and immunogenicity by testing reactivity of T cells against target cells expressing HLA alleles and peptides of interest. These peptides can be exogenously pulsed onto target cells, or encoded by genes naturally present in the genome or artificially introduced into target cells, thereby revealing whether the peptides are endogenously processed. Application of T-cell assays is, however, hindered by the limited availability of T cells with known specificity for the peptide-HLA complex of interest. In addition to experimental approaches, peptide-HLA binding can be predicted *in silico* (29). These machine learning-based algorithms, which have been trained on large sets of previously identified HLA ligands, can predict binding of peptides to different HLA class I or II allotypes. Algorithms for HLA class I outperform those for HLA class II. Prediction algorithms are useful for selecting potential HLA-binding peptides from large sets of protein sequences or candidate peptides and can be used to predict which HLA alleles bind to ligands identified by mass spectrometry.

T cells in cancer immunotherapy

T cells are key mediators of anti-tumor immunity

T cells play a central role in anti-cancer immunity and can eliminate cancer cells through recognition of tumor-associated and -specific antigens (30, 31). These antigens may be released after cancer cell death, taken up by professional APCs, in particular dendritic cells (DCs), and presented to patrolling naive T cells after DC migration to tumor-draining lymph nodes. Upon recognition of HLA-presented tumor antigens, naive T cells are primed. In addition to the interaction between a TCR and peptide-HLA complex, T-cell priming requires binding of the CD28 costimulatory receptor on T cells with CD80 or CD86 ligands on professional APCs. T-cell priming

results in the formation of effector T cells that migrate via the blood to the tumor site, where they extravasate and infiltrate the tumor. Within the tumor, effector T cells can recognize and kill malignant cells presenting their cognate antigens, resulting in release of more tumor antigens and amplification of the immune response. Since cancer cells primarily express HLA class I, direct elimination of malignant cells is mostly mediated by cytotoxic CD8 T cells. CD4 T cells contribute indirectly by providing help (32-34). For instance, CD4 T cells interact with DCs to induce DC maturation and release cytokines, which promote CD8 T-cell priming and enhance effector and memory functions in anti-cancer immunity. Some cancer types express HLA class II, which can make them susceptible to direct CD4 T-cell-mediated cytotoxicity (2). Malignant cells can exploit intrinsic mechanisms to resist T-cell cytotoxicity (35). For instance, downregulation or loss of HLA or tumor antigen expression prevents recognition and lysis by cytotoxic T cells, leading to tumor immune evasion or escape. Tumor immune evasion can also be facilitated by the tumor microenvironment, which is an ecosystem composed of cancer cells and non-cancerous cells, including immune, stromal and vascular cells (36). For example, tumor cells and other cells within the tumor microenvironment can express immune checkpoint molecules that impede tumor-infiltrating effector T cells by inhibiting TCR signaling and contributing to a dysfunctional state of T-cell exhaustion in which T-cell effector functions are impaired (37). Natural anti-tumor T-cell responses can thus be hampered by tumor cell intrinsic as well as extrinsic resistance mechanisms. T-cell-based cancer immunotherapies aim to overcome these resistance mechanisms by stimulating potent anti-tumor T-cell responses.

Natural anti-tumor T-cell immunity can be enhanced by immunotherapy

Various immunotherapeutic approaches aim to boost naturally occurring anti-tumor CD8 and CD4 T-cell responses against tumor-associated or -specific antigens. These include tumor-infiltrating lymphocyte (TIL) therapy, immune checkpoint therapy (ICT) and various cancer vaccination strategies. The efficacy of TIL therapy depends on tumor-reactive T cells present within the tumor. These TILs are grown *in vitro* from resected tumor tissue, expanded to large numbers and reinfused into the patient after lymphodepleting treatment (38). TIL therapy has shown clinical benefit, particularly in patients with metastatic melanoma (39). In ICT, immune checkpoint molecules that inhibit T-cell function are blocked with monoclonal antibodies to restore impaired anti-tumor immunity (40). The best studied checkpoint molecules are cytotoxic T-lymphocyte-associated protein 4 (CTLA-4), programmed cell death 1 (PD-1) and programmed death ligand 1 (PD-L1), and ICTs targeting these molecules are included in the standard treatment of multiple tumor types. Whereas TIL therapy and ICT boost tumor-reactive T cells with unidentified antigen specificity, most cancer vaccination strategies target preselected tumor-associated or -specific antigens. This selection is complicated by the difficulty of predicting which

antigens will be immunogenic *in vivo* (41). Selected antigens are incorporated into different vaccine strategies as synthetic peptides, mRNA or DNA vectors or plasmids, either alone or loaded onto DCs, which are then administered to the patient to elicit or augment tumor antigen-specific T-cell responses (42). Clinical benefit of cancer vaccines targeting tumor-specific antigens has been observed for some tumor types in trials.

Allogeneic T cells can induce anti-tumor reactivity in patients with hematological malignancies

Allogeneic hematopoietic stem cell transplantation (alloSCT) is a potential curative treatment for patients with hematological malignancies (43). Hematological malignancies are heterogenous tumors originating from diverse hematopoietic cell types. These cell types are produced in the bone marrow by hematopoiesis, a process in which hematopoietic stem cells give rise to myeloid and lymphoid cells through successive steps of differentiation and maturation (44). Following hematopoiesis, lymphoid cells travel to the lymph nodes where they can be activated to differentiate into effector cells. Malignant transformation can occur at different stages during and after hematopoiesis. AlloSCT facilitates the eradication of malignant cells by replacing the diseased hematopoietic system of the patient with a healthy hematopoietic system of a donor. To abrogate patient hematopoiesis, patients are treated with chemotherapy, which can be combined with radiotherapy, prior to alloSCT (43). This conditioning regimen aims to eliminate malignant and healthy hematopoietic cells, leading to tumor eradication and destruction of the functioning hematopoietic system. Elimination of healthy hematopoietic cells by the conditioning regimen as well as by administration of (T) lymphocyte depleting antibodies also reduces the risk of stem cell graft rejection by patient T cells caused by genetic differences between patient and donor (45). To restore hematopoiesis, patients receive donor-derived hematopoietic stem cells that, after successful engraftment, reconstitute a healthy hematopoietic system of donor origin (43). Both healthy and malignant hematopoietic cells of patient origin may survive the conditioning regimen. Following alloSCT, donor T cells can target these patient-derived hematopoietic cells, thereby inducing a desired anti-tumor effect called graft-versus-tumor (GvT) or graft-versus-leukemia (GvL) reactivity (46). Healthy hematopoietic cells of donor origin will be spared, leaving healthy hematopoiesis unaffected. If donor T cells target patient non-hematopoietic tissues, side-effects known as graft-versus-host disease (GvHD) may develop. GvHD can range from mild to severe and even lethal, and represents a major obstacle in alloSCT. T cells can be depleted from the donor stem cell graft to reduce the frequency and severity of GvHD. This, however, also increases the risk of relapse and infections. To re-install GvT reactivity and protection against infections, donor T cells can be administered as donor lymphocyte infusions several months after alloSCT (47).

AlloSCT forms an effective treatment for previously incurable hematological malignancies, but its efficacy can be hampered by opportunistic infections, GvHD and disease relapse (43). However, improved management of GvHD and the use of novel T-cell-engineered immunotherapies have increased the application of alloSCT as treatment for patients with hematological malignancies.

T-cell engineering produces large numbers of tumor-reactive T cells for immunotherapy

Chimeric antigen receptor (CAR) T-cell therapy has transformed cancer immunotherapy in hematological malignancies (48). CAR T-cell therapy redirects the specificity of patient T cells towards malignant cells through introduction of a CAR. A CAR is an artificial antigen receptor that typically contains an antibody-derived single-chain variable fragment as antigen-binding domain linked to a transmembrane domain, costimulatory domain and CD3ζ signaling domain of a TCR (49). As such, CARs bind to extracellular surface antigens in their native form independent of HLA. CAR T cells are produced from patient T cells, which are genetically engineered to express a CAR, expanded and reinfused into the patient (50). CAR T-cell therapies targeting different cell surface molecules have demonstrated clinical benefit in various hematological malignancies, particularly in B cell malignancies (49, 51). The anti-tumor efficacy of CAR T cells can be complicated by substantial toxicities related to T-cell activation, most frequently cytokine release syndrome and immune effector cell-associated neurotoxicity syndrome, or to expression of the target antigen on healthy tissues (50). The identification of target antigens with restricted expression on tumor cells is a fundamental challenge of CAR T-cell therapy and hinders its broad applicability. Most CAR therapies are currently directed against cell surface lineage-restricted antigens (49). Lineage-restricted antigens are antigens that are present in all or most cells within a certain cell lineage and on tumor cells derived from these lineages. Since these antigens are expressed at similar levels on healthy and malignant cells, lineage-restricted antigens can only be targeted if they are presented on healthy tissues performing non-vital or replaceable functions (52). A limited number of such antigens has been identified for certain hematological malignancies, whereas for the majority of cancer types, in particular solid tumors, such antigens have not yet been discovered. To increase the number of targetable tumor antigens, patient T cells can instead be redirected towards malignant cells by the introduction of a transgenic TCR (53). In contrast to CARs, TCRs recognize antigens derived from intracellular proteins that are presented on the cell surface by HLA, thereby limiting their applicability to patients with specific HLA types, yet enabling the targeting of a large repertoire of intracellular antigens. Numerous intracellular tumor antigens presented by different HLA molecules have been targeted by TCR-engineered T-cell therapies in clinical studies and clinical responses have been observed in hematological as well as solid tumors (53). Similar

to CAR T-cell therapies, TCR-engineered T-cell therapies offer the possibility to generate large numbers of tumor-reactive T cells by genetically modifying patient T cells with a transgenic TCR and reinfusing engineered T cells into the patient after expansion (50). An important benefit of TCR T-cell therapy is the ability to select for potent and safe TCRs with predefined anti-tumor specificities that have been extensively tested *in vitro* and *in vivo* in preclinical models (53). Transgenic TCR α and β chain sequences can be integrated into the genome of patient T cells using retro- or lentiviral vectors, or non-viral genome editing. TCR transduction with viral vectors is well-established and relatively efficient, but results in semirandom integration of variable copy numbers of TCR transgenes (53). This can cause heterogenous TCR expression which can result in variable T-cell functionality (54). Insertional mutagenesis forms another risk of using viral vectors (55) and can potentially cause malignant transformation. In contrast to viral vector-based approaches, non-viral genome editing methods are less efficient and carry the risk of introducing off-target double-strand DNA breaks, but they enable targeted insertion of defined copy numbers of TCR transgenes at selected genomic locations (53). Non-viral genome editing methods can also be employed to disrupt endogenous TCR genes, thereby reducing or preventing mispairing between endogenous and introduced TCR α and β chains (56-58). TCR chain mispairing reduces expression of the introduced TCR and generates new TCRs with unknown specificity, which may be autoreactive (59, 60). Other approaches to promote preferential pairing of introduced TCR chains include substitution of transgenic TCR human constant α and β regions with murine regions (61) or introduction of cysteine residues in transgenic TCR constant α and β regions to form a stable interchain disulfide bridge (62).

Tumor antigens targeted by T-cell-based immunotherapies

Tumor antigens can be derived from self-proteins

Although immunotherapies stimulating or initiating natural, allogeneic or engineered T-cell responses each have their specific benefits and limitations, the efficacy and toxicity of each approach is largely determined by the type of tumor antigen that is targeted. Self-proteins encoded by unmutated wild-type (wt) genes can give rise to tumor antigens. These tumor antigens include cancer germline antigens, overexpressed tumor antigens and tissue differentiation antigens (63). Cancer germline antigens are expressed in cancer cells, but their encoding genes are presumed to be epigenetically silenced in all normal tissues, except for germline and trophoblast cells. Overexpressed tumor antigens are overexpressed in tumor cells, but low expression levels are also found in certain healthy tissues. Tissue differentiation antigens are expressed at similar levels on differentiated cell types

within certain healthy tissues and tumor cells originating from these cell types. For tissue differentiation antigens that are expressed at high levels in certain healthy tissues, T cells with high-affinity TCRs are expected to be deleted during thymic selection, as these T cells can mediate substantial on-target off-tumor toxicity against healthy tissues. For overexpressed tumor antigens that are expressed at low levels in certain healthy tissues, T cells with relatively low-affinity TCRs recognizing high antigen expression on tumor cells, but not low antigen expression on healthy cells, may have survived thymic selection and be present in the T-cell repertoire (64). For cancer germline antigens that are not expressed in healthy tissues, T cells with high-affinity TCRs may be present in the T-cell repertoire. Immunotherapies targeting tissue differentiation antigens have a high risk for on-target off-tumor toxicity, due to high expression of the antigen on healthy tissues (65, 66). Immunotherapies targeting overexpressed tumor antigens also carry a substantial risk for on-target off-tumor toxicity, since these antigens can be expressed at low levels on certain healthy tissues (67). Immunotherapies targeting cancer germline antigens have a low risk for on-target off-tumor toxicity, since germline and trophoblast cells lack HLA expression and are therefore protected against T-cell attack.

Minor histocompatibility antigens (MiHAs) arise from polymorphic proteins after alloSCT

After (partially) HLA-mismatched alloSCT, mismatched HLA alleles that are expressed by the patient but not by the donor can induce strong allo-HLA-reactive donor T-cell responses against patient cells. Although this allo-HLA reactivity often leads to a potent GvT effect, it can also elicit life-threatening GvHD. For this reason, patient and donor are preferably matched for all or most HLA alleles (68, 69). Following HLA-matched alloSCT, donor T cells mediate GvT reactivity and GvHD by targeting polymorphic peptides presented in HLA on the surface of patient cells (70). These polymorphic peptides are known as MiHAs and arise as a result of single nucleotide polymorphism (SNP) differences between patient and donor. The majority of MiHA-encoding SNP differences encode single polymorphic amino acids (70, 71). Polymorphic peptides recognized by donor T cells on patient cells are MiHAs, whereas the corresponding peptides on donor cells are called allelic variants (70). In addition to SNP mismatches, genes specific to the Y chromosome can encode MiHAs known as H-Y antigens in female-to-male transplantations (72). The distribution of MiHAs on patient tissues significantly influences the balance between GvT reactivity and GvHD (70). Donor T cells targeting MiHAs on hematopoietic cells are expected to elicit GvT reactivity, whereas donor T cells specific for MiHAs on healthy non-hematopoietic cells are expected to provoke GvHD. Most MiHAs are broadly expressed on hematopoietic and non-hematopoietic tissues and donor T cells targeting these antigens are presumed to contribute to both GvT reactivity and GvHD (71, 73). However, various MiHAs are exclusively presented on hematopoietic

tissues and are of special interest, as donor T cells against these antigens are expected to induce GvT reactivity without GvHD (71, 73, 74).

Mutated proteins give rise to tumor-specific antigens

Acquisition of somatic mutations by healthy cells can result in malignant transformation. After transformation, cancer cells gain additional mutations, some of which contribute to tumor progression. Mutations that are essential for tumor initiation and progression are called driver mutations (75). Driver mutations are, however, rare and most acquired mutations are passenger mutations. In contrast to driver mutations, passenger mutations are not essential for tumor development. Both driver and passenger mutations can encode mutated proteins which, after endogenous processing, can result in presentation of mutated peptides in HLA on the cell surface of malignant cells. HLA-presented mutated peptides on cancer cells that are recognized by T cells are called neoantigens (76, 77). In contrast to cancer germline antigens, overexpressed tumor antigens and tissue differentiation antigens, neoantigens are tumor-specific antigens created by genetic aberrations that are present in cancer cells, but absent in normal cells. As such, T cells targeting neoantigens are unlikely to induce on-target off-tumor toxicity against healthy tissues. In addition, T cells with high-affinity TCRs against neoantigens are expected to survive negative selection in the thymus. For these reasons, neoantigens are promising targets for immunotherapy. Naturally occurring neoantigen-specific CD8 and CD4 T-cell responses have been detected in patient TIL products (77, 78) and in patients treated with ICT (77). After infusion of TIL products, clinical responses have been observed in patients with diverse tumor types, indicating that T-cell reactivity against neoantigens plays a direct role in tumor control (79-81). Although natural T-cell responses against neoantigens are induced, most somatic mutations in cancer cells do not create neoantigens (76, 77). To create neoantigens, somatic mutations need to be present in genes that are expressed. Additionally, the resulting mutated proteins need to be endogenously processed to produce mutated peptides, which need to be presented on the cell surface by HLA molecules that are expressed by the patient. Finally, the mutated peptide-HLA complexes need to be recognized by T cells carrying specific TCRs that are able to bind to these complexes. Most somatic mutations fail to meet all these requirements for neoantigen formation. The probability of neoantigen formation is dependent on the number of nonsynonymous somatic mutations present in the genome of a tumor, known as the tumor mutational burden or load, which differs between tumor types and patients (82). Cancers with a high mutational burden are more likely to present neoantigens than cancers with a low mutational load (76, 77). Tumor mutational burden is associated with clinical benefit from ICT across different tumor types (83), providing indirect evidence that cancers with a high mutational load present more neoantigens and that T-cell responses against neoantigens contribute to tumor control after ICT. In addition to

neoantigen quantity, the type of mutation encoding a neoantigen may influence the anti-tumor efficacy of T-cell-based immunotherapies. T-cell reactivity against neoantigens encoded by passenger mutations can result in immune escape due to loss of these mutations by the tumor (84), whereas loss of driver mutations and their resulting neoantigens is less likely due to their essential role in tumorigenesis (85). The type of mutation encoding a neoantigen is of less importance for tumors with a high mutational burden, in which polyclonal T-cell responses can be induced against numerous neoantigens presented by diverse HLA molecules on different tumor populations, thereby reducing the risk of immune escape by antigen loss. Polyclonal anti-tumor T-cell responses can be boosted by TIL therapy and ICT, and these therapies are most effective in cancers with a high mutational load. In cancers with a low mutational burden that present few neoantigens, induction of polyclonal T-cell responses is not feasible. Instead, these tumors are suitable candidates for TCR-engineered T-cell therapies directed against one or a few carefully selected neoantigens (86). Public neoantigens encoded by driver mutations that are clonally expressed in all tumor cells and are present in multiple patients are especially preferable as target antigens, since TCR-engineered T-cell therapies against these antigens are broadly applicable and expected to induce anti-tumor responses with no or low risk of immune escape by antigen loss (85). Immune evasion can, however, still occur through loss of the HLA allele presenting the targeted neoantigen by tumor cells (35).

Neoantigen identification and isolation of neoantigen-specific T cells

Neopeptides encoded by somatic mutations are candidate neoantigens

Most mutations in a tumor do not encode mutated peptides that fulfill all criteria for neoantigen formation, and predicting which mutations give rise to a neoantigen is difficult (76, 77, 87). The discovery of neoantigens is therefore challenging and different identification strategies can be followed (87). Many strategies start with identifying somatic mutations that are present in the whole tumor genome, exome or in selected genomic regions by whole genome or exome sequencing of tumor and healthy tissue samples from patients. Alternatively, mutations can be identified from public databases, such as Catalogue Of Somatic Mutations In Cancer (COSMIC), that collect and catalogue data on somatic mutations from scientific literature and open access cancer genome data portals (88). The number of identified mutations is often extensive and screening each mutation for neoantigen formation can be laborious and expensive. To filter the number of mutations that need to be screened, mutations can be examined for encoding mutated peptides or neopeptides that are likely to fulfill the requirements of neoantigen formation (87). Candidate neoantigens can be filtered for gene expression using RNA sequencing data, and *in silico*

algorithms can be used to predict immunobiological features of neopeptides, for instance HLA binding affinity, proteasomal processing and/or TAP transport (87, 89). RNA expression data and tools to predict HLA binding, such as NetMHC algorithms (90), are most frequently used in computational pipelines to identify and prioritize candidate neoantigens. Although computational pipelines significantly reduce the number of neopeptides that need to be screened, a major drawback of these pipelines remains that most selected candidate neoantigens are false-positives that cannot be validated as true neoantigens (77, 87, 91). Candidate neoantigens can also be identified using mass spectrometry to measure the HLA ligandome of tumor cells or cells expressing mutations of interest (87, 92). In contrast to *in silico* prediction, mass spectrometry directly identifies neopeptides that are presented by HLA on the cell surface. Mass spectrometry typically requires large cell numbers and identifies peptides that are abundantly present on the cell surface and have strong HLA binding affinity (87). All candidate neoantigens, whether preselected by computational pipelines or mass spectrometry, ultimately need to be screened for T-cell reactivity to be validated as true neoantigens.

T-cell recognition is necessary for validation of neoantigens

To be validated as true neoantigens, candidate neoantigens need to be recognized by a specific T cell within the human T-cell repertoire. Neoantigen-specific T cells can be searched in T-cell repertoires from patients or healthy donors (53, 87). For patients, TILs or peripheral blood mononuclear cells (PBMCs) can be screened (93). TILs can be enriched for tumor-reactive T cells, including neoantigen-specific T cells, but are not available from all patients (53, 87). In contrast, peripheral blood can be easily collected from most patients and permits isolation of large numbers of PBMCs, although the frequency of neoantigen-specific T cells is generally considerably lower than in TILs. Neoantigen-specific T cells can also be searched in PBMCs from healthy donors (94). Whereas neoantigen-specific T cells in patients can be derived from the memory and naive T-cell compartment, neoantigen-specific T cells in healthy donors have not previously encountered their cognate antigen and are therefore expected to be derived from the naive T-cell compartment. Despite their extremely low frequency in peripheral blood, the number of neoantigen-specific T cells that can be isolated from healthy donors is compensated by the vast amount of available donor PBMCs. In addition, the naive T-cell compartment in healthy donors contains T cells with a broad range of specificities that have not been subjected to immunosuppressive mechanisms employed by tumors (53, 95). Generally, the frequency of neoantigen-specific T cells in the human T-cell repertoire is low and the chance of isolating these T cells may be increased by enriching TILs or PBMCs using peptide-HLA multimers or *in vitro* stimulation (53, 87). Peptide-HLA multimers consist of multiple HLA complexes with predefined neopeptides and are typically conjugated with fluorochromes to enable isolation of antigen-specific T cells by flow cytometry.

In vitro stimulation of TILs or PBMCs can be performed by coculturing T cells with autologous tumor cells, or with autologous or HLA-matched allogeneic cells that are exogenously pulsed with neopeptides or modified to express genes encoding candidate neoantigens. T cells isolated from (enriched) TILs or PBMCs can be cultured in bulk or as single T-cell clones. To assess the presence of neoantigen-specific T cells, reactivity of bulk T cells or T-cell clones can be tested, for instance by measuring cytokine secretion or cytotoxicity, against stimulator cells that are exogenously loaded with individual or pooled neopeptides or transduced with gene constructs encoding one or more neopeptides (87). As stimulator cells, autologous APCs can be used or allogeneic cells or cell lines in which the HLA alleles of interest are naturally expressed or artificially introduced. Upon T-cell recognition, neopeptide pools or gene constructs encoding multiple neopeptides are deconvoluted to evaluate T-cell reactivity against individual neopeptides and elucidate which neoantigen is recognized. Neoantigen-specific T cells can be further tested *in vitro* against malignant and healthy cell types that are positive or negative for the neoantigen and/or restricting HLA allele to characterize their specificity, potency and safety (53). Neoantigens are ultimately validated by demonstrating T-cell reactivity against tumor cells naturally expressing the neoantigen-encoding mutation and respective HLA allele. TCRs from T cells specific for identified neoantigens may be promising candidates for TCR-engineered T-cell therapy (53, 87). TCR α and β chains can be sequenced and introduced into CD8 and/or CD4 T cells from patients or healthy donors for extensive preclinical characterization of their safety and potency.

Acute myeloid leukemia (AML)

AML is a hematological malignancy with a poor prognosis

AML is a malignancy of the myeloid lineage that arises during hematopoiesis. Genetic aberrations that accumulate in hematopoietic stem cells and myeloid progenitor cells may lead to malignant transformation into leukemic cells (96). These leukemic cells, or AML blasts, are arrested in differentiation and show uncontrolled clonal expansion. The resulting malignant leukocytosis hinders normal hematopoiesis, causing myelosuppression. Failure of normal hematopoiesis can produce diverse symptoms in patients with AML, such as increased bleeding tendency or susceptibility to infections. Approximately 800 people are diagnosed with AML each year in the Netherlands (97). AML mainly affects older individuals and the median age at diagnosis is 68 years (96). Diagnostic evaluation includes examination of peripheral blood and bone marrow samples by morphology, immunophenotyping, cytogenetics and molecular genetics, and assessment of patient fitness (96, 98). This diagnostic evaluation allows AML classification, informs

prognosis and risk stratification, and guides treatment decisions. AML is classified mainly based on cytogenetic and molecular disease characteristics using the WHO (99) or ICC (100) diagnostic classification systems. Cytogenetic and molecular abnormalities also substantially influence patient outcome and are used to stratify patients into prognostic risk groups with the ELN risk classification (98). The ELN risk stratification and patient fitness play an essential role in therapy selection (96, 98). Treatment of patients with AML consists of induction therapy with the aim to induce complete remission, followed by consolidation therapy to deepen the remission and prevent disease recurrence. Induction therapy can consist of (combinations of) chemotherapy, hypomethylating agents, BCL-2 inhibitor and targeted small molecule inhibitors for selected mutations, while consolidation therapy can also include autologous or allogeneic stem cell transplantation. The choice of consolidation therapy also relies on the persistence of low numbers of leukemic cells during complete remission, called measurable residual disease, which can be assessed by flow cytometry or quantitative PCR for specific genetic aberrations. Most patients achieve complete remission following induction and/or consolidation therapy, but many patients relapse within a few years after diagnosis (101, 102). Disease relapse is a major concern in patients with AML and significantly contributes to its poor prognosis.

AML has a heterogenous clonal architecture

The accumulation of genetic aberrations in hematopoietic and leukemic cells is a stepwise process that is shaped by Darwinian selection (103, 104). Each acquired mutation is expressed by the respective mutated cell as well as its progeny, which in turn can acquire additional mutations. As a result, leukemic cells possess mutational patterns that are formed by the initial and all subsequent genetic aberrations that have been gained. Most mutations are acquired passenger mutations with no individual effect on cell fitness (103). In contrast, a single driver mutation does confer a fitness advantage, leading to clonal outgrowth of cells with this mutation. A single driver mutation can sometimes be sufficient for leukemic transformation, giving rise to an AML founding clone. This founding clone can gain subsequent driver mutations, creating AML subclones with distinct mutational patterns (103, 104). This process of mutation accumulation followed by clonal selection is called clonal evolution. Because of clonal evolution, AML often has a clonal architecture composed of multiple AML subclones at varying frequencies. AML subclones can differ in their susceptibility to therapy (104-106). Subclones with mutations that convey resistance to therapy may survive treatment and cause refractory or relapsed disease. Disease relapse is believed to be driven by therapy-resistant leukemic stem cells, which are stem-cell like cells that are capable of long-term self-renewal and leukemia initiation and maintenance (107).

Recurrent driver mutations are common in AML

The tumor mutational burden in AML is low compared to other cancer types (82, 108). Next-generation sequencing of 200 adult AML cases demonstrated an average of 13 coding somatic mutations per AML genome (108). Almost half of these mutations occur in genes that are mutated in multiple patients. These recurrently mutated genes include genes that have been identified as driver genes in AML (109, 110). Nucleophosmin 1 (*NPM1*) and DNA methyltransferase 3A (*DNMT3A*) are amongst the most frequently mutated driver genes in AML (108, 109). Hotspot mutations in *NPM1* and *DNMT3A* are present in approximately 30-35% (108, 109, 111) and 15% (108, 109, 112) of adult patients with AML, respectively. Hotspot mutations in *NPM1* are 4 base pair insertions in the last exon causing a shift in protein translation (111, 113). These 4 base pair insertions, which can differ in exact sequence, almost all produce the same C-terminal alternative reading frame of 11 amino acids, thereby extending the mutated protein by 4 amino acids compared to the wt protein. *NPM1* mutations are early driver events in leukemogenesis, indicating their importance for tumor initiation and progression (110, 114). *NPM1* mutations are often present in all AML subclones and are infrequently lost by AML cells (115-117). Hotspot mutations in *DNMT3A* are single nucleotide variants in exon 23 creating single amino acid substitutions at position R882 (112). *DNMT3A* mutations can arise in preleukemic hematopoietic stem cells (118) and cause clonal expansion of hematopoietic cells, leading to clonal hematopoiesis of indeterminate potential (CHIP) or clonal cytopenia of undetermined significance (CCUS) (119). CHIP and CCUS mainly affect elderly individuals and convey an increased risk of developing hematological malignancies. The low mutational burden combined with the presence of driver mutations that are shared between patients, like mutations in *NPM1* and *DNMT3A*, makes AML a promising candidate for TCR-engineered T-cell therapy. Therefore, there is a strong need to identify neoantigens that are derived from such common recurrent driver mutations in AML.

Aim of the thesis

Since patients with AML frequently relapse after achieving complete remission with current standard treatments, there is an urgent need for new and effective therapies. Immunotherapy targeting neoantigens is a promising new treatment strategy for patients with AML. In AML, there are a limited number of recurrent driver mutations (109, 110). Neoantigens encoded by these mutations are especially attractive targets for immunotherapy, since they are shared between patients and unlikely to be lost as a form of immune escape (85). The aim of this thesis is to identify neoantigens encoded by recurrent driver mutations that can serve as targets for T-cell-based immunotherapy to treat patients with AML (Figure 1).

Neoantigen identification pipelines often incorporate *in silico* prediction algorithms to filter neopeptides that need to be screened for neoantigen formation (87, 89). The value of these computational tools for neoantigen discovery varies between algorithms and is dependent on their ability to reduce the number of false positives, while retaining true neoantigens. In **chapter 2**, we aim to investigate the potential of various *in silico* prediction algorithms for the discovery of T-cell ligands. Using algorithms that predict different immunobiological features, we will determine *in silico* characteristics for a set of autosomal HLA class I-binding MiHAs that have been identified as true T-cell ligands. MiHAs and neoantigens are conceptually similar, as both are encoded by genetic variants and recognized by T cells (76). The *in silico* characteristics of MiHAs will be compared with a reference set, consisting of peptides with predicted HLA binding that have not been identified as T-cell ligands. Data from MiHAs and reference peptides will be used to determine the specificity and sensitivity of the different algorithms.

One of the most frequently mutated driver genes in patients with AML is *NPM1* (108, 109). The 4 base pair hotspot insertion in *NPM1* is an early driver mutation (110, 114) that is often clonally expressed and rarely lost by AML blasts (115-117). Neoantigens encoded by mutated *NPM1* are therefore desirable targets for T-cell-based immunotherapies. In **chapter 3**, we aim to identify HLA class I-binding neoantigens that are derived from the alternative reading frame of mutated NPM1 as created by hotspot frameshift mutations. First, we aim to identify neopeptides derived from mutated NPM1 that are naturally processed and presented by HLA on AML cells. We will generate and search HLA class I ligandome data from patient-derived *NPM1*-mutated AML cells for neopeptides binding to different HLA molecules. Next, to confirm that these neopeptides are true neoantigens that are targeted by T cells, we will search for T cells specific for one HLA-A*02:01-binding NPM1 neopeptide by screening patient and healthy donor PBMCs using peptide-

HLA tetramers. Reactivity of isolated T-cell clones against HLA-A*02:01 positive patient-derived AML cells with wt or mutated *NPM1* will be assessed in cytokine secretion assays. Finally, we aim to examine the value of TCRs from potent NPM1 neoantigen-specific T-cell clones for TCR-engineered T-cell therapy of AML. TCRs will be sequenced, introduced into CD8 and CD4 T cells from healthy donors and TCR-engineered T cells will be tested for reactivity against HLA-A*02:01 positive patient-derived AML cells with wt or mutated *NPM1* in cytokine secretion and cytotoxicity assays. *In vivo* efficacy of NPM1 neoantigen-specific TCR-engineered T cells will be evaluated in a murine model engrafted with a human *NPM1*-mutated AML cell line.

Identification of neoantigens for different HLA molecules increases the number of patients that can be treated with NPM1 neoantigen-directed T-cell-based immunotherapies. In **chapter 4**, we aim to investigate whether another naturally processed NPM1 neopeptide that binds to both HLA-A*03:01 and HLA-A*11:01 is a neoantigen that can be targeted on AML by T-cell-based immunotherapy. To achieve this aim, similar methods as described for the HLA-A*02:01-binding NPM1 neopeptide will be employed to isolate specific T cells from healthy donors and to generate TCR-engineered T cells that will be evaluated for reactivity against AML cells *in vitro* and *in vivo*.

CD4 T cells are crucial for effective anti-tumor immunity by providing help to other immune cells (32-34). In addition, CD4 T cells can be cytolytic and directly kill tumor cells that express HLA class II (2). Since AML blasts frequently express HLA class II, HLA class II-binding neoantigens may be particularly relevant for T-cell-based immunotherapy of AML. In **chapter 5**, we aim to identify neoantigens encoded by recurrent driver mutations in AML that are presented in HLA class II. Because isolation of neoantigen-specific CD4 T cells by peptide-HLA class II tetramers is challenging, we aim to develop an *in vitro* T-cell stimulation and isolation method. Using public database COSMIC (88), long neopeptides encoded by recurrent genetic aberrations in AML will be synthesized and used to stimulate and isolate CD4 T cells from healthy donors. These peptides will be selected for predicted binding to common HLA class II molecules using an *in silico* algorithm (120). Isolated CD4 T-cell clones will be tested in cytokine secretion and cytotoxicity assays to determine their HLA restriction as well as their potency and specificity. Reactivity will be tested against cells that are exogenously pulsed with the neopeptides of interest and cells expressing the relevant driver mutation artificially after introduction of the mutated gene or naturally as expressed on patient-derived AML blasts.

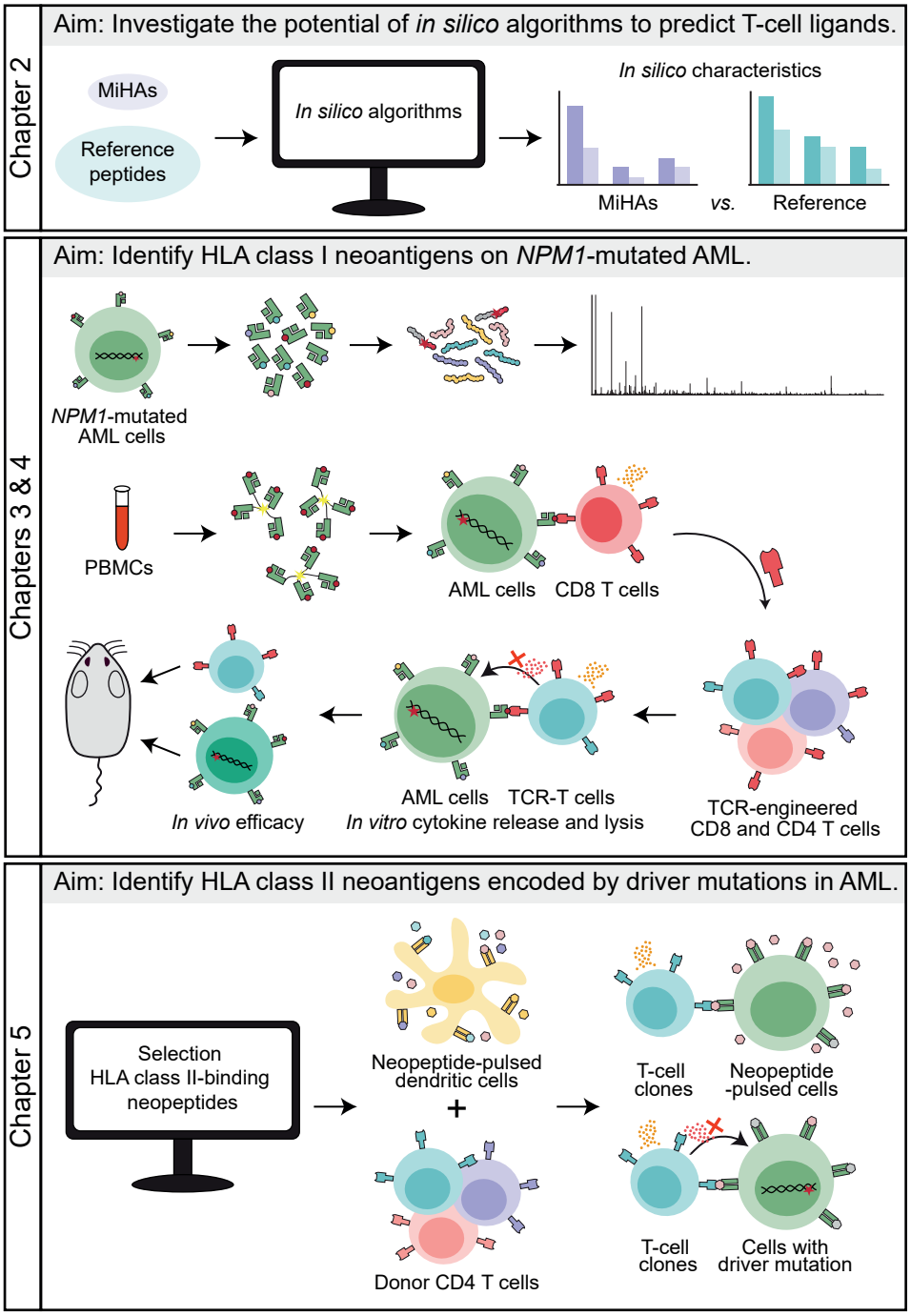

Figure 1. Outline of the thesis.

References

1. Chi H, Pepper M, Thomas PG. Principles and therapeutic applications of adaptive immunity. Cell. 2024;187(9):2052-78.
2. van Wandeloo IMB, Bol K, van Herpen C, et al. Cytotoxic CD4+ T cells in cancer: an emerging target for next-generation anticancer immunotherapy? J Immunother Cancer. 2025;13(12):e013461.
3. Lam N, Lee Y, Farber DL. A guide to adaptive immune memory. Nat Rev Immunol. 2024;24(11):810-29.
4. Djaoud Z, Parham P. HLAs, TCRs, and KIRs, a Triumvirate of Human Cell-Mediated Immunity. Annu Rev Biochem. 2020;89:717-39.
5. Rossjohn J, Gras S, Miles JJ, et al. T cell antigen receptor recognition of antigen-presenting molecules. Annu Rev Immunol. 2015;33:169-200.
6. Arstila TP, Casrouge A, Baron V, et al. A direct estimate of the human alphabeta T cell receptor diversity. Science. 1999;286(5441):958-61.
7. Bassing CH, Swat W, Alt FW. The mechanism and regulation of chromosomal V(D)J recombination. Cell. 2002;109 Suppl:S45-55.
8. Weiss A, Stobo JD. Requirement for the coexpression of T3 and the T cell antigen receptor on a malignant human T cell line. J Exp Med. 1984;160(5):1284-99.
9. Mariuzza RA, Agnihotri P, Orban J. The structural basis of T-cell receptor (TCR) activation: An enduring enigma. J Biol Chem. 2020;295(4):914-25.
10. Ashby KM, Hogquist KA. A guide to thymic selection of T cells. Nat Rev Immunol. 2024;24(2):103-17.
11. Wieczorek M, Abualrous ET, Sticht J, et al. Major Histocompatibility Complex (MHC) Class I and MHC Class II Proteins: Conformational Plasticity in Antigen Presentation. Front Immunol. 2017;8:292.
12. Madden DR. The three-dimensional structure of peptide-MHC complexes. Annu Rev Immunol. 1995;13:587-622.
13. Rammensee HG, Friede T, Stevanoviíc S. MHC ligands and peptide motifs: first listing. Immunogenetics. 1995;41(4):178-228.
14. Nguyen AT, Szeto C, Gras S. The pockets guide to HLA class I molecules. Biochem Soc Trans. 2021;49(5):2319-31.
15. Shiina T, Hosomichi K, Inoko H, et al. The HLA genomic loci map: expression, interaction, diversity and disease. J Hum Genet. 2009;54(1):15-39.
16. Barker DJ, Maccari G, Georgiou X, et al. The IPD-IMGT/HLA Database. Nucleic Acids Res. 2023;51(D1):D1053-d60. Available at https://www.ebi.ac.uk/ipd/imgt/hla/about/statistics/.
17. Greenbaum J, Sidney J, Chung J, et al. Functional classification of class II human leukocyte antigen (HLA) molecules reveals seven different supertypes and a surprising degree of repertoire sharing across supertypes. Immunogenetics. 2011;63(6):325-35.
18. Sette A, Sidney J. Nine major HLA class I supertypes account for the vast preponderance of HLA-A and -B polymorphism. Immunogenetics. 1999;50(3-4):201-12.
19. Zhang S, Liu J, Cheng H, et al. Structural basis of cross-allele presentation by HLA-A*0301 and HLA-A*1101 revealed by two HIV-derived peptide complexes. Mol Immunol. 2011;49(1-2):395-401.
20. Gonzalez-Galarza FF, McCabe A, Santos E, et al. Allele frequency net database (AFND) 2020 update: gold-standard data classification, open access genotype data and new query tools. Nucleic Acids Res. 2020;48(D1):D783-d8. Available at https://www.allelefrequencies.net/top10freqs.asp.
21. Pishesha N, Harmand TJ, Ploegh HL. A guide to antigen processing and presentation. Nat Rev Immunol. 2022;22(12):751-64.

22. Murata S, Takahama Y, Kasahara M, et al. The immunoproteasome and thymoproteasome: functions, evolution and human disease. Nat Immunol. 2018;19(9):923-31.
23. Inholz K, Anderl JL, Klawitter M, et al. Proteasome composition in immune cells implies special immune-cell-specific immunoproteasome function. Eur J Immunol. 2024;54(4):e2350613.
24. Stern LJ, Santambrogio L. The melting pot of the MHC II peptidome. Curr Opin Immunol. 2016;40:70-7.
25. Sidney J, Peters B, Sette A. Epitope prediction and identification- adaptive T cell responses in humans. Semin Immunol. 2020;50:101418.
26. Tan TL, Geluk A, Toebes M, et al. A novel, highly efficient peptide-HLA class I binding assay using unfolded heavy chain molecules: identification of HIV-1 derived peptides that bind to HLA-A*0201 and HLA-A*0301. J Immunol Methods. 1997;205(2):201-9.
27. Freudenmann LK, Marcu A, Stevanović S. Mapping the tumour human leukocyte antigen (HLA) ligandome by mass spectrometry. Immunology. 2018;154(3):331-45.
28. Zhang B, Bassani-Sternberg M. Current perspectives on mass spectrometry-based immunopeptidomics: the computational angle to tumor antigen discovery. J Immunother Cancer. 2023;11(10).
29. Peters B, Nielsen M, Sette A. T Cell Epitope Predictions. Annu Rev Immunol. 2020;38:123-45.
30. Chen DS, Mellman I. Oncology meets immunology: the cancer-immunity cycle. Immunity. 2013;39(1):1-10.
31. Mellman I, Chen DS, Powles T, et al. The cancer-immunity cycle: Indication, genotype, and immunotype. Immunity. 2023;56(10):2188-205.
32. Borst J, Ahrends T, Bąbała N, et al. CD4(+) T cell help in cancer immunology and immunotherapy. Nat Rev Immunol. 2018;18(10):635-47.
33. Speiser DE, Chijioke O, Schaeuble K, et al. CD4(+) T cells in cancer. Nat Cancer. 2023;4(3):317-29.
34. Montauti E, Oh DY, Fong L. CD4(+) T cells in antitumor immunity. Trends Cancer. 2024;10(10):969-85.
35. Ghorani E, Swanton C, Quezada SA. Cancer cell-intrinsic mechanisms driving acquired immune tolerance. Immunity. 2023;56(10):2270-95.
36. de Visser KE, Joyce JA. The evolving tumor microenvironment: From cancer initiation to metastatic outgrowth. Cancer Cell. 2023;41(3):374-403.
37. Waldman AD, Fritz JM, Lenardo MJ. A guide to cancer immunotherapy: from T cell basic science to clinical practice. Nat Rev Immunol. 2020;20(11):651-68.
38. Rosenberg SA, Restifo NP. Adoptive cell transfer as personalized immunotherapy for human cancer. Science. 2015;348(6230):62-8.
39. Klobuch S, Seijkens TTP, Schumacher TN, et al. Tumour-infiltrating lymphocyte therapy for patients with advanced-stage melanoma. Nat Rev Clin Oncol. 2024;21(3):173-84.
40. Sharma P, Goswami S, Raychaudhuri D, et al. Immune checkpoint therapy-current perspectives and future directions. Cell. 2023;186(8):1652-69.
41. Katsikis PD, Ishii KJ, Schliehe C. Challenges in developing personalized neoantigen cancer vaccines. Nat Rev Immunol. 2024;24(3):213-27.
42. Zaidi N, Jaffee EM, Yarchoan M. Recent advances in therapeutic cancer vaccines. Nat Rev Cancer. 2025;25(7):517-33.
43. Singh AK, McGuirk JP. Allogeneic Stem Cell Transplantation: A Historical and Scientific Overview. Cancer Res. 2016;76(22):6445-51.
44. Doulatov S, Notta F, Laurenti E, et al. Hematopoiesis: a human perspective. Cell Stem Cell. 2012;10(2):120-36.
45. Handgretinger R, Arendt AM, Maier CP, et al. Ex vivo and in vivo T-cell depletion in allogeneic transplantation: towards less or non-cytotoxic conditioning regimens. Expert Rev Clin Immunol. 2022;18(12):1285-96.

46. Falkenburg JHF, Jedema I. Graft versus tumor effects and why people relapse. Hematology Am Soc Hematol Educ Program. 2017;2017(1):693-8.
47. Falkenburg JHF, Schmid C, Kolb HJ, et al. Delayed Transfer of Immune Cells or the Art of Donor Lymphocyte Infusion (DLI) 2.0. In: Sureda A, Corbacioglu S, Greco R, Kröger N, Carreras E, editors. The EBMT Handbook: Hematopoietic Cell Transplantation and Cellular Therapies. Cham (CH): Springer; 2024:531-9.
48. June CH, Sadelain M. Chimeric Antigen Receptor Therapy. N Engl J Med. 2018;379(1):64-73.
49. Labanieh L, Mackall CL. CAR immune cells: design principles, resistance and the next generation. Nature. 2023;614(7949):635-48.
50. Brudno JN, Maus MV, Hinrichs CS. CAR T Cells and T-Cell Therapies for Cancer: A Translational Science Review. Jama. 2024;332(22):1924-35.
51. Cappell KM, Kochenderfer JN. Long-term outcomes following CAR T cell therapy: what we know so far. Nat Rev Clin Oncol. 2023;20(6):359-71.
52. Morris EC, Falkenburg JHF. What Defines a Good Tumour Antigen? In: Kröger N, Gribben J, Chabannon C, Yakoub-Agha I, Einsele H, editors. The EBMT/EHA CAR-T Cell Handbook. Cham (CH): Springer; 2022:11-4.
53. Klebanoff CA, Chandran SS, Baker BM, et al. T cell receptor therapeutics: immunological targeting of the intracellular cancer proteome. Nat Rev Drug Discov. 2023;22(12):996-1017.
54. Müller TR, Jarosch S, Hammel M, et al. Targeted T cell receptor gene editing provides predictable T cell product function for immunotherapy. Cell Rep Med. 2021;2(8):100374.
55. Ottaviano G, Qasim W. Current landscape of vector safety and genotoxicity after hematopoietic stem or immune cell gene therapy. Leukemia. 2025;39(6):1325-33.
56. Roth TL, Puig-Saus C, Yu R, et al. Reprogramming human T cell function and specificity with non-viral genome targeting. Nature. 2018;559(7714):405-9.
57. Morton LT, Reijmers RM, Wouters AK, et al. Simultaneous Deletion of Endogenous TCRαβ for TCR Gene Therapy Creates an Improved and Safe Cellular Therapeutic. Mol Ther. 2020;28(1):64-74.
58. Foy SP, Jacoby K, Bota DA, et al. Non-viral precision T cell receptor replacement for personalized cell therapy. Nature. 2023;615(7953):687-96.
59. van Loenen MM, de Boer R, Amir AL, et al. Mixed T cell receptor dimers harbor potentially harmful neoreactivity. Proc Natl Acad Sci U S A. 2010;107(24):10972-7.
60. Bendle GM, Linnemann C, Hooijkaas AI, et al. Lethal graft-versus-host disease in mouse models of T cell receptor gene therapy. Nat Med. 2010;16(5):565-70.
61. Cohen CJ, Zhao Y, Zheng Z, et al. Enhanced antitumor activity of murine-human hybrid T-cell receptor (TCR) in human lymphocytes is associated with improved pairing and TCR/CD3 stability. Cancer Res. 2006;66(17):8878-86.
62. Kuball J, Dossett ML, Wolfl M, et al. Facilitating matched pairing and expression of TCR chains introduced into human T cells. Blood. 2007;109(6):2331-8.
63. Leko V, Rosenberg SA. Identifying and Targeting Human Tumor Antigens for T Cell-Based Immunotherapy of Solid Tumors. Cancer Cell. 2020;38(4):454-72.
64. Roex MCJ, Hageman L, Veld SAJ, et al. A minority of T cells recognizing tumor-associated antigens presented in self-HLA can provoke antitumor reactivity. Blood. 2020;136(4):455-67.
65. Johnson LA, Morgan RA, Dudley ME, et al. Gene therapy with human and mouse T-cell receptors mediates cancer regression and targets normal tissues expressing cognate antigen. Blood. 2009;114(3):535-46.
66. Parkhurst MR, Yang JC, Langan RC, et al. T cells targeting carcinoembryonic antigen can mediate regression of metastatic colorectal cancer but induce severe transient colitis. Mol Ther. 2011;19(3):620-6.
67. Lamers CH, Sleijfer S, van Steenbergen S, et al. Treatment of metastatic renal cell carcinoma with CAIX CAR-engineered T cells: clinical evaluation and management of on-target toxicity. Mol Ther. 2013;21(4):904-12.

68. Hansen JA, Petersdorf EW, Lin MT, et al. Genetics of allogeneic hematopoietic cell transplantation. Role of HLA matching, functional variation in immune response genes. Immunol Res. 2008;41(1):56-78.
69. Petersdorf EW. The major histocompatibility complex: a model for understanding graft-versus-host disease. Blood. 2013;122(11):1863-72.
70. Griffioen M, van Bergen CA, Falkenburg JH. Autosomal Minor Histocompatibility Antigens: How Genetic Variants Create Diversity in Immune Targets. Front Immunol. 2016;7:100.
71. Fuchs KJ, van de Meent M, Honders MW, et al. Expanding the repertoire reveals recurrent, cryptic, and hematopoietic HLA class I minor histocompatibility antigens. Blood. 2024;143(18):1856-72.
72. Wang W, Meadows LR, den Haan JM, et al. Human H-Y: a male-specific histocompatibility antigen derived from the SMCY protein. Science. 1995;269(5230):1588-90.
73. Fuchs KJ, Falkenburg JHF, Griffioen M. Minor histocompatibility antigens to predict, monitor or manipulate GvL and GvHD after allogeneic hematopoietic cell transplantation. Best Pract Res Clin Haematol. 2024;37(2):101555.
74. Krakow EF, Brault M, Summers C, et al. HA-1-targeted T-cell receptor T-cell therapy for recurrent leukemia after hematopoietic stem cell transplantation. Blood. 2024;144(10):1069-82.
75. Pon JR, Marra MA. Driver and passenger mutations in cancer. Annu Rev Pathol. 2015;10:25-50.
76. Schumacher TN, Schreiber RD. Neoantigens in cancer immunotherapy. Science. 2015;348(6230):69-74.
77. Schumacher TN, Scheper W, Kvistborg P. Cancer Neoantigens. Annu Rev Immunol. 2019;37:173-200.
78. Brough SC, Skonieczny KL, Leibou S, et al. Facts and Hopes for Neoantigen-Enriched TIL. Clin Cancer Res. 2025;31(24):5128-36.
79. Tran E, Turcotte S, Gros A, et al. Cancer immunotherapy based on mutation-specific CD4+ T cells in a patient with epithelial cancer. Science. 2014;344(6184):641-5.
80. Tran E, Robbins PF, Lu YC, et al. T-Cell Transfer Therapy Targeting Mutant KRAS in Cancer. N Engl J Med. 2016;375(23):2255-62.
81. Zacharakis N, Chinnasamy H, Black M, et al. Immune recognition of somatic mutations leading to complete durable regression in metastatic breast cancer. Nat Med. 2018;24(6):724-30.
82. Alexandrov LB, Nik-Zainal S, Wedge DC, et al. Signatures of mutational processes in human cancer. Nature. 2013;500(7463):415-21.
83. Budczies J, Kazdal D, Menzel M, et al. Tumour mutational burden: clinical utility, challenges and emerging improvements. Nat Rev Clin Oncol. 2024;21(10):725-42.
84. Verdegaal EM, de Miranda NF, Visser M, et al. Neoantigen landscape dynamics during human melanoma-T cell interactions. Nature. 2016;536(7614):91-5.
85. Pearlman AH, Hwang MS, Konig MF, et al. Targeting public neoantigens for cancer immunotherapy. Nat Cancer. 2021;2(5):487-97.
86. Leidner R, Sanjuan Silva N, Huang H, et al. Neoantigen T-Cell Receptor Gene Therapy in Pancreatic Cancer. N Engl J Med. 2022;386(22):2112-9.
87. Garcia-Garijo A, Fajardo CA, Gros A. Determinants for Neoantigen Identification. Front Immunol. 2019;10:1392.
88. Sondka Z, Dhir NB, Carvalho-Silva D, et al. COSMIC: a curated database of somatic variants and clinical data for cancer. Nucleic Acids Res. 2024;52(D1):D1210-d7.
89. Lang F, Schrörs B, Löwer M, et al. Identification of neoantigens for individualized therapeutic cancer vaccines. Nat Rev Drug Discov. 2022;21(4):261-82.
90. Nilsson JB, Greenbaum J, Peters B, et al. NetMHCpan-4.2: improved prediction of CD8+ epitopes by use of transfer learning and structural features. Front Immunol. 2025;16:1616113.
91. Wells DK, van Buuren MM, Dang KK, et al. Key Parameters of Tumor Epitope Immunogenicity Revealed Through a Consortium Approach Improve Neoantigen Prediction. Cell. 2020;183(3):818-34.e13.

92. Bassani-Sternberg M, Bräunlein E, Klar R, et al. Direct identification of clinically relevant neoepitopes presented on native human melanoma tissue by mass spectrometry. Nat Commun. 2016;7:13404.
93. Cohen CJ, Gartner JJ, Horovitz-Fried M, et al. Isolation of neoantigen-specific T cells from tumor and peripheral lymphocytes. J Clin Invest. 2015;125(10):3981-91.
94. Strønen E, Toebes M, Kelderman S, et al. Targeting of cancer neoantigens with donor-derived T cell receptor repertoires. Science. 2016;352(6291):1337-41.
95. Karpanen T, Olweus J. The Potential of Donor T-Cell Repertoires in Neoantigen-Targeted Cancer Immunotherapy. Front Immunol. 2017;8:1718.
96. DiNardo CD, Erba HP, Freeman SD, et al. Acute myeloid leukaemia. Lancet. 2023;401(10393):2073-86.
97. Nederlandse Kankerregistratie (NKR), IKNL. Available at https://nkr-cijfers.iknl.nl/. Accessed 13 August, 2025.
98. Döhner H, Wei AH, Appelbaum FR, et al. Diagnosis and management of AML in adults: 2022 recommendations from an international expert panel on behalf of the ELN. Blood. 2022;140(12):1345-77.
99. Khoury JD, Solary E, Abla O, et al. The 5th edition of the World Health Organization Classification of Haematolymphoid Tumours: Myeloid and Histiocytic/Dendritic Neoplasms. Leukemia. 2022;36(7):1703-19.
100. Arber DA, Orazi A, Hasserjian RP, et al. International Consensus Classification of Myeloid Neoplasms and Acute Leukemias: integrating morphologic, clinical, and genomic data. Blood. 2022;140(11):1200-28.
101. Döhner H, Weisdorf DJ, Bloomfield CD. Acute Myeloid Leukemia. N Engl J Med. 2015;373(12):1136-52.
102. Döhner H, Estey E, Grimwade D, et al. Diagnosis and management of AML in adults: 2017 ELN recommendations from an international expert panel. Blood. 2017;129(4):424-47.
103. Welch JS, Ley TJ, Link DC, et al. The origin and evolution of mutations in acute myeloid leukemia. Cell. 2012;150(2):264-78.
104. Morita K, Wang F, Jahn K, et al. Clonal evolution of acute myeloid leukemia revealed by high-throughput single-cell genomics. Nat Commun. 2020;11(1):5327.
105. Ding L, Ley TJ, Larson DE, et al. Clonal evolution in relapsed acute myeloid leukaemia revealed by whole-genome sequencing. Nature. 2012;481(7382):506-10.
106. Parkin B, Ouillette P, Li Y, et al. Clonal evolution and devolution after chemotherapy in adult acute myelogenous leukemia. Blood. 2013;121(2):369-77.
107. Shlush LI, Mitchell A, Heisler L, et al. Tracing the origins of relapse in acute myeloid leukaemia to stem cells. Nature. 2017;547(7661):104-8.
108. Ley TJ, Miller C, Ding L, et al. Genomic and epigenomic landscapes of adult de novo acute myeloid leukemia. N Engl J Med. 2013;368(22):2059-74.
109. Papaemmanuil E, Gerstung M, Bullinger L, et al. Genomic Classification and Prognosis in Acute Myeloid Leukemia. N Engl J Med. 2016;374(23):2209-21.
110. Kishtagari A, Levine RL, Viny AD. Driver mutations in acute myeloid leukemia. Curr Opin Hematol. 2020;27(2):49-57.
111. Falini B, Mecucci C, Tiacci E, et al. Cytoplasmic nucleophosmin in acute myelogenous leukemia with a normal karyotype. N Engl J Med. 2005;352(3):254-66.
112. Ley TJ, Ding L, Walter MJ, et al. DNMT3A mutations in acute myeloid leukemia. N Engl J Med. 2010;363(25):2424-33.
113. Thiede C, Koch S, Creutzig E, et al. Prevalence and prognostic impact of NPM1 mutations in 1485 adult patients with acute myeloid leukemia (AML). Blood. 2006;107(10):4011-20.
114. Falini B, Brunetti L, Sportoletti P, et al. NPM1-mutated acute myeloid leukemia: from bench to bedside. Blood. 2020;136(15):1707-21.

115. Krönke J, Bullinger L, Teleanu V, et al. Clonal evolution in relapsed NPM1-mutated acute myeloid leukemia. Blood. 2013;122(1):100-8.
116. Höllein A, Meggendorfer M, Dicker F, et al. NPM1 mutated AML can relapse with wild-type NPM1: persistent clonal hematopoiesis can drive relapse. Blood Adv. 2018;2(22):3118-25.
117. Cocciardi S, Dolnik A, Kapp-Schwoerer S, et al. Clonal evolution patterns in acute myeloid leukemia with NPM1 mutation. Nat Commun. 2019;10(1):2031.
118. Shlush LI, Zandi S, Mitchell A, et al. Identification of pre-leukaemic haematopoietic stem cells in acute leukaemia. Nature. 2014;506(7488):328-33.
119. Weeks LD, Ebert BL. Causes and consequences of clonal hematopoiesis. Blood. 2023;142(26):2235-46.
120. Jensen KK, Andreatta M, Marcatili P, et al. Improved methods for predicting peptide binding affinity to MHC class II molecules. Immunology. 2018;154(3):394-406.

Chapter 2

The value of online algorithms to predict T-cell ligands created by genetic variants

Dyantha I. van der Lee[1], Margot J. Pont[1,2], J.H. Frederik Falkenburg[1], Marieke Griffioen[1]

[1] Department of Hematology, Leiden University Medical Center, Leiden, The Netherlands
[2] Program in Immunology, Clinical Research Division, Fred Hutchinson Cancer Research Center, Seattle, Washington, United States of America

PLoS One. 2016 Sep 12;11(9):e0162808
DOI: 10.1371/journal.pone.0162808

Abstract

Allogeneic stem cell transplantation can be a curative treatment for hematological malignancies. After HLA-matched allogeneic stem cell transplantation, beneficial anti-tumor immunity as well as detrimental side-effects can develop due to donor-derived T-cells recognizing polymorphic peptides that are presented by HLA on patient cells. Polymorphic peptides on patient cells that are recognized by specific T-cells are called minor histocompatibility antigens (MiHA), while the respective peptides in donor cells are allelic variants. MiHA can be identified by reverse strategies in which large sets of peptides are screened for T-cell recognition. In these strategies, selection of peptides by prediction algorithms may be relevant to increase the efficiency of MiHA discovery. We investigated the value of online prediction algorithms for MiHA discovery and determined the *in silico* characteristics of 68 autosomal HLA class I-restricted MiHA that have been identified as natural ligands by forward strategies in which T-cells from *in vivo* immune responses after allogeneic stem cell transplantation are used to identify the antigen. Our analysis showed that HLA class I binding was accurately predicted for 87% of MiHA of which a relatively large proportion of peptides had strong binding affinity (56%). Weak binding affinity was also predicted for a considerable number of antigens (31%) and the remaining 13% of MiHA were not predicted as HLA class I binding peptides. Besides prediction for HLA class I binding, none of the other online algorithms significantly contributed to MiHA characterization. Furthermore, we demonstrated that the majority of MiHA do not differ from their allelic variants in *in silico* characteristics, suggesting that allelic variants can potentially be processed and presented on the cell surface. In conclusion, our analyses revealed the *in silico* characteristics of 68 HLA class I-restricted MiHA and explored the value of online algorithms to predict T-cell ligands that are created by genetic variants.

Introduction

Allogeneic stem cell transplantation (alloSCT) can be a curative treatment for hematological malignancies (1, 2). After HLA-matched alloSCT, a desired anti-tumor or graft-versus-leukemia (GvL) effect can be mediated by donor-derived T-cells recognizing polymorphic peptides in the context of HLA on the malignant cells of the patient. These polymorphic peptides or minor histocompatibility antigens (MiHA) arise as a result of differences in single nucleotide polymorphisms (SNP) in the genome between the recipient and stem cell donor (3-6). These SNP differences often lead to a change in a single non-synonymous amino acid, resulting in presentation of the MiHA on the patient cell and expression of its allelic variant in the donor cell. Unfortunately, donor T-cells can also cause undesired graft-versus-host disease (GvHD) when MiHA are targeted that are expressed on healthy non-hematopoietic tissues (7, 8). Research focuses on characterization of MiHA with hematopoiesis-restricted expression, since donor T-cells for these MiHA attack the malignant cells of the patient, while sparing healthy hematopoietic cells of donor origin. As such, hematopoiesis-restricted MiHA can be used as targets for T-cell therapy to stimulate GvL reactivity without GvHD.

In 1995, HA-2 has been identified as first autosomal MiHA by mass spectrometry analysis of peptides eluted from HLA surface molecules (9). Since then, methods for MiHA discovery developed in rapid succession and include screening of cDNA libraries and genetic approaches such as genetic linkage analysis and whole genome association scanning (4-6). In these forward strategies, T-cells isolated from *in vivo* immune responses after alloSCT are used to identify MiHA and all peptides are thus characterized as natural T-cell ligands. Drawbacks of forward strategies are that large numbers of T-cells need to be isolated and expanded and that antigens have to be examined in detail for their tissue distribution to identify hematopoiesis-restricted MiHA with therapeutic relevance.

In reverse approaches, candidate MiHA encoded by genes with hematopoiesis-restricted expression can be selected to search for specific T-cells (10-12). Selection of predefined antigens is frequently based on HLA class I binding affinity as predicted by online algorithms. A major drawback of reverse strategies is that many candidates cannot be confirmed as antigens that are endogenously processed and presented and recognized by specific T-cells. Inclusion of an additional step in which candidate antigens are selected for presence in the HLA-ligandome ensures endogenous processing and presentation, but does not guarantee that a donor T-cell exists with a T-cell receptor (TCR) that is capable of reacting with the antigen *in vivo*.

Similar to MiHA, neoantigens are peptides with amino acid changes that are recognized by specific T-cells (13, 14). In contrast to MiHA, neoantigens are created by tumor-specific mutations and can be targeted by autologous T-cells from the patient. In neoantigen discovery, tumor-specific mutations in coding exons as identified by whole exome or genome sequencing are searched for peptides with predicted binding to the HLA class I alleles as expressed by the patient and candidate neoantigens encoded by genes that are expressed in the tumor are selected to search for specific T-cells.

In reverse strategies for MiHA or neoantigen discovery, large sets of peptides need to be screened in order to discover antigens. Therefore, selection of peptides with predicted HLA class I binding affinity, peptide-HLA complex stability, proteasomal cleavage, affinity for the transporter associated with antigen processing and presentation (TAP) or *in vivo* immunogenicity may enhance the efficiency of antigen discovery. In this study, we explored the value of online prediction algorithms and determined the *in silico* characteristics for a set of 68 autosomal HLA class I-restricted MiHA that have been identified as natural T-cell ligands by forward approaches. We demonstrate that the algorithm for HLA class I binding accurately predicted 87% of MiHA of which a relatively large proportion (56%) are peptides with strong predicted binding to HLA class I. Besides prediction for HLA class I binding, none of the other online algorithms significantly contributed to MiHA characterization. We also demonstrate that the majority of MiHA do not differ from their allelic variants in *in silico* characteristics, suggesting that allelic variants can potentially be processed and presented on the cell surface and may therefore be relevant T-cell targets after alloSCT.

Materials and methods

Minor histocompatibility antigens

A total of 68 autosomal HLA class I-restricted MiHA that have been identified as natural T-cell ligands by forward approaches have been included in the analyses. Epitopes which were restricted to multiple HLA-molecules (ACC-2D, LB-APOBEC3B-1K, LB-DHX33-1C, LB-GEMIN4-1V and UGT2B17) or length variants from a single epitope (LB-ERAP1-1R) were considered as different MiHA. Allelic variants exist for 60 MiHA and two MiHA (ACC-1Y and HB-1H) have allelic variants that have also been identified as *in vivo* T-cell targets (15, 16). For these two MiHA, the epitope that was first identified and published as *in vivo* T-cell target is indicated as MiHA, whereas its counterpart is indicated as allelic variant.

Reference set of peptides

For accurate analysis of the value of online prediction algorithms for MiHA characterization, we composed a set of reference peptides. All peptides in the reference set were derived from 21 proteins for which HLA-A*02:01-restricted (*n* = 12) or HLA-B*07:02-restricted (*n* = 9) MiHA have been identified in the normal open reading frame. Whole protein sequences were screened for peptides with predicted binding to HLA-A*02:01 and HLA-B*07:02 using the online prediction algorithm NetMHCpan 2.8. Predicted strong and weak binding peptides as designated by default thresholds were included, leading to a total set of 1370 peptides of which 906 peptides were predicted to bind to HLA-A*02:01 and 464 peptides were predicted to bind to HLA-B*07:02.

Online prediction algorithms

To predict binding affinity for HLA class I, stability of the peptide-HLA class I complex, proteasomal cleavage at the C-terminus, affinity for TAP and *in vivo* immunogenicity, the online available algorithms NetMHCpan 2.8 (17), NetMHCstab 1.0 (18), NetChop 3.1 (19), TAPPred (20) and the MHC I Immunogenicity tool from the immune epitope database (IEDB) (21) were used, respectively. In addition, NetCTLpan 1.1 (22) was used to integrate predicted HLA class I binding affinity, C-terminal proteasomal cleavage and TAP transport efficiency.

In NetMHCpan 2.8, NetMHCstab 1.0 and NetChop 3.1, predictions are made using artificial neural networks (ANNs). ANNs of NetMHCpan 2.8 and NetMHCstab 1.0 have been trained for >150 and 10 different HLA-molecules based on >150.000 quantitative binding data and 5509 distinct peptide stability measurements, respectively. Predictions can be made for HLA-A or –B in NetMHCstab 1.0 and for HLA-A, -B, -C and -E in NetMHCpan 2.8. ANNs of the C-term 3.0 network of NetChop 3.1 have been trained on 1260 HLA class I ligands. In NetMHCpan 2.8, predictions are given as IC_{50} values in nM and %-Rank, which designates the rank of the predicted affinity of a certain epitope as compared to a set of 200.000 random natural peptides (17). When using standard thresholds, epitopes are indicated as strong binding peptides (SB) if $IC_{50} \leq 50$ nM or %-Rank≤0.5 and as weak binding peptides (WB) if $IC_{50} \leq 500$ nM or %-Rank≤2. We defined peptides with $IC_{50} > 500$ nM and %-Rank>2 as non-binding peptides (NB). NetMHCstab 1.0 predicts the half-life of peptide-HLA class I complexes in hours (18). The relative contribution of the predicted binding affinity of an epitope for its respective HLA-allele (as determined by NetMHCcons 1.0 (23)) to NetMHCstab 1.0 is 0.85 by default. Standard cut off values for highly stable complexes (HS) and weakly stable complexes (WS) are >6 hrs and >2 hrs, respectively. We indicated peptides with predicted stability ≤2 hrs as non-stable complexes (NS). Exact epitope sequences were fed into NetMHCpan 2.8 and NetMHCstab 1.0, whereas whole protein sequences were entered into NetChop

3.1. In NetChop 3.1, we used the C-term 3.0 network to predict C-terminal proteasomal cleavage (19). Output is displayed as a score ranging 0-1, in which 0 signifies a low and 1 a high likelihood of proteasomal cleavage. The standard threshold for proteasomal cleavage is a score >0.5.

Affinity for the TAP transporter was predicted by TAPPred (20). TAPPred uses a support vector machine (SVM)-based method which is trained on experimentally determined IC_{50} values of 431 peptides that bind to TAP with different affinities. The cascade SVM-based method was used to predict TAP transporter affinity. Output is given as a scale on which a score of 0 corresponds to a normalized IC_{50}>1000 nM and a score of 10 to a normalized IC_{50}<0.003 nM. Exact peptide sequences were entered into the algorithm and, using standard cut off values, were divided in high (>6), intermediate (>3) or low (≤3) affinity peptides for the TAP transporter.

NetCTLpan 1.1 predicts T-cell epitopes in protein sequences based on an integrated approach of HLA class I binding affinity, C-terminal proteasomal cleavage and TAP transport efficiency as predicted by NetMHC pan 2.3, the C-term 3.0 network of NetChop 3.0 and a weight matrix based method, respectively (22). In this algorithm, the default weight on HLA class I binding affinity, C-terminal proteasomal cleavage and TAP transport efficiency is 0.750, 0.225 and 0.025, respectively. Predictions are given as %-Rank, which designates the rank of the predicted affinity of a certain epitope as compared to a set of 200.000 random natural peptides. Whole protein sequences were entered into the algorithm and the standard threshold of %-Rank<1 was used for epitope identification.

Epitope immunogenicity, which is defined as the ability of a certain epitope to be recognized by a specific TCR, was determined by the MHC I Immunogenicity tool from the Immune Epitope Database and Analysis Resource (IEDB) (21). Exact peptide sequences were entered and thresholds for *in vivo* immunogenicity with 90% specificity were determined for HLA-A*02:01 (>0.27) and HLA-B*07:02 (>0.22) based on analysis of prediction data for MiHA and reference peptides by receiver operating characteristics (ROC) curves. In the IEDB tool, amino acid residues at anchor positions are masked to avoid bias by HLA class I binding affinity according to binding motifs as available in http://www.cbs.dtu.dk/biotools/MHCMotifViewer/Human_alleles.html (24).

Statistical analysis

Fisher's exact test was used to compare *in silico* characteristics between MiHA and reference peptides and to compare predicted C-terminal proteasomal cleavage and *in vivo* immunogenicity between MiHA and their allelic variants. For comparison of predicted HLA class I binding affinity, stability of the peptide-HLA class I complexes

and *in vivo* immunogenicity between MiHA and their allelic variants, Wilcoxon signed rank test was used. P-values <0.05 were considered significant. ROC curves were plotted to determine the sensitivity and specificity of default thresholds and to define the thresholds for the MHC I Immunogenicity tool from the IEDB. The performance of the online algorithms was evaluated by the area under the ROC curve (AUC) in which p-values <0.05 were considered significant.

Results

HLA class I-restricted minor histocompatibility antigens

HLA class I-restricted MiHA that have been identified by forward approaches are antigens that are targeted by T-cells *in vivo*. These natural T-cell ligands follow by definition all rules that are required for endogenous processing and presentation and antigen recognition by specific T-cells. We therefore selected these antigens to explore the value of online available tools for prediction of HLA class I binding affinity, stability of the peptide-HLA class I complex, proteasomal cleavage, TAP transporter affinity and *in vivo* immunogenicity. Autosomal HLA class I-restricted MiHA that have been identified by forward approaches (reviewed by Griffioen et al. (6), (25) and unpublished work) are listed in Table 1 (n = 68) and the results of *in silico* analyses are shown in Table 2. Of the 68 MiHA as shown in Table 1, 34 antigens are 9-mer peptides, 17 antigens are 10-mer peptides and 16 antigens are 11-mer peptides. LB-NADK-1K is the only peptide of 13 amino acids in length. Overall, the 68 MiHA bind to 19 different HLA class I-alleles, of which HLA-A*02:01 (n = 17) and HLA-B*07:02 (n = 18) are most frequent.

Table 1. HLA class I-restricted minor histocompatibility antigens

MiHA name	Sequence[A]	Length	Gene	SNP	HLA-allele
ACC-1Y[B]	DYLQ[**Y**/C]VLQI	9	*BCL2A1*	rs1138357	A*24:02
ACC-2D	KEFED[**D**/G]IINW	10	*BCL2A1*	rs3826007	B*44:02
ACC-2D	KEFED[**D**/G]IINW	10	*BCL2A1*	rs3826007	B*44:03
ACC-6	MEIFIEVFSHF	11	*HMSD*	rs9945924[C]	B*44:03
CTSH(R)/A31	ATLPLLCA[**R**/G]	9	*CTSH*	rs2289702	A*31:01
CTSH(R)/A33	WATLPLLCA[**R**/G]	10	*CTSH*	rs2289702	A*33:03
DPH1	S[**V**/L]LPEVDVW	9	*DPH1*	rs35394823	B*57:01
HA-1	VL[**H**/R]DDLLEA	9	*HMHA1*	rs1801284	A*02:01
HA-2	YIGEVLVS[**V**/M]	9	*MYO1G*	rs61739531	A*02:01
HA-3T	V[**T**/M]EPGTAQY	9	*AKAP13*	rs2061821	A*01:01
HA-8R	[**R**/P]TLDKVLEV	9	*KIAA0020*	rs2173904	A*02:01
HB-1H[B]	EEKRGSL[**H**/Y]VW	10	*HMHB1*	rs161557	B*44:03
HEATR1-1E	ISKERA[**E**/G]AL	9	*HEATR1*	rs2275687	B*08:01
HwA11-S	CIPPD[**S**/T]LLFPA	11	*C19ORF48*	rs3745526[D]	A*02:01
LB-ADIR-1F	SVAPALAL[**F**/S]PA	11	*TOR3A*	rs2296377[D]	A*02:01
LB-APOBEC3B-1K	[**K**/E]PQYHAEMCF	10	*APOBEC3B*	rs2076109	B*07:02
LB-APOBEC3B-1K	[**K**/E]PQYHAEMCF	10	*APOBEC3B*	rs2076109	B*08:01
LB-ARHGDIB-1R	LPRACW[**R**/P]EA	9	*ARHGDIB*	rs4703[D]	B*07:02
LB-BCAT2-1R	QP[**R**/T]RALLFVIL	11	*BCAT2*	rs11548193	B*07:02
LB-C16ORF-1R	[**R**/W]PCPSVGLSFL	11	*C16ORF*	rs305087[D]	B*07:02
LB-C19ORF48-2E	TAWPGAP[**E**/G]V	9	*C19ORF48*	rs4801853	B*51:01
LB-CCL4-1T	CADPSE[**T**/S]WV	9	*CCL4*	rs1719152	A*02:01
LB-CLYBL-1Y	SLAA[**Y**/D]IPRL	9	*CLYBL*	rs17577293	A*02:01
LB-CYBA-1Y	STMERWGQK[**Y**/H]	10	*CYBA*	rs4673	A*01:01
LB-DHX33-1C	YLYEGGIS[**C**/R]	9	*DHX33*	rs8069315	A*02:01
LB-DHX33-1C	YLYEGGIS[**C**/R]	9	*DHX33*	rs8069315	C*03:03
LB-EBI3-1I	RPRARYY[**I**/V]QV	10	*EBI3*	rs4740	B*07:02
LB-ECGF-1H	RP[**H**/R]AIRRPLAL	11	*TYMP*	rs112723255[D]	B*07:02
LB-ERAP1-1R	HP[**R**/P]QEQIAL	9	*ERAP1*	rs26653	B*07:02
LB-ERAP1-1R	HP[**R**/P]QEQIALLA	11	*ERAP1*	rs26653	B*07:02
LB-FUCA2-1V	RLRQ[**V**/M]GSWL	9	*FUCA2*	rs3762002	B*07:02
LB-GEMIN4-1V	FPALRFVE[**V**/E]	9	*GEMIN4*	rs4968104	B*07:02
LB-GEMIN4-1V	FPALRFVE[**V**/E]	9	*GEMIN4*	rs4968104	B*08:01
LB-GLE1-1V	GQ[**V**/I]RLRALY	9	*GLE1*	rs2275260	B*15:01
LB-GSTP1-1V	DLRCKY[**V**/I]SL	9	*GSTP1*	rs1695	B*08:01
LB-ITGB2-1	GQAGFFPSPF	10	*ITGB2*	rs760462[C]	B*15:01
LB-MOB3A-1C	[**C**/S]PRPGTWTC	9	*MOB3A*	rs11541046[D]	B*07:02

Table 1. ***Continued***

MiHA name	Sequence[A]	Length	Gene	SNP	HLA-allele
LB-NADK-1K	AVHNGLGE[**K**/N]GSQA	13	*NADK*	rs4751	A*03:01
LB-NCAPD3-1Q	WL[**Q**/R]GVVPVV	9	*NCAPD3*	rs12292394	A*02:01
LB-NDC80-1P	HLEEQI[**P**/A]KV	9	*NDC80*	rs9051	A*02:01
LB-NUP133-1R	SEDLILC[**R**/Q]L	9	*NUP133*	rs1065674	B*40:01
LB-OAS1-1R	ETDDPR[**R**/T]YQKY	11	*OAS1*	rs1051042	A*01:01
LB-PDCD11-1F	GPDSSKT[**F**/L]LCL	11	*PDCD11*	rs2986014	B*07:02
LB-PFAS-1P	A[**P**/S]GHTRRKL	9	*PFAS*	rs9891699	B*07:02
LB-PNP-1S	TQAQIFDY[**S**/G]EI	11	*PNP*	rs1049564	B*13:02
LB-PRCP-1D	FMWDVAE[**D**/E]LKA	11	*PRCP*	rs2298668	A*02:01
LB-SON-1R	SETKQ[**R**/C]TVL	9	*SON*	rs13047599	B*40:01
LB-SRGN-1R	ESSVQGYPT[**R**/Q]R	11	*SRGN*	rs2805910	A*68:01
LB-SSR1-1S	[**S**/L]LAVAQDLT	9	*SSR1*	rs10004	A*02:01
LB-SWAP70-1Q	MEQLE[**Q**/E]LEL	9	*SWAP70*	rs415895	B*40:01
LB-TMEM8A-1I	RPRSVT[**I**/V]QPLL	11	*TMEM8A*	rs2071915	B*07:02
LB-TRIP10-1EPC	G[**E**/G][**P**/S]QDL[**C**/G]TL	9	*TRIP10*	rs1049229[D] rs1049230[D] rs1049232[D]	B*40:01
LB-TTK-1D	RLH[**D**/E]GRVFV	9	*TTK*	rs240226[D]	A*02:01
LB-USP15-1I	MPSHLRN[**I**/T]LL	10	*USP15*	rs11174420[D]	B*07:02
LB-WNK1-1I	RTLSPE[**I**/M]ITV	10	*WNK1*	rs12828016	A*02:01
LB-ZDHHC6-1Y	RPR[**Y**/H]WILLVKI	11	*ZDHHC6*	rs4918752[D]	B*07:02
LB-ZNFX1-1Q	NEIEDVW[**Q**/H]LDL	11	*ZNFX1*	rs238221	B*40:01
LRH-1	TPNQRQNVC	9	*P2RX5*	rs3215407[C]	B*07:02
P2RX7	WFHHC[**H**/R]PKY	9	*P2RX7*	rs7958311	A*29:02
PANE1	RVWDLPGVLK	10	*CENPM*	rs5758511[C]	A*03:01
SLC1A5	AE[**A**/P]TANGGLAL	11	*SLC1A5*	rs3027956	B*40:02
SP110	SLP[**R**/G]GTSTPK	10	*SP110*	rs1365776	A*03:01
TRIM22	MAVPPC[**C**/R]IGV	10	*TRIM22*	rs187416296	A*02:01
UGT2B17	CVATMIFMI	9	*UGT2B17*	Gene deletion	A*02:01
UGT2B17	AELLNIPFLY	10	*UGT2B17*	Gene deletion	A*29:02
UGT2B17	AELLNIPFLY	10	*UGT2B17*	Gene deletion	B*44:03
UTA2-1	QL[**L**/P]NSVLTL	9	*KIAA1551*	rs2166807	A*02:01
ZAPHIR	IPRDSWWVEL	10	*ZNF419*	rs2074071[C]	B*07:02

[A] Polymorphic amino acids are shown in brackets. Amino acids as present in MiHA are indicated in bold. [B] MiHA for which the allelic variant has also been identified as *in vivo* T-cell target. The epitope which was first identified and published as *in vivo* T-cell target is indicated as MiHA, whereas its counterpart is indicated as allelic variant. [C] SNP does not directly encode MiHA but creates a new protein from which MiHA is derived. [D] SNP encoding MiHA in an alternative reading frame.

Table 2. *In silico* analysis of minor histocompatibility antigens

MiHA name	Sequence[A]	HLA-allele	NetMHCpan 2.8 (nM/%-Rank)	NetMHCstab 1.0 t½ (hrs)
ACC-1Y	DYLQ[**Y**/C]VLQI	A*24:02	82.21/0.40	5.87
ACC-2D	KEFED[**D**/G]IINW	B*44:02	72.66/0.12	n.a.
ACC-2D	KEFED[**D**/G]IINW	B*44:03	35.30/0.10	n.a.
ACC-6	MEIFIEVFSHF	B*44:03	64.04/0.15	n.a.
CTSH(R)/A31	ATLPLLCA[**R**/G]	A*31:01	17.34/0.30	n.a.
CTSH(R)/A33	WATLPLLCA[**R**/G]	A*33:03	194.66/1.50	n.a.
DPH1	S[**V**/L]LPEVDVW	B*57:01	77.67/0.25	n.a.
HA-1	VL[**H**/R]DDLLEA	A*02:01	21.96/1.00	1.70
HA-2	YIGEVLVS[**V**/M]	A*02:01	5.92/0.20	7.96
HA-3T	V[**T**/M]EPGTAQY	A*01:01	30.55/0.08	4.11
HA-8R	[**R**/P]TLDKVLEV	A*02:01	80.99/2.00	2.49
HB-1H	EEKRGSL[**H**/Y]VW	B*44:03	98.36/0.25	n.a.
HEATR1-1E	ISKERA[**E**/G]AL	B*08:01	588.87/1.50	n.a.
HwA11-S	CIPPD[**S**/T]LLFPA	A*02:01	829.68/6.00	0.50
LB-ADIR-1F	SVAPALAL[**F**/S]PA	A*02:01	50.89/1.50	0.79
LB-APOBEC3B-1K	[**K**/E]PQYHAEMCF	B*07:02	215.46/1.00	2.11
LB-APOBEC3B-1K	[**K**/E]PQYHAEMCF	B*08:01	6146.92/9.00	n.a.
LB-ARHGDIB-1R	LPRACW[**R**/P]EA	B*07:02	40.16/0.40	2.12
LB-BCAT2-1R	QP[**R**/T]RALLFVIL	B*07:02	20.34/0.17	4.14
LB-C16ORF-1R	[**R**/W]PCPSVGLSFL	B*07:02	93.99/0.80	2.83
LB-C19ORF48-2E	TAWPGAP[**E**/G]V	B*51:01	n.a./0.50	n.a.
LB-CCL4-1T	CADPSE[**T**/S]WV	A*02:01	5048.30/15.00	0.35
LB-CLYBL-1Y	SLAA[**Y**/D]IPRL	A*02:01	4.28/0.12	6.41
LB-CYBA-1Y	STMERWGQK[**Y**/H]	A*01:01	243.43/0.25	0.61
LB-DHX33-1C	YLYEGGIS[**C**/R]	A*02:01	24.03/1.00	3.31
LB-DHX33-1C	YLYEGGIS[**C**/R]	C*03:03	1662.22/7.00	n.a.
LB-EBI3-1I	RPRARYY[**I**/V]QV	B*07:02	11.77/0.10	5.89
LB-ECGF-1H	RP[**H**/R]AIRRPLAL	B*07:02	2.49/0.01	6.71
LB-ERAP1-1R 9-mer	HP[**R**/P]QEQIAL	B*07:02	4.63/0.03	5.65
LB-ERAP1-1R 11-mer	HP[**R**/P]QEQIALLA	B*07:02	107.63/0.80	1.97
LB-FUCA2-1V	RLRQ[**V**/M]GSWL	B*07:02	78.61/0.80	1.48
LB-GEMIN4-1V	FPALRFVE[**V**/E]	B*07:02	32.34/0.30	2.99
LB-GEMIN4-1V	FPALRFVE[**V**/E]	B*08:01	21.52/0.08	n.a.
LB-GLE1-1V	GQ[**V**/I]RLRALY	B*15:01	61.54/0.80	7.74
LB-GSTP1-1V	DLRCKY[**V**/I]SL	B*08:01	9.92/0.03	n.a.
LB-ITGB2-1	GQAGFFPSPF	B*15:01	10.28/0.05	9.37

Table 2. ***Continued***

MiHA name	Sequence[A]	HLA-allele	NetMHCpan 2.8 (nM/%-Rank)	NetMHCstab 1.0 t½ (hrs)
LB-MOB3A-1C	[**C**/S]PRPGTWTC	B*07:02	470.83/1.50	3.59
LB-NCAPD3-1Q	WL[**Q**/R]GVVPVV	A*02:01	10.56/0.50	6.59
LB-NDC80-1P	HLEEQI[**P**/A]KV	A*02:01	70.32/2.00	3.15
LB-NUP133-1R	SEDLILC[**R**/Q]L	B*40:01	139.60/0.80	1.22
LB-OAS1-1R	ETDDPR[**R**/T]YQKY	A*01:01	133.89/0.15	2.85
LB-PDCD11-1F	GPDSSKT[**F**/L]LCL	B*07:02	585.68/1.50	1.38
LB-PFAS-1P	A[**P**/S]GHTRRKL	B*07:02	19.95/0.17	3.03
LB-PNP-1S	TQAQIFDY[**S**/G]EI	B*13:02	n.a./0.80	n.a.
LB-PRCP-1D	FMWDVAE[**D**/E]LKA	A*02:01	11.09/0.50	2.51
LB-SON-1R	SETKQ[**R**/C]TVL	B*40:01	98.73/0.80	1.37
LB-SRGN-1R	ESSVQGYPT[**R**/Q]R	A*68:01	60.54/1.50	n.a.
LB-SWAP70-1Q	MEQLE[**Q**/E]LEL	B*40:01	24.68/0.20	1.06
LB-TMEM8A-1I	RPRSVT[**I**/V]QPLL	B*07:02	6.88/0.05	6.30
LB-TRIP10-1EPC	G[**E**/G][**P**/S]QDL[**C**/G]TL	B*40:01	271.70/1.00	1.51
LB-TTK-1D	RLH[**D**/E]GRVFV	A*02:01	30.45/1.50	5.32
LB-USP15-1I	MPSHLRN[**I**/T]LL	B*07:02	11.79/0.10	2.42
LB-WNK1-1I	RTLSPE[**I**/M]ITV	A*02:01	388.11/4.00	1.34
LB-ZDHHC6-1Y	RPR[**Y**/H]WILLVKI	B*07:02	31.86/0.30	3.17
LB-ZNFX1-1Q	NEIEDVW[**Q**/H]LDL	B*40:01	51.33/0.40	0.85
LRH-1	TPNQRQNVC	B*07:02	1219.83/3.00	1.61
P2RX7	WFHHC[**H**/R]PKY	A*29:02	29.98/0.50	n.a.
PANE1	RVWDLPGVLK	A*03:01	45.68/0.25	2.91
SLC1A5	AE[**A**/P]TANGGLAL	B*40:02	40.81/0.40	n.a.
SP110	SLP[**R**/G]GTSTPK	A*03:01	405.03/1.50	1.47
UGT2B17	CVATMIFMI	A*02:01	432.65/4.00	0.96
UGT2B17	AELLNIPFLY	A*29:02	509.05/3.00	n.a.
UGT2B17	AELLNIPFLY	B*44:03	22.25/0.05	n.a.
UTA2-1	QL[**L**/P]NSVLTL	A*02:01	92.30/2.00	4.61
ZAPHIR	IPRDSWWVEL	B*07:02	10.21/0.10	4.42

[A] Polymorphic amino acids are shown in brackets. Amino acids as present in MiHA are indicated in bold.
n.a. HLA class I allele not available in the algorithm.

Table 2. ***Continued***

MiHA name	HLA-allele	NetChop 3.1	TAPPred	NetCTLpan 1.1 (%-Rank)	IEDB
ACC-1Y	A*24:02	0.91	5.01	0.20	-0.16
ACC-2D	B*44:02	0.41	8.41	0.30	0.42
ACC-2D	B*44:03	0.41	8.41	0.15	0.42
ACC-6	B*44:03	0.96	7.71	0.01	0.42
CTSH(R)/A31	A*31:01	0.27	3.84	0.30	-0.06
CTSH(R)/A33	A*33:03	0.27	4.00	2.00	-0.05
DPH1	B*57:01	0.45	5.80	0.80	0.16
HA-1	A*02:01	0.96	6.96	0.80	0.09
HA-2	A*02:01	0.97	7.95	0.10	0.08
HA-3T	A*01:01	0.98	5.80	0.05	0.02
HA-8R	A*02:01	0.97	4.17	1.00	-0.10
HB-1H	B*44:03	0.90	5.84	0.80	-0.11
HEATR1-1E	B*08:01	0.70	6.12	1.50	0.24
HwA11-S	A*02:01	0.81	7.19	5.00	-0.08
LB-ADIR-1F	A*02:01	0.91	8.35	1.00	0.15
LB-APOBEC3B-1K	B*07:02	0.26	6.97	1.50	-0.06
LB-APOBEC3B-1K	B*08:01	0.26	6.97	16.00	-0.05
LB-ARHGDIB-1R	B*07:02	0.42	-0.73	0.80	0.31
LB-BCAT2-1R	B*07:02	0.94	7.26	0.20	0.31
LB-C16ORF-1R	B*07:02	0.90	5.62	0.40	-0.20
LB-C19ORF48-2E	B*51:01	0.97	4.05	0.80	0.18
LB-CCL4-1T	A*02:01	0.29	4.89	32.00	0.09
LB-CLYBL-1Y	A*02:01	0.97	3.94	0.05	0.19
LB-CYBA-1Y	A*01:01	0.79	4.08	0.15	0.17
LB-DHX33-1C	A*02:01	0.04	8.31	1.50	0.18
LB-DHX33-1C	C*03:03	0.04	8.31	50.00	0.18
LB-EBI3-1I	B*07:02	0.96	8.40	0.15	0.14
LB-ECGF-1H	B*07:02	0.92	5.86	0.01	0.28
LB-ERAP1-1R 9-mer	B*07:02	0.96	0.76	0.05	0.02
LB-ERAP1-1R 11-mer	B*07:02	0.12	4.45	1.50	0.04
LB-FUCA2-1V	B*07:02	0.90	4.07	0.40	-0.04
LB-GEMIN4-1V	B*07:02	0.98	1.42	0.30	0.19
LB-GEMIN4-1V	B*08:01	0.98	1.42	0.05	0.26
LB-GLE1-1V	B*15:01	0.88	3.84	1.00	0.13
LB-GSTP1-1V	B*08:01	0.77	5.41	0.05	-0.12
LB-ITGB2-1	B*15:01	0.54	8.62	0.80	0.12

Table 2. ***Continued***

MiHA name	HLA-allele	NetChop 3.1	TAPPred	NetCTLpan 1.1 (%-Rank)	IEDB
LB-MOB3A-1C	B*07:02	0.70	8.46	1.50	0.28
LB-NCAPD3-1Q	A*02:01	0.91	-1.08	0.20	0.09
LB-NDC80-1P	A*02:01	0.97	7.62	1.50	0.01
LB-NUP133-1R	B*40:01	0.91	3.84	0.40	0.10
LB-OAS1-1R	A*01:01	0.85	6.84	0.10	-0.11
LB-PDCD11-1F	B*07:02	0.97	5.70	1.50	-0.42
LB-PFAS-1P	B*07:02	0.94	6.12	0.30	0.05
LB-PNP-1S	B*13:02	0.57	6.47	0.80	0.08
LB-PRCP-1D	A*02:01	0.06	7.80	1.50	0.16
LB-SON-1R	B*40:01	0.92	3.85	0.80	-0.21
LB-SRGN-1R	A*68:01	0.79	4.10	0.40	-0.04
LB-SWAP70-1Q	B*40:01	0.95	7.40	0.15	-0.01
LB-TMEM8A-1I	B*07:02	0.97	7.18	0.05	-0.07
LB-TRIP10-1EPC	B*40:01	0.96	7.14	0.80	-0.13
LB-TTK-1D	A*02:01	0.89	4.01	0.80	0.22
LB-USP15-1I	B*07:02	0.66	5.05	0.20	0.12
LB-WNK1-1I	A*02:01	0.97	6.76	1.50	0.18
LB-ZDHHC6-1Y	B*07:02	0.97	4.03	0.30	0.25
LB-ZNFX1-1Q	B*40:01	0.94	4.37	0.30	0.32
LRH-1	B*07:02	0.13	-0.88	16.00	-0.16
P2RX7	A*29:02	0.96	4.61	0.40	-0.11
PANE1	A*03:01	0.56	6.78	0.40	0.13
SLC1A5	B*40:02	0.96	4.02	0.10	0.16
SP110	A*03:01	0.98	6.09	0.80	-0.01
UGT2B17	A*02:01	0.10	3.89	5.00	0.00
UGT2B17	A*29:02	0.97	3.90	1.50	0.19
UGT2B17	B*44:03	0.97	3.90	0.05	0.19
UTA2-1	A*02:01	0.98	3.99	1.50	-0.12
ZAPHIR	B*07:02	0.97	3.84	0.05	0.40

HLA class I binding affinity

Binding of antigens to HLA class I is a strict requirement for provoking CD8 T-cell responses. Therefore, we predicted HLA class I binding affinity by NetMHCpan 2.8 and compared the characteristics of MiHA with a reference set of peptides (Figure 1A). When using standard thresholds to designate strong binding peptides (SB; ≤0.5%-Rank or IC_{50}≤50 nM) and weak binding peptides (WB; ≤2%-Rank or IC_{50}≤500 nM), 38 (56%) antigens of the total set of 68 MiHA were predicted as SB peptides,

21 (31%) antigens as WB peptides and 9 (13%) antigens as NB peptides. For 3 MiHA that have been identified as NB peptides (LB-NADK-1K, LB-SSR1-1S and TRIM22), it is unclear whether the peptide as reported in Table 1 is the actual minimal epitope. For LB-NADK-1K and TRIM22, other 9-11-mer peptide variants can be found with weak predicted binding to HLA-A*03:01 and HLA-A*02:01, respectively, but T-cell recognition of these peptides has not been tested (LB-NADK-1K; own observations) or reported (TRIM22; (26)). For LB-SSR1-1S, no other 9-11-mer peptide variant with predicted HLA binding can be found, but T-cell recognition of the peptide as reported in Table 1 requires concentrations >5.000 nM, suggesting that the peptide may not be the actual minimal epitope (27). These 3 MiHA were excluded from our dataset, resulting in a total number of 65 HLA class I-restricted MiHA containing 15 antigens that bind to HLA-A*02:01 and 18 antigens that bind to HLA-B*07:02 that were used for further analyses to determine the value of online prediction algorithms. Analysis of the 6 remaining NB peptides revealed that 5 (83%) antigens contain a cysteine residue either as anchor (*n* = 2) or as residue adjacent to the anchor (*n* = 3). In contrast, only 13 (22%) of the 59 MiHA that are predicted as SB or WB peptides contain a cysteine residue and of these 13 antigens, only 6 peptides contained the cysteine residue as anchor (*n* = 1) or as residue adjacent to the anchor (*n* = 5). The data suggest that NetMHCpan 2.8 is less accurate in predicting binding affinity for peptides with cysteine residues at anchor or adjacent positions.

For accurate analysis of the value of online prediction algorithms for MiHA characterization, we compared prediction data for HLA-A*02:01- and HLA-B*07:02-restricted MiHA with a reference set of peptides. Of the 15 HLA-A*02:01-restricted MiHA, 13 antigens were predicted to bind to HLA-A*02:01 of which 7 (54%) antigens were SB peptides and 6 (46%) antigens were WB peptides. The remaining 2 antigens were NB peptides. Of the 18 HLA-B*07:02-restricted MiHA, 17 antigens were predicted to bind to HLA-B*07:02 of which 11 (65%) antigens were SB peptides and 6 (35%) antigens were WB peptides. Only one HLA-B*07:02-restricted MiHA was a NB peptide. The reference set consisted of 1370 peptides (9-11-mer peptides) with predicted binding to HLA-A*02:01 (*n* = 906) or HLA-B*07:02 (*n* = 464) as determined by NetMHCpan 2.8 using default thresholds. All peptides were derived from 21 proteins for which HLA-A*02:01-restricted MiHA (*n* = 12) or HLA-B*07:02-restricted MiHA (*n* = 9) have been identified in the normal open reading frame. Analysis revealed that 26% of the reference peptides were SB peptides and 74% were WB peptides. The percentages SB and WB peptides in the reference set were comparable for HLA-A*02:01 and HLA-B*07:02 (28% SB and 72% WB peptides for HLA-A*02:01; 24% SB and 76% WB peptides for HLA-B*07:02). As expected, the proportion of SB peptides in the group of MiHA is higher than in the reference set of peptides and this difference is more pronounced for HLA-B*07:02 (65% *versus* 24%;

p = 0.0005) than for HLA-A*02:01 (54% *versus* 28%; p = 0.0581). In addition, NetMHCpan 2.8 failed to predict HLA class I binding for 2 (13%) HLA-A*02:01-restricted MiHA (HwA11-S CIPPDSLLFPA; LB-CCL4-1T CADPSETWV) and one (6%) HLA-B*07:02-restricted MiHA (LRH-1 TPNQRQNVC).

To evaluate the performance of NetMHCpan 2.8, ROC curves were plotted separately for HLA-A*02:01 and HLA-B*07:02 (Figure 1B). For both HLA restriction alleles, comparison of the overall performance of %-Rank and IC_{50} revealed similar AUC values. Furthermore, sensitivity and specificity values for default thresholds for SB and WB peptides demonstrated that MiHA are characterized with low sensitivity but high specificity by selecting SB peptides, whereas selection of WB peptides leads to characterization of MiHA with high sensitivity but low specificity.

Stability of the peptide-HLA class I complex

Since NetMHCpan 2.8 failed to predict 6 MiHA (including 2 HLA-A*02:01-restricted MiHA and one HLA-B*07:02-restricted MiHA) using default settings, we explored whether MiHA are more accurately predicted as stable peptide-HLA class I complexes by NetMHCstab 1.0 (Figure 2A). In NetMHCstab 1.0, HLA class I restriction alleles were available for 46 MiHA as shown in Table 2 and we therefore restricted the analysis to HLA-A*02:01- and HLA-B*07:02-restricted MiHA. Of the 15 HLA-A*02:01-restricted MiHA, 3 (20%) antigens were predicted as highly stable complexes (HS; half-life>6 hrs), 6 (40%) antigens as weakly stable complexes (WS; >2 hrs and ≤6 hrs) and 6 (40%) antigens as non-stable complexes (NS;≤2 hrs). Of the 18 HLA-B*07:02-restricted MiHA, 2 (11%), 12 (67%) and 4 (22%) antigens were predicted as HS, WS and NS complexes, respectively. In conclusion, MiHA are predicted as HLA class I binding peptides by NetMHCpan 2.8 with higher sensitivity than as stable peptide-HLA complexes by NetMHCstab 1.0.

In NetMHCstab 1.0, stability predictions are based for 85% on HLA class I binding affinity as predicted by the online algorithm NetMHCcons 1.0. ROC curves were plotted for NetMHCstab 1.0 and NetMHCcons 1.0 separately for HLA-A*02:01 and HLA-B*07:02 (Supplemental Figure S1). Comparison of AUC showed that NetMHCstab 1.0 is slightly superior to NetMHCcons 1.0 for HLA-B*07:02, but not for HLA-A*02:01. Moreover, ROC analysis confirmed the low sensitivity of NetMHCstab 1.0 to characterize MiHA, but demonstrated that the specificity of the algorithm is high.

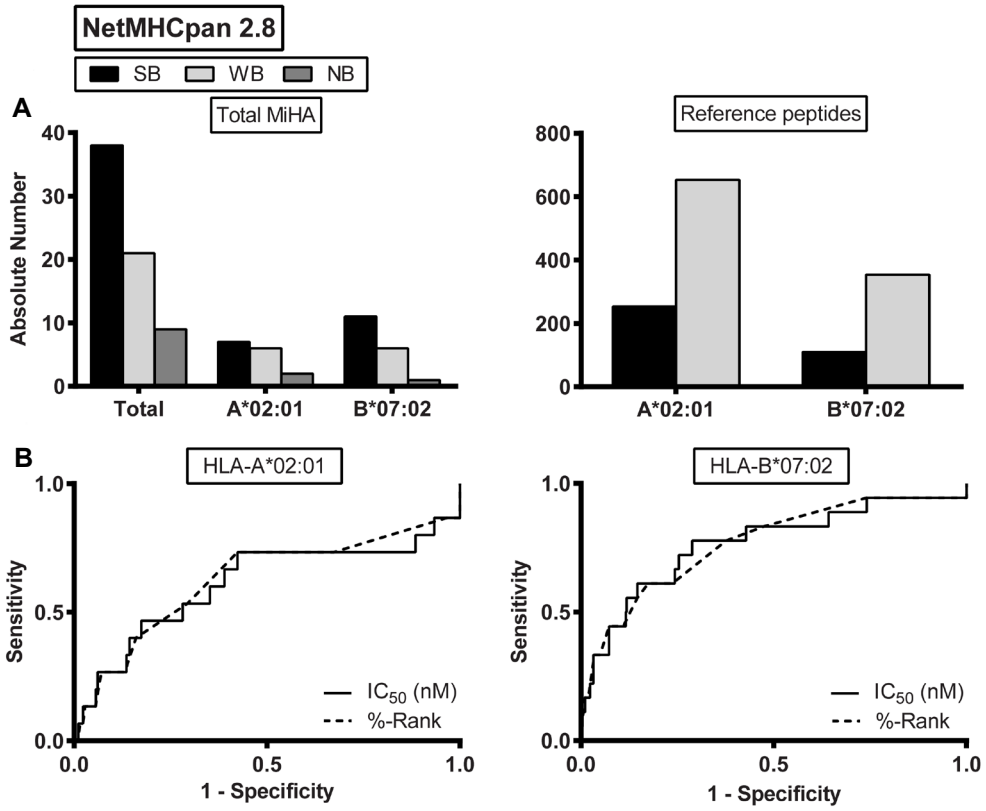

	Sensitivity	Specificity
SB IC50	47%	72%
SB %-Rank	27%	93%
WB IC50	87%	0%
WB %-Rank	73%	58%

	Sensitivity	Specificity
SB IC50	61%	83%
SB %-Rank	61%	76%
WB IC50	89%	33%
WB %-Rank	94%	0%

Figure 1. Predicted HLA class I binding affinity. (**A**) HLA class I binding affinity as predicted by NetMHCpan 2.8 for MiHA that have been identified as natural T-cell ligands by forward strategies. Results are shown for the total group of MiHA (*n* = 68) and for HLA-A*02:01-restricted MiHA (*n* = 15) and HLA-B*07:02-restricted MiHA (*n* = 18) (left) as compared to reference peptides with predicted binding affinity to HLA-A*02:01 (*n* = 906) or HLA-B*07:02 (*n* = 464) (right). Indicated are absolute numbers of peptides with strong predicted binding (SB; black bars), weak predicted binding (WB; light grey bars) and non-binding (NB; dark grey bars).The data show that the proportion of SB peptides in the group of MiHA is higher than in the reference set of peptides (54% *versus* 28% with p = 0.0581 for HLA-A*02:01; 65% *versus* 24% with p = 0.0005 for HLA-B*07:02 using Fisher's exact test). (**B**) ROC curves for HLA class I binding affinity as predicted by NetMHCpan 2.8 for HLA-A*02:01 (left) and HLA-B*07:02 (right). Sensitivity and 1-specificity are shown on the Y- and X-axis, respectively. Curves for IC_{50} (solid line) and %-Rank (dashed line) are plotted based on prediction data for MiHA and reference peptides. Sensitivity and specificity are indicated for default values for SB (≤0.5%-Rank or IC_{50}≤50 nM) and WB (≤2%-Rank or IC_{50}≤500 nM). For HLA-A*02:01, AUC values for %-Rank and IC_{50} are 0.625 and 0.609, respectively (p = 0.0964 for %-Rank; p = 0.1486 for IC_{50}). For HLA-B*07:02, AUC values for %-Rank and IC_{50} are 0.767 and 0.765, respectively (p = 0.0001 for %-Rank; p = 0.0001 for IC_{50}).

Proteasomal cleavage

Surface presentation of an antigen by HLA class I requires intracellular processing of the protein by the proteasome. It has been demonstrated that the exact C-terminus of an antigenic peptide is generated by the proteasome, whereas the N-terminus is trimmed by amino peptidases (28). We investigated the presence of a proteasomal cleavage site at the exact C-terminus of the MiHA by NetChop 3.1 (Figure 2B). Whole protein sequences were fed into the algorithm and MiHA that are presented by two different HLA class I restriction alleles (ACC-2D, LB-APOBEC3B-1K, LB-DHX33-1C, LB-GEMIN4-1V and UGT2B17) were analyzed only once, resulting in a total number of 60 different MiHA that were examined. Of the 60 MiHA, 48 (80%) antigens were predicted to be cleaved immediately after the C-terminal amino acid. Since proteasomal cleavage is not influenced by HLA class I binding affinity, we compared predicted proteasomal cleavage between MiHA and reference peptides using the same sets as described above. Of the 30 MiHA with predicted binding to HLA-A*02:01 or HLA-B*07:02, 24 (80%) antigens were predicted to be cleaved after the C-terminus as compared to 70% of the reference peptides, indicating that predicted proteasomal cleavage by NetChop 3.1 is similar between MiHA and reference peptides (sensitivity 80% and specificity 30% by ROC analysis).

TAP transporter affinity

Transport of peptides from the cytosol into the endoplasmic reticulum occurs via the TAP transporter and can be predicted by TAPPred (Figure 2C). Of the 60 different MiHA, 24 (40%) antigens were predicted as peptides with high binding affinity for TAP (>6), 31 (52%) antigens as peptides with intermediate binding affinity (>3) and 5 (8%) antigens as peptides with low binding affinity (≤3). Similar as for proteasomal cleavage, TAP affinity is not influenced by HLA class I binding affinity and we therefore compared the same set of MiHA and reference peptides. Analysis of the 30 MiHA with predicted binding to HLA-A*02:01 or HLA-B*07:02 revealed that 13 (43%) epitopes had high binding affinity, 13 (43%) epitopes had intermediate binding affinity and 4 (13%) epitopes had low binding affinity for TAP. Similar percentages were predicted for peptides in the reference set (54% high, 39% intermediate and 7% low binding affinity), indicating that also TAP transport as predicted by TAPPred is similar between MiHA and reference peptides (sensitivity 40% and specificity 46% for high affinity threshold; sensitivity 92% and specificity 7% for intermediate affinity threshold by ROC analysis).

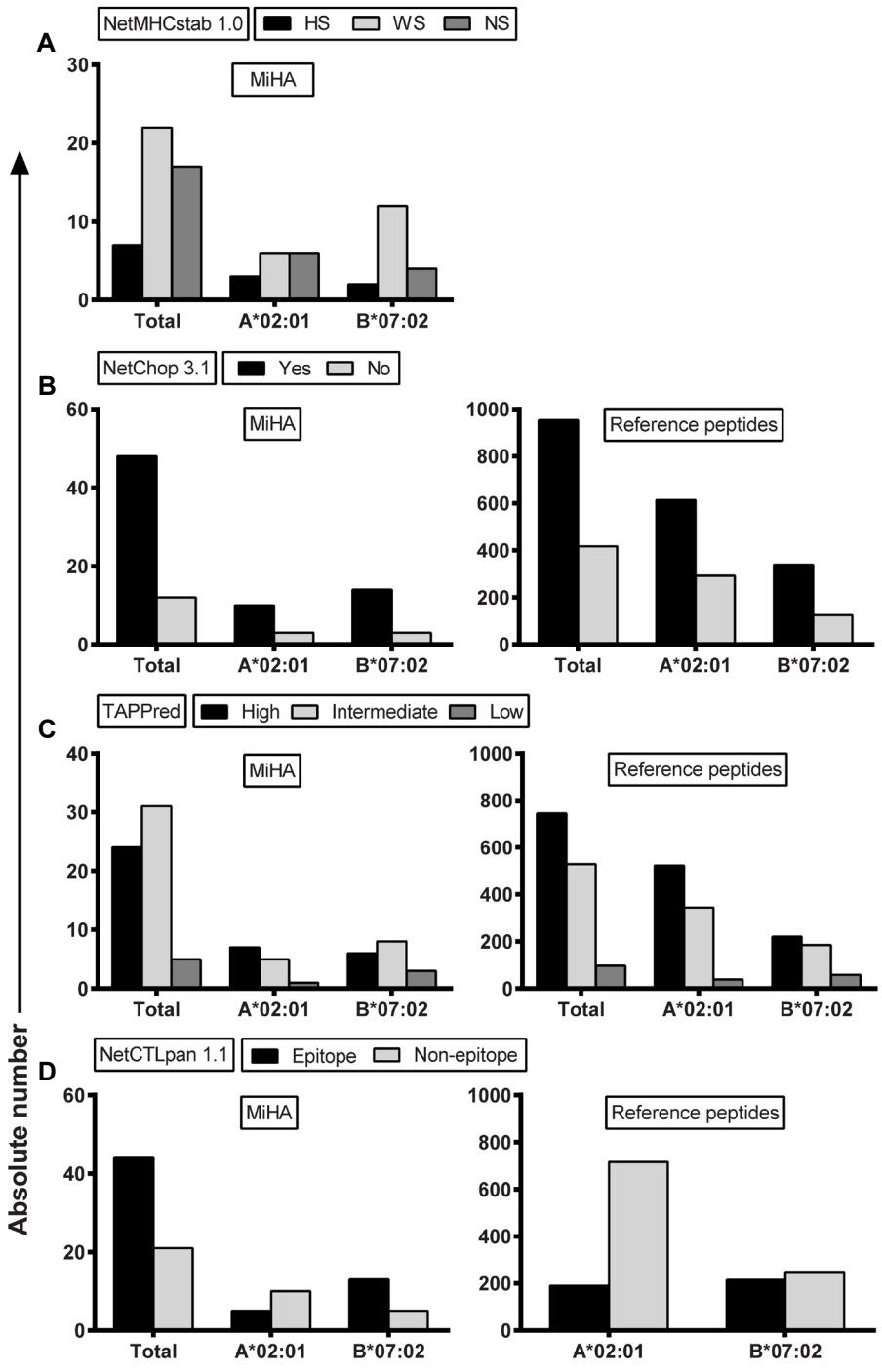
A
NetMHCstab 1.0
HS
WS
NS
MiHA
30
20
10
0
Total
A*02:01
B*07:02
B
NetChop 3.1
Yes
No
MiHA
60
40
20
0
Total
A*02:01
B*07:02
Reference peptides
1000
800
600
400
200
0
Total
A*02:01
B*07:02
C
TAPPred
High
Intermediate
Low
MiHA
40
30
20
10
0
Total
A*02:01
B*07:02
Reference peptides
1000
800
600
400
200
0
Total
A*02:01
B*07:02
D
NetCTLpan 1.1
Epitope
Non-epitope
MiHA
60
40
20
0
Total
A*02:01
B*07:02
Reference peptides
1000
800
600
400
200
0
A*02:01
B*07:02
Absolute number

Figure 2. Predicted stability of the peptide-HLA class I complex, proteasomal cleavage, TAP transport and their integration. (**A**) Peptide-HLA class I complex stability as predicted by NetMHCstab 1.0 with default settings for all MiHA for which HLA class I restriction alleles are available in the algorithm (*n* = 46), HLA-A*02:01-restricted MiHA (*n* = 15) and HLA-B*07:02-restricted MiHA (*n* = 18). Indicated are absolute numbers of MiHA that are predicted as highly stable (HS; black bars), weakly stable (WS; light grey bars) or non-stable (NS; dark grey bars) complexes. The data show that NetMHCstab 1.0 accurately predicted 29 of the 46 MiHA, including 9 HLA-A*02:01-restricted MiHA and 14 HLA-B*07:02-restricted MiHA. (**B**) Proteasomal cleavage at the C-terminus as predicted by NetChop 3.1 for all different MiHA peptides (*n* = 60) and for MiHA that are predicted to bind to HLA-A*02:01 (*n* = 13) or HLA-B*07:02 (*n* = 17) by NetMHCpan 2.8. Whole protein sequences were fed into the algorithm and default settings were used to predict proteasomal cleavage. Indicated are absolute numbers of peptides with predicted cleavage at the C-terminus for MiHA (left) and the reference set of peptides (right). No significant difference was observed in proportion of peptides with predicted cleavage at the C-terminus between MiHA and reference peptides (80% for MiHA *versus* 70% for reference peptides, p = 0.3141 using Fisher's exact test). (**C**) Affinity for the TAP transporter as predicted by TAPPred with default settings for all different MiHA peptides (*n* = 60) and for MiHA that are predicted to bind to HLA-A*02:01 (*n* = 13) or HLA-B*07:02 (*n* = 17) by NetMHCpan 2.8. Indicated are absolute numbers of peptides with high (black bars), intermediate (light grey bars) and low (dark grey bars) affinity for TAP for the MiHA (left) and the reference peptides (right). No significant difference was observed in proportion of peptides with high or weak affinity for TAP between MiHA (43% high, 43% intermediate and 13% low affinity) and the reference peptides (54% high, 39% intermediate and 7% low affinity). (**D**) Epitope prediction by NetCTLpan 1.1 with default settings for the total set of MiHA (*n* = 65) and for HLA-A*02:01-restricted MiHA (*n* = 15) and HLA-B*07:02-restricted MiHA (*n* = 18) (left) as compared to reference peptides (right). Indicated are absolute numbers of peptides that are predicted as epitopes (black bars) or non-epitopes (grey bars). For HLA-A*02:01, the proportion of peptides that are predicted as T-cell epitopes is similar between MiHA and reference peptides (33% *versus* 21%, p = 0.3338), whereas for HLA-B*07:02, the proportion of peptides that are predicted as T-cell epitopes is higher for MiHA than for reference peptides although it did not reach statistical significance (72% *versus* 46%, p = 0.0514). *Figure on opposite page.*

Integration of HLA class I binding affinity, C-terminal proteasomal cleavage and TAP transport

Predictions for HLA class I binding affinity, C-terminal proteasomal cleavage and TAP transporter efficiency are integrated in the combined algorithm NetCTLpan 1.1. In the algorithm, the weight on HLA class I binding affinity, C-terminal proteasomal cleavage and TAP transport efficiency is 0.750, 0.225 and 0.025 by default, respectively. Using the default threshold for epitope identification (<1%-Rank), 44 (68%) of the 65 MiHA were predicted as epitopes, including 5 (33%) of the 15 HLA-A*02:01-restricted MiHA and 13 (72%) of the 18 HLA-B*07:02-restricted MiHA (Figure 2D). Notably, NetCTLpan 1.1 also failed to identify the 6 MiHA that were predicted as NB peptides by NetMHCpan 2.8. In the reference set of peptides, 21% of peptides with predicted binding to HLA-A*02:01 and 46% of peptides with predicted binding to HLA-B*07:02 were predicted as potential epitopes. These data demonstrate that HLA-B*07:02-restricted MiHA are more accurately predicted by NetCTLpan 1.1 (72% *versus* 46%, p = 0.0514) than HLA-A*02:01-restricted MiHA (33% *versus* 21%, p = 0.3338). ROC curves were plotted to determine the

contribution of each algorithm to the overall predictive performance of the integrated algorithm of NetCTLpan 1.1 (Supplemental Figure S2A) and to compare NetCTLpan 1.1 and NetMHCpan 2.8 (Supplemental Figure S2B). The data demonstrated that MiHA cannot be more accurately characterized by an approach in which predicted C-terminal proteasomal cleavage and TAP transport are integrated with HLA class I binding affinity as compared to prediction tools for HLA class I binding affinity alone.

***In vivo* immunogenicity**

The final step in the HLA class I pathway is antigen recognition by CD8 T-cells. The Immune Epitope Database and Analysis Resource (IEDB) has designed an online tool to predict *in vivo* immunogenicity of peptide antigens. Immunogenicity scores for the 65 MiHA in Table 2 were homogenously distributed with a range from -0.42 to 0.42 and a median score of 0.09. Individual values and median immunogenicity scores for the total set of MiHA as well as for MiHA with predicted binding to HLA-A*02:01 and HLA-B*07:02 and their reference peptides are shown in Figure 3A. Based on ROC curves as shown in Figure 3B, we determined thresholds with 90% specificity to predict *in vivo* immunogenicity of peptides binding to HLA-A*02:01 (>0.27) and HLA-B*07:02 (>0.22). Using the threshold of >0.27, none of the 13 HLA-A*02:01-restricted MiHA were predicted to be immunogenic as compared to 10% of the reference peptides. For HLA-B*07:02, however, 7 (41%) of the 17 antigens were predicted to be immunogenic using the threshold of >0.22 as compared to 10% of reference peptides. These data demonstrate that the MHC I immunogenicity tool of IEDB can be used to predict *in vivo* immunogenicity for peptides binding to HLA-B*07:02. However, it should be noted that classifying peptides into immunogenic and non-immunogenic peptides using a score >0.22 leads to a considerable number of HLA-B*07:02-restricted MiHA (59%) that are designated as non-immunogenic peptides, indicating that this threshold has a low sensitivity to characterize MiHA.

***In silico* characteristics of MiHA and their allelic variants**

MiHA arise as a result of SNP differences between patient and donor, which often lead to a change in a single non-synonymous amino acid between the MiHA as expressed on the patient cell and its allelic variant in the donor cell. Of the 65 HLA class I-restricted MiHA in Table 2, allelic variants do not exist for 8 MiHA (ACC-6, LB-ITGB2-1, LRH-1, PANE1, 3 MiHA encoded by *UGT2B17* and ZAPHIR). For the remaining 57 MiHA, allelic variants do exist. The majority of these allelic variants have not been identified as *in vivo* T-cell targets. This can be explained by insufficient searching for specific T-cells, but may also indicate that allelic variants cannot be processed or presented on the cell surface or that no specific TCRs are present in the naive repertoire of donor lymphocytes. Therefore, we explored whether MiHA differ from their allelic variants in *in silico* characteristics as determined by online prediction algorithms.

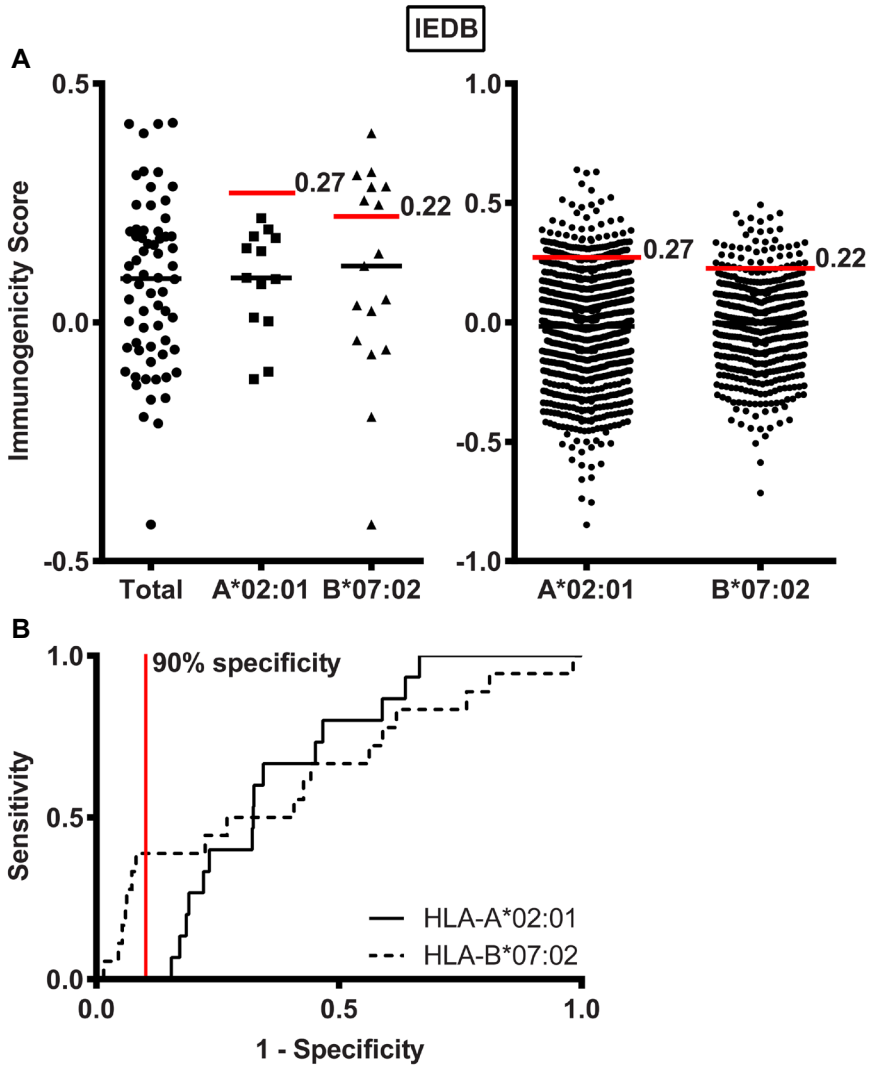

Figure 3. Predicted *in vivo* immunogenicity. (**A**) *In vivo* immunogenicity as predicted by the MHC I immunogenicity tool of the IEDB for the total group of MiHA (*n* = 65) and for MiHA with predicted binding to HLA-A*02:01 (*n* = 13) or HLA-B*07:02 (*n* = 17) by NetMHCpan 2.8. Indicated are immunogenicity scores for MiHA (left) and reference peptides (right). Designated are median immunogenicity scores (black horizontal lines) and thresholds of 0.27 and 0.22 to define immunogenic peptides for MiHA binding to HLA-A*02:01 or HLA-B*07:02, respectively (red lines). The data show a significant difference in proportion of immunogenic peptides between HLA-B*07:02-restricted MiHA and reference peptides (41% *versus* 10% with p = 0.0014 using Fisher's exact test), but no significant difference between HLA-A*02:01-restricted MiHA and reference peptides (0% *versus* 10% with p = 0.3825 using Fisher's exact test). (**B**) ROC curves for *in vivo* immunogenicity as predicted by the online tool of the IEDB for HLA-A*02:01 (solid line) and HLA-B*07:02 (dashed line) based on prediction data for MiHA and reference peptides. Thresholds with 90% specificity are indicated by the red vertical line.

First, we examined and compared HLA class I binding affinity as predicted by NetMHCpan 2.8 between MiHA and their allelic variants (Figure 4). Of the 57 pairs of MiHA and allelic variants, two MiHA (ACC-1Y and HB-1H) have allelic variants that can be targeted by T-cells *in vivo*, indicating that these peptides are immunogenic in two directions. For these bi-allelic MiHA, the epitope that was first identified and published as *in vivo* T-cell target is indicated as MiHA and the counterpart is indicated as allelic variant. We divided the MiHA and their allelic variants into two groups based on whether the polymorphic amino acids are present at anchor positions or TCR contact positions. Anchor residue motifs that are used for HLA class I binding are shown in Table 3. HLA class I binding affinity was examined for 57 pairs of MiHA and allelic variants. Of these 57 pairs, 12 pairs contained polymorphic residues at anchor positions. As expected, for all pairs with polymorphic amino acids at anchor positions, predicted HLA class I binding affinity for MiHA was significantly higher than for their allelic variants ($p = 0.0005$). Of the 45 pairs with polymorphic amino acids at TCR contact residues, 9 MiHA had predicted HLA class I binding affinities that were significantly higher than their allelic variants ($p = 0.0039$). In all these peptides, the polymorphic amino acid was located immediately adjacent to the N-terminal anchor residue at position 2. For the remaining 36 pairs, predicted HLA class I binding affinity was similar between MiHA and allelic variants ($p = 0.1965$).

We also compared MiHA and their allelic variants in predicted stability of the peptide-HLA class I complex by NetMHCstab 1.0 (Supplemental Figure S3A). HLA class I restriction alleles were available for 41 pairs of MiHA and allelic variants. For 7 pairs with polymorphic amino acids at anchor residues, predicted stability of the peptide-HLA class I complex was significantly higher for MiHA than for their allelic variants ($p = 0.0156$), while predicted stability was similar for the majority of 34 pairs with polymorphic amino acids at TCR contact residues ($p = 0.0781$).

Finally, 57 pairs of MiHA and allelic variants were compared for predicted proteasomal cleavage, TAP affinity and *in vivo* immunogenicity (Supplemental Figure S3B-D). No difference was observed in predicted proteasomal cleavage by NetChop 3.1 (81% for MiHA *versus* 81% for allelic variants, $p = 1.000$) and TAP affinity by TAPPred (40% high, 53% intermediate and 8% low affinity peptides for MiHA *versus* 47% high, 43% intermediate and 9% low affinity peptides for allelic variants). Moreover, immunogenicity scores as determined by the online tool of the IEDB were similar between MiHA (range between -0.42 and 0.42 with a median score of 0.09) and allelic variants (range between -0.54 and 0.46 with a median score of 0.05) ($p = 0.2871$). When a threshold of >0.25 was applied to define immunogenic peptides, 8 (14%) MiHA and 10 (18%) allelic variants were predicted to be immunogenic, including 5 pairs of MiHA and allelic variants for HLA-B*07:02.

In conclusion, the data show that predicted HLA class I binding affinity for 12 MiHA with polymorphic amino acids at anchor positions is significantly higher than for their allelic variants as well as for 9 MiHA with polymorphic amino acids at TCR contact residues in which the variant residue is located immediately adjacent to the anchor residue at position 2. The majority of MiHA (*n* = 36), however, do not differ from their allelic variants in *in silico* characteristics, indicating that these allelic variants can potentially be presented on the cell surface.

Table 3. Binding motifs for HLA class I alleles[A]

HLA-allele	Peptide length	Anchor residues
A*01:01	9-11	P_2, P_3, P_{end}
A*02:01	9-11	P_2, P_{end}
A*03:01	9-11	P_2, P_3, P_{end}
A*24:02	9-11	P_2, P_{end}
A*29:02	9-11	P_{end}
A*31:01	9-11	P_{end}
A*33:03	9-11	P_{end}
A*68:01	9-11	P_2, P_{end}
C*03:03	9-11	P_1, P_2, P_{end}
B*07:02	9-11	P_2, P_{end}
B*08:01	9-11	P_3, P_5, P_{end}
B*13:02	9-11	P_2, P_3, P_{end}
B*15:01	9-11	P_2, P_{end}
B*40:01	9-11	P_2, P_{end}
B*40:02	9-11	P_2, P_{end}
B*44:02	9-11	P_2, P_{end}
B*44:03	9-11	P_2, P_{end}
B*51:01	9-11	P_2, P_{end}
B*57:01	9-11	P_2, P_{end}

[A] Binding motifs as available at http://www.cbs.dtu.dk/biotools/MHCMotifViewer/Human_alleles.html (24).

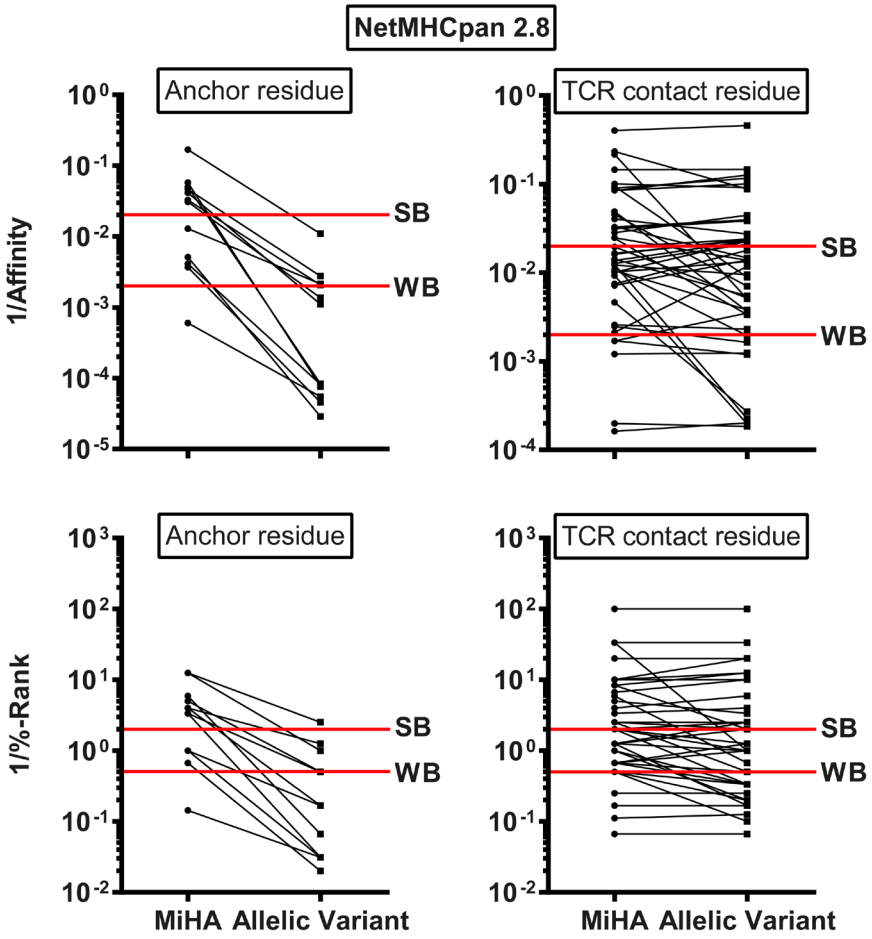

Figure 4. Predicted HLA class I binding affinity for MiHA and allelic variants. HLA class I binding affinity as predicted for MiHA and their allelic variants by NetMHCpan 2.8. Predicted affinity (1/affinity (nM); upper) and %-Rank (1/%-Rank; lower) are shown for all MiHA with allelic variants (*n* = 57) divided into two groups based on whether the polymorphic amino acid is an anchor residue (*n* = 12; left) or TCR contact residue (*n* = 45; right). Default thresholds for SB and WB peptides are indicated by red lines. The data show that predicted HLA class I binding for the 12 MiHA with polymorphic amino acids at anchor positions was significantly higher than for their allelic variants (p = 0.0005 using Wilcoxon signed rank test). For the MiHA with polymorphic amino acids at TCR contact residues (*n* = 45), predicted HLA class I binding as compared to their allelic variants was higher for 9 MiHA with the variant residue immediately adjacent to the anchor at position 2 (p = 0.0039 using Wilcoxon signed rank test), but similar for the remaining 36 antigens (p = 0.1965 using Wilcoxon signed rank test).

Discussion

MiHA can be identified by forward and reverse strategies. In forward strategies, T-cells from *in vivo* immune responses after alloSCT are used to identify the antigen, whereas peptides are used to search for specific T-cells in reverse strategies (4-6). Particularly in reverse strategies, selection of candidate peptides by prediction algorithms for HLA class I binding affinity, stability of the peptide-HLA complex, proteasomal cleavage, TAP transport and *in vivo* immunogenicity may be relevant to increase the efficiency of MiHA discovery. To explore the value of online prediction algorithms, we determined the *in silico* characteristics of 68 autosomal HLA class I-restricted MiHA which have all been identified as natural T-cell ligands by forward strategies. As such, these MiHA should follow all rules for endogenous processing and presentation and antigen recognition by specific T-cells.

Of the 68 HLA class I-restricted MiHA that were analyzed, NetMHCpan 2.8 accurately predicted 38 (56%) antigens as SB peptides and 21 (31%) antigens as WB peptides. We also compared HLA class I binding affinity between MiHA and reference peptides and showed that the proportion of SB peptides is higher in the group of MiHA (54% for HLA-A*02:01 and 65% for HLA-B*07:02) than in the reference set (28% for HLA-A*02:01 and 24% for HLA-B*07:02). Using a more robust and quantitative approach, sensitivity and specificity were determined by ROC analysis for the default thresholds of NetMHCpan 2.8 based on prediction data for MiHA and reference peptides for HLA-A*02:01 and HLA-B*07:02. Our data showed that the threshold for SB has a high specificity but low sensitivity, whereas the threshold for WB has a high sensitivity but low specificity. This implies that in reverse strategies, selection of SB peptides has a high chance that the peptide is a true MiHA, but many MiHA will be missed, whereas selection of WB peptides has a low chance that true MiHA are missed, but the strategy is rather inefficient and many peptides need to be synthesized and screened.

Of the 9 antigens that were predicted as NB peptides, 3 antigens were excluded from further analyses, since experimental data confirming that the peptide sequences as reported in Table 1 are the actual minimal epitope are lacking. Of the remaining 6 NB antigens, we noticed that 5 (83%) antigens contained a cysteine residue as anchor (n = 2) or as residue adjacent to the anchor (n = 3). In contrast, 13 (23%) of the 59 antigens that were predicted as SB or WB peptides contained a cysteine residue and of these 13 antigens, only 6 antigens contained the cysteine as anchor (n = 1) or as residue adjacent to the anchor (n = 5). Since peptides with cysteine residues are highly underrepresented in databases used to train prediction

algorithms for HLA class I binding, our data suggest that the accuracy of NetMHCpan 2.8 to predict HLA class I binding of cysteine containing peptides may be low.

NetMHCstab 1.0 is an algorithm that predicts stability of the peptide-HLA complex. We demonstrated that this algorithm failed to predict 10 (30%) of the 33 HLA-A*02:01- and HLA -B*07:02-restricted MiHA as stable peptide-HLA complexes. As such, MiHA are predicted as stable peptide-HLA complexes by NetMHCstab 1.0 with lower sensitivity than as HLA-binding peptides by NetMHCpan 2.8, which failed to predict 3 (9%) of these 33 MiHA. Specificity of NetMHCstab 1.0 as determined by ROC analysis, however, is high, illustrating that the chance that a peptide selected based on high predicted stability as determined by NetMHCstab 1.0 is a true MiHA is high. Unfortunately, only 13 HLA class I alleles are currently available in NetMHCstab 1.0 as compared to more than 2900 HLA class I alleles in NetMHCpan 2.8.

By comparing MiHA with reference peptides, we demonstrated that predicted proteasomal cleavage by NetChop 3.1 and predicted affinity for TAP by TAPPred was similar in both groups, suggesting that MiHA characterization cannot be improved by applying these algorithms. In NetCTLpan 1.1, predictions for HLA class I binding affinity, C-terminal proteasomal cleavage and TAP transporter efficiency are integrated in a combined algorithm with weights of 0.750, 0.225 and 0.025 by default, respectively. NetCTLpan 1.1 failed to identify the same 6 MiHA that were predicted as NB peptides by NetMHCpan 2.8, indicating that predicted C-terminal proteasomal cleavage and TAP transport affinity in the combined algorithm cannot compensate for weak HLA class I binding affinity. We also analyzed the predictive performance of NetCTLpan 1.1 by ROC analysis and demonstrated that the curve for the combined algorithm was similar as the curve for HLA class I binding affinity, illustrating that MiHA cannot be more accurately characterized by an approach in which predicted C-terminal proteasomal cleavage and TAP transport are integrated with HLA class I binding affinity as compared to prediction tools for HLA class I binding affinity alone.

The Immune Epitope Database and Analysis Resource (IEDB) has designed an online tool to predict *in vivo* immunogenicity of peptide antigens. We defined the thresholds for immunogenic peptides for MiHA binding to HLA-A*02:01 and HLA-B*07:02 by ROC analysis and demonstrated that the MHC I immunogenicity tool of IEDB can be used to predict *in vivo* immunogenicity of peptides binding to HLA-B*07:02. As such, selection of peptides with an immunogenicity score >0.22 may be considered as additional step to HLA class I binding prediction to improve discovery of HLA-B*07:02-restricted MiHA. The value of the online tool of IEDB has also been reported by Bassani-Sternberg et al. (29), who demonstrated that within the HLA-

ligandome as analyzed by mass spectrometry, peptides that are known T-cell epitopes from cancer-associated proteins were more often predicted to be immunogenic than other HLA class I binding peptides from the same proteins. However, it should be emphasized that the sensitivity of the online tool of IEDB is low and that it failed to predict immunogenicity for 10 (59%) MiHA with predicted binding to HLA-B*07:02 as well as for all MiHA with predicted binding to HLA-A*02:01. It can be speculated that HLA-A*02:01-restricted epitopes allow more diversity in their TCR contact residues than HLA-B*07:02-restricted epitopes. This may explain why, despite use of many HLA-A*02:01-restricted epitopes for training of the algorithm, the sensitivity of the online tool of IEDB to predict *in vivo* immunogenicity of peptides binding to HLA-A*02:01 is lower than for HLA-B*07:02-binding peptides.

For the majority of HLA class I-restricted MiHA as shown in Table 2, allelic variants have not been identified as *in vivo* T-cell targets. This can be explained by insufficient searching for specific T-cells, but may also indicate that allelic variants cannot be processed or presented on the cell surface or that no specific TCRs are present in the naive repertoire of donor lymphocytes. To investigate processing and presentation of allelic variants, we determined whether the *in silico* characteristics as predicted by online algorithms are different between MiHA and their allelic variants. Our data showed that of the 57 pairs of MiHA and allelic variants that were analyzed, a minority of MiHA have amino acid substitutions at anchor positions (n = 12). As expected, HLA class I binding affinities for these MiHA are significantly higher than for their allelic variants. Predicted HLA class I binding affinity was also higher for a number of MiHA with amino acid substitutions at TCR contact residues (n = 9) in which the polymorphic residue is located immediately adjacent to the N-terminal anchor residue at position 2. For the majority of MiHA (n = 36), however, no difference in predicted HLA class I binding affinity was observed between MiHA and their allelic variants. Similar results were obtained for peptide-HLA class I complex stability as predicted by NetMHCstab 1.0 and also other prediction algorithms for proteasomal cleavage, TAP affinity and *in vivo* immunogenicity did not reveal any difference between MiHA and their allelic variants. Fritsch et al. (30) investigated 40 HLA class I-restricted neoantigens and also demonstrated that mutated amino acids are often present at TCR contact residues and that predicted HLA class I binding affinity is similar between mutated and native peptides. However, Duan et al. (31) showed in a reverse strategy for neoantigens that a relative score based on difference in HLA class I binding affinity as predicted by NetMHC 3.0 between mutant and wild-type peptides (differential agretopicity index; DAI) is superior in predicting *in vivo* immunogenicity in anti-tumor responses in mice than absolute values for HLA class I binding affinity as predicted for mutant peptides only. High DAI mostly resulted from amino acid substitutions at anchor residues between mutant and native

peptides. Although it can be argued that peptides with amino acid changes at anchor positions may be more immunogenic as a result of lack of central tolerance, the majority of the 65 HLA class I-restricted MiHA that have been identified as *in vivo* T-cell targets in anti-tumor responses after alloSCT contain amino acid changes at TCR contact residues. Therefore, we recommend the use of prediction algorithms for HLA class I binding affinity for discovery of MiHA or neoantigens, but do not favor a strategy in which peptides are only selected for a difference in predicted HLA class I binding affinity between the two peptides as created by the genetic variants. Furthermore, since no evidence was obtained for improper processing or presentation for the majority of allelic variants, our data suggest that lack of *in vivo* immunogenicity of allelic variants is most likely due to insufficient searching for specific T-cells or absence of specific TCRs in the naive repertoire of donor lymphocytes.

In conclusion, our data showed that 87% of the HLA class I-restricted MiHA (56% SB and 31% WB peptides) were accurately predicted by NetMHCpan 2.8, but that besides HLA class I binding affinity, none of the other algorithms significantly contributed to MiHA characterization. Our results are relevant for discovery of T-cell ligands that are created by polymorphic (MiHA) or mutated (neoantigens) genetic variants.

References

1. Horowitz MM, Bortin MM. Current status of allogeneic bone marrow transplantation. Clin Transpl. 1990:41-52.
2. Falkenburg JH, Warren EH. Graft versus leukemia reactivity after allogeneic stem cell transplantation. Biol Blood Marrow Transplant. 2011;17(1 Suppl):S33-8.
3. Warren EH, Zhang XC, Li S, et al. Effect of MHC and non-MHC donor/recipient genetic disparity on the outcome of allogeneic HCT. Blood. 2012;120(14):2796-806.
4. Spierings E. Minor histocompatibility antigens: past, present, and future. Tissue Antigens. 2014;84(4):374-60.
5. Zilberberg J, Feinman R, Korngold R. Strategies for the identification of T cell-recognized tumor antigens in hematological malignancies for improved graft-versus-tumor responses after allogeneic blood and marrow transplantation. Biol Blood Marrow Transplant. 2015;21(6):1000-7.
6. Griffioen M, van Bergen CA, Falkenburg JH. Autosomal Minor Histocompatibility Antigens: How Genetic Variants Create Diversity in Immune Targets. Front Immunol. 2016;7:100.
7. Ferrara JL, Levine JE, Reddy P, et al. Graft-versus-host disease. Lancet. 2009;373(9674):1550-61.
8. Stern M, de Wreede LC, Brand R, et al. Sensitivity of hematological malignancies to graft-versus-host effects: an EBMT megafile analysis. Leukemia. 2014;28(11):2235-40.
9. den Haan JM, Sherman NE, Blokland E, et al. Identification of a graft versus host disease-associated human minor histocompatibility antigen. Science. 1995;268(5216):1476-80.
10. Broen K, Greupink-Draaisma A, Woestenenk R, et al. Concurrent detection of circulating minor histocompatibility antigen-specific CD8+ T cells in SCT recipients by combinatorial encoding MHC multimers. PLoS One. 2011;6(6):e21266.
11. Hombrink P, Hadrup SR, Bakker A, et al. High-throughput identification of potential minor histocompatibility antigens by MHC tetramer-based screening: feasibility and limitations. PLoS One. 2011;6(8):e22523.
12. Hombrink P, Hassan C, Kester MG, et al. Identification of Biological Relevant Minor Histocompatibility Antigens within the B-lymphocyte-Derived HLA-Ligandome Using a Reverse Immunology Approach. Clin Cancer Res. 2015;21(9):2177-86.
13. Schumacher TN, Schreiber RD. Neoantigens in cancer immunotherapy. Science. 2015;348(6230):69-74.
14. Tran E, Ahmadzadeh M, Lu YC, et al. Immunogenicity of somatic mutations in human gastrointestinal cancers. Science. 2015;350(6266):1387-90.
15. Kawase T, Nannya Y, Torikai H, et al. Identification of human minor histocompatibility antigens based on genetic association with highly parallel genotyping of pooled DNA. Blood. 2008;111(6):3286-94.
16. Dolstra H, de Rijke B, Fredrix H, et al. Bi-directional allelic recognition of the human minor histocompatibility antigen HB-1 by cytotoxic T lymphocytes. Eur J Immunol. 2002;32(10):2748-58.
17. Nielsen M, Lundegaard C, Blicher T, et al. NetMHCpan, a method for quantitative predictions of peptide binding to any HLA-A and -B locus protein of known sequence. PLoS One. 2007;2(8):e796. Available at http://www.cbs.dtu.dk/services/NetMHCpan/.
18. Jørgensen KW, Rasmussen M, Buus S, et al. NetMHCstab - predicting stability of peptide-MHC-I complexes; impacts for cytotoxic T lymphocyte epitope discovery. Immunology. 2014;141(1):18-26. Available at http://www.cbs.dtu.dk/services/NetMHCstab-1.0/.
19. Nielsen M, Lundegaard C, Lund O, et al. The role of the proteasome in generating cytotoxic T-cell epitopes: insights obtained from improved predictions of proteasomal cleavage. Immunogenetics. 2005;57(1-2):33-41. Available at http://www.cbs.dtu.dk/services/NetChop/.

20. Bhasin M, Raghava GP. Analysis and prediction of affinity of TAP binding peptides using cascade SVM. Protein Sci. 2004;13(3):596-607. Available at http://www.imtech.res.in/raghava/tappred/.
21. Calis JJ, Maybeno M, Greenbaum JA, et al. Properties of MHC class I presented peptides that enhance immunogenicity. PLoS Comput Biol. 2013;9(10):e1003266. Available at http://tools.iedb.org/immunogenicity/.
22. Stranzl T, Larsen MV, Lundegaard C, et al. NetCTLpan: pan-specific MHC class I pathway epitope predictions. Immunogenetics. 2010;62(6):357-68. Available at http://www.cbs.dtu.dk/services/NetCTLpan/.
23. Karosiene E, Lundegaard C, Lund O, et al. NetMHCcons: a consensus method for the major histocompatibility complex class I predictions. Immunogenetics. 2012;64(3):177-86.
24. Rapin N, Hoof I, Lund O, et al. The MHC motif viewer: a visualization tool for MHC binding motifs. Curr Protoc Immunol. 2010;Chapter 18:18.7.1-.7.3. Available at http://www.cbs.dtu.dk/biotools/MHCMotifViewer/Human_alleles.html.
25. Pont MJ, van der Lee DI, van der Meijden ED, et al. Integrated Whole Genome and Transcriptome Analysis Identified a Therapeutic Minor Histocompatibility Antigen in a Splice Variant of ITGB2. Clin Cancer Res. 2016;22(16):4185-96.
26. Wölfel C, Lennerz V, Lindemann E, et al. Dissection and molecular analysis of alloreactive CD8+ T cell responses in allogeneic haematopoietic stem cell transplantation. Cancer Immunol Immunother. 2008;57(6):849-57.
27. Van Bergen CA, Rutten CE, Van Der Meijden ED, et al. High-throughput characterization of 10 new minor histocompatibility antigens by whole genome association scanning. Cancer Res. 2010;70(22):9073-83.
28. Rock KL, York IA, Goldberg AL. Post-proteasomal antigen processing for major histocompatibility complex class I presentation. Nat Immunol. 2004;5(7):670-7.
29. Bassani-Sternberg M, Pletscher-Frankild S, Jensen LJ, et al. Mass spectrometry of human leukocyte antigen class I peptidomes reveals strong effects of protein abundance and turnover on antigen presentation. Mol Cell Proteomics. 2015;14(3):658-73.
30. Fritsch EF, Rajasagi M, Ott PA, et al. HLA-binding properties of tumor neoepitopes in humans. Cancer Immunol Res. 2014;2(6):522-9.
31. Duan F, Duitama J, Al Seesi S, et al. Genomic and bioinformatic profiling of mutational neoepitopes reveals new rules to predict anticancer immunogenicity. J Exp Med. 2014;211(11):2231-48.

Supplemental information

S1 Dataset. Tables showing the *in silico* analyses of MiHA, allelic variants and the reference set of peptides are available at https://doi.org/10.1371/journal.pone.0162808.s001.

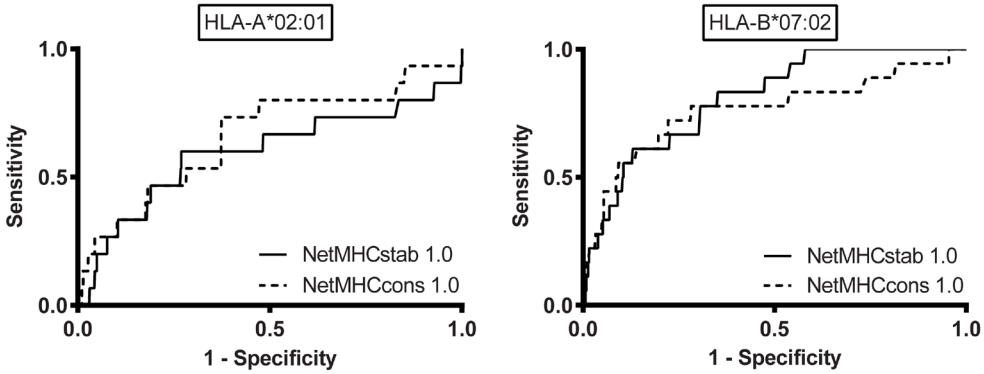

	Sensitivity	Specificity
HS	20%	94%
WS	60%	61%

	Sensitivity	Specificity
HS	11%	99%
WS	78%	66%

Figure S1. Comparison of predictive performance of NetMHCstab 1.0 and NetMHCcons 1.0. ROC curves for NetMHCstab 1.0 and NetMHCcons 1.0 for HLA-A*02:01 (left) and HLA-B*07:02 (right). Curves for NetMHCcons 1.0 (dashed line) and the integrated algorithm of NetMHCstab 1.0 (solid line) are plotted based on prediction data for MiHA and reference peptides. Sensitivity and specificity are indicated for default values for HS (>6 hrs) and WS (>2 hrs) complexes as predicted by NetMHCstab 1.0. For HLA-A*02:01, the AUC for NetMHCcons 1.0 and NetMHCstab 1.0 are 0.659 ($p = 0.0341$) and 0.596 ($p = 0.2033$), respectively. For HLA-B*07:02, the AUC for NetMHCcons 1.0 and NetMHCstab 1.0 are 0.763 ($p = 0.0002$) and 0.811 ($p < 0.0001$), respectively. These data demonstrate that NetMHCstab 1.0 is slightly superior to NetMHCcons 1.0 for HLA-B*07:02, but not for HLA-A*02:01.

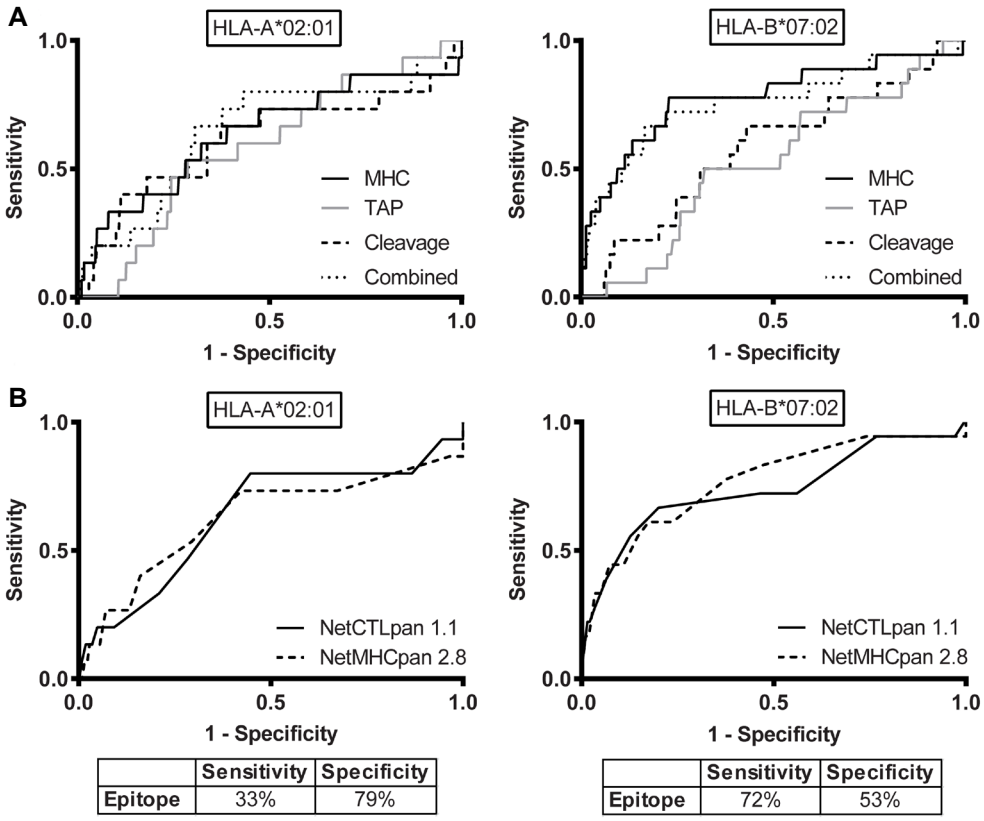

	Sensitivity	Specificity
Epitope	33%	79%

	Sensitivity	Specificity
Epitope	72%	53%

Figure S2. Predictive performance of NetCTLpan 1.1. (**A**) ROC curves for HLA class I binding affinity as predicted by NetMHCpan 2.3 (MHC; solid black line), TAP transport efficiency (TAP; solid grey line), C-terminal proteasomal cleavage as predicted by NetChop 3.0 (Cleavage; dashed line) and their combination (Combined; dotted line) are shown for HLA-A*02:01 (left) and HLA-B*07:02 (right). Graphs are plotted based on prediction data for MiHA and reference peptides. For HLA-A*02:01, the AUC for the MHC, TAP, Cleavage and Combined curves are 0.638 ($p = 0.0663$), 0.585 ($p = 0.2598$), 0.614 ($p = 0.1295$) and 0.646 ($p = 0.0525$), respectively. For HLA-B*07:02, the AUC for the MHC, TAP, Cleavage and Combined curves were 0.778 ($p < 0.0001$), 0.526 ($p = 0.7082$), 0.579 ($p = 0.2539$) and 0.760 ($p = 0.0002$), respectively. (**B**) ROC curves for NetCTLpan 1.1 (solid line) and NetMHCpan 2.8 (dashed line) are shown for HLA-A*02:01 (left) and HLA-B*07:02 (right). Graphs are plotted based on prediction data for MiHA and reference peptides. Sensitivity and specificity are indicated for the default value for epitope prediction (<1%-Rank) as used by NetCTLpan 1.1. For HLA-A*02:01, the AUC for NetCTLpan 1.1 and NetMHCpan 2.8 are 0.634 ($p = 0.0758$) and 0.625 ($p = 0.0964$), respectively. For HLA-B*07:02, the AUC for NetCTLpan 1.1 and NetMHCpan 2.8 are 0.737 ($p = 0.0007$) and 0.767 ($p = 0.0001$), respectively. The data show that MiHA cannot be more accurately characterized by NetCTLpan 1.1 in which C-terminal proteasomal cleavage and TAP transport efficiency are integrated with HLA class I binding affinity, as compared to prediction tools for HLA class I binding affinity alone.

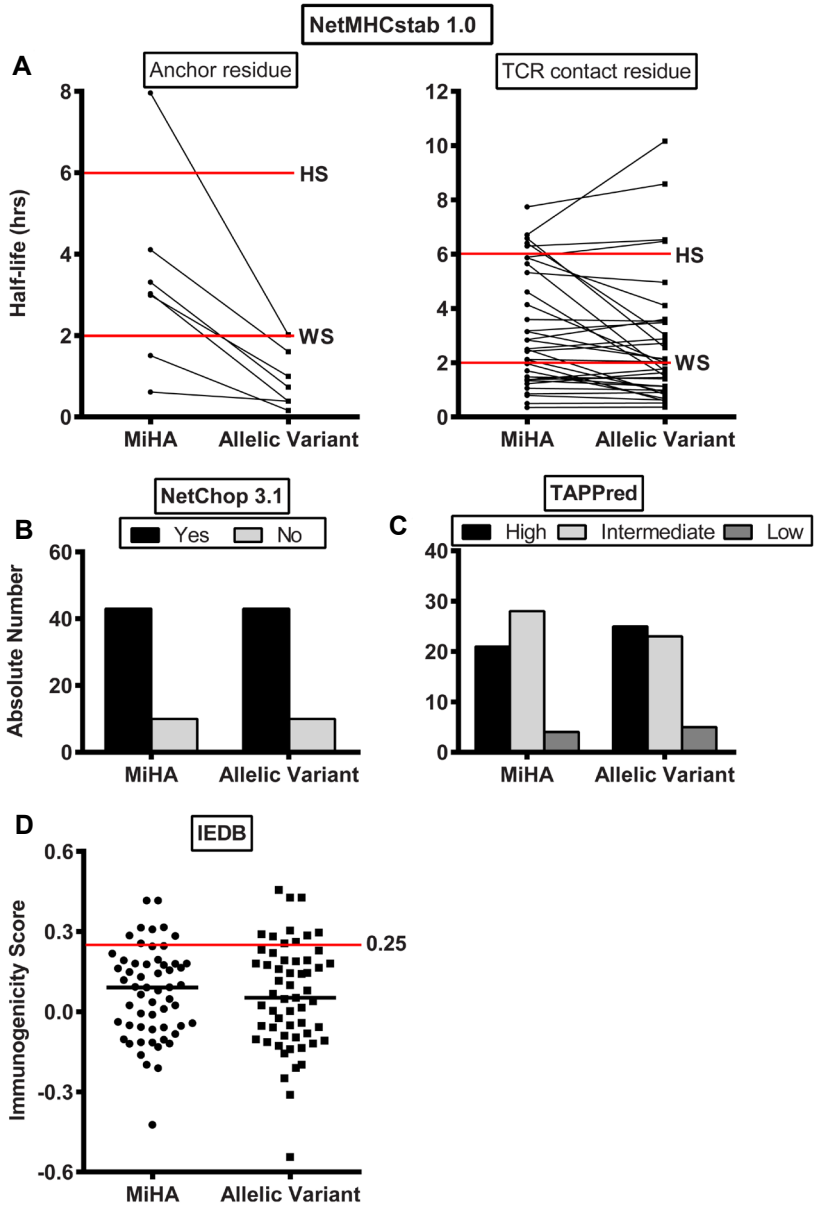

Figure S3. Predicted stability of the peptide-HLA class I complex, proteasomal cleavage, TAP transport and *in vivo* immunogenicity for MiHA and allelic variants. (**A**) Peptide-HLA class I complex stability as predicted for MiHA and their allelic variants by NetMHCstab 1.0. Predicted half-life (hrs) is shown for all MiHA and allelic variants for which HLA class I restriction alleles are available in the algorithm (n = 41) divided into two groups based on whether the polymorphic amino acid is present at an anchor residue (n = 7; left) or TCR contact residue (n = 34; right). Default thresholds for HS and WS peptides are indicated by red lines. The data show that predicted peptide-HLA class I complex stability for the 7 MiHA with polymorphic amino acids at anchor positions was significantly higher than for their allelic variants (p = 0.0156 using Wilcoxon signed rank test), whereas predicted peptide-HLA class I complex stability was

similar between MiHA and their allelic variants for the majority of 34 pairs with polymorphic amino acids at TCR contact residues (p = 0.0781 using Wilcoxon signed rank test). (**B**) Proteasomal cleavage at the C-terminus as predicted by NetChop 3.1 for all MiHA and their allelic variants (*n* = 53). Whole protein sequences were fed into the algorithm and default settings were used to predict proteasomal cleavage. Indicated are absolute numbers of peptides with predicted cleavage at the C-terminus. No significant difference was observed in proportion of peptides with predicted cleavage at the C-terminus between MiHA and allelic variants (81% for MiHA *versus* 81% for allelic variants, p = 1.000 using Fisher's exact test). (**C**) Affinity for the TAP transporter as predicted by TAPPred with default settings for all MiHA and their allelic variants (*n* = 53). Indicated are absolute numbers of peptides with high (black bars), intermediate (light grey bars) and low (dark grey bars) affinity for TAP. No significant difference was observed in proportion of peptides with high or weak affinity for TAP between MiHA (40% high, 53% intermediate and 8% low affinity) and allelic variants (47% high, 43% intermediate and 9% low affinity). (**D**) *In vivo* immunogenicity as predicted by the MHC I immunogenicity tool of the IEDB for the total group of MiHA and allelic variants (*n* = 57). Median immunogenicity scores are indicated by black horizontal lines. Using a threshold of 0.25 (red line), no significant difference in proportion of immunogenic peptides was observed between MiHA (14%) and allelic variants (18%) (p = 0.798 using Fisher's exact test).

Chapter 3

Mutated nucleophosmin 1 as immunotherapy target in acute myeloid leukemia

Dyantha I. van der Lee[1], Rogier M. Reijmers[1], Maria W. Honders[1], Renate S. Hagedoorn[1], Rob C.M. de Jong[1], Michel G.D. Kester[1], Dirk M. van der Steen[1], Arnoud H. de Ru[2], Christiaan Kweekel[1], Helena M. Bijen[1], Inge Jedema[1], Hendrik Veelken[1], Peter A. van Veelen[2], Mirjam H.M. Heemskerk[1], J.H. Frederik Falkenburg[1*], Marieke Griffioen[1*]

[1] Department of Hematology, Leiden University Medical Center, Leiden, The Netherlands
[2] Center for Proteomics and Metabolomics, Leiden University Medical Center, Leiden, The Netherlands
[*] Shared senior authorship

The Journal of Clinical Investigation. 2019 Feb 1;129(2):774-785
DOI: 10.1172/JCI97482

Abstract

The most frequent subtype of acute myeloid leukemia (AML) is defined by mutations in the nucleophosmin 1 (*NPM1*) gene. Mutated *NPM1* (ΔNPM1) is an attractive target for immunotherapy, since it is an essential driver gene and 4 bp frameshift insertions occur in the same hotspot in 30%–35% of AMLs, resulting in a C-terminal alternative reading frame of 11 aa. By searching the HLA class I ligandome of primary AMLs, we identified multiple ΔNPM1-derived peptides. For one of these peptides, HLA-A*02:01–binding CLAVEEVSL, we searched for specific T cells in healthy individuals using peptide-HLA tetramers. Tetramer-positive $CD8^+$ T cells were isolated and analyzed for reactivity against primary AMLs. From one clone with superior antitumor reactivity, we isolated the T cell receptor (TCR) and demonstrated specific recognition and lysis of HLA-A*02:01–positive ΔNPM1 AML after retroviral transfer to $CD8^+$ and $CD4^+$ T cells. Antitumor efficacy of TCR-transduced T cells was confirmed in immunodeficient mice engrafted with a human AML cell line expressing ΔNPM1. In conclusion, the data show that ΔNPM1-derived peptides are presented on AML and that CLAVEEVSL is a neoantigen that can be efficiently targeted on AML by ΔNPM1 TCR gene transfer. Immunotherapy targeting ΔNPM1 may therefore contribute to treatment of AML.

Introduction

Acute myeloid leukemia (AML) is characterized by accumulation of malignant myeloid precursor cells that are arrested in differentiation in the bone marrow. Standard therapy of AML consists of induction chemotherapy followed by intensive consolidation chemotherapy or high-dose therapy in combination with autologous or allogeneic hematopoietic stem cell transplantation (alloSCT) (1, 2). Although most patients respond to therapy and achieve complete remission, relapses occur frequently. Patients with relapsed or refractory AML after intensive chemotherapy or alloSCT have an extremely poor prognosis, and there is a strong need for new and effective therapies to treat these patients.

Molecular characterization of AML using whole-genome and exome sequencing demonstrated that AML has a low mutational load with an average of 10–13 coding mutations per patient (3-5). In contrast to what occurs in most other cancer types, somatic abnormalities in AML often occur in the same genes (3, 6) and antigens arising from hotspot mutations in these genes are therefore attractive targets for immunotherapy. Nucleophosmin 1 (*NPM1*) is a driver gene that is mutated in 30%–35% of AMLs (3, 6). Although AMLs are often heterogeneous mixtures of different leukemic subclones (3, 7), mutations in *NPM1* are initiating mutations that are present in all leukemic cells, illustrating that these mutations are clonal and essential for malignant transformation early in leukemogenesis. Patients with mutated *NPM1* (ΔNPM1) carry a characteristic 4 bp frameshift insertion in exon 12 of the gene. The resulting ΔNPM1 protein is 4 aa longer than the WT counterpart, and its C-terminal 11 aa are translated in an alternative reading frame (CLAVEEVSLRK) (8). The 4 bp frameshift insertions occur at restricted positions in the coding sequence and, although the exact 4 bp sequence can differ, the majority of mutations encode the same 11 aa alternative reading frame.

Immunotherapy by *in vivo* vaccination or adoptive transfer of T cells that are produced *in vitro* can be very effective. In particular, chimeric antigen receptor (CAR) and T cell receptor (TCR) gene therapy targeting lineage-restricted or cancer-associated antigens have shown promising results (9-11). However, due to (low) antigen expression in healthy tissues, antitumor immunity can be accompanied by severe toxicity (9, 10, 12). In contrast with antigens encoded by unmutated genes, neoantigens arise from tumor-specific mutations and their formation and expression are restricted to malignant cells (13-15). The majority of neoantigens, however, are encoded by patient-specific passenger mutations that can be lost as a result of immune editing and lead to tumor evasion (16). Immune escape for neoantigens created by driver mutations is less likely, since tumor cells need to express the driver

gene in order to retain their malignant phenotype (13). Since ΔNPM1 is a driver mutation that occurs in 30%–35% of AMLs, its C-terminal 11 aa alternative reading frame may be an ideal target for immunotherapy.

In this study, we searched in the HLA class I ligandome of primary AMLs and identified multiple peptides from the alternative reading frame of ΔNPM1. For one of these peptides, the HLA-A*02:01–binding peptide CLAVEEVSL, we demonstrated its relevance as a therapeutic neoantigen that can be efficiently targeted on AML by TCR gene transfer, indicating that ΔNPM1 is a relevant target for immunotherapy of AML.

Materials and methods

Sample collection and cell culture

Peripheral blood and bone marrow samples were collected from patients with AML and healthy individuals. Peripheral blood and bone marrow mononuclear cells were isolated by Ficoll-Isopaque separation and cryopreserved. For isolation of PBMCs from HLA-A*02:01–typed healthy individuals, buffy coats were ordered from Sanquin. T cells were cultured in T cell medium (TCM) consisting of Iscove's Modified Dulbecco's Medium (IMDM) (Lonza) supplemented with 5% heat-inactivated FBS (Gibco, Thermo Fisher Scientific), 5% human serum, 1.5% 200 mM l-glutamine (Lonza), 1% 10,000 U/ml penicillin/streptomycin (Lonza), and 100 IU/ml IL-2 (Novartis). AML cell lines expressing WTNPM1 (OCI-AML2) and ΔNPM1 (OCI-AML3) were ordered from DSMZ. AML cell lines and primary AML, EBV-LCL, and T2 cells (ATCC) were cultured in IMDM containing 10% FBS, 1.5% l-glutamine, and 1% penicillin/streptomycin. Monocytes were isolated from PBMCs by magnetic-activated cell sorting (MACS) (Miltenyi Biotec) with CliniMACS CD14 beads (Miltenyi Biotec), and mature DCs were cultured as described previously (17). All cell lines were mycoplasma negative, as determined by regular testing using the PlasmoTest Mycoplasma Detection Kit (InvivoGen).

HLA class I ligandome of primary AML

Peptide elution was performed as outlined previously (18). In brief, cell pellets of 12 primary AMLs were lysed in 50 mM Tris-HCl, 150 mM NaCl, 5 mM ethylenediaminetetraacetate, and 0.5% Zwittergent 3-12 (pH 8.0) supplemented with cOmplete Protease Inhibitor (Sigma-Aldrich). After 2 hours of tumbling in lysis buffer at 4°C, cell lysates were centrifuged for 10 minutes at 1000 *g* at 4°C. The supernatant was subsequently centrifuged for 35 minutes at 13,000 *g* at 4°C, precleared with Protein A Sepharose CL-4B beads (GE Healthcare Life Sciences), and subjected to an immunoaffinity column with dimethyl pimelidate–immobilized

W6/32 antibody (3 mg/ml resin) on Protein A Sepharose CL-4B beads with a flow rate of 1 ml/min. After washing with 5 to 10 column volumes of lysis buffers and 10 mM Tris-HCl (pH 8.0) buffers with 1 M, 120 mM, and no NaCl, bound HLA class I–peptide complexes were eluted from the column and dissociated with 3 to 4 column volumes of 10% acetic acid. Peptides were separated from HLA class I molecules via passage through a 10 kDa membrane (Macrosep Advance Centrifugal Devices With Supor Membrane, Pall Corp.). The filtrate was freeze dried.

Eluted peptide pools were fractionated by strong cation exchange chromatography (SCX) with a homemade 15 cm SCX column (320 µm inner diameter; polysulfoethyl A, 3 µm, Poly LC) run at 4 µl/min. Gradients were run for 10 minutes at 100% solvent A (100/0.1 water/trifluoroacetic acid v/v), after which a linear gradient started to reach 100% solvent B (65/35/0.1 250 mM KCl/acetonitrile/trifluoroacetic acid v/v/v) over 15 minutes, followed by 100% solvent C (65/35/0.1 500 mM KCl/acetonitrile/trifluoroacetic acid v/v/v) over the next 15 minutes. The gradient remained at 100% solvent C for 5 minutes and then switched again to 100% solvent A. Twenty 4 µl fractions were collected in vials prefilled with 20 µl 95/3/0.1 water/acetonitrile/formic acid v/v/v. Peptide fractions were lyophilized, dissolved in 95/3/0.1 water/acetonitril/formic acid v/v/v and subsequently analyzed by data-dependent MS/MS on either an LTQ FT Ultra equipped with a nanoflow liquid chromatography 1100 HPLC system (Agilent Technologies), as previously described (19), or a Q Exactive mass spectrometer equipped with an easy-nLC 1000 (Thermo Fisher Scientific). Peptides were trapped at 6–10 µl/min on a 1.5 cm column (100 µm internal diameter; ReproSil-Pur C18-AQ, 3 µm, Dr. Maisch HPLC GmbH) and eluted to a 20 cm column (50 µm internal diameter; ReproSil-Pur C18-AQ, 3 µm) at 150 nl/min. The column was developed with a 120-minute gradient from 0% to 40% acetonitrile in 0.1% formic acid. The end of the column was drawn to a tip (internal diameter about 5 µm) from which the eluent was sprayed into the mass spectrometer. Full-scan MS spectra were acquired in the FT-ICR with a resolution of 25,000 at a target value of 3,000,000. The 2 most intense ions were isolated for accurate mass measurements by a selected ion monitoring scan in FT-ICR with a resolution of 50,000 at a target accumulation value of 50,000. The selected ions were then fragmented in the linear ion trap using collision-induced dissociation at a target value of 10,000. The Q Exactive mass spectrometer was operated in top10 mode. Parameters were resolution 70,000 at an AGC target value of 3,000,000/maximum fill time of 20 ms (full scan) and resolution 17,500 at an AGC target value of 100,000/maximum fill time of 60 ms for MS/MS at an intensity threshold of 17,000. Apex trigger was set to 1 to 10 seconds, and allowed charges were 2–6. The Orbitrap Fusion LUMOS mass spectrometer was operated in data-dependent MS/MS (top-N mode), with collision energy at 32 V and recording of the MS2 spectrum in the orbitrap. In the master scan (MS1), the resolution was 60,000 and the scan range

300–1400 at an AGC target of 400,000 at maximum fill time of 50 ms. The dynamic exclusion was set after n = 1 with an exclusion duration of 20 seconds. Charge states 1–4 were included. For MS2, precursors were isolated with the quadrupole with an isolation width of 1.2 Da. HCD collision energy was set to 32 V. First mass was set to 110 Da. The MS2 scan resolution was 30,000, with an AGC target of 50,000 at maximum fill time of 100 ms. Proteome Discoverer version 2.1 (Thermo Fisher Scientific) was used for peptide and protein identification, using the mascot node for identification, using mascot version 2.2.04 with the UniProt Homo Sapiens database (UP000005640; Jan 2015; 67,911 entries). Methionine oxidation and cysteinylation of cysteine were set as a variable modification. Peptide assignments were made with a precursor tolerance of 10 ppm and MS/MS fragment tolerance of 20 mmu for the Q Exactive data and 2 ppm and 0.5 Da for LTQ FT Ultra data. Identification of the ΔNPM1-derived peptide was confirmed by its synthetic counterpart.

Peptide synthesis and pHLA tetramer production

Peptides were synthesized by standard Fmoc chemistry and dissolved in DMSO. Cysteinylation of peptides was performed by treating 1 mM peptide with 2 mM 1,4-dithiothreitol in 50 mM ammonium bicarbonate for 15 minutes at 50°C, followed by addition of 10 mM free cysteine and 15 mM H_2O_2 for 30 minutes at room temperature (RT). pHLA tetramers were produced as outlined previously, with minor modifications (20, 21). In brief, monomers consisting of recombinant HLA-A*02:01 heavy chain and human B2M were purified by gel-filtration HPLC and biotinylated. After folding with the appropriate peptide, pHLA tetramers were generated by adding PE- or APC-conjugated streptavidin (Invitrogen, Thermo Fisher Scientific). UV-exchange pHLA tetramers were produced by exposing biotinylated HLA-A*02:01 monomers containing UV-sensitive peptide to 366 nm UV light in the presence of cysteinylated ΔNPM1 peptide. After 1 hour of peptide exchange, monomers were incubated for 1 hour at 4°C followed by centrifugation at 4000 *g* for 10 minutes at 15°C. pHLA tetramers were produced by adding streptavidin-conjugated PE to supernatants and were stored at 4°C.

Antibodies and FACS analysis

T cells were stained with FITC-conjugated antibodies against CD3 (catalog 555339), CD4 (catalog 555346), CD8 (catalog 555366) (BD Biosciences), and TCR-Vβ5.1 (catalog IM1552, Beckman Coulter); APC-conjugated antibodies against CD3 (catalog 555342), CD4 (catalog 555349), CD8 (catalog 555369), and mouse TCR-Cβ (catalog 553174); and PE-conjugated pHLA tetramers and antibodies against CD3 (catalog 555340), CD4 (catalog 555347), and CD8 (catalog 555367) (BD Biosciences). Cells were measured on a BD FACSCalibur II (BD Biosciences) using BD CellQuest Pro software (BD Biosciences), and analysis was performed with FlowJo software.

T cell isolation and culture

pHLA tetramer–positive $CD8^+$ T cells were isolated from PBMCs from AML patients and healthy individuals as previously described (22). In short, PBMCs from HLA-*02:01–positive AML patients and healthy individuals were stained with PE-conjugated pHLA tetramers containing ΔNPM1 peptides for 1 hour at 4°C followed by MACS isolation using anti-PE MicroBeads (Miltenyi Biotec). Isolated cells were stained with Alexa Fluor–conjugated anti-CD8 (catalog MHCD0829) (Invitrogen), FITC-conjugated anti-CD4, anti-CD14 (catalog 555397), and anti-CD19 (catalog 555412) (BD Biosciences), and tetramer-positive $CD8^+$ T cells were single cell sorted by a BD FACSAria III cell sorter (BD Biosciences) using BD FACSDiva version 6 software. Single T cells were stimulated with 50,000 irradiated allogeneic PBMCs, 5,000 irradiated allogeneic EBV-LCL, and 0.8 µg/ml PHA (Oxoid Microbiology Products, Thermo Fisher Scientific) in 100 µl TCM per well in 96-well U-bottom culture plates (Costar, Sigma-Aldrich). Growing T cell clones were restimulated every 10–14 days with irradiated feeder cells and PHA.

T cell reactivity assays

T cell recognition was measured by IFN-γ ELISA (Sanquin). Stimulator cells (30,000 or 10,000 cells for EBV-LCL) were coincubated with T cells (2000 cells) in 40 µl TCM per well in 384-well flat-bottom plates (Greiner Bio-One). After overnight coincubation, culture supernatants were harvested to measure IFN-γ release. In peptide recognition assays, T2 cells (15,000 cells) were preincubated for 30 minutes at 37°C with titrated peptide concentrations and washed twice before coincubation with T cells. In blocking assays, target cells (10,000 cells) were preincubated for 60 minutes at RT with antibodies blocking HLA class I (W6/32) or HLA class II (PdV5.2) before addition of T cells. T cell–mediated cytotoxicity was measured in ^{51}chromium release assays. AML cells were labeled with 100 µCi $Na_2{}^{51}CrO_4$ for 1 hour at 37°C, washed, and coincubated with T cells at various effector-to-target (E:T) ratios in 100 µl TCM per well in 96-well U-bottom culture plates (Costar). Spontaneous and maximum ^{51}Cr release were measured in separate plates containing 100 µl TCM or 100 µl TCM with 1% Triton-X 100 per well (Sigma-Aldrich), respectively. After 9 hours of coincubation, 25 µl supernatants were harvested and transferred to 96-well LumaPlates (PerkinElmer). ^{51}Cr release in cpm was measured on a 2450 Microbeta^2 plate counter (PerkinElmer).

TCR cloning and production of retroviral supernatants

TCR α and β chain usage of clone 1A2 was determined as previously described with minor modifications (23). In brief, T cells were lysed and mRNA was isolated by the Dynabeads mRNA DIRECT Kit (Invitrogen). TCR-specific cDNA was generated using 2 TCR-Cβ primers, a TCR-Cα primer, an SA.rt anchor template-switching oligonucleotide (TSO), and SMARTScribe Reverse Transcriptase (Takara, Clontech)

(24). During first-strand cDNA synthesis, SMARTScribe reverse transcriptase adds a 3′ nontemplated polycytosine terminus, which allows for annealing of the TSO and second-strand cDNA synthesis (24). TCR amplification was performed by PCR using Phusion Flash (Thermo Fisher Scientific), an anchor-specific primer, and nested primers annealing to TCR-Cα or -Cβ regions. TCR sequences for clone 1A2 were identified as TRAV12-2 and TRBV5-1 by Sanger sequencing (Macrogen) and the ImMunoGeneTics (IMGT) database (25). Codon-optimized TRAV12-2 and TRBV5-1 sequences were synthesized and cloned in MP71-TCR-flex retroviral vector by GenScript. In MP71-TCR-flex, murine TCR-Cα and -Cβ regions with additional cysteine residues to promote preferential pairing of the TCR are linked by a P2A sequence (26). The construct was transfected into packaging cells ϕ-NX-A (ATCC), and retroviral supernatants 48 and 72 hours after transfection were harvested and frozen at –80°C. The MP71-TCR-flex vector and MP71-TCR-flex encoding a TCR for HLA-A*02:01–binding CMV peptide NLVPMVATV was provided by T.N. Schumacher (Division of Immunology, Netherlands Cancer Institute, Amsterdam, Netherlands).

TCR gene transfer

PBMCs from 3 HLA-A*02:01–positive healthy individuals (donor 1, 2 and 3) were thawed, and $CD4^+$ and $CD8^+$ T cells were isolated by MACS using anti-CD4 MicroBeads (Miltenyi Biotec) followed by the $CD8^+$ T cell Isolation Kit (Miltenyi Biotec). $CD8^+$ and $CD4^+$ T cells were stimulated with irradiated autologous feeders and 0.8 μg/ml PHA in 24-well flat-bottom culture plates (Costar). Two days after stimulation, T cells were transferred to 24-well flat-bottom suspension culture plates (Greiner Bio-One) for retroviral transduction. Prior to the addition of T cells, the plates were coated with 30 μg/ml retronectin (Takara, Clontech) and blocked with 2% human serum albumin (Sanquin). Retroviral supernatants were added, and plates were centrifuged at 3000 *g* for 20 minutes at 4°C. T cells were added to the plates with viral supernatants at 300,000 cells per well. After overnight incubation, T cells were transferred to 24-well flat-bottom culture plates. At day 6 after transduction, TCR-transduced T cells were stained with APC-conjugated anti-mouse TCR-Cβ for 15 minutes at 4°C, followed by MACS isolation using anti-APC MicroBeads (Miltenyi Biotec). TCR-transduced T cells were restimulated on days 10–14 with irradiated allogeneic PBMCs, EBV-LCL, and 0.8 μg/ml PHA and enriched by MACS using APC-conjugated anti-mouse TCR-Cβ and anti-APC MicroBeads prior to analysis.

***In vivo* antitumor efficacy**

Male NOD.Cg-*Prkdc*(scid)*Il2rg*(tm1Wjl)/SzJ (NOD *scid* gamma, NSG) mice (The Jackson Laboratory) were maintained in individually ventilated cages in groups, and food and water were provided ad libitum. Mice of 8 to 12 weeks were injected i.v. with 1×10^6 OCI-AML3 cells that were transduced with luciferase (pCDH-EF1-Luc2-

P2A-tdTomato Red; a gift from Kazuhiro Oka, Department of Molecular & Cellular Biology, Baylor College of Medicine, Houston, Texas, USA) (Addgene plasmid, catalog 72486) and sorted to greater than 98% purity by flow cytometry. For tumor visualization, mice were injected i.p. with 200 µl 7.5 mM d-luciferine (Cayman Chemical Co.) and anesthetized with 3%–4% isoflurane. Bioluminescent images were obtained using a CCD camera (IVIS spectrum, PerkinElmer). Two weeks after tumor cell inoculation, mice were injected i.v. with 4×10^6 TCR-transduced $CD8^+/CD4^+$ T cells (2:3 ratio) or left untreated.

Data and materials availability

pHLA tetramers for CLAVEEVSL, C*LAVEEVSL, and NLVPMVATV, retroviral vectors and supernatants for mutant and WT *NPM1*, the allo-HLA-A*02:01 clone, and primary AML must be obtained through a material transfer agreement (MTA).

Statistics

Statistical significance of survival data was assessed using the log-rank (Mantel-Cox) test. Statistical analyses were performed using Prism software (GraphPad Software, version 6). $P < 0.05$ was considered significant.

Study approval

For this study, materials were used from the Leiden University Medical Center Biobank for Hematological Diseases. This study was approved by the Institutional Review Board of the Leiden University Medical Center (IRB LUMC approval number B16.039). Materials from patients and healthy individuals were collected after written informed consent according to the Declaration of Helsinki. All animal studies were conducted in accordance with institutional guidelines after obtaining permission from the national Ethical Committee for Animal Research (AVD116002017891) and in accordance with Dutch laws on animal experiments.

Results

ΔNPM1 peptides in the HLA class I ligandome of primary AMLs

To investigate whether ΔNPM1 peptides are processed and presented on AML, we immunoprecipitated HLA class I surface molecules from 12 primary AMLs, eluted the peptides from the binding groove, and analyzed the peptidome by tandem mass spectrometry (MS/MS). Table 1 shows HLA typing of these 12 AMLs as well as their mutational status for *NPM1*. Eight of the 12 AMLs were positive for ΔNPM1 by routine diagnostics. All patients had normal karyotypes by cytogenetics except for 1 AML, which carried chromosomal translocation inv(16)(p13q22), resulting in the *CBFB-MYH11* fusion gene. Blast percentages in peripheral blood or bone marrow samples used for peptidome analysis ranged between 55% and 98%.

The 4 bp hotspot insertion in exon 12 results in a ΔNPM1 protein that is 4 aa longer than its WT counterpart, with 11 aa (CLAVEEVSLRK) at the C terminus translated in an alternative reading frame (Figure 1). From this ΔNPM1 protein, a sequence spanning 10 N-terminal residues in the normal reading frame followed by the 11 C-terminal aa in the alternative reading frame (MTDQEAIQDLCLAVEEVSLRK) was used to search for matching peptides in the HLA class I ligandomes of the 12 primary AMLs. This search revealed two 8-mer peptides (VEEVSLRK and AVEEVSLR), two 9-mer peptides (CLAVEEVSL and AVEEVSLRK), and one 11-mer peptide (CLAVEEVSLRK) in ΔNPM1 AML, but not in WT *NPM1* (WTNPM1) AML (Table 1). All 5 ligands as eluted from 7 AMLs were validated by comparing tandem mass spectra with synthetic peptides (Figure 2 and Supplemental Figure S1). Tandem mass spectra of the eluted CLAVEEVSL and CLAVEEVSLRK ligands were confirmed upon cysteinylation of the first residue of the synthetic peptide, indicating that cysteinylated variants of these peptides are presented on primary AMLs. Using NetMHCpan 3.0 (27), CLAVEEVSL was predicted to bind to HLA-A*02:01 and AVEEVSLRK and CLAVEEVSLRK to HLA-A*03:01 as well as HLA-A*11:01 (Supplemental Table S1), which was confirmed by appropriate peptide folding in the respective HLA class I monomers.

Figure 1. DNA and protein sequences for WTNPM1 and ΔNPM1. Nucleic and amino acid sequences are shown for WTNPM1 (upper) and ΔNPM1 (lower). Indicated is a TCTG insertion between c.863_864 in the coding sequence of *NPM1*, which is the most frequent frameshift mutation in the hotspot region. Translated aa sequences are shown until the termination sequence (stop, indicated by asterisks). As a consequence of the TCTG insertion, the C-terminal aa CLAVEEVSLRK of ΔNPM1 are translated in an alternative reading frame. WT and mutant aa are indicated in gray and red, respectively.

Table 1. ΔNPM1 peptides in the HLA class I ligandome of primary AMLs

Patient	HLA class I	ΔNPM1[A]	Karyotype	Blasts[B]	Eluted peptide	No. spectra[C]
AML10197	A*01:01 A*02:01 B*08:01 B*44:03 C*07:01 C*16:01	+	46, XX	98%	CLAVEEVSL	11,232
AML3361	A*02:01 A*11 B*13 B*35 C*04 C*06	+	46, XX	79%	CLAVEEVSL AVEEVSLRK VEEVSLRK	7,992
AML6395	A*02:01 A*24:03 B*38:01 B*51:01 C*02:02 C*12:03	+	46, XY	80%	-	3,915[D]
AML9448	A*03:01 A*32:01 B*07:02 B*08:01 C*07:01 C*07:10	+	46, XX	77%	CLAVEEVSLRK AVEEVSLRK	10,352
AML5444	A*03:01 B*07:02 B*35:01 C*04:01 C*07:02	+	46, XX	55%	AVEEVSLRK	6,209
AML5518	A*01:01 A*24:02 B*35:03 B*44:03 C*04:01 C*16:01	+	46, XX	95%	AVEEVSLRK AVEEVSLR	8,479
AML6498	A*11:01 A*68:01 B*35:01 B*35:03 C*04:01	+	46, XX	94%	CLAVEEVSLRK AVEEVSLRK	12,233
AML4443	A*01:01 B*08:01 C*07:01	+	46, XX	82%	AVEEVSLRK	4,037
AML1775	A*24 A*02:01 B*51 B*40:01 C*10 C*03	-	46, XY, inv(16)(p13q22)	89%	-	524[D]
AML2250	A*02:01 A*01:01 B*62 B*15:01 C*10 C*03	-	46, XY	95%	-	4,286[D]
AML1143	A*02:01 A*03:01 B*07:02 B*35:01 C*04:01 C*07:02	-	46, XY	90%	-	5,571
AML3009	A*11 A*02:01 B*15:01 B*07:02 C*03 C*07	-	46, XY	70%	-	4,466[D]

[A] ΔNPM1 are 4 bp insertions in exon 12 of *NPM1* causing a frameshift at the C terminus of the protein. [B] Blast percentages in peripheral blood or bone marrow samples used for peptidome analysis. [C] Number of Mascot-identified unique 8- to 11-mer peptide sequences in the UniProt Homo Sapiens database with MIS ≥ 35. [D] AML samples for which peptide-HLA complexes were immunoprecipitated by BB7.2 (anti-HLA-A*02:01) antibody. For all other AML samples, W6/32 (anti-HLA class I) antibody was used.

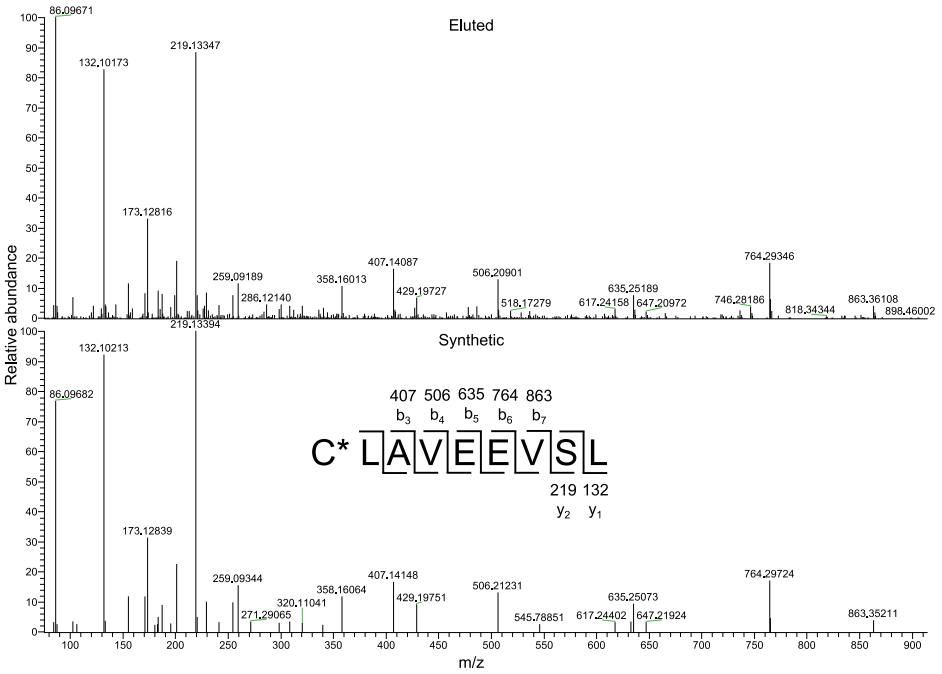

Figure 2. Validation of C*LAVEEVSL as peptide eluted from HLA-A*02:01–positive AML with ΔNPM1. C*LAVEEVSL was validated as peptide eluted from HLA-A*02:01–positive AML with ΔNPM1 by comparing MS/MS between eluted peptides and synthetic peptide C*LAVEEVSL. Matching MS/MS are shown for an eluted peptide from AML10197 (upper panel) and synthetic peptide C*LAVEEVSL (lower panel). C*, cysteinylation of the Cys residue.

CLAVEEVSL as ΔNPM1-derived neoantigen

Since HLA-A*02:01 is expressed in 50% of the White population, we selected CLAVEEVSL to explore its relevance as therapeutic neoantigen and searched for specific T cells in AML patients. Phycoerythrin-conjugated (PE-conjugated) peptide-HLA (pHLA) tetramers were produced for CLAVEEVSL (ΔNPM1-CLA) and its cysteinylated variant C*LAVEEVSL (ΔNPM1-C*LA), and a mix of these tetramers was used to isolate specific T cells from PBMCs from 6 HLA-A*02:01–positive AML patients with ΔNPM1 who were in remission after chemotherapy. T cells binding to 1 or both pHLA tetramers were enriched by magnetic anti-PE beads, and single tetramer-positive $CD8^+$ T cells were isolated by flow cytometry (Supplemental Table S2). A total of 41 tetramer-positive $CD8^+$ T cells were isolated from 34×10^6 PBMCs from 4 patients; of these, 5 clones from 3 patients expanded. None of these 5 T cell clones, however, stained with the ΔNPM1-CLA or ΔNPM1-C*LA tetramer. In addition to direct T cell isolation, we also screened for tetramer-positive T cells after *in vitro* peptide stimulation, but failed to detect these T cells above background in any of the 4 patients analyzed (Supplemental Table S3 and Supplemental Figure S2). These

data indicate that T cells for ΔNPM1 did not exist at frequencies that could be detected in limited numbers of PBMCs, as available from AML patients in remission after chemotherapy. Since we and others previously demonstrated that tumor-specific T cells can be present at low frequencies in healthy individuals (28, 29), we followed the same strategy as described above and directly isolated tetramer-positive T cells from large numbers of PBMCs from 6 HLA-A*02:01–positive healthy individuals (Table 2). A variable number of 8 to 55 tetramer-positive $CD8^+$ T cells were isolated from 460–1970 × 10^6 PBMCs from each individual. Of these cells, 31 clones from 5 individuals expanded and 13 T cell clones from 4 individuals were positive for the ΔNPM1-CLA tetramer. Of these 13 clones, 3 T cell clones also stained with the ΔNPM1-C*LA tetramer (Figure 3A).

Table 2. Direct isolation of ΔNPM1-specific T cells from healthy individuals

Donor	PBMC[A] (×10^6)	Sorted T cells[B]	Growing clones	ΔNPM1-CLA tetramer[C]	ΔNPM1-C*LA tetramer[D]	Reactive clones
1	460	14	4	2	1	1
2	700	8	6	4	ND	0
3	970	20	7	3	0	0
4	560	24	8	0	0	-
5	545	13	0	-	-	-
6	1970	55	6	4	2	1

[A] Indicated are numbers of PBMCs from HLA-A*02:01–positive healthy individuals that are used for T cell isolation. [B] PBMCs were stained with anti-CD8-Alexa Fluor 700 and a mix of PE-conjugated pHLA tetramers for CLAVEEVSL and its cysteinylated variant, C*LAVEEVSL. Indicated are numbers of tetramer-positive $CD8^+$ T cells that are sorted. [C] Number of growing T cell clones positive for the ΔNPM1-CLA tetramer. [D] Number of growing T cell clones positive for the ΔNPM1-C*LA tetramer. ND. Not done.

To determine whether the 13 tetramer-positive $CD8^+$ clones were reactive against their target peptide, clones were tested for reactivity against HLA-A*02:01–positive T2 cells exogenously loaded with CLAVEEVSL, the cysteinylated variant C*LAVEEVSL, or an irrelevant HLA-A*02:01–binding CMV peptide, NLVPMVATV. Of the 13 ΔNPM1-CLA tetramer-positive clones, 2 T cell clones (1A2 and 4A8) showed specific reactivity against T2 cells loaded with CLAVEEVSL, but not control peptide NLVPMVATV (Figure 3B). Clone 1A2 also showed recognition of C*LAVEEVSL. These results are in line with tetramer data and demonstrate that clone 1A2 recognizes uncysteinylated as well as cysteinylated ΔNPM1, whereas only uncysteinylated ΔNPM1 is recognized by clone 4A8.

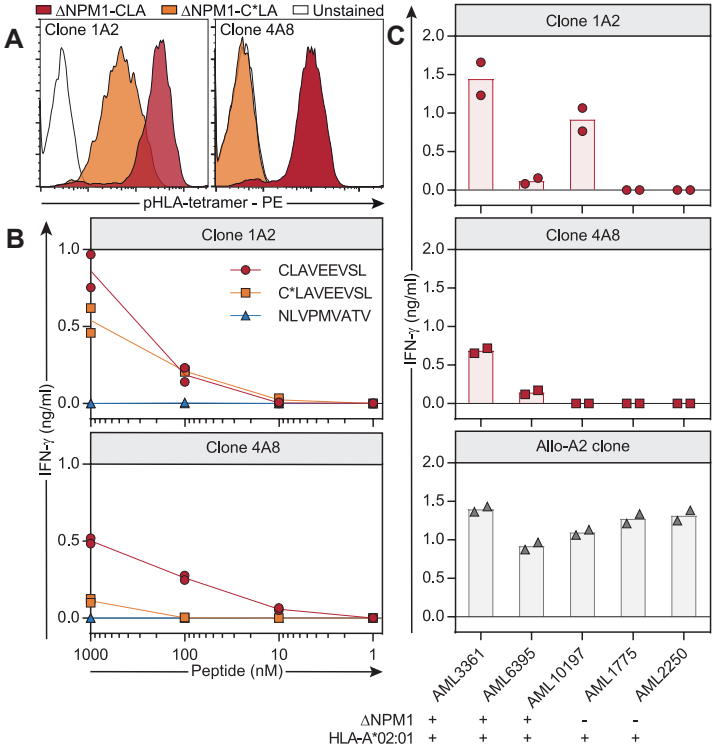

Figure 3. CLAVEEVSL as ΔNPM1-derived neoantigen. CD8$^+$ T cells specific for ΔNPM1 were single cell isolated from PBMCs from HLA-A*02:01–positive healthy individuals using a mix of ΔNPM1-CLA and ΔNPM1-C*LA pHLA tetramers. (**A**) T cell clones were stained with pHLA tetramers. T cell clones 1A2 (left) and 4A8 (right) were both positive for the ΔNPM1-CLA tetramer (red), whereas only clone 1A2 stained with ΔNPM1-C*LA (orange). (**B**) T cell clones 1A2 (upper panel) and 4A8 (lower panel) were tested for reactivity against HLA-A*02:01–positive T2 cells exogenously loaded with titrated concentrations of ΔNPM1 peptide CLAVEEVSL (red circles), the cysteinylated variant C*LAVEEVSL (orange squares), or an irrelevant HLA-A*02:01–binding CMV peptide NLVPMVATV (blue triangles) by IFN-γ ELISA. Both T cell clones showed recognition of CLAVEEVSL, and clone 1A2 also showed recognition of C*LAVEEVSL. Release of IFN-γ (ng/ml) in duplicate wells is shown. (**C**) Clones 1A2 (upper panel) and 4A8 (middle panel) were tested for reactivity against 5 HLA-A*02:01–positive primary AMLs by IFN-γ ELISA. The panel included 3 AMLs with ΔNPM1 and 2 AMLs with WTNPM1. T cell clone 1A2 reacted against all 3 AMLs with ΔNPM1, whereas clone 4A8 recognized 2 AMLs. An HLA-A*02:01–specific alloreactive T cell clone (Allo-A2 clone) was included as a positive control. Release of IFN-γ (ng/ml) in duplicate wells is shown; bars represent mean IFN-γ release.

To investigate the antitumor potential of clones 1A2 and 4A8, T cell reactivity was measured against 5 HLA-A*02:01–positive primary AMLs, including 3 samples with ΔNPM1 and 2 samples with WTNPM1. T cell clone 1A2 showed reactivity against all 3 AMLs with ΔNPM1, whereas clone 4A8 showed reactivity against 2 of these samples (Figure 3C). Superior reactivity against AML by clone 1A2 may be explained by its capacity to recognize cysteinylated ΔNPM1 as identified on the surface of

primary AML by MS. No T cell reactivity was observed against HLA-A*02:01–positive AML with WTNPM1 (Figure 3C). These data indicate that ΔNPM1 tetramer-positive T cells are present in healthy individuals and that a minority of these T cells are able to react to ΔNPM1-positive primary AML.

TCR gene transfer to target ΔNPM1 on AML

Since ΔNPM1 is a driver mutation that occurs in 30%–35% of AMLs and HLA-A*02:01 is expressed in 50% of the White population, we considered CLAVEEVSL an attractive target for TCR gene transfer. Since primary AMLs were most strongly recognized by clone 1A2, mRNA was isolated from this clone and cDNA was generated to sequence the variable regions of the TCR α and β chains for ΔNPM1. Codon-optimized gene sequences for TRAV12-2 and TRBV5-1 as expressed by clone 1A2 were synthesized and cloned into a modified MP71-TCR-flex retroviral vector (26). To facilitate preferential binding and expression of the TCR α and β chains, the variable regions of the TCR were cloned in-frame with murine constant regions linked by a P2A sequence. The TCR for ΔNPM1 and, as a control, a TCR for HLA-A*02:01–binding CMV pp65 peptide NLVPMVATV were introduced into $CD8^+$ and $CD4^+$ T cells isolated from PBMCs from HLA-A*02:01–positive healthy individuals (donors 1, 2, and 3). At day 6 after transduction, TCR-transduced $CD8^+$ and $CD4^+$ T cells were purified using an allophycocyanin (APC)-conjugated antibody against mouse TCR-Cβ and magnetic anti-APC beads. Flow cytometry demonstrated specific binding of the ΔNPM1-CLA tetramer to $CD8^+$ T cells transduced with the TCR for ΔNPM1 (CD8ØNPM1), but not to $CD8^+$ T cells transduced with the CMV-specific TCR (CD8ØCMV) (Figure 4A). Conversely, the CMV-NLV tetramer did not bind to $CD8^+$ T cells transduced with the TCR for ΔNPM1, whereas it clearly stained $CD8^+$ T cells transduced with the CMV-specific TCR. For TCR-transduced $CD4^+$ T cells (CD4ØNPM1 and CD4ØCMV), results were similar, indicating that the ΔNPM1-CLA tetramer binds to ΔNPM1 TCR–transduced T cells independently of the CD8 coreceptor. TCR-transduced $CD8^+$ and $CD4^+$ T cells were also stained with an antibody against mouse TCR-Cβ, and $CD8^+$ and $CD4^+$ T cells transduced with the TCR for ΔNPM1 also showed specific binding to an antibody against human TCR-Vβ5.1 (Supplemental Figure S3).

Next, we analyzed the functionality of $CD8^+$ and $CD4^+$ T cells transduced with the TCR for ΔNPM1 and demonstrated specific release of IFN-γ upon incubation with HLA-A*02:01–positive T2 cells loaded with CLAVEEVSL, but not CMV peptide NLVPMVATV (Figure 4B). Specific release of IFN-γ was also observed upon stimulation with HLA-A*02:01–positive and ΔNPM1-mutated AML cell line OCI-AML3, but not HLA-A*02:01–positive WTNPM1 AML cell line OCI-AML2. Blocking experiments confirmed that recognition of OCI-AML3 by TCR-modified $CD8^+$ and $CD4^+$ T cells was mediated by HLA class I (Figure 4C).

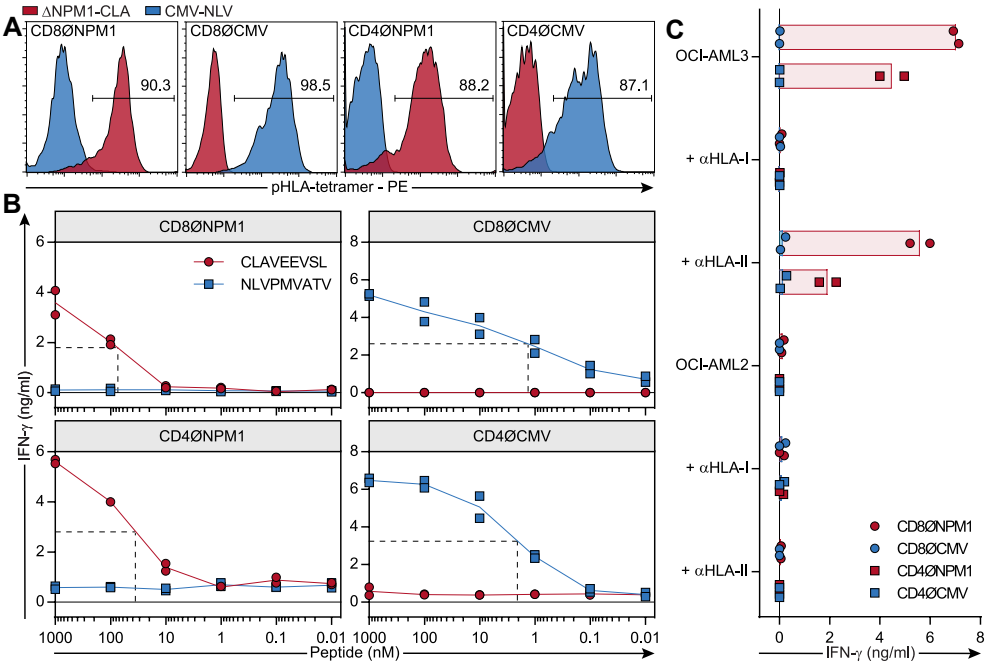

Figure 4. Targeting ΔNPM1 by TCR gene transfer. CD8$^+$ and CD4$^+$ T cells isolated from HLA-A*02:01–positive healthy individuals were transduced with the TCR for ΔNPM1 from clone 1A2 and a TCR for HLA-A*02:01–binding CMV peptide NLVPMVATV. TCR-transduced T cells were purified by MACS. (**A**) TCR-transduced T cells were analyzed by flow cytometry using ΔNPM1-CLA (red) and CMV-NLV (blue) pHLA tetramers. CD8$^+$ (CD8ØNPM1) and CD4$^+$ (CD4ØNPM1) T cells transduced with the TCR for ΔNPM1 stained with the ΔNPM1-CLA tetramer, whereas CD8$^+$ (CD8ØCMV) and CD4$^+$ (CD4ØCMV) T cells transduced with the CMV-specific TCR showed binding to the CMV-NLV tetramer. Results are shown for donor 1. (**B**) TCR-transduced T cells were analyzed for reactivity against T2 cells exogenously loaded with titrated concentrations of CLAVEEVSL (red circles) or NLVPMVATV (blue squares) by IFN-γ ELISA. CD8ØNPM1 (upper left panel) and CD4ØNPM1 (lower left panel) showed half-maximum recognition of CLAVEEVSL at concentrations of 30–100 nM (dotted lines), but no recognition of NLVPMVATV. Conversely, CD8ØCMV (upper right panel) and CD4ØCMV (lower right panel) reacted against NLVPMVATV, but not CLAVEEVSL. Release of IFN-γ (ng/ml) in duplicate wells is shown for donor 1. (**C**) TCR-transduced T cells were tested for recognition of HLA-A*02:01–positive AML cell lines with ΔNPM1 (OCI-AML3) or WTNPM1 (OCI-AML2) in the absence or presence of blocking antibodies against HLA class I (αHLA-I) or HLA class II (αHLA-II) by IFN-γ ELISA. Recognition of OCI-AML3 by CD8$^+$ and CD4$^+$ T cells transduced with the TCR for ΔNPM1 is mediated by HLA class I. Release of IFN-γ (ng/ml) in duplicate wells is shown for donor 2. Bars represent mean IFN-γ release.

TCR-transduced CD8$^+$ and CD4$^+$ T cells were subsequently tested for reactivity against a panel of 13 HLA-A*02:01–positive primary AMLs, including 9 samples with ΔNPM1 and 4 samples with WTNPM1. Upon transduction with the TCR for ΔNPM1, CD8$^+$ and CD4$^+$ T cells both showed recognition of all 9 AMLs with ΔNPM1, whereas no specific recognition of AML with WTNPM1 was observed (Figure 5). Despite variable expression of HLA-A*02:01 and costimulatory and adhesion molecules on leukemic cells (Supplemental Table S4), the TCR for ΔNPM1 was strongly reactive against all AML analyzed, except for AML10594, which has a low percentage of leukemic blasts (27%). We also analyzed ΔNPM1 gene expression and variant allele frequencies using RNA-Seq data for these AMLs (Supplemental Table S5). RNA-Seq analysis revealed high gene expression and variant allele frequencies, thereby confirming strong and clonal expression of ΔNPM1 in all AML cases tested.

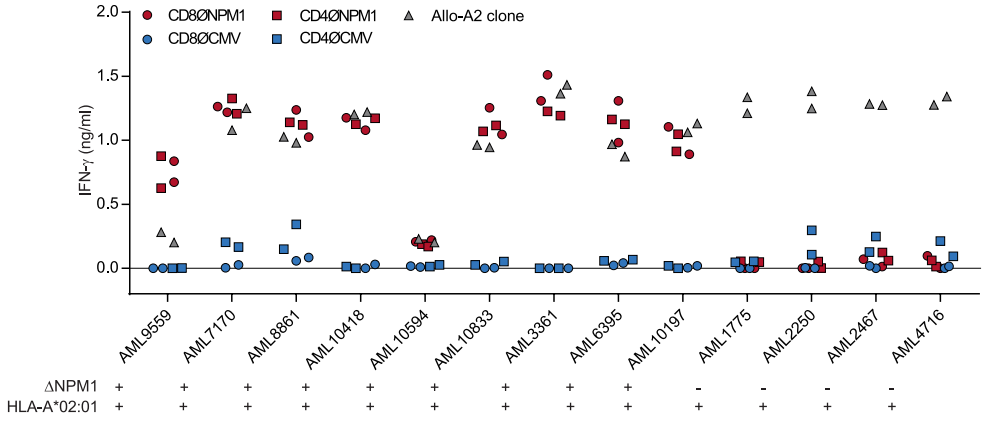

Figure 5. Recognition of primary AMLs after ΔNPM1 TCR gene transfer. TCR-transduced CD8$^+$ and CD4$^+$ T cells were tested for reactivity against a panel of 13 HLA-A*02:01–positive primary AMLs, including 9 samples with ΔNPM1 and 4 samples with WTNPM1 by IFN-γ ELISA (Supplemental Table S4). CD8$^+$ (CD8ØNPM1; red circles) and CD4$^+$ (CD4ØNPM1; red squares) T cells transduced with the TCR for ΔNPM1 reacted against all 9 AMLs with ΔNPM1, whereas none of the AMLs were specifically recognized by CD8$^+$ (CD8ØCMV; blue circles) or CD4$^+$ (CD4ØCMV; blue squares) T cells after transfer of the CMV-specific TCR. The allo-A2 clone (gray triangles) was included as a positive control. Release of IFN-γ (ng/ml) in duplicate wells is shown for donor 1.

CD8$^+$ and CD4$^+$ T cells transduced with the TCR for ΔNPM1 lacked reactivity against HLA-A*02:01–negative AML with ΔNPM1. There was also no reactivity against HLA-A*02:01–positive mature monocyte-derived DC and a panel of HLA-A*02:01–positive EBV-LCL (Supplemental Figure S4), excluding production of a peptide resembling CLAVEEVSL by alternative translation of the WTNPM1 gene and off-target reactivity against a ubiquitous peptide presented by HLA-A*02:01 or other

common HLA alleles. In summary, the data show that the TCR for ΔNPM1 upon gene transfer to CD8⁺ and CD4⁺ T cells results in specific recognition of CLAVEEVSL as an endogenous neoantigen presented by HLA-A*02:01 on primary AML with ΔNPM1.

Next, we tested the cytolytic capacity of TCR-transduced CD8⁺ and CD4⁺ T cells against primary AML. TCR-transduced T cells were tested against 6 HLA-A*02:01–positive AMLs, including 4 samples with ΔNPM1 and 2 samples with WTNPM1 in a 9-hour ^{51}chromium release assay. CD8⁺ as well as CD4⁺ T cells transduced with the TCR for ΔNPM1 showed specific lysis of ΔNPM1 AML, but not WTNPM1 AML (Figure 6), indicating that CLAVEEVSL is a neoantigen that can be efficiently targeted on AML by ΔNPM1 TCR gene transfer in a CD8 coreceptor–independent fashion.

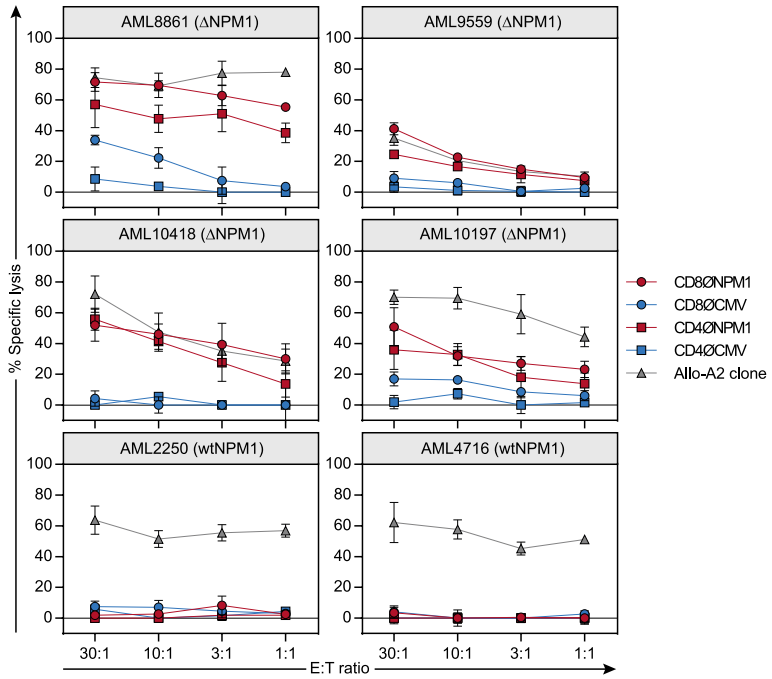

Figure 6. Lysis of primary AMLs after ΔNPM1 TCR gene transfer. TCR-transduced CD8⁺ and CD4⁺ T cells were tested for cytolytic capacity by a 9-hour 51Cr-release assay on 6 HLA-A*02:01–positive primary AMLs, including 4 samples with ΔNPM1 and 2 samples with WTNPM1. CD8⁺ (CD8ØNPM1; red circles) and CD4⁺ (CD4ØNPM1; red squares) T cells transduced with the TCR for ΔNPM1 showed specific lysis of all 4 AMLs with ΔNPM1, whereas none of the AMLs were specifically lysed by CD8⁺ (CD8ØCMV; blue circles) or CD4⁺ (CD4ØCMV; blue squares) T cells after transfer of the CMV-specific TCR. The allo-A2 clone (gray triangles) was included as a positive control. Data represent mean percentage of specific lysis in triplicate wells ± SD for donor 2.

Finally, *in vivo* efficacy of TCR-transduced T cells was investigated in immunodeficient NSG mice engrafted with HLA-A*02:01–positive OCI-AML3 cells with ΔNPM1. Two weeks after inoculation of 1 × 10^6 OCI-AML3 cells transduced with luciferase, mice were either left untreated (n = 4) or received a single dose of 4 × 10^6 $CD8^+/CD4^+$ T cells (ratio 2:3) transduced with the TCR for ΔNPM1 (n = 5) or with the CMV-specific control TCR (n = 2). The data showed a clear antitumor effect in mice treated with the ΔNPM1-specific TCR by bioluminescent imaging (Figure 7A-B), resulting in significantly better overall survival than that seen in untreated mice or mice treated with the CMV-specific TCR (Figure 7C). In conclusion, T cells transduced with the TCR for ΔNPM1 efficiently kill AML cells *in vivo*, resulting in prolonged overall survival.

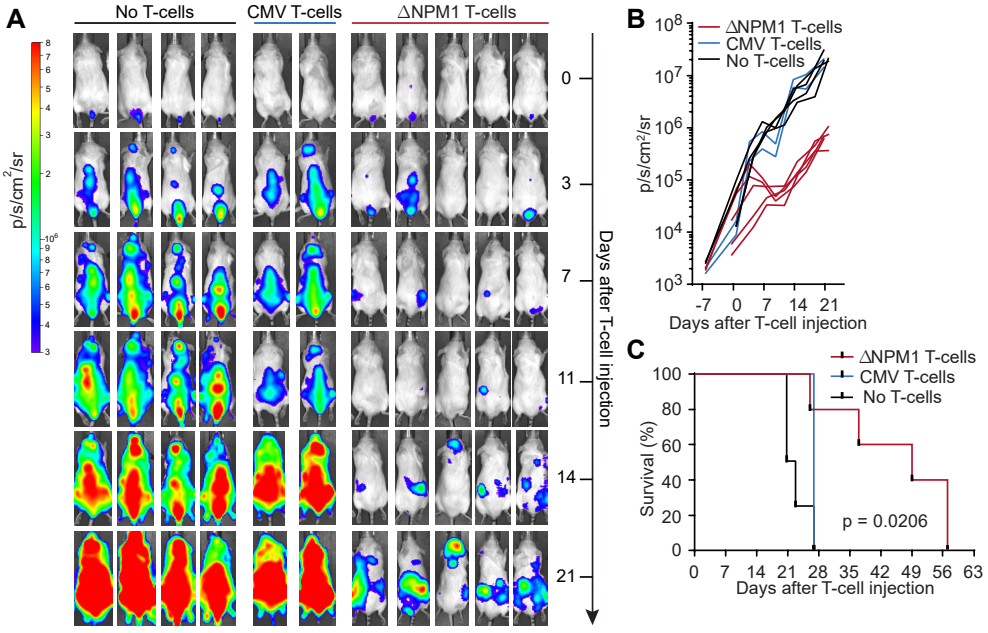

Figure 7. *In vivo* antitumor efficacy after ΔNPM1 TCR gene transfer. Male NSG mice were engrafted with 1 × 10^6 HLA-A*02:01–positive OCI-AML3 cells with ΔNPM1. OCI-AML3 cells were transduced with luciferase to follow *in vivo* tumor growth by bioluminescence imaging. Two weeks after tumor inoculation, mice were either left untreated or injected i.v. with 4 × 10^6 $CD8^+/CD4^+$ T cells (2:3 ratio) transduced with the TCR for ΔNPM1 or with the CMV-specific control TCR. TCR-transduced T cells were produced from HLA-A*02:01–positive healthy donor 3. (**A** and **B**) After T cell injection, tumor burden was followed twice per week for 21 days. In mice receiving $CD8^+/CD4^+$ T cells transduced with the TCR for ΔNPM1 (ΔNPM1 T cells; n = 5; red), tumor load was significantly reduced within 2 weeks of T cell transfer, resulting in delayed tumor outgrowth as compared with that in untreated mice (no T cells; n = 4; black) and mice treated with $CD8^+/CD4^+$ T cells transduced with the CMV-specific control TCR (CMV T cells; n = 2; blue). (**C**) Kaplan-Meier curve showing better overall survival of mice treated with the ΔNPM1-specific TCR (n = 5; red line) as compared with untreated mice (n = 4; black line) or mice treated with the CMV-specific control TCR (n = 2; blue line). P = 0.0206, log-rank (Mantel-Cox) test.

Discussion

In this study, we demonstrate the relevance of ΔNPM1 as a target for immunotherapy of AML. *NPM1* is a driver gene that is mutated in 30%–35% of patients with AML, and although the exact 4 bp insertion may differ, the same C-terminal 11 aa alternative reading frame is produced by the majority of hotspot mutations. By searching the HLA class I ligandome of 12 primary AMLs, multiple peptides were identified from the alternative reading frame of ΔNPM1. For one of these peptides, HLA-A*02:01–binding CLAVEEVSL, we isolated a TCR and demonstrated its *in vitro* and *in vivo* potential to target ΔNPM1 AML upon introduction into $CD8^+$ and $CD4^+$ T cells.

Interestingly, patients carrying ΔNPM1 without *FLT3* mutations or with low allelic ratio (<0.5) *FLT3* mutations have a relatively favorable prognosis after chemotherapy (1, 2, 6, 30, 31), raising the question of whether an effective *in vivo* immune response is induced against ΔNPM1. NPM1 is a nucleocytoplasmic shuttling protein, and as a result of the mutation, ΔNPM1 is dislocated from the nucleolus to the cytoplasm, where it is susceptible to proteasomal degradation and processing by the HLA class I antigen presentation pathway (8). Greiner et al. (32) investigated whether *in vitro* T cell responses could be induced against 9 HLA-A*02:01–binding ΔNPM1 peptides using PBMCs from healthy individuals and patients with AML. After coculture of $CD8^+$ T cells with peptide-loaded PBMCs, T cell responses against AIQDLCLAV and AIQDLCVAV, but not against CLAVEEVSL, were observed. These 2 peptides were subsequently used to screen 25 AML patients with ΔNPM1 for *in vivo* T cell responses, and it was shown that overall survival of patients with detectable immune responses was higher than that of patients without immune responses (33). We analyzed 6 HLA-A*02:01–positive AML patients with ΔNPM1 who were in remission after chemotherapy for *in vivo* immune responses against CLAVEEVSL, but were unable to detect tetramer-positive T cells, indicating that *in vivo* immune responses against CLAVEEVSL in these 6 patients were below the threshold of detection and emphasizing the need to develop immunotherapy to target this ΔNPM1 neoantigen on AML.

Although only cysteinylated C*LAVEEVSL was identified in the HLA class I ligandome of primary AML by MS/MS, clone 1A2 recognized both C*LAVEEVSL and CLAVEEVSL when pulsed as synthetic peptides on T2 cells and could be stained with ΔNPM1-CLA as well as ΔNPM1-C*LA tetramers. In contrast, clone 4A8 recognized CLAVEEVSL, but not C*LAVEEVSL, and only the ΔNPM1-CLA tetramer could bind to the clone. Despite its failure to recognize cysteinylated C*LAVEEVSL, clone 4A8 reacted against 2 of the 3 AMLs tested. Although this suggests that

uncysteinylated ΔNPM1 peptides can also be presented on AML, our elution data demonstrate that cysteinylated ΔNPM1 peptides are more abundant, since C*LAVEEVSL and C*LAVEEVSLRK were identified as HLA class I ligands on 4 different AMLs, while uncysteinylated variants were not detected. Based on its capacity to recognize C*LAVEEVSL, the TCR from clone 1A2 was isolated and investigated for its potential to target ΔNPM1 AML after TCR gene transfer.

Current immunotherapies often exploit cancer-associated antigens to stimulate antitumor immunity (9, 10). Whereas most vaccination trials have shown limited clinical efficacy, possibly due to central T cell tolerance as a result of low antigen expression on healthy tissues, clinical efficacy of CAR and TCR gene therapy can be strong. However, due to low antigen expression on healthy tissues, antitumor immunity is often accompanied by severe side effects (9, 10, 12). For instance, CAR therapy targeting CD123 on AML shows promising antitumor responses in preclinical models (34), but also severe myeloablation, probably due to low CD123 expression on healthy hematopoietic stem cells (35). PRAME and WT1 are promising antigens for targeting AML by TCR gene therapy, but low antigen expression on healthy tissues remains a risk for toxicity (36-38). In contrast with cancer-associated antigens, which are encoded by unmutated genes, neoantigens are created by tumor-specific mutations that are absent in healthy tissues, and high-affinity T cells are therefore not deleted by thymic selection (13-15). This may explain why neoepitope vaccination induces broad and diverse immune responses in stage III/IV melanoma patients (39-41). Likewise, due to absence in healthy tissues, TCR gene transfer for neoantigens is expected to mediate antitumor immunity with no or limited side effects (13, 15).

Since CLAVEEVSL is a neoantigen, on-target toxicity is not expected for the ΔNPM1-specific TCR. This is supported by lack of detection of ΔNPM1 in clonal hematopoiesis, which is characterized by clonal expansion of blood cells with one or more somatic mutations (42, 43), and the fact that the ΔNPM1-specific TCR has been isolated from an HLA-A*02:01–positive healthy individual, who apparently did not have a deletion of this TCR in the thymus. Although on-target toxicity was not anticipated, we measured reactivity of the ΔNPM1-specific TCR against HLA-A*02:01–positive mature dendritic cells and EBV-LCL, which also express a variety of other HLA alleles. The TCR for ΔNPM1 lacked reactivity against these healthy cells, with strong antigen processing and presentation capacity, thereby excluding on-target reactivity against a peptide resembling CLAVEEVSL produced by alternative translation of the WTNPM1 gene and off-target reactivity against a ubiquitous peptide presented by HLA-A*02:01 or another common HLA allele. However, potential off-target reactivity against a tissue-restricted peptide or a

ubiquitous peptide presented by a rare HLA allele cannot be excluded and should be further evaluated before start of a clinical ΔNPM1 TCR gene study.

Clinical efficacy of TCR gene therapy is dependent on specificity and expression of the target antigen, but also relies on affinity of the transferred TCR (44). Our data showed that the TCR for ΔNPM1 is able to recognize and lyse primary AML in a CD8 coreceptor–independent manner. Although $CD4^+$ T cells are traditionally known to provide help to $CD8^+$ T cells, there is now substantial evidence that $CD4^+$ T cells can also mediate tumor rejection in the absence of $CD8^+$ T cells and that they may even be essential for effective antitumor immunity (45-48). Coadministration of $CD8^+$ and $CD4^+$ T cells expressing the same antigen receptor may thus be preferable and might result in superior antitumor immunity. This is supported by mouse studies (49, 50) and by Turtle et al. (51, 52), who demonstrated in humans that adoptive transfer of $CD8^+$ and $CD4^+$ T cells expressing the same CD19-specific CAR resulted in complete remission in a substantial number of patients with relapsed or refractory B cell malignancies.

An advantage of gene therapy is that the CAR or TCR can be introduced into distinct T cell subsets with superior *in vivo* persistence and antitumor efficacy, such as stem cell memory and central memory T cells. Notably, the culture period to produce tumor-specific T cells is relatively short and permits conditions for maintaining a less differentiated T cell phenotype and infusion of a well-defined T cell product (53, 54). On the other hand, gene therapy could lead to immune escape of the tumor by loss of antigen expression (55). In particular, HLA class I downregulation through loss of heterozygosity of HLA alleles or *B2M* mutations is an escape mechanism that may hamper efficacy of TCR gene therapy (41, 56-58). Other escape mechanisms mainly affect genes involved in the IFN-γ signaling pathway, such as apelin receptor (*APLNR*) and Janus kinases (*JAK1* and *JAK2*), which are also crucial in antitumor responses by CAR gene therapy and other immunotherapeutic approaches (58-60). Finally, another specific drawback of TCR gene therapy is the risk of TCR chain mispairing between introduced and endogenous TCR α and β chains, resulting in reduced efficacy and potential toxicity by new TCRs with unknown specificities (61, 62). Although preferential pairing of the introduced TCR can be stimulated by a disulfide bridge between α and β chains (63), mispairing cannot entirely be prevented. It is noteworthy that strategies including gene editing by TALEN, zinc-finger nucleases, and CRISPR/Cas9 completely abrogate expression of endogenous TCRs and can provide a solution for unwanted TCR chain mispairing (37, 64-66).

In conclusion, since patients with relapsed or refractory AML after intensive chemotherapy or alloSCT have an extremely poor prognosis (1, 2), ΔNPM1 TCR

gene therapy may significantly contribute to survival and potential cure of these patients for whom there are often no other treatment options. Recently, ΔNPM1 has also been shown as a reliable marker for measuring minimal residual disease (67). Persistence of ΔNPM1 transcripts as detected by quantitative reverse transcriptase PCR in AML patients after chemotherapy strongly predicted disease relapse within 3 years of follow-up. These findings support that ΔNPM1 is a clonal driver mutation that is retained in AML cells to maintain their malignant phenotype and suggest that ΔNPM1 as a marker for disease status can be used for optimal timing and treatment of patients with relapsed or refractory AML by preemptive ΔNPM1 TCR gene therapy. If proven successful, it may even replace alloSCT as effective therapy for AML across all risk categories. Altogether, this emphasizes the relevance of ΔNPM1 as a target for T cell immunotherapy and clinical potential of this ΔNPM1-specific TCR.

Patents

The HLA-A*02:01-restricted TCR for CLAVEEVSL as well as AVEEVSLRK and CLAVEEVSL as HLA class I-binding ΔNPM1 peptides on primary AML are protected by patent publication number WO/2019/004831.

References

1. Döhner H, Weisdorf DJ, Bloomfield CD. Acute Myeloid Leukemia. N Engl J Med. 2015;373(12):1136-52.
2. Ferrara F, Schiffer CA. Acute myeloid leukaemia in adults. Lancet. 2013;381(9865):484-95.
3. Ley TJ, Miller C, Ding L, et al. Genomic and epigenomic landscapes of adult de novo acute myeloid leukemia. N Engl J Med. 2013;368(22):2059-74.
4. Alexandrov LB, Nik-Zainal S, Wedge DC, et al. Signatures of mutational processes in human cancer. Nature. 2013;500(7463):415-21.
5. Kandoth C, McLellan MD, Vandin F, et al. Mutational landscape and significance across 12 major cancer types. Nature. 2013;502(7471):333-9.
6. Papaemmanuil E, Gerstung M, Bullinger L, et al. Genomic Classification and Prognosis in Acute Myeloid Leukemia. N Engl J Med. 2016;374(23):2209-21.
7. Welch JS, Ley TJ, Link DC, et al. The origin and evolution of mutations in acute myeloid leukemia. Cell. 2012;150(2):264-78.
8. Falini B, Mecucci C, Tiacci E, et al. Cytoplasmic nucleophosmin in acute myelogenous leukemia with a normal karyotype. N Engl J Med. 2005;352(3):254-66.
9. Coulie PG, Van den Eynde BJ, van der Bruggen P, et al. Tumour antigens recognized by T lymphocytes: at the core of cancer immunotherapy. Nat Rev Cancer. 2014;14(2):135-46.
10. Rosenberg SA, Restifo NP. Adoptive cell transfer as personalized immunotherapy for human cancer. Science. 2015;348(6230):62-8.
11. June CH, Sadelain M. Chimeric Antigen Receptor Therapy. N Engl J Med. 2018;379(1):64-73.
12. Hinrichs CS, Restifo NP. Reassessing target antigens for adoptive T-cell therapy. Nat Biotechnol. 2013;31(11):999-1008.
13. Blankenstein T, Leisegang M, Uckert W, et al. Targeting cancer-specific mutations by T cell receptor gene therapy. Curr Opin Immunol. 2015;33:112-9.
14. Schumacher TN, Schreiber RD. Neoantigens in cancer immunotherapy. Science. 2015;348(6230):69-74.
15. Tran E, Robbins PF, Rosenberg SA. 'Final common pathway' of human cancer immunotherapy: targeting random somatic mutations. Nat Immunol. 2017;18(3):255-62.
16. Verdegaal EM, de Miranda NF, Visser M, et al. Neoantigen landscape dynamics during human melanoma-T cell interactions. Nature. 2016;536(7614):91-5.
17. Kremer AN, van der Meijden ED, Honders MW, et al. Endogenous HLA class II epitopes that are immunogenic in vivo show distinct behavior toward HLA-DM and its natural inhibitor HLA-DO. Blood. 2012;120(16):3246-55.
18. Hassan C, Kester MG, de Ru AH, et al. The human leukocyte antigen-presented ligandome of B lymphocytes. Mol Cell Proteomics. 2013;12(7):1829-43.
19. Meiring HD, van der Heeft E, ten Hove GJ, et al. Nanoscale LC–MS(n): technical design and applications to peptide and protein analysis. J Sep Sci. 2002;25(9):557-68.
20. Burrows SR, Kienzle N, Winterhalter A, et al. Peptide-MHC class I tetrameric complexes display exquisite ligand specificity. J Immunol. 2000;165(11):6229-34.
21. Rodenko B, Toebes M, Hadrup SR, et al. Generation of peptide-MHC class I complexes through UV-mediated ligand exchange. Nat Protoc. 2006;1(3):1120-32.
22. Jahn L, Hombrink P, Hagedoorn RS, et al. TCR-based therapy for multiple myeloma and other B-cell malignancies targeting intracellular transcription factor BOB1. Blood. 2017;129(10):1284-95.
23. van Bergen CA, van Luxemburg-Heijs SA, de Wreede LC, et al. Selective graft-versus-leukemia depends on magnitude and diversity of the alloreactive T cell response. J Clin Invest. 2017;127(2):517-29.
24. Koning MT, Kielbasa SM, Boersma V, et al. ARTISAN PCR: rapid identification of full-length immunoglobulin rearrangements without primer binding bias. Br J Haematol. 2017;178(6):983-6.

25. Lefranc MP, Giudicelli V, Ginestoux C, et al. IMGT, the international ImMunoGeneTics database. Nucleic Acids Res. 1999;27(1):209-12.
26. Linnemann C, Heemskerk B, Kvistborg P, et al. High-throughput identification of antigen-specific TCRs by TCR gene capture. Nat Med. 2013;19(11):1534-41.
27. Nielsen M, Andreatta M. NetMHCpan-3.0; improved prediction of binding to MHC class I molecules integrating information from multiple receptor and peptide length datasets. Genome Med. 2016;8(1):33.
28. Hombrink P, Hassan C, Kester MG, et al. Identification of Biological Relevant Minor Histocompatibility Antigens within the B-lymphocyte-Derived HLA-Ligandome Using a Reverse Immunology Approach. Clin Cancer Res. 2015;21(9):2177-86.
29. Strønen E, Toebes M, Kelderman S, et al. Targeting of cancer neoantigens with donor-derived T cell receptor repertoires. Science. 2016;352(6291):1337-41.
30. Arber DA, Orazi A, Hasserjian R, et al. The 2016 revision to the World Health Organization classification of myeloid neoplasms and acute leukemia. Blood. 2016;127(20):2391-405.
31. Pratcorona M, Brunet S, Nomdedéu J, et al. Favorable outcome of patients with acute myeloid leukemia harboring a low-allelic burden FLT3-ITD mutation and concomitant NPM1 mutation: relevance to post-remission therapy. Blood. 2013;121(14):2734-8.
32. Greiner J, Ono Y, Hofmann S, et al. Mutated regions of nucleophosmin 1 elicit both CD4(+) and CD8(+) T-cell responses in patients with acute myeloid leukemia. Blood. 2012;120(6):1282-9.
33. Greiner J, Schneider V, Schmitt M, et al. Immune responses against the mutated region of cytoplasmatic NPM1 might contribute to the favorable clinical outcome of AML patients with NPM1 mutations (NPM1mut). Blood. 2013;122(6):1087-8.
34. Mardiros A, Forman SJ, Budde LE. T cells expressing CD123 chimeric antigen receptors for treatment of acute myeloid leukemia. Curr Opin Hematol. 2015;22(6):484-8.
35. Gill S, Tasian SK, Ruella M, et al. Preclinical targeting of human acute myeloid leukemia and myeloablation using chimeric antigen receptor-modified T cells. Blood. 2014;123(15):2343-54.
36. Amir AL, van der Steen DM, van Loenen MM, et al. PRAME-specific Allo-HLA-restricted T cells with potent antitumor reactivity useful for therapeutic T-cell receptor gene transfer. Clin Cancer Res. 2011;17(17):5615-25.
37. Provasi E, Genovese P, Lombardo A, et al. Editing T cell specificity towards leukemia by zinc finger nucleases and lentiviral gene transfer. Nat Med. 2012;18(5):807-15.
38. Morris EC, Stauss HJ. Optimizing T-cell receptor gene therapy for hematologic malignancies. Blood. 2016;127(26):3305-11.
39. Carreno BM, Magrini V, Becker-Hapak M, et al. Cancer immunotherapy. A dendritic cell vaccine increases the breadth and diversity of melanoma neoantigen-specific T cells. Science. 2015;348(6236):803-8.
40. Ott PA, Hu Z, Keskin DB, et al. An immunogenic personal neoantigen vaccine for patients with melanoma. Nature. 2017;547(7662):217-21.
41. Sahin U, Derhovanessian E, Miller M, et al. Personalized RNA mutanome vaccines mobilize poly-specific therapeutic immunity against cancer. Nature. 2017;547(7662):222-6.
42. Xie M, Lu C, Wang J, et al. Age-related mutations associated with clonal hematopoietic expansion and malignancies. Nat Med. 2014;20(12):1472-8.
43. Bowman RL, Busque L, Levine RL. Clonal Hematopoiesis and Evolution to Hematopoietic Malignancies. Cell Stem Cell. 2018;22(2):157-70.
44. Stone JD, Harris DT, Kranz DM. TCR affinity for p/MHC formed by tumor antigens that are self-proteins: impact on efficacy and toxicity. Curr Opin Immunol. 2015;33:16-22.
45. Corthay A, Skovseth DK, Lundin KU, et al. Primary antitumor immune response mediated by CD4+ T cells. Immunity. 2005;22(3):371-83.
46. Perez-Diez A, Joncker NT, Choi K, et al. CD4 cells can be more efficient at tumor rejection than CD8 cells. Blood. 2007;109(12):5346-54.

47. Tran E, Turcotte S, Gros A, et al. Cancer immunotherapy based on mutation-specific CD4+ T cells in a patient with epithelial cancer. Science. 2014;344(6184):641-5.
48. Kreiter S, Vormehr M, van de Roemer N, et al. Mutant MHC class II epitopes drive therapeutic immune responses to cancer. Nature. 2015;520(7549):692-6.
49. Morris EC, Tsallios A, Bendle GM, et al. A critical role of T cell antigen receptor-transduced MHC class I-restricted helper T cells in tumor protection. Proc Natl Acad Sci U S A. 2005;102(22):7934-9.
50. Fujiwara H, Ochi T, Ochi F, et al. Antileukemia multifunctionality of CD4(+) T cells genetically engineered by HLA class I-restricted and WT1-specific T-cell receptor gene transfer. Leukemia. 2015;29(12):2393-401.
51. Turtle CJ, Hanafi LA, Berger C, et al. Immunotherapy of non-Hodgkin's lymphoma with a defined ratio of CD8+ and CD4+ CD19-specific chimeric antigen receptor-modified T cells. Sci Transl Med. 2016;8(355):355ra116.
52. Turtle CJ, Hanafi LA, Berger C, et al. CD19 CAR-T cells of defined CD4+:CD8+ composition in adult B cell ALL patients. J Clin Invest. 2016;126(6):2123-38.
53. Busch DH, Fräßle SP, Sommermeyer D, et al. Role of memory T cell subsets for adoptive immunotherapy. Semin Immunol. 2016;28(1):28-34.
54. Gattinoni L, Speiser DE, Lichterfeld M, et al. T memory stem cells in health and disease. Nat Med. 2017;23(1):18-27.
55. Beatty GL, Gladney WL. Immune escape mechanisms as a guide for cancer immunotherapy. Clin Cancer Res. 2015;21(4):687-92.
56. Tran E, Robbins PF, Lu YC, et al. T-Cell Transfer Therapy Targeting Mutant KRAS in Cancer. N Engl J Med. 2016;375(23):2255-62.
57. McGranahan N, Rosenthal R, Hiley CT, et al. Allele-Specific HLA Loss and Immune Escape in Lung Cancer Evolution. Cell. 2017;171(6):1259-71.e11.
58. Zaretsky JM, Garcia-Diaz A, Shin DS, et al. Mutations Associated with Acquired Resistance to PD-1 Blockade in Melanoma. N Engl J Med. 2016;375(9):819-29.
59. Patel SJ, Sanjana NE, Kishton RJ, et al. Identification of essential genes for cancer immunotherapy. Nature. 2017;548(7669):537-42.
60. Manguso RT, Pope HW, Zimmer MD, et al. In vivo CRISPR screening identifies Ptpn2 as a cancer immunotherapy target. Nature. 2017;547(7664):413-8.
61. Bendle GM, Linnemann C, Hooijkaas AI, et al. Lethal graft-versus-host disease in mouse models of T cell receptor gene therapy. Nat Med. 2010;16(5):565-70.
62. van Loenen MM, de Boer R, Amir AL, et al. Mixed T cell receptor dimers harbor potentially harmful neoreactivity. Proc Natl Acad Sci U S A. 2010;107(24):10972-7.
63. Kuball J, Dossett ML, Wolfl M, et al. Facilitating matched pairing and expression of TCR chains introduced into human T cells. Blood. 2007;109(6):2331-8.
64. Berdien B, Mock U, Atanackovic D, et al. TALEN-mediated editing of endogenous T-cell receptors facilitates efficient reprogramming of T lymphocytes by lentiviral gene transfer. Gene Ther. 2014;21(6):539-48.
65. Mastaglio S, Genovese P, Magnani Z, et al. NY-ESO-1 TCR single edited stem and central memory T cells to treat multiple myeloma without graft-versus-host disease. Blood. 2017;130(5):606-18.
66. Roth TL, Puig-Saus C, Yu R, et al. Reprogramming human T cell function and specificity with non-viral genome targeting. Nature. 2018;559(7714):405-9.
67. Ivey A, Hills RK, Simpson MA, et al. Assessment of Minimal Residual Disease in Standard-Risk AML. N Engl J Med. 2016;374(5):422-33.

Supplemental information

Supplemental materials and methods

In vitro peptide stimulation

PBMCs harvested from AML patients who were in remission after chemotherapy were peptide stimulated *in vitro* following three different strategies. In strategy 1, PBMCs were stimulated with HLA-A*02:01–positive allogeneic irradiated EBV-LCLs that were pulsed with 10 μM CLAVEEVSL for 2 hours at 37°C in IMDM supplemented with 2% FBS, 1.5% l-glutamine and 1% penicillin/streptomycin at a ratio of 5:1 (PBMCs:EBV-LCLs). PBMCs were cultured in TCM without cytokines at a concentration of 0.5×10^6 cells/ml in 48-well flat-bottom culture plates. After 2 and 5 days, 100 IU/ml IL-2 and 10 ng/ml IL-15 (Miltenyi Biotec) were added. On day 11, bulk cultures were separately analyzed by flow cytometry. In strategy 2, PBMCs were stimulated with 20 μM CLAVEEVSL at a concentration of 10^7 cells/ml in IMDM supplemented with 2% FBS, 1.5% l-glutamine and 1% penicillin/streptomycin. After 2 hours of incubation at 37°C, PBMCs were diluted to 0.5×10^6 cells/ml in 48-well flat-bottom culture plates in TCM with 20 IU/ml IL-2. After 3 and 6 days, 100 IU/ml IL-2 and 10 ng/ml IL-15 were added. On day 11, PBMCs were restimulated with HLA-A*02:01–positive allogeneic irradiated PBMCs that were pulsed with 10 μM CLAVEEVSL as described above at a ratio of 5:1 (allogeneic PBMCs:PBMCs) in TCM with 100 IU/ml IL-2. On day 21, bulk cultures were separately analyzed by flow cytometry. In strategy 3, PBMCs were stimulated as described for strategy 2 with the exception that PBMCs were restimulated on day 11 with HLA-A*02:01–positive allogeneic PBMCs in the presence of 0.8 μg/ml PHA but absence of CLAVEEVSL. For all 3 strategies flow cytometric analysis was performed on PBMCs directly after thawing before peptide stimulation and on day 11 or 21 after peptide stimulation. For FACS analysis, all bulk cultures of approximately 1×10^6 peptide-stimulated PBMCs each were stained with FITC-conjugated antibodies against CD4, CD14, CD16 (catalog 335035) and CD19, a Pacific Blue-conjugated antibody against CD8 (catalog 558207) (BD Biosciences) and ΔNPM1-CLA tetramers conjugated to APC and PE to allow for combinatorial coding. Zombie Aqua was included as live/dead dye. Cells were measured on a BD LSR II using BD FACSDiva version 6 software and analysis was performed with FlowJo software.

Antibodies and FACS analysis of primary AMLs

Primary AMLs were stained with Alexa Fluor 700-conjugated anti-CD33 (catalog 561160), Brilliant Violet 421-conjugated anti-CD34 (catalog 562577), FITC-conjugated anti-CD58 (catalog 555920), PE-conjugated anti-CD80 (catalog 557227), PE-CF594-conjugated anti-CD86 (catalog 562390) (BD Biosciences) and APC-conjugated anti-CD54 (catalog 353112, Biolegend). HLA-A*02:01 staining was

performed indirectly with a mouse antibody against human HLA-A*02:01 (BB7.2) and FITC-conjugated goat anti-mouse Ig (catalog 349031, BD Biosciences). After HLA-A*02:01 staining, cells were blocked with 5% mouse serum, washed and stained with Alexa Fluor 700-conjugated anti-CD33 or Brilliant Violet 421-conjugated anti-CD34. Zombie Aqua was included as live/dead dye. Cells were measured on a BD LSR II using BD FACSDiva version 6 software and analysis was performed with FlowJo software.

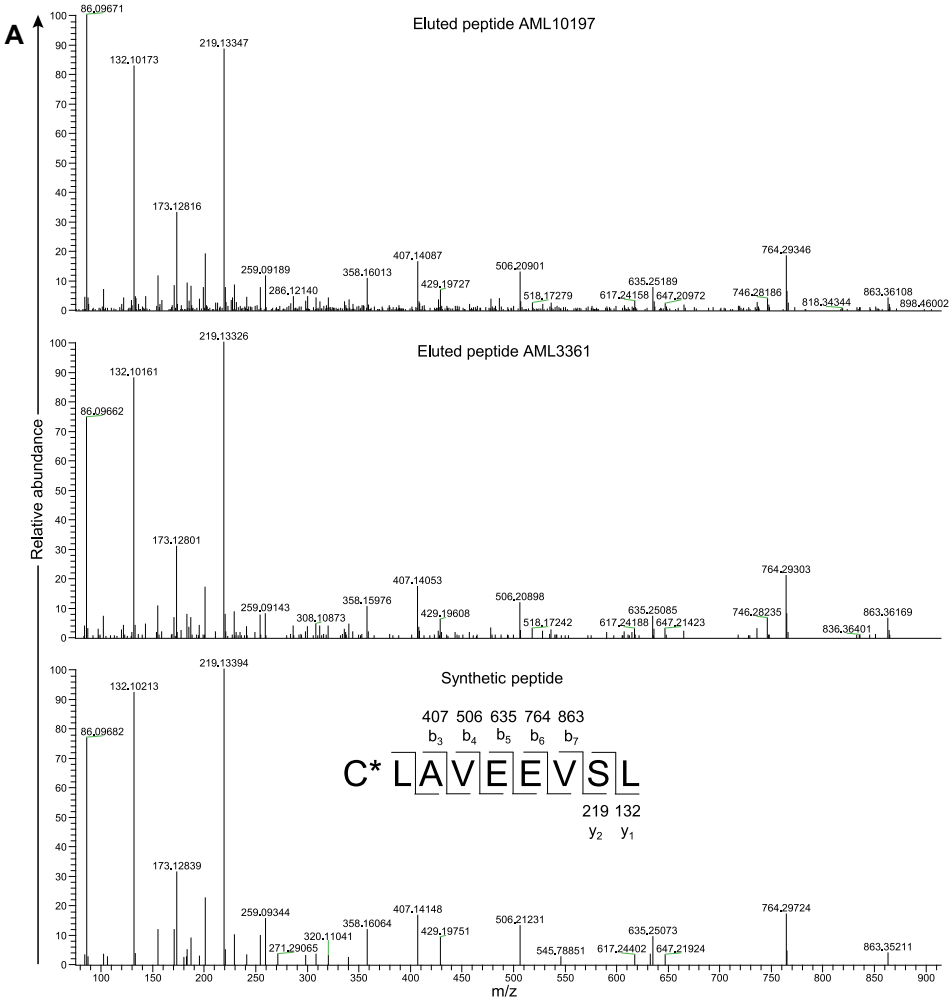
A
Eluted peptide AML10197
Eluted peptide AML3361
Synthetic peptide
407 506 635 764 863
b3 b4 b5 b6 b7
C* LAVEEVSL
219 132
y2 y1
Relative abundance
m/z

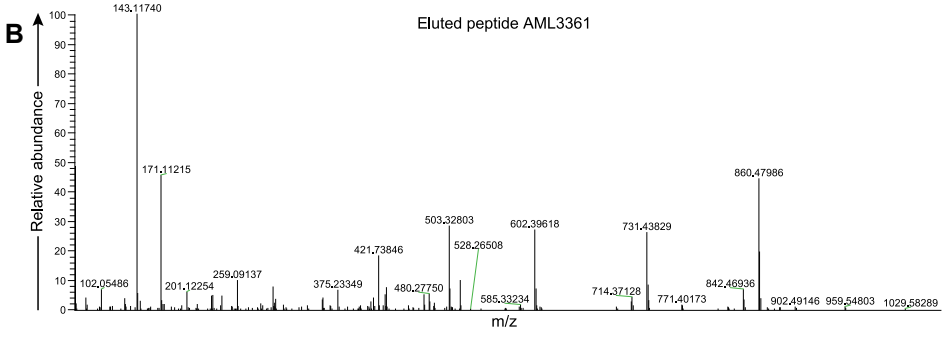
B
Eluted peptide AML3361
Relative abundance
m/z

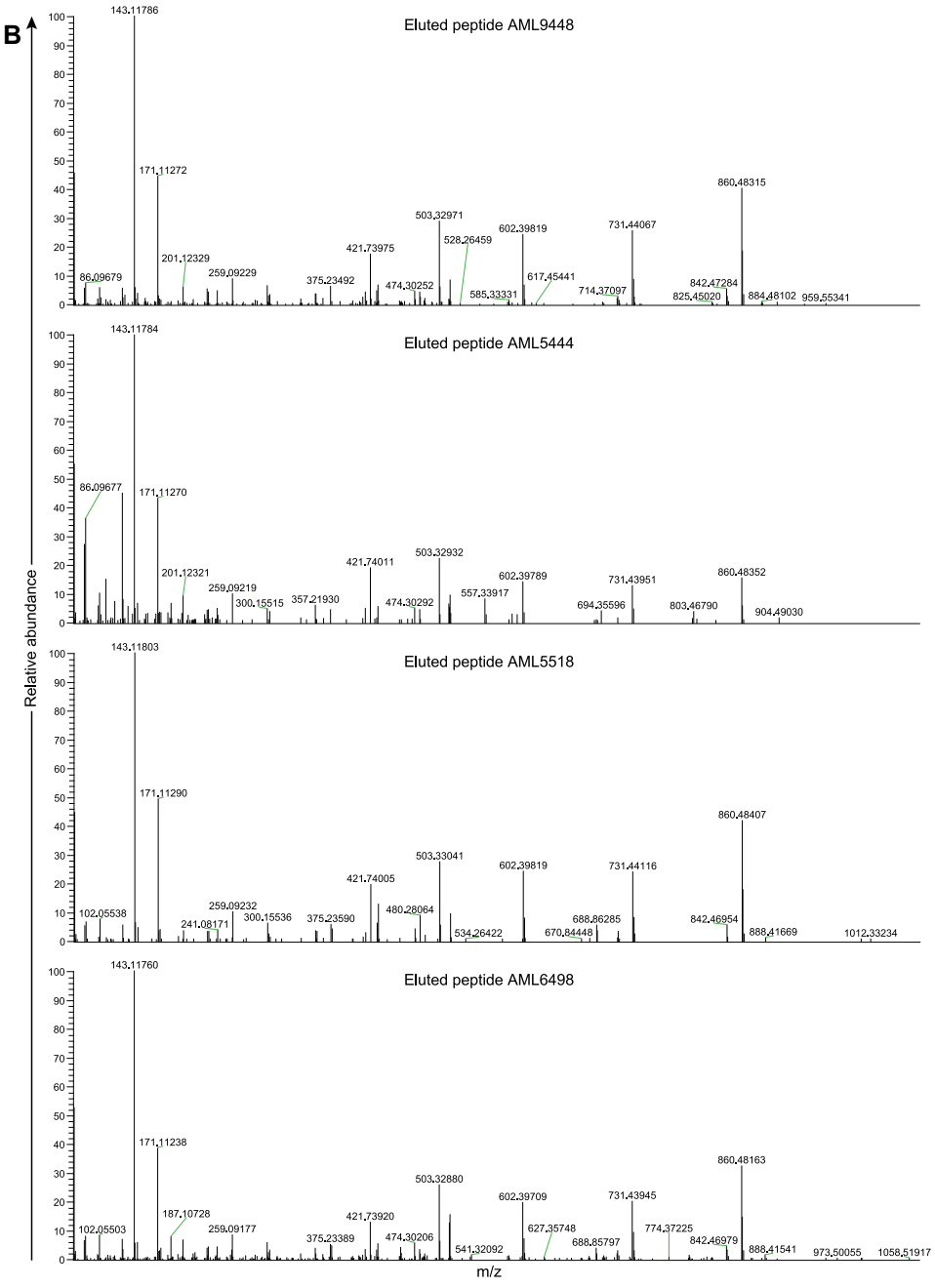
B
Eluted peptide AML9448
143.11786
171.11272
860.48315
503.32971
602.39819
731.44067
528.26459
421.73975
201.12329
86.09679
259.09229
375.23492
474.30252
617.45441
585.33331
714.37097
842.47284
825.45020
884.48102
959.55341
Eluted peptide AML5444
143.11784
86.09677
171.11270
503.32932
421.74011
602.39789
731.43951
860.48352
201.12321
259.09219
300.15515
357.21930
474.30292
557.33917
694.35596
803.46790
904.49030
Eluted peptide AML5518
143.11803
171.11290
860.48407
503.33041
602.39819
731.44116
421.74005
259.09232
102.05538
300.15536
375.23590
480.28064
241.08171
688.86285
842.46954
534.26422
670.84448
888.41669
1012.33234
Eluted peptide AML6498
143.11760
171.11238
860.48163
503.32880
602.39709
731.43945
187.10728
421.73920
102.05503
259.09177
375.23389
474.30206
627.35748
774.37225
688.85797
842.46979
541.32092
888.41541
973.50055
1058.51917
Relative abundance
m/z

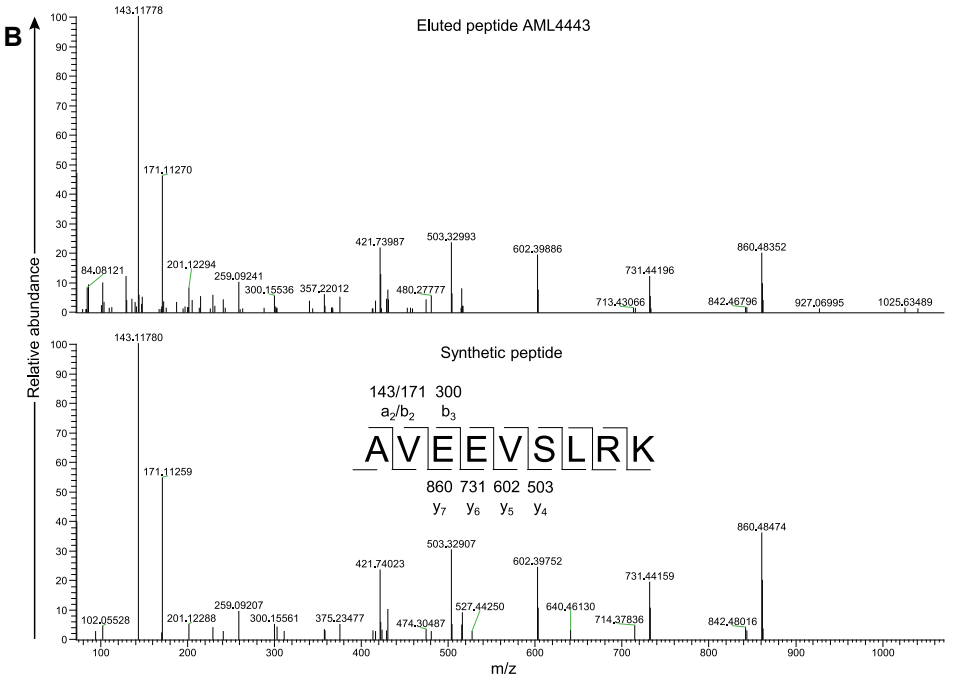
B
Eluted peptide AML4443
Synthetic peptide
143/171 300
a2/b2 b3
AVEEVSLRK
860 731 602 503
y7 y6 y5 y4
Relative abundance
m/z

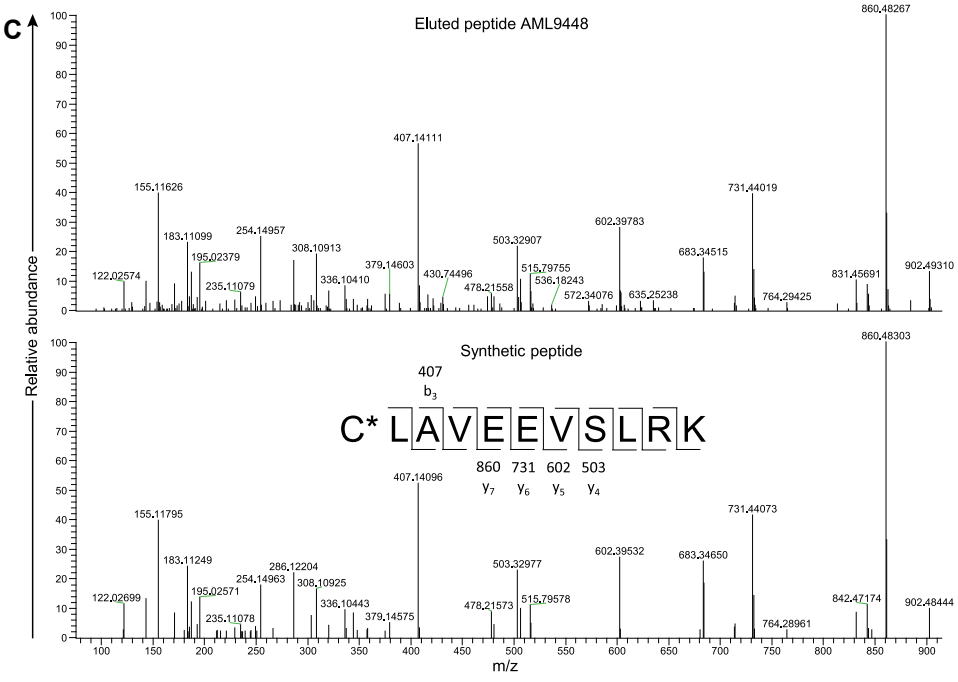
C
Eluted peptide AML9448
Synthetic peptide
407
b3
C* LAVEEVSLRK
860 731 602 503
y7 y6 y5 y4
Relative abundance
m/z

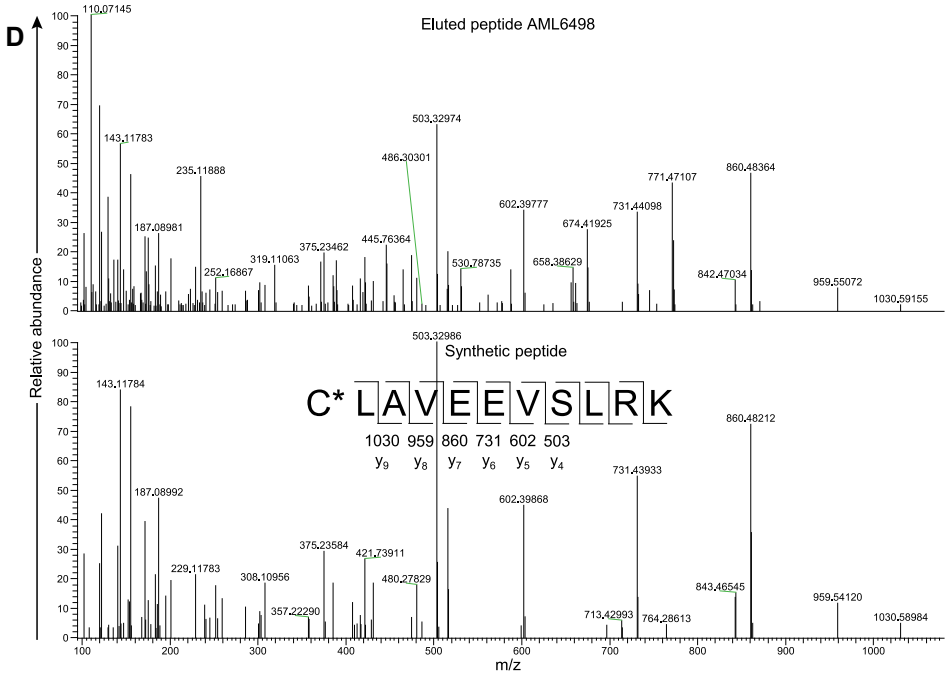
D
Eluted peptide AML6498
Relative abundance
110.07145
143.11783
235.11888
187.08981
252.16867
319.11063
375.23462
445.76364
486.30301
503.32974
530.78735
602.39777
658.38629
674.41925
731.44098
771.47107
842.47034
860.48364
959.55072
1030.59155
Synthetic peptide
503.32986
C* L A V E E V S L R K
1030 959 860 731 602 503
y9 y8 y7 y6 y5 y4
143.11784
187.08992
229.11783
308.10956
357.22290
375.23584
421.73911
480.27629
602.39868
731.43933
843.46545
860.48212
959.54120
1030.58984
713.42993
764.28613
m/z

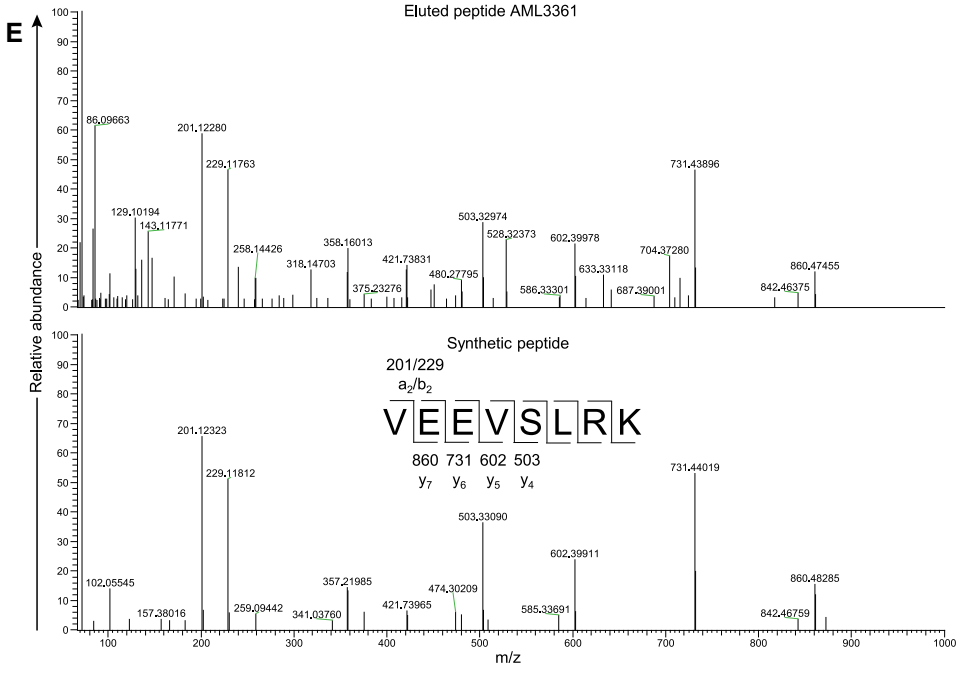
E
Eluted peptide AML3361
Relative abundance
86.09663
129.10194
143.11771
201.12280
229.11763
258.14426
318.14703
358.16013
375.23276
421.73831
480.27795
503.32974
528.32373
586.33301
602.39978
633.33118
687.39001
704.37280
731.43896
842.46375
860.47455
Synthetic peptide
201/229
a2/b2
V E E V S L R K
860 731 602 503
y7 y6 y5 y4
102.05545
157.38016
201.12323
229.11812
259.09442
341.03760
357.21985
421.73965
474.30209
503.33090
585.33691
602.39911
731.44019
842.46759
860.48285
m/z

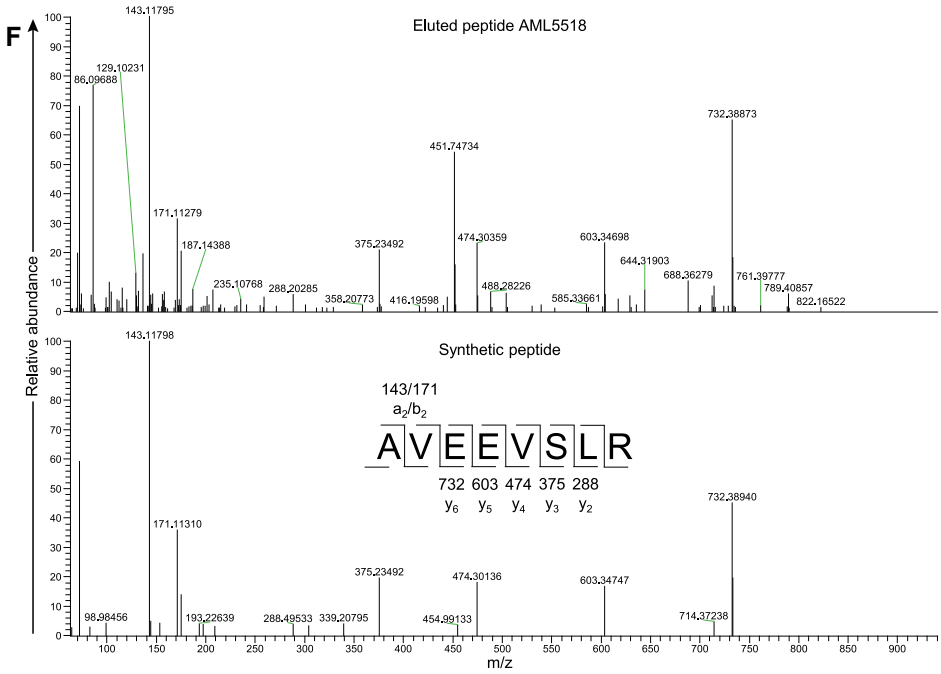

Figure S1. Validation of ΔNPM1-derived peptides eluted from primary AML. ΔNPM1-derived peptides were validated as HLA–binding peptides on primary AML by comparing tandem mass spectra between eluted peptides from AML and synthetic peptides. Matching tandem mass spectra are shown. C*, cysteinylation of the Cys residue. (**A**) Tandem mass spectra for eluted peptides from AML10197 (upper panel) and AML3361 (middle panel) and synthetic peptide C*LAVEEVSL (lower panel). (**B**) Tandem mass spectra for eluted peptides from AML3361 (first panel), AML9448 (second panel), AML5444 (third panel), AML5518 (fourth panel), AML6498 (fifth panel) and AML4443 (sixth panel) and synthetic peptide AVEEVSLRK (last panel). (**C**) Tandem mass spectra for an eluted peptide from AML9448 (upper panel) and synthetic peptide C*LAVEEVSLRK (lower panel). (**D**) Tandem mass spectra for an eluted peptide from AML6498 (upper panel) and synthetic peptide C*LAVEEVSLRK (lower panel). (**E**) Tandem mass spectra for an eluted peptide from AML3361 (upper panel) and synthetic peptide VEEVSLRK (lower panel). (**F**) Tandem mass spectra for an eluted peptide from AML5518 (upper panel) and synthetic peptide AVEEVSLR (lower panel).

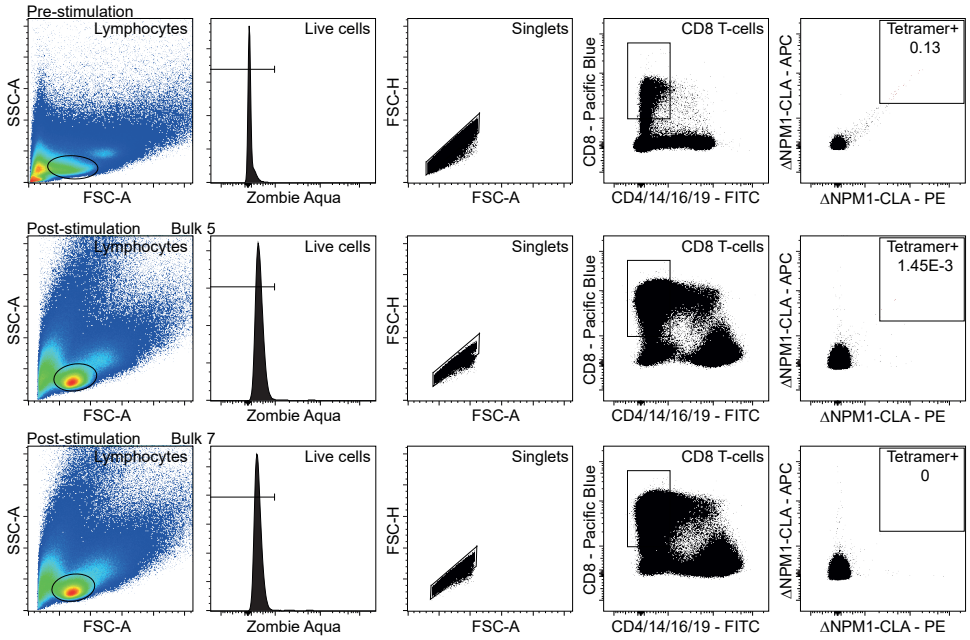

Figure S2. Screening for ΔNPM1-specific T cells in a representative patient with AML after *in vitro* peptide stimulation. PBMCs from AML patients who were in remission after chemotherapy were thawed and stimulated *in vitro* with CLAVEEVSL. A minimum of 1 × 10^6 total events were analyzed by flow cytometry before (pre-stimulation) and after (post-stimulation) peptide stimulation. Cells were stained with a Pacific Blue anti-CD8 antibody, a mix of FITC-conjugated anti-CD4, anti-CD14, anti-CD16 and anti-CD19 antibodies and ΔNPM1-CLA tetramers conjugated to APC and PE. Zombie Aqua was used as live/dead dye. A representative screening for ΔNPM1-specific T cells using combinatorial coding APC- and PE-conjugated ΔNPM1-CLA tetramers is shown for patient AML11282. Viable Zombie Aqua-negative single cells were selected and gated for Pacific Blue-positive FITC-negative $CD8^+$ T cells. Within this $CD8^+$ population, T cells that were double positive for APC- and PE-conjugated ΔNPM1-CLA tetramers were counted. Data are shown for PBMCs before peptide stimulation (upper panels) and two of the 14 bulk cultures after peptide stimulation (culture 5: middle panels; culture 7: lower panels).

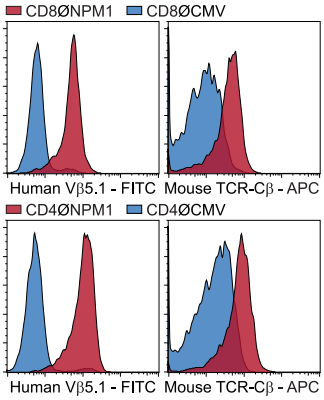

Figure S3. TCR staining after ΔNPM1 TCR gene transfer. TCR-transduced T cells were analyzed by flow cytometry at day 7 after transduction using anti-mouse TCR-Cβ - APC and anti-human TCR-Vβ5.1 - FITC antibodies. All TCR-transduced T cells stained positive for mouse TCR-Cβ. T cells transduced with the TCR for ΔNPM1 (CD8ØNPM1 and CD4ØNPM) were also positive for human TCR-Vβ5.1 (left panels). Results are shown for donor 1.

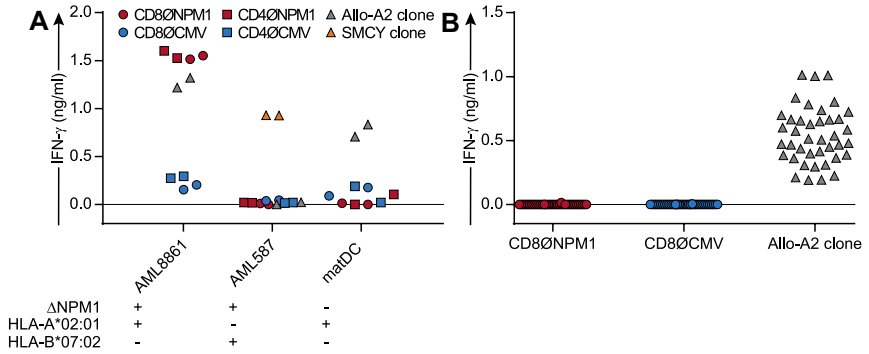

Figure S4. Lack of T cell reactivity against control samples. (**A**) TCR-transduced T cells were tested for reactivity against autologous monocyte-derived mature DCs (matDC) and AMLs with ΔNPM1 that were HLA-A*02:01–positive (AML8861) or –negative (AML587) by IFN-γ ELISA. $CD8^+$ (CD8ØNPM1; red circles) and $CD4^+$ (CD4ØNPM1; red squares) T cells with the TCR for ΔNPM1 reacted against AML8861, but not against AML587 or autologous mature DCs, whereas $CD8^+$ (CD8ØCMV; blue circles) and $CD4^+$ (CD4ØCMV; blue squares) T cells with the CMV-specific TCR failed to recognize both AML samples and autologous mature DCs. The allo-A2 clone (grey triangles) is included as a positive control for the autologous matDCs and AML8861. The HLA-B*07:02–restricted SMCY-specific $CD8^+$ T cell clone (orange triangles) is included as a positive control for the HLA-A*02:01–negative, but HLA-B*07:02–positive AML587 which was loaded with an HLA-B*07:02–binding SMCY peptide. Release of IFN-γ (ng/ml) in duplicate wells is shown for donor 2. (**B**) TCR-transduced $CD8^+$ T cells were tested for recognition of a panel of 40 HLA-A*02:01–positive allogeneic EBV-LCLs by IFN-γ ELISA. No reactivity against EBV-LCLs was observed for either CD8ØNPM1 (red circles) or CD8ØCMV (blue circles). The allo-A2 clone (grey triangles) is included as positive control. Mean release of IFN-γ (ng/ml) in duplicate wells is shown for donor 1.

Table S1. HLA class I binding prediction by NetMHCpan 3.0

Peptide	Predicted HLA class I binding affinity (nM)				
	A*01:01	A*02:01	A*03:01	A*11:01	Other HLA class I alleles[A]
CLAVEEVSL	27798.0	592.2	NA	33678.3	≥3562.6
AVEEVSLRK	16147.9	36154.8	534.4	58.2	≥1755.9
CLAVEEVSLRK	NA	NA	498.2	1111.8	≥5404.5
AVEEVSLR	31753.2	NA	NA	NA	≥39787.9
VEEVSLRK	NA	44597.1	NA	15474.5	≥38325.9

[A] Predicted binding affinity (nM) for all other HLA class I alleles as expressed by primary AMLs from which the indicated peptide has been eluted. NA. Not applicable.

Table S2. Direct isolation of ΔNPM1-specific T cells from patients with AML

Patient	Days after diagnosis[A]	PBMC[B] ($\times 10^6$)	Sorted T cells[C]	Growing clones	Tetramer clones[D]
AML10833	89	8.6	21	1	0
AML9559	107	6.4	2	2	0
AML6395	69	10.6	6	2	0
AML11282	81	8.0	12	0	-
AML9423	98	9.0	0	-	-
AML10418	108	7.5	0	-	-

[A] Number of days after diagnosis when peripheral blood for T cell isolation was collected. [B] Indicated are numbers of PBMCs from HLA-A*02:01–positive AML patients with ΔNPM1 that are used for T cell isolation. [C] PBMCs were stained with anti-CD8-Alexa Fluor 700 and a mix of PE-conjugated pHLA tetramers for CLAVEEVSL and its cysteinylated variant C*LAVEEVSL. Indicated are numbers of tetramer-positive $CD8^+$ T cells that are sorted. [D] Number of growing T cell clones positive for the ΔNPM1-CLA or ΔNPM1-C*LA tetramer.

Table S3. ΔNPM1-specific T cells in patients with AML after *in vitro* peptide stimulation

IVS[A]	Patient	Days after diagnosis[B]	PBMC[C] (×10^6)	No. bulks	CD8$^+$ T cells	
					% Tetramer[D] pre-stimulation	% Tetramer[E] post-stimulation
1	AML10833	89	4.9	10	0.051	0.000-0.005
	AML9559	107	3.2	7	0.044	0.000-0.009
2	AML10833	89	4.9	10	0.180	0.000-0.061
	AML9559	107	2.9	6	0.170	0.004-0.120
3	AML11282	81	7.0	14	0.130	0.000-0.001
	AML10418	108	6.5	13	0.083	0.000-0.002

[A] IVS, *in vitro* peptide stimulation strategy. Three different strategies for *in vitro* peptide stimulation have been followed as described in the supplemental methods. [B] Number of days after diagnosis when peripheral blood for T cell isolation was collected. [C] Indicated are numbers of PBMCs from HLA-A*02:01–positive AML patients with ΔNPM1 that are used for peptide stimulation. [D] Percentage of CD8$^+$ T cells that are positive for combinatorial coding ΔNPM1-CLA-APC and ΔNPM1-CLA-PE tetramers prior to peptide stimulation. [E] Percentage of CD8$^+$ T cells that are positive for combinatorial coding ΔNPM1-CLA-APC and ΔNPM1-CLA-PE tetramers after *in vitro* peptide stimulation. For each patient, the range of tetramer-positive CD8$^+$ T cells in different bulk cultures is shown.

Table S4. Flow cytometric analysis of primary AMLs

AML	Leukemic cells (%)[A]	HLA-A*02:01 (ΔMFI[B])	CD80 (MFI)	CD86 (MFI)	CD54 (MFI)	CD58 (MFI)
9559	93	1126	455	3821	8918	2135
7170	92	1558	201	1178	5786	1379
8861	98	380	55	198	186	369
10418	99	159	46	92	152	319
10594	27	444	81	491	2451	524
10833	92	1437	262	1440	3438	1413
3361	100	1236	108	294	1218	720
6395	84	1195	233	1254	11287	2061
10197	90	331	71	439	3896	451
1775	80	514	58	91	1682	414
2250	61	880	54	115	1954	774
2467	40	895	77	281	8722	612
4716	80	690	61	100	1563	589
EBV-LCL	-	4245	7555	22823	24005	5072

[A] Percentages of leukemic cells as determined by CD33 or CD34 expression in peripheral blood samples used for flow cytometric analysis. [B] HLA-A*02:01 staining was performed indirectly with a mouse antibody against human HLA-A*02:01 (BB7.2) and FITC-conjugated goat anti-mouse Ig. ΔMFI indicates the difference in geometric mean fluorescence intensity between AML stained with BB7.2 and goat anti-mouse Ig and AML stained with goat anti-mouse Ig only.

Table S5. ΔNPM1 gene expression and variant allele frequencies by RNA-sequencing[A]

AML	NPM1 CDS[B]	VAF[C]	ΔNPM1 protein	NPM1 reads	Total reads	NPM1/ total reads
9559	c.859_860insTCTG	34.47	p.Trp288CysfsTer12	9498	103961552	0.0000913607
7170	c.859_860insTCTG	35.28	p.Trp288CysfsTer12	12988	111732282	0.000116242
8861	c.860_861insCTGC	27.21	p.Trp288CysfsTer12	21735	101868266	0.000213364
10418	c.859_860insTCTG	37.08	p.Trp288CysfsTer12	30907	139712362	0.000221219
10594	c.859_860insTCTG	33.29	p.Trp288CysfsTer12	17041	148624447	0.000114658
10833	c.859_860insTCTG	32.17	p.Trp288CysfsTer12	10129	128443731	0.0000788594
3361	c.859_860insTCTG	46.33	p.Trp288CysfsTer12	21222	118571640	0.00017898
6395	c.859_860insTCTG	31.97	p.Trp288CysfsTer12	6310	160372609	0.0000393459
10197	c.860_861insCTGC	35.74	p.Trp288CysfsTer12	15039	105485637	0.000142569

[A] Paired-end RNA sequencing with a read length of 126 bp was performed on an Illumina HiSeq 2500 v4 sequencer to at least 12.5 Gbp per case. Mutations were detected by VARSCAN. [B] Indicated is the position and type of *NPM1* mutation in the coding sequence (CDS). [C] VAF, variant allele frequency.

Chapter 4

An HLA-A*11:01-binding neoantigen from mutated NPM1 as target for TCR gene therapy in AML

Dyantha I. van der Lee[1], Georgia Koutsoumpli[1], Rogier M. Reijmers[1], M. Willy Honders[1], Rob C. M. de Jong[1], Dennis F. G. Remst[1], Tassilo L. A. Wachsmann[1], Renate S. Hagedoorn[1], Kees L. M. C. Franken[2], Michel G. D. Kester[1], Karl J. Harber[1], Lisanne M. Roelofsen[1], Annemiek M. Schouten[1], Arend Mulder[2], Jan W. Drijfhout[2], Hendrik Veelken[1], Peter A. van Veelen[3], Mirjam H. M. Heemskerk[1], J.H. Frederik Falkenburg[1], Marieke Griffioen[1]

[1] Department of Hematology, Leiden University Medical Center, Leiden, The Netherlands
[2] Department of Immunology, Leiden University Medical Center, Leiden, The Netherlands
[3] Center for Proteomics and Metabolomics, Leiden University Medical Center, Leiden, The Netherlands

Cancers (Basel). 2021 Oct 27;13(21):5390
DOI: 10.3390/cancers13215390

Abstract

Acute myeloid leukemia (AML) is a hematological malignancy caused by clonal expansion of myeloid progenitor cells. Most patients with AML respond to chemotherapy, but relapses often occur and infer a very poor prognosis. Thirty to thirty-five percent of AMLs carry a four base pair insertion in the nucleophosmin 1 gene (*NPM1*) with a C-terminal alternative reading frame of 11 amino acids. We previously identified various neopeptides from the alternative reading frame of mutant NPM1 (dNPM1) on primary AML and isolated an HLA-A*02:01-restricted T-cell receptor (TCR) that enables human T-cells to kill AML cells upon retroviral gene transfer. Here, we isolated T-cells recognizing the dNPM1 peptide AVEEVSLRK presented in HLA-A*11:01. The TCR cloned from a T-cell clone recognizing HLA-A*11:01+ primary AML cells conferred *in vitro* recognition and lysis of AML upon transfer to CD8 T-cells, but failed to induce an anti-tumor effect in immunodeficient NSG mice engrafted with dNPM1 OCI-AML3 cells. In conclusion, our data show that AVEEVSLRK is a dNPM1 neoantigen on HLA-A*11:01+ primary AMLs. CD8 T-cells transduced with an HLA-A*11:01-restricted TCR for dNPM1 were reactive against AML *in vitro*. The absence of reactivity in a preclinical mouse model requires further preclinical testing to predict the potential efficacy of this TCR in clinical development.

Introduction

Acute myeloid leukemia (AML) is a hematological malignancy that is caused by clonal expansion of myeloid progenitor cells. Currently, intensive induction chemotherapy followed by consolidation chemotherapy or allogeneic hematopoietic stem cell transplantation remains the mainstay of treatment (1, 2). Although most patients respond to induction chemotherapy, complete remission without minimal residual disease is achieved in only half of patients (2, 3). Moreover, most patients that reach complete remission after induction or consolidation therapy eventually relapse (3). Despite the recent development of novel treatment modalities, curative options for patients with refractory or relapsed AML are limited.

Nucleophosmin 1 (*NPM1*) is the most frequently mutated gene in AML and occurs in 30–35% of patients (4, 5). Mutations in *NPM1* consist of four base pair insertions in exon 12, resulting in elongation of the mutated protein (dNPM1) by 4 amino acids and translation of the C-terminal 11 amino acids in an alternative reading frame (CLAVEEVSLRK) (6, 7). These recurrent *NPM1* mutations are essential leukemogenic driver events with expression of dNPM1 in all evolving leukemic subclones (8). Mutated *NPM1* is also retained by tumor cells in AML relapses (9-12). This makes dNPM1 an attractive target for immunotherapy of AML.

We previously demonstrated that multiple dNPM1-derived peptides are presented by HLA class I on primary AML. One of these peptides, HLA-A*02:01 (HLA-A2)-binding CLAVEEVSL, is a neoantigen that can be targeted by T-cell receptor (TCR) gene therapy (13). In addition to CLAVEEVSL, AVEEVSLRK has been eluted from primary AML as a dNPM1 peptide with predicted binding to HLA-A*03:01 (HLA-A3) and HLA-A*11:01 (HLA-A11) (13, 14). In this study, we investigated whether AVEEVSLRK is also a neoantigen that can be targeted by TCR gene therapy. We isolated various T-cells for AVEEVSLRK and cloned the TCR from one T-cell clone that reacted against HLA-A11+ dNPM1 primary AMLs. The TCR showed specific recognition and lysis of primary AMLs *in vitro* upon transfer to CD8 T-cells, but failed to induce an anti-tumor response in immunodeficient NSG mice engrafted with dNPM1 OCI-AML3 cells. The results confirm that AVEEVSLRK is a neoantigen on HLA-A11+ dNPM1 primary AMLs that can be targeted *in vitro* by CD8 T-cells transduced with the TCR for dNPM1. Whether the affinity of the TCR is sufficient to treat patients remains unclear.

Materials and methods

Cell collection and culture

Peripheral blood and bone marrow samples were collected from AML patients at diagnosis or relapse and from healthy individuals. Peripheral blood and bone marrow mononuclear cells (PBMCs and BMMCs) were separated with Ficoll-amidotrizoate (Leiden University Medical Center pharmacy) and cryopreserved. For assays, PBMCs and BMMCs from AML patients were thawed and cultured overnight in Iscove's Modified Dulbecco's Medium (IMDM) (Lonza, Novartis, Basel, Switzerland) with 10% heat-inactivated human ABO serum (hABOs) (Sanquin, Amsterdam, The Netherlands). B-cells and monocytes were isolated from PBMCs by magnetic-activated cell sorting (MACS) using CD19 MicroBeads and CliniMACS CD14 Reagent (Miltenyi Biotec, Bergisch Gladbach, Germany), respectively. B-cells or PBMCs were infected with Epstein–Barr virus (EBV) to create EBV-transformed lymphoblastoid cell lines (EBV-LCLs) (15). Mature dendritic cells (matDCs) were generated from monocytes as outlined previously (16). Cell lines T2 (ATCC, Manassas, VA, USA), K562 (ATCC), OCI-AML2 (DSMZ, Braunschweig, Germany) and OCI-AML3 (DSMZ) as well as EBV-LCLs and bone marrow samples from mice were cultured in IMDM with 10% heat-inactivated fetal bovine serum (FBS) (Gibco, Thermo Fisher Scientific, Waltham, MA, USA) and 1.5% 200 mM L-glutamine (Lonza). T-cells were cultured in T-cell medium (TCM) consisting of IMDM with 5% heat-inactivated FBS, 5% heat-inactivated hABOs, 1.5% L-glutamine and 100 IU/mL IL-2 (Novartis). T-cells were stimulated every 10–14 days with TCM containing irradiated (40 Gy) allogeneic PBMCs as feeder cells at a T-cell:feeder cell ratio of 1:5 and 0.8 µg/mL phytohemagglutinin (PHA) (Oxoid Limited, Thermo Fisher Scientific, Basingstoke, UK).

Peptide and peptide-HLA tetramer production

Peptides were synthesized in-house by standard Fmoc chemistry, dissolved in DMSO (Merck, Darmstadt, Germany) and stored at −20 °C. Monomers were produced as described previously (17), with minor adjustments. In short, β2M and recombinant HLA-A3 or -A11 heavy chains, as produced in *Escherichia coli*, were folded with peptides to create monomers that were subsequently biotinylated and purified by gel-filtration HPLC. Peptide-HLA (pHLA) tetramers were assembled by adding PE- or APC-conjugated streptavidin (Invitrogen, Thermo Fisher Scientific, Waltham, MA, USA) and stored at −80 °C.

Peptide-HLA class I binding assays

The dNPM1 AVEEVSLRK peptide and human immunodeficiency virus (HIV)-derived HLA-A3 and -A11-binding positive control peptide QVPLRPMTYK were dissolved in

DMSO to 10 mM and binding assays were performed as previously outlined (18). In short, 10-fold serial peptide dilutions were made in binding buffer consisting of 100 mM phosphate, 75 mM NaCl and 1 mM CHAPS at a final pH of 7 in a low protein-binding polypropylene 96-well microtiter plate (Costar, Corning, Corning, NY, USA). A mixture of 25 pmol HLA-A3 or -A11 heavy chain, 25 pmol β2M, 2 µL cOmplete Protease Inhibitor Cocktail (one tablet per 50 mL) (Roche, Basel, Switzerland), 100 fmol fluorescently labeled standard peptide KVFPC(FI)ALINK and 10 µL AVEEVSLRK or QVPLRPMTYK peptide dilution was incubated for 24 h at RT at a final volume of 100 µL per well in binding buffer. After incubation, 50 µL of the mixtures were analyzed on a Jasco AS-950 HPLC (JASCO, Easton, MD, USA) equipped with a 250 mm × 4.6 mm SynChropak GPC100 column (Eprogen, Downers Grove, IL, USA) that was isocratically run at 0.7 mL/min, with running buffer consisting of 100 mM phosphate, 75 mM NaCl, 1 mM CHAPS and 5% acetonitrile, at a final pH of 7. The column effluent was measured with a Jasco FP-920 fluorescence detector (JASCO) with excitation at 493 nm and emission at 516 nm. Two fluorescent peaks containing HLA-bound and unbound fluorescent peptide were detected at approximately 3.5 and 8 min, respectively. The HLA binding affinities of the peptides were deduced from their abilities to compete with the fluorescent peptide for pHLA-complex formation. Binding affinity was calculated from the dose-response curve and expressed as an IC50 value, indicating the concentration of peptide at which a 50% reduction of the area of the fluorescent pHLA-complex peak at 3.5 min was observed.

Isolation of dNPM1-specific T-cells

PBMCs were collected from fresh buffy coats of HLA-A3+ or -A11+ healthy individuals and stained with PE-conjugated pHLA-tetramers for 1 h at 4 °C. PBMCs were washed and incubated for 15 min with anti-PE MicroBeads (Miltenyi Biotec) at 4 °C and PE+ cells were isolated by MACS. Isolated cells were subsequently stained with anti-CD8 Alexa Fluor 700 (catalog MHCD0829) (Invitrogen) and anti-CD4 (catalog 555346), -CD14 (catalog 561712) and -CD19 (catalog 555412) FITC antibodies (BD Biosciences, Franklin Lakes, NJ, USA) for 30 min at 4 °C. CD8+ pHLA-tetramer+ T-cells were single-cell sorted by fluorescence-activated cell sorting (FACS) in 96-well tissue culture plates (Corning, Corning, NY, USA) containing 100 µL TCM, 50,000 irradiated (40 Gy) allogeneic PBMCs, 5000 irradiated (55 Gy) allogeneic EBV-LCLs and 0.8 µg/mL PHA per well.

Transduction of cell lines

The cell lines T2, K562, OCI-AML2 and OCI-AML3 were transduced with constructs encoding HLA-A3, HLA-A11, wild-type NPM1 (wtNPM1) or dNPM1 in combination with tNGFR or CD34 as markers. Cells were transduced in 24-well suspension culture plates (Greiner Bio-One, Kremsmünster, Austria) that had been coated with

30 µg/mL RetroNectin (TaKaRa Bio, Kusatsu, Japan) and blocked with 2% 200 g/L human serum albumin (Sanquin) in PBS (Fresenius Kabi, Bad Homburg, Germany). Retroviral supernatant was added and plates were centrifuged at 2000 *g* for 20 min at 4 °C. The retroviral supernatants were removed and 500 µL of cells, at a concentration of 400,000–600,000 cells/mL, was added to the wells. After overnight incubation, cells were transferred to 24-well tissue culture plates (Corning). The transduced cells were purified by MACS or FACS and their purity was assessed by FACS before their use in our experiments.

Generation of TCR-transduced T-cells for *in vitro* assays

The TCR α and β chain usage of dNPM1-specific clone 6F11 and EBV-specific clone 20–16 were determined as described previously (13, 19). Codon-optimized variable α and β chain sequences were synthesized and cloned in the MP71-TCR-flex retroviral vector containing murine–TCR-constant regions (20) by BaseClear. The constructs were transfected in phoenix-AMPHO packaging cells and the supernatants were harvested and stored at −80 °C. For TCR gene transfer, PBMCs from healthy individuals were thawed, resuspended in TCM and stimulated with T-cell TransAct (Miltenyi Biotec). After 2 days, cells were transduced with TCRs using the transduction protocol as described for cell lines. On day 11, TCR-transduced CD8 and CD4 T-cells were sorted by FACS using anti-CD8 PE (catalog 555367), anti-CD4 Pacific Blue (catalog 558116) and anti-mouse TCR β chain APC (catalog 553174) antibodies (BD Biosciences) and stimulated with TCM containing irradiated allogeneic PBMCs at a T-cell:feeder cell ratio of 1:5 and 0.8 µg/mL PHA. Experiments with TCR-transduced T-cells were performed 10–13 days after the second stimulation.

Antibodies and flow cytometry experiments

Cell sorting was performed with a BD FACS Aria II 3L or III 4L cell sorter and analyses were done with a BD FACS LSR II 4L Full or Fortessa 4L using BD FACSDiva software (BD Biosciences) at the Flow Cytometry Core Facility of the Leiden University Medical Center. FlowJo software (FlowJo, BD Biosciences, Ashland, OR, USA) was used to analyze data. Cells were stained in 96-well V-bottom plates (Greiner Bio-One) and incubated for 30 min at RT with the viability dye Zombie Aqua (BioLegend, San Diego, CA, USA) before additional incubations. The blocking of cells with PBS with 2% 200 g/L human serum albumin and 2.5% heat-inactivated hABOs was done for 15 min at 4 °C and antibody and pHLA-tetramer staining was done for 30 min at 4 °C. To analyze T-cells, 30,000–100,000 cells per well were blocked, followed by addition of anti-mouse TCR β chain APC antibody or pHLA-tetramers conjugated to PE or APC. Next, cells were washed and incubated with anti-CD8 FITC (catalog 555366) (BD Biosciences) and, in initial experiments, with anti-CD4 Pacific Blue antibodies. Primary AML cells were seeded at 30,000 cells per

well and blocked before the addition of antibody mixes containing anti-CD45 PE (catalog 555483) or FITC (catalog 345808), anti-CD33 Alexa Fluor 700 (catalog 561160) (BD Biosciences) and either anti-CD40 FITC (catalog MCA1590F), anti-CD54 PE (catalog MCA1615PE) (Bio-Rad, Hercules, CA, USA), anti-CD58 FITC (catalog 555920), anti-CD80 PE (catalog 557227), anti-CD86 PE (catalog 555658) (BD Biosciences) or anti-HLA-ABC FITC (catalog MCA81F) (Bio-Rad). Bone marrow samples from mice were thawed and 50,000 or 100,000 cells per well were blocked. For the staining of OCI-AML.bm10 cells in bone marrow, cells were washed and anti-CD40 FITC, anti-CD54 APC (catalog 353112) (BioLegend), anti-CD58 FITC, anti-CD80 FITC (catalog IM1853U) (Beckman Coulter Life Sciences, Indianapolis, IN, USA), anti-CD86 FITC (catalog 555657) or anti-PD-L1 Brilliant Violet 421 (catalog 563738) (BD Biosciences) antibodies were added. HLA-A2 and -A11 were stained indirectly by unlabeled mouse anti-HLA-A2 (clone BB7.2) (Leiden University Medical Center) or human anti-HLA-A11/-A3 (clone MUL4C8) (Department of Immunology, Leiden University Medical Center) primary antibodies, followed by goat anti-mouse IgG Alexa Fluor 647 (catalog A-21236) (Invitrogen) or rabbit anti-human IgG FITC (catalog F0056) (Dako, Agilent, Santa Clara, CA, USA) secondary antibodies, respectively (21). Cells that were stained with human anti-HLA-A11 were not blocked with heat-inactivated hABOs to prevent binding of the secondary rabbit anti-human IgG FITC antibody to non-relevant human IgG. For staining of T-cells in bone marrow, PE-conjugated pHLA-tetramers were added after blocking. Cells were washed and anti-CD8 Pacific Blue (catalog 558207), anti-PD-1 PE-Cy7 (catalog 561272), anti-HLA-DR FITC (catalog 347400) (BD Biosciences) and anti-mouse TCR β chain APC antibodies were added.

T-cell assays

T-cell recognition assays were performed in 384-well tissue culture plates (Greiner Bio-One) by co-culture of 2000 T-cells with varying numbers of stimulator cells in 40–80 µL of TCM per well. After overnight incubation, IFN-γ secretion was measured by enzyme-linked immunosorbent assay (ELISA) (Sanquin). Peptide pulsing of stimulator cells was performed for 2 h at 37 °C, after which cells were washed and incubated with T-cells. Chromium-51 release assays were performed as previously described (13). Percentage of specific lysis was calculated by: ((chromium-51 release of test—mean spontaneous chromium-51 release)/(mean maximum chromium-51 release—mean spontaneous chromium-51 release)) × 100%.

***In vivo* experiments**

In vivo experiments were conducted as previously outlined (13), with some modifications. Male NOD.Cg-*Prkdc*^{scid}*Il2rg*^{tm1Wjl}/SzJ (NOD *scid* gamma, NSG) mice (The Jackson Laboratory, Bar Harbor, ME, USA), 7–12 weeks of age, were inoculated i.v. with 1 × 10^6 OCI-AML3.bm10 cells. OCI-AML3.bm10 cells were

derived from an NSG mouse engrafted with the parental OCI-AML3 cell line transduced with luciferase (pCDH-EF1-Luc2-P2A-tdTomato Red; a gift from Kazuhiro Oka, Addgene plasmid #72486). OCI-AML3 cells that homed to the bone marrow were harvested and expanded *in vitro* to generate OCI-AML3.bm10 cells. In contrast to mice engrafted with parental OCI-AML3 cells, mice engrafted with OCI-AML3.bm10 cells do not develop solid tumors and are therefore more representative as model for human AML. OCI-AML3.bm10 cells were transduced with HLA-A11 coupled to tNGFR and sorted on tNGFR+ tdTomato Red+ cells by FACS. TCR-transduced T-cells were generated from an HLA-A2+ and -A11+ healthy individual. CD8 T-cells were isolated from PBMCs by MACS using CD8 MicroBeads (Miltenyi Biotec) and stimulated with T-cell TransAct. T-cells were transduced with a TCR on day 2, purified for TCR expression on day 8 by MACS using anti-mouse TCR β chain APC antibody and anti-APC MicroBeads and infused on day 11. Mice were infused i.v. with PBS only or with 6×10^6 T-cells in PBS with 2% heat-inactivated hABOs and 20 IU/mL IL-2 on day 11 after tumor inoculation. To monitor tumor growth, mice were infused i.p. with 200 µL 7.5 mM d-luciferin (Cayman Chemical, Ann Arbor, MI, USA) and anesthetized with 3–4% isoflurane. A CCD camera (IVIS spectrum, PerkinElmer, Waltham, MA, USA) was used to obtain bioluminescent images. Two weeks after T-cell injection, mice were sacrificed and bone marrow cells were harvested and cryopreserved.

Study approval

Materials were used from the Leiden University Medical Center Biobank for Hematological Diseases and were collected from individuals after written informed consent. The study was conducted according to the guidelines of the Declaration of Helsinki, and approved by the Institutional Review Board of the Leiden University Medical Center (approval number B16.039). Animal studies were conducted in accordance with institutional guidelines after obtaining permission from the national Ethical Committee for Animal Research (AVD116002017891) and in accordance with Dutch laws on animal experiments.

Results

AVEEVSLRK is an HLA-A11-binding neoantigen on primary AML

To validate HLA binding of AVEEVSLRK, a competition-based peptide-HLA class I binding assay was performed, in which soluble HLA molecules mixed with a fluorescein-labeled peptide were added to serial dilutions of AVEEVSLRK or QVPLRPMTYK, which is an HIV-derived positive control peptide that binds to HLA-A3 and -A11 (Figure 1A). AVEEVSLRK showed high affinity binding to HLA-A11 with an IC50 of 50.9 nM, which was similar to the IC50 of 51.2 nM for the HIV peptide. HLA-A3 binding affinity was lower, with an IC50 of 1332 nM as compared with 304 nM for the HIV peptide. These results confirm binding of AVEEVSLRK as dNPM1 peptide in HLA-A11 and -A3.

To investigate whether AVEEVSLRK is a neoantigen that can be targeted by specific T-cells, PBMCs from healthy individuals were screened using pHLA-tetramers for AVEEVSLRK in HLA-A3 and -A11 (Supplemental Table S1). Various tetramer+ T-cells were isolated and expanded for both HLA alleles, but only three HLA-A11-restricted T-cell clones produced IFN-γ upon coincubation with HLA-A11-transduced T2 cells pulsed with AVEEVSLRK (Figure 1B). These T-cells required higher peptide concentrations than the control T-cell clone, which recognizes EBV-derived AVFDRKSDAK in HLA-A11. Of the three T-cell clones, one clone (clone 6F11) was also reactive against three out of four HLA-A11+ primary AMLs with dNPM1 (9899, 10535 and 12364), while AML6498 with dNPM1 and two HLA-A11+ wtNPM1 AMLs were not recognized (Figure 1C and Supplemental Figure S1). CD8 T-cells transduced with an EBV-specific TCR for AVFDRKSDAK, which were included as positive control, also failed to react against dNPM1 AML6498 after peptide pulsing, whereas the other three dNPM1 AMLs and the two wtNPM1 AMLs were strongly recognized, illustrating that AML6498 has a general defect in stimulating T-cells. The reason for this failure may be absence or low surface expression of CD40, CD54, CD58, CD80, CD86 or HLA class I, as assessed by flow cytometry (Supplemental Figure S2). These data demonstrate that AVEEVSLRK is a dNPM1-derived neoantigen that could specifically be recognized on HLA-A11+ primary AMLs by clone 6F11.

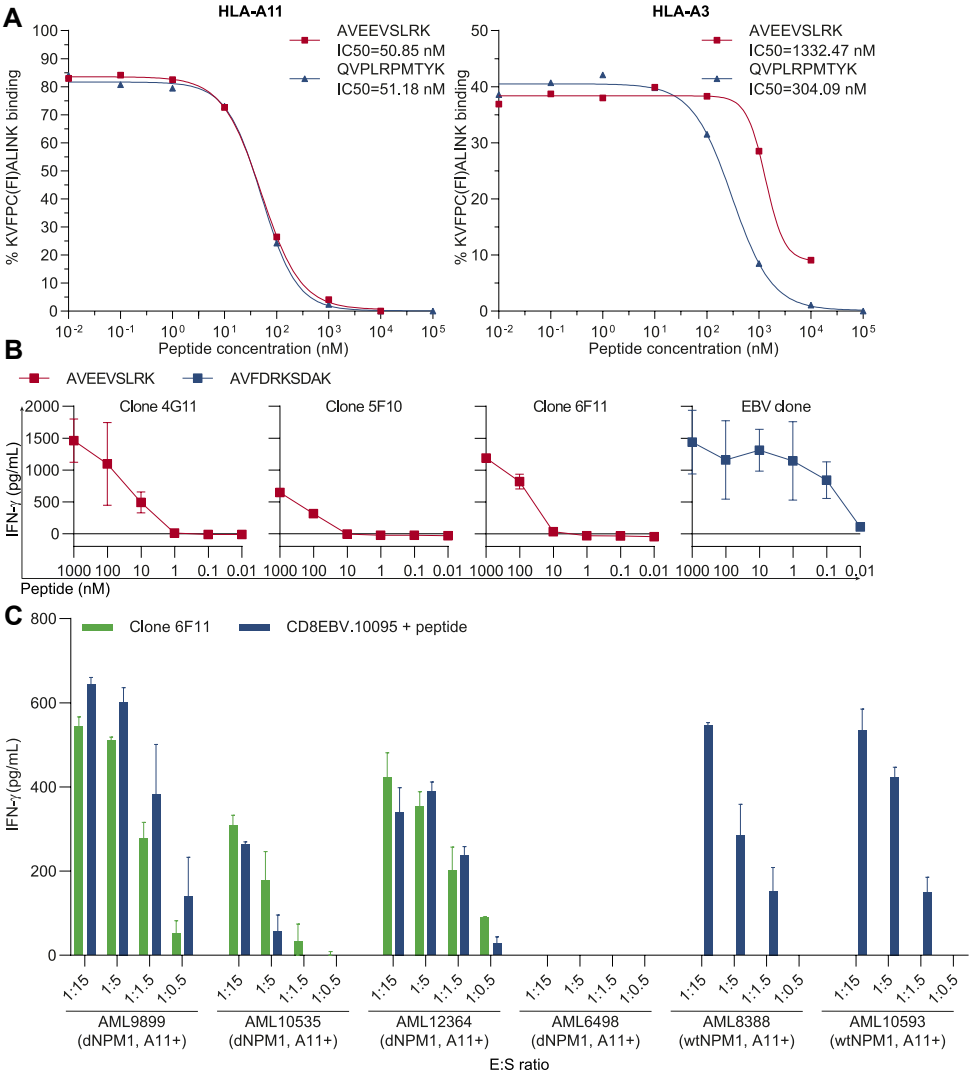

Figure 1. Clone 6F11 specifically recognizes dNPM1-derived AVEEVSLRK in HLA-A11. (**A**) Affinity of AVEEVSLRK for HLA-A*11:01 (HLA-A11) (left panel) and -A*03:01 (-A3) (right panel) was measured by a competition-based peptide-HLA class I binding assay in which fluorescein-labeled KVFPC(FI)ALINK and soluble HLA-A11 or -A3 were added to 10-fold dilutions of AVEEVSLRK (red line and squares) or QVPLRPMTYK (blue line and triangles), which is an human immunodeficiency virus (HIV) positive control peptide that binds to HLA-A11 as well as HLA-A3. After overnight incubation, fluorescence was measured by HPLC with a fluorescence detector and % binding of KVFPC(FI)ALINK was calculated. High-affinity binding was observed for AVEEVSLRK in HLA-A11 with an IC50 of 51 nM, which is similar to the IC50 of 51 nM for the positive control. Binding of AVEEVSLRK to HLA-A3 was lower, with an IC50 of 1332 nM as compared with the positive control with an IC50 of 304 nM. (**B**) Peripheral blood mononuclear cells (PBMCs) from HLA-A11+ healthy individuals were stained with peptide-HLA tetramers (pHLA-tetramers) consisting of AVEEVSLRK in HLA-A11, and tetramer+ CD8 T-cells were single-cell sorted by fluorescence-activated cell sorting (FACS). Expanded T-cell clones were incubated overnight with HLA-

A11-transduced T2 cells pulsed with titrated concentrations of AVEEVSLRK (red lines and squares) at an effector:stimulator (E:S) ratio of 1:7.5. IFN-γ secretion was measured by ELISA. Clones 4G11, 5F10 and 6F11 produced IFN-γ after coculture and required higher peptide concentrations than the control T-cell clone recognizing the Epstein–Barr virus (EBV)-derived peptide AVFDRKSDAK in HLA-A11 (blue line and squares). Symbols represent mean ± SD of duplicate wells. (**C**) T-cell clone 6F11 was tested for recognition of 6 HLA-A11+ primary acute myeloid leukemias (AMLs) at different E:S ratios. After overnight incubation, IFN-γ production was measured by ELISA. Clone 6F11 (green bars) reacted against three of four AMLs with mutated nucleophosmin 1 (dNPM1), while dNPM1 AML6498 and two AMLs with wild type NPM1 (wtNPM1) were not recognized. CD8 T-cells from donor 10095 transduced with an EBV-specific T-cell receptor (TCR) for AVFDRKSDAK in HLA-A11 (blue bars), which were included as positive control, also failed to recognize AML6498 after loading with 500 nM EBV peptide, whereas clear reactivity was observed against the other five peptide-loaded AMLs. Bars represent mean + SD of duplicate wells.

The HLA-A11-restricted TCR for dNPM1 specifically targets primary AML

To evaluate whether the TCR of clone 6F11 could be used to treat AML by gene therapy, the TCR was sequenced, cloned into the MP71-TCR-flex retroviral vector containing murine–TCR-constant regions and introduced into PBMCs from two HLA-A11+ healthy individuals (donors 10095 and 5963). The EBV-specific TCR recognizing AVFDRKSDAK in HLA-A11 was, again, included as a positive control. TCR-transduced CD8 and CD4 T-cells were separately sorted by FACS using antibodies against CD8, CD4 and the mouse TCR β chain, stimulated with irradiated allogeneic PBMCs, PHA and IL-2 and expanded for 10–13 days before analyses. Flow cytometry showed that 45% of CD8 T-cells and 11% of CD4 T-cells with the dNPM1 TCR specifically bound the NPM1-AVE-A11 tetramer, whereas 58% of CD8 T-cells and 29% of CD4 T-cells with the EBV TCR stained with the EBV-AVF-A11 tetramer (Figure 2A). Flow cytometry thus indicates that both TCRs were successfully introduced into CD8 and CD4 T-cells and that pHLA-tetramer binding is dependent on the CD8 co-receptor.

To examine functional activity, TCR-transduced T-cells were incubated with T2 cells transduced with HLA-A11 or -A3 that were exogenously pulsed with dNPM1 AVEEVSLRK or EBV AVFDRKSDAK (Figure 2B). CD8 T-cells with the dNPM1 TCR reacted against HLA-A11+ T2 cells with AVEEVSLRK, as did clone 6F11, but not against T2 cells with HLA-A3 or EBV peptide. CD4 T-cells with the dNPM1 TCR did not recognize peptide-pulsed T2 cells, supporting the observation that this TCR requires the CD8 co-receptor. CD8 T-cells with the dNPM1 TCR were also tested against K562 cells transduced with HLA-A11 or -A3 in combination with the dNPM1 or wtNPM1 gene (Figure 2C). Clone 6F11, as well as T-cells with the dNPM1 TCR, specifically secreted IFN-γ upon incubation with K562 cells with HLA-A11 and dNPM1. Furthermore, the HLA-A11-transduced cell line OCI-AML3 expressing endogenous dNPM1 was also recognized by T-cells with the dNPM1 TCR and clone 6F11, but not HLA-A11-transduced OCI-AML2 cells expressing wtNPM1 (Figure 2D).

Lastly, the potential off-target reactivity of the dNPM1 TCR was tested by screening reactivity against autologous matDCs, EBV-LCLs and PBMCs from both donors and EBV-LCLs from donor 11894, from whom clone 6F11 was isolated (Figure 2E). No reactivity against healthy hematopoietic cells was seen, except for EBV-LCLs from donor 11894, which showed weak recognition by dNPM1 TCR T-cells from donor 10095, but not by dNPM1 TCR T-cells from donor 5963 or clone 6F11. The functional activity of TCR-transduced T-cells was similar for both donors (Supplemental Figure S3). These data show that, upon transfer to CD8 T-cells, the HLA-A11-restricted TCR for dNPM1, as isolated from clone 6F11, is able to specifically target AVEEVSLRK on cell lines that are positive for HLA-A11 and dNPM1.

Figure 2. dNPM1-derived AVEEVSLRK in HLA-A11 can be targeted by TCR gene transfer. PBMCs from two HLA-A11+ healthy individuals (donors 10095 and 5963) were transduced with the TCR from clone 6F11 recognizing dNPM1 AVEEVSLRK in HLA-A11 and a control TCR for EBV AVFDRKSDAK in HLA-A11. The TCR-transduced CD8 and CD4 T-cells were sorted by FACS, stimulated and tested after 10–13 days. T-cells were incubated overnight with stimulator cells at an E:S ratio of 1:7.5 and IFN-γ secretion was measured by ELISA. In (**C**–**E**), stimulator cells were also pulsed with a mix of dNPM1 and EBV peptides at a concentration of 500 nM per peptide. Results are shown for donor 10095. Results for donor 5963 are shown in Supplemental Figure S3. (**A**) Purity of TCR-transduced T-cells was assessed by flow cytometry using antibodies against CD8 and CD4 and pHLA-tetramers. Staining with the NPM1-AVE-A11 tetramer was observed for 44.6% of CD8 and 11% of CD4 T-cells with the dNPM1 TCR (red) and 99.2% of clone 6F11 (green), whereas 58.2% and 29.2% of CD8 and CD4 T-cells with the EBV TCR (blue) stained with the EBV-AVF-A11 tetramer, respectively. (**B**) T2 cells transduced with HLA-A11 (squares) or -A3 (triangles) were pulsed with titrated concentrations of AVEEVSLRK (red) or AVFDRKSDAK (blue) and incubated with T-cells. Recognition of AVEEVSLRK in HLA-A11 was seen for CD8 T-cells with the dNPM1 TCR and clone 6F11, whereas CD8 and CD4 T-cells with the EBV TCR recognized AVFDRKSDAK in HLA-A11. CD4 T-cells with the dNPM1 TCR did not secrete IFN-γ, indicating that the function of the dNPM1 TCR is dependent on the CD8 co-receptor. (**C**) K562 cells transduced with dNPM1 or wtNPM1 and HLA-A11 or -A3 were tested for recognition by CD8 T-cells. T-cells with the dNPM1 TCR (red bars) and clone 6F11 (green bars) only reacted against K562 cells with HLA-A11 and dNPM1. After peptide pulsing, K562 cells with HLA-A11 were recognized by T-cells with the dNPM1 TCR regardless of NPM1 transduction status, as well as by T-cells with the EBV TCR (blue bars). (**D**) CD8 T-cells were tested against the AML cell lines OCI-AML3 with dNPM1 and OCI-AML2 with wtNPM1 transduced with HLA-A11 or -A3. T-cells with the dNPM1 TCR (red bars) and clone 6F11 (green bars) secreted IFN-γ upon incubation with OCI-AML3 with HLA-A11, but not OCI-AML2. Peptide-pulsed OCI-AML2 with HLA-A11 was only recognized by T-cells with the EBV TCR (blue bars), indicating poor exogenous pulsing of AVEEVSLRK. (**E**) CD8 T-cells were incubated with autologous PBMCs, mature dendritic cells (matDCs) and EBV-transformed lymphoblastoid cell lines (EBV-LCLs) from donors 10095 and 5963, and EBV-LCLs from donor 11894 from whom clone 6F11 was isolated. Except for EBV-LCLs from donor 11894, which showed weak recognition by T-cells with the dNPM1 TCR (red bars), healthy hematopoietic cells were not recognized by T-cells with the dNPM1 TCR or clone 6F11 (green bars), whereas T-cells with the EBV TCR (blue bars) reacted against EBV-LCLs from all three donors. EBV-LCLs were also recognized by dNPM1 T-cells after peptide loading, while peptide loaded matDCs and PBMCs were not recognized, again demonstrating the poor exogenous pulsing of AVEEVSLRK. Symbols and bars represent mean + SD of duplicate wells. *Figure on opposite page.*

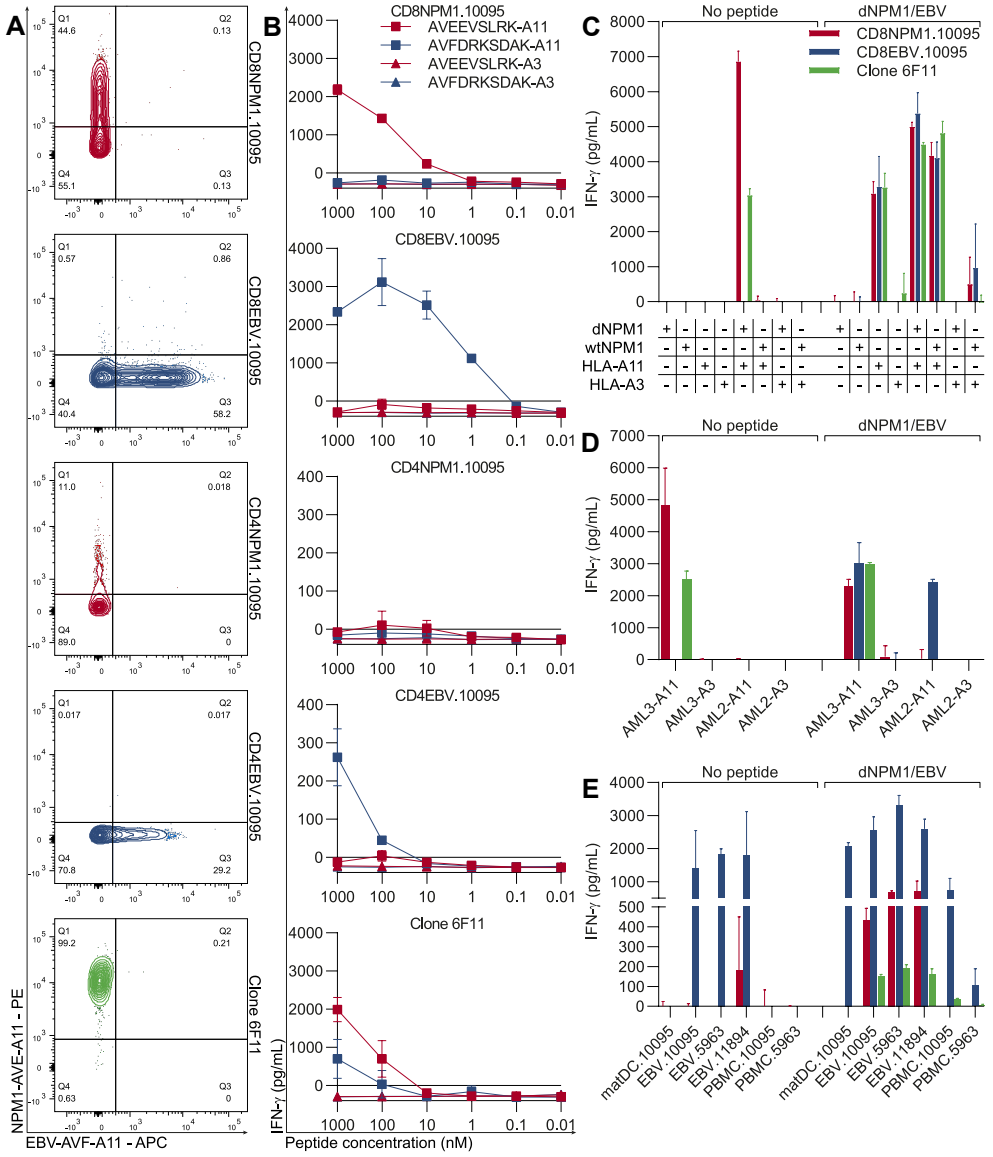

To investigate its potential use for therapy, CD8 T-cells from two HLA-A11+ healthy individuals (donors 10095 and 10231) were transduced with the dNPM1 TCR and tested for reactivity against 5 HLA-A11+ primary AMLs, including three dNPM1 and two wtNPM1 samples (Figure 3A). Similar as clone 6F11, CD8 T-cells with the dNPM1 TCR reacted against AMLs with dNPM1, while wtNPM1 AMLs were not recognized. Lastly, we examined T-cell-mediated killing of these five HLA-A11+

primary AMLs in a 9-h chromium-51 release assay (Figure 3B). Clone 6F11 as well as CD8 T-cells with the dNPM1 TCR showed specific lysis of dNPM1 AMLs, but not of wtNPM1 AMLs. The results were similar for both donors (Supplemental Figure S4). In conclusion, these results demonstrate that AVEEVSLRK is an HLA-A11-binding dNPM1 neoantigen that can be targeted on primary AML by TCR gene transfer.

The HLA-A11-restricted TCR for dNPM1 fails to target AML in mice

Since the TCR for dNPM1 is able to recognize and kill primary AML *in vitro*, we investigated its therapeutic potential in a mouse model. Male NSG mice were inoculated with 1 × 10^6 HLA-A2+ dNPM1 OCI-AML3.bm10 cells that were transduced with HLA-A11 and luciferase. After 11 days of tumor engraftment, mice were injected with PBS (*n* = 3) or 6 × 10^6 CD8 T-cells transduced with the HLA-A11-restricted dNPM1 TCR (*n* = 8), the HLA-A11-restriced EBV TCR as negative control (*n* = 7) or the HLA-A2-restricted dNPM1 TCR as positive control (*n* = 5). TCRs were introduced in CD8 T-cells from donor 3944, who was positive for both HLA-A2 and -A11, and TCR-transduced T-cells were purified for mouse TCR β chain expression by MACS (Supplemental Figure S5). Following T-cell injection, tumor growth was measured biweekly for 2 weeks, after which mice were sacrificed and their bone marrow was harvested. In contrast to HLA-A2 dNPM1 T-cells, which induced an anti-tumor response, no reduction in tumor load was observed in mice receiving HLA-A11 dNPM1 T-cells (Figure 4A). On the day of T-cell infusion, T-cells were also tested for recognition of OCI-AML3.bm10 *in vitro*. The HLA-A11 dNPM1 TCR clearly reacted against OCI-AML3.bm10, although IFN-γ release was lower than levels produced by T-cells with the HLA-A2 dNPM1 TCR (Figure 4B). We measured the frequencies of human T-cells in bone marrow samples harvested 2 weeks after infusion. Human T-cells were not detectable irrespective of the introduced TCR (Supplemental Figure S6). No major changes were observed in the phenotype of AML cells in bone marrow samples. Bone marrow samples were also cultured for 3 weeks and samples that showed outgrowth of OCI-AML3.bm10 cells were tested for T-cell recognition (Figure 4C). The data showed that HLA-A11 dNPM1 T-cells were able to recognize the AML cells, although IFN-γ levels were again lower than for HLA-A2 dNPM1 T-cells. In conclusion, despite clear reactivity *in vitro*, data from a preclinical mouse model suggest that the affinity of the HLA-A11 dNPM1 TCR is too low to provoke an anti-tumor response in NSG mice engrafted with OCI-AML3.bm10.

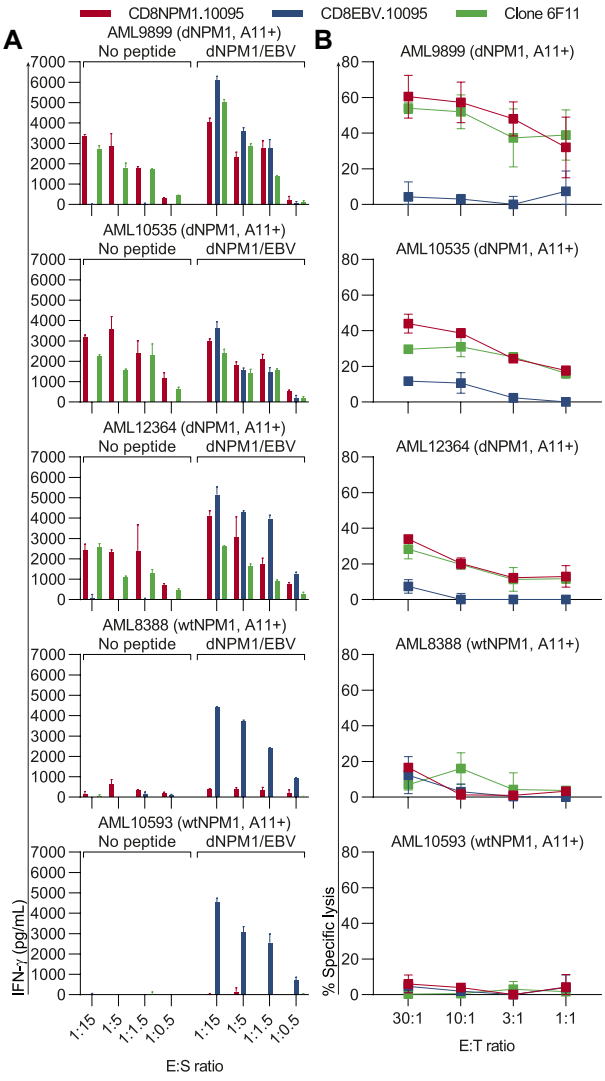

Figure 3. The HLA-A11-restricted dNPM1 TCR targets primary AML. CD8 T-cells transduced with the dNPM1 or EBV TCR were generated from two HLA-A11+ healthy individuals (donors 10095 and 10231). Results are shown for donor 10095. Results for donor 10231 are shown in Supplemental Figure S4. (**A**) T-cells were incubated overnight with five HLA-A11+ primary AMLs at different E:S ratios and IFN-γ secretion was measured by ELISA. AML cells were also pulsed with a mix of dNPM1 and EBV peptides at a concentration of 500 nM per peptide. T-cells with the dNPM1 TCR (red bars) and clone 6F11 (green bars) reacted against dNPM1 AMLs, while wtNPM1 AMLs were not recognized. T-cells with the EBV TCR (blue bars) recognized all five AMLs after peptide loading. Bars represent mean + SD of duplicate wells. (**B**) A 9-h chromium-51 release assay was performed to test T-cell cytotoxicity against five HLA-A11+ primary AMLs at different effector:target (E:T) ratios. T-cells with the dNPM1 TCR (red line) and clone 6F11 (green line) lysed dNPM1 AMLs, while wtNPM1 AMLs were not killed. T-cells with the EBV TCR (blue line) did not show lysis of primary AMLs. Symbols represent mean ± SD of triplicate wells.

Figure 4. The HLA-A11-restricted TCR for dNPM1 does not target AML in mice. Male NSG mice were injected i.v. with 1 × 10^6 OCI-AML3.bm10 (HLA-A*02:01+, dNPM1) cells that were transduced with HLA-A11 and luciferase. CD8 T-cells from an HLA-A*02:01+ (HLA-A2) and HLA-A11+ healthy individual (donor 3944) were transduced with a TCR on day 2, purified on mouse TCR β chain expression on day 8 and injected on day 11. After 11 days of tumor engraftment, mice were infused i.v. with PBS or 6 × 10^6 CD8 T-cells transduced with the HLA-A11 dNPM1 or EBV TCR or the HLA-A2 dNPM1 TCR. Tumor growth was monitored for 2 weeks after T-cell injection, after which mice were sacrificed and bone marrow was harvested. (**A**) *In vivo* growth of luciferase-transduced OCI-AML3.bm10 cells was measured twice per week by bioluminescent imaging. Depicted is the tumor burden in individual mice (left panel) and per treatment group (right panel). No effect was observed in mice treated with T-cells with the HLA-A11 dNPM1 TCR (*n* = 8, red line) or EBV TCR (*n* = 7, blue line) or in mice receiving PBS (*n* = 3, black line), whereas mice receiving HLA-A2 dNPM1 T-cells (*n* = 5, green line) showed a reduction in tumor growth. Symbols represent mean ± SD. (**B**) T-cells were tested on the day of infusion for recognition of OCI-AML3.bm10 cells *in vitro* at different E:S ratios. IFN-γ secretion was measured after overnight incubation by ELISA. T-cells transduced with the HLA-A11 dNPM1 TCR (red bars) clearly recognized OCI-AML3.bm10 cells, although IFN-γ production was lower as compared to the HLA-A2 dNPM1 TCR (green bars) or EBV TCR (blue bars; OCI-AML3.bm10 loaded with 1 μM EBV peptide). Bars represent mean + SD of duplicate wells. (**C**) Mouse bone marrow samples harvested 2 weeks after T-cell infusion were thawed and cultured for 3 weeks, and samples that showed outgrowth of AML cells were tested for T-cell recognition at an E:S ratio of 1:7.5. IFN-γ release was measured by ELISA after overnight incubation. TCR-transduced T-cells that were frozen on the day of infusion were thawed, stimulated and expanded for 11 days before testing. AML cells were also pulsed with a mix of dNPM1 and EBV peptides at a concentration of 500 nM per peptide. All AML samples were recognized by T-cells with the HLA-A11 dNPM1 TCR (red bars) or HLA-A2 dNPM1 TCR (green bars) and by T-cells with the EBV TCR (blue bars) after peptide loading, but IFN-γ release by T-cells with the HLA-A11 dNPM1 TCR was lower. Bars represent mean + SD of duplicate wells. *Figure on opposite page.*

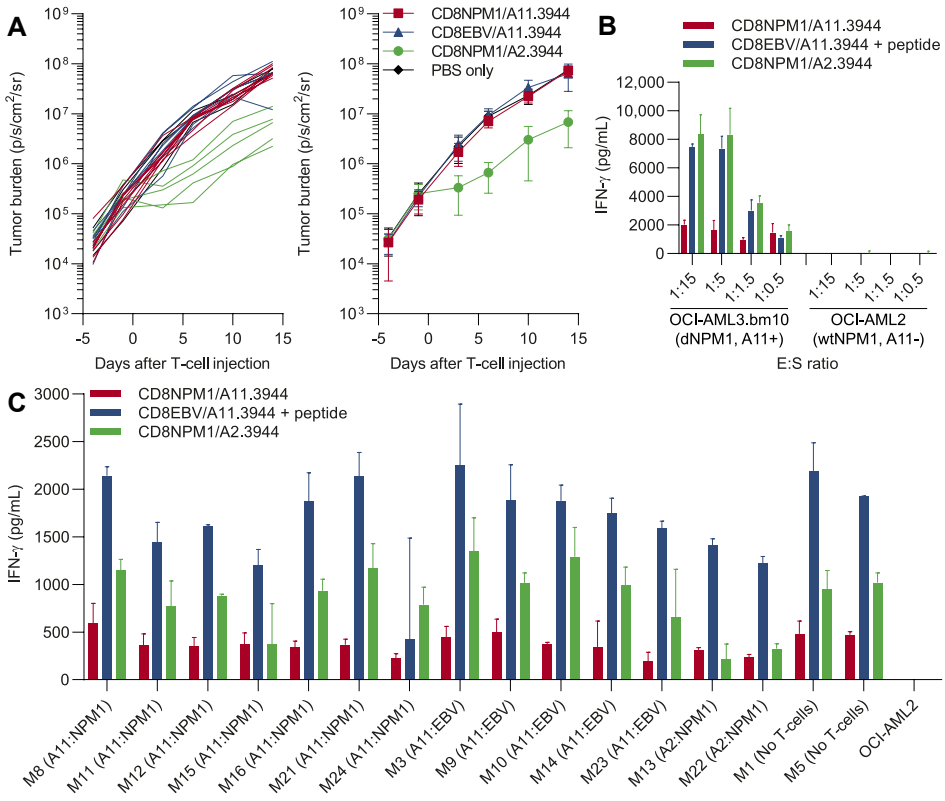
A
Tumor burden (p/s/cm²/sr)
Days after T-cell injection
CD8NPM1/A11.3944
CD8EBV/A11.3944
CD8NPM1/A2.3944
PBS only
B
CD8NPM1/A11.3944
CD8EBV/A11.3944 + peptide
CD8NPM1/A2.3944
IFN-γ (pg/mL)
1:15
1:5
1:1.5
1:0.5
OCI-AML3.bm10 (dNPM1, A11+)
OCI-AML2 (wtNPM1, A11-)
E:S ratio
C
CD8NPM1/A11.3944
CD8EBV/A11.3944 + peptide
CD8NPM1/A2.3944
IFN-γ (pg/mL)
M8 (A11:NPM1)
M11 (A11:NPM1)
M12 (A11:NPM1)
M15 (A11:NPM1)
M16 (A11:NPM1)
M21 (A11:NPM1)
M24 (A11:NPM1)
M3 (A11:EBV)
M9 (A11:EBV)
M10 (A11:EBV)
M14 (A11:EBV)
M23 (A11:EBV)
M13 (A2:NPM1)
M22 (A2:NPM1)
M1 (No T-cells)
M5 (No T-cells)
OCI-AML2

Discussion

Mutated *NPM1* is an attractive target for the immunotherapy of AML, since this driver mutation, which is present in 30–35% of patients, creates an alternative reading frame that leads to the presentation of multiple HLA-binding peptides on the leukemic cell surface. In this study, we isolated a T-cell clone for AVEEVSLRK in HLA-A11 that was able to specifically target HLA-A11+ primary AMLs *in vitro*. After gene transfer to CD8 T-cells, the TCR of this clone also showed recognition and lysis of primary AML *in vitro*. However, despite clear reactivity *in vitro*, TCR-transduced T-cells failed to induce an anti-tumor effect in NSG mice engrafted with dNPM1 OCI-AML3.bm10 cells. Our data thus demonstrate that AVEEVSLRK is a dNPM1-derived neoantigen on HLA-A11+ primary AML that can be recognized by specific T-cells. It remains unclear, however, whether the TCR that has been isolated for this neoantigen is of sufficient affinity to target AML in patients.

Although clone 6F11 clearly reacted against three dNPM1 AMLs, one dNPM1 AML was not recognized. This AML, when pulsed with EBV peptide, also failed to stimulate CD8 T-cells transduced with an EBV-specific TCR, indicating that this AML has a general defect in stimulating T-cells. This defect may be explained by the low expression of HLA class I and co-stimulation (CD40, CD80, CD86) and adhesion (CD54, CD58) molecules. Co-stimulation and adhesion molecules are essential for T-cell recognition (22), as confirmed by Brouwer et al. (23), who showed that the upregulation of CD40, CD54 and CD58 enhanced CD8 T-cell-mediated killing of two of three primary AMLs tested. This enhanced cytolytic effect was almost completely abolished by the simultaneous blocking of CD11a, CD54 and CD58. In another study (24), CD4 T-cells demonstrated less proliferation and cytokine release when stimulated with allogeneic primary AML in the presence of blocking antibodies against both CD80 and CD86. Similar to adhesion and co-stimulation molecules, several studies have demonstrated that T-cell responses against AMLs are impaired when HLA class I expression is low or absent (25-27). Altogether, these studies suggest that the failure of AML6498 to stimulate T-cells can be explained by its immune-evasive phenotype.

Despite clear recognition and lysis *in vitro*, T-cells with the dNPM1 HLA-A11 TCR did not induce an anti-tumor effect in immunodeficient mice engrafted with OCI-AML3.bm10. In contrast, similar as in our previous experiments (13), T-cells with the dNPM1 HLA-A2 TCR did reduce tumor load, although such control was temporary and did not prevent tumor outgrowth. Analysis of bone marrow samples collected 2 weeks after T-cell infusion indicated that the survival of human T-cells in NSG mice is poor, since no T-cells were found in any of the treatment groups. This is

independent of the antigen that is targeted, but rather due to a hostile environment in which human cytokines and supportive cell types are lacking, which are essential for the *in vivo* survival of *in vitro*-cultured human T-cells. As a result, only a short interaction can take place between human T-cells with dNPM1 TCRs and OCI-AML3.bm10 cells, which is insufficient to mediate tumor clearance. Therefore, the anti-tumor potential of dNPM1 TCRs are probably underestimated in this preclinical model.

In this study, NSG mice were only treated with CD8 T-cells, since the dNPM1 HLA-A11 TCR is not functional when introduced into CD4 T-cells (Figure 2B). This is in contrast to the dNPM1 HLA-A2 TCR, which is clearly reactive against AML after transfer to CD4 T-cells (13). We, therefore, treated NSG mice in previous experiments with a mix of CD8 and CD4 T-cells to investigate the efficacy of the dNPM1 HLA-A2 TCR, but did not expect any advantage of co-infusing CD8 and CD4 T-cells for the dNPM1 HLA-A11 TCR. However, co-infusion of CD4 T-cells expressing another TCR that is able to mediate cytokine release upon encountering AML cells or peptide vaccination may be considered to stimulate the *in vivo* expansion and survival of CD8 T-cells and, thereby, the capacity of the dNPM1 HLA-A11 TCR to induce an anti-tumor response.

Although efficacy cannot be accurately assessed in NSG mice, our *in vivo* data demonstrated a clear difference in tumor control between the HLA-A11 dNPM1 TCR and HLA-A2 dNPM1 TCR. For TCR gene therapy, it therefore seems advisable to identify an HLA-A11 TCR with higher affinity for dNPM1. One approach to identifying such a TCR is to follow the same or a similar strategy as that employed in this study and to continue searching for specific T-cells in individuals who are positive for the relevant HLA restriction allele. The advantage of isolating neoantigen-specific T-cells from healthy individuals is that such T-cells have not been subjected to immunosuppression by tumor cells (28). High-affinity TCRs can also be identified by searching for specific T-cells in healthy individuals who are negative for the relevant HLA restriction allele (29, 30). Various high-affinity TCRs for lineage- and tumor-associated antigens have successfully been isolated from HLA-mismatched individuals (29). However, since these T-cells have been educated in the thymus in the absence of the HLA allele of interest, high-affinity TCRs isolated from mismatched individuals require intensive screening for potential off-target toxicity. Besides searching for new TCRs, the affinity of an existing TCR can be enhanced by genetic engineering. This can be performed by random mutagenesis of CDR regions in the α and β chains, followed by the selection of high-affinity mutated TCRs by yeast (31), phage (32) or mammalian display (33). Also, more targeted methods for the mutagenesis of CDR regions have been described, including alanine-scanning to identify key amino acids in the interaction of TCRs with pHLA (34) and

structure-based designs (35, 36) to predict affinity-enhancing point mutations. Recently, high-affinity TCRs have also been created by somatic hypermutation in host cells transduced with activation-induced cytidine deaminase (37). Besides the genetic engineering of TCR regions directly interacting with pHLA, Thomas et al. (38) described amino acid replacements in framework regions of the α and β chain, thereby creating TCRs with improved cell surface expression and enhanced effector functions. Although these techniques show promising results in terms of efficacy, affinity-enhanced TCRs also carry the risk of toxicity through the targeting of HLA-binding peptides in healthy tissues. These peptides can be the target epitope that is expressed at low levels in healthy tissues (on-target toxicity) (39) or peptides similar to or completely different from the target epitope in the same or another HLA molecule (off-target toxicity) (40-42). However, promising clinical results have also been described (43) and genetic engineering may be considered to enhance the affinity of the HLA-A11 dNPM1 TCR as identified in this study.

In conclusion, we have here shown that AVEEVSLRK is a dNPM1 neoantigen on HLA-A11+ primary AML that can be recognized by T-cells. We isolated a TCR that targets AVEEVSLRK on primary AML *in vitro*, but this TCR lacked reactivity in a preclinical mouse model. Therefore, identification of an HLA-A11 TCR with enhanced affinity for dNPM1 for TCR gene therapy seems advisable. In addition to TCR gene therapy, AVEEVSLRK may also be a promising target for other immunotherapeutic strategies, such as neoantigen vaccination (44). These dNPM1-directed immunotherapies could provide new and effective treatment options for patients with relapsed or refractory AML.

Acknowledgments

The authors gratefully acknowledge the Flow cytometry Core Facility (FCF) of the Leiden University Medical Center in Leiden, The Netherlands for cell sorting assistance.

References

1. Short NJ, Rytting ME, Cortes JE. Acute myeloid leukaemia. Lancet. 2018;392(10147):593-606.
2. Döhner H, Estey E, Grimwade D, et al. Diagnosis and management of AML in adults: 2017 ELN recommendations from an international expert panel. Blood. 2017;129(4):424-47.
3. Döhner H, Weisdorf DJ, Bloomfield CD. Acute Myeloid Leukemia. N Engl J Med. 2015;373(12):1136-52.
4. Papaemmanuil E, Gerstung M, Bullinger L, et al. Genomic Classification and Prognosis in Acute Myeloid Leukemia. N Engl J Med. 2016;374(23):2209-21.
5. Ley TJ, Miller C, Ding L, et al. Genomic and epigenomic landscapes of adult de novo acute myeloid leukemia. N Engl J Med. 2013;368(22):2059-74.
6. Thiede C, Koch S, Creutzig E, et al. Prevalence and prognostic impact of NPM1 mutations in 1485 adult patients with acute myeloid leukemia (AML). Blood. 2006;107(10):4011-20.
7. Falini B, Mecucci C, Tiacci E, et al. Cytoplasmic nucleophosmin in acute myelogenous leukemia with a normal karyotype. N Engl J Med. 2005;352(3):254-66.
8. Falini B, Brunetti L, Sportoletti P, et al. NPM1-mutated acute myeloid leukemia: from bench to bedside. Blood. 2020;136(15):1707-21.
9. Cocciardi S, Dolnik A, Kapp-Schwoerer S, et al. Clonal evolution patterns in acute myeloid leukemia with NPM1 mutation. Nat Commun. 2019;10(1):2031.
10. Höllein A, Meggendorfer M, Dicker F, et al. NPM1 mutated AML can relapse with wild-type NPM1: persistent clonal hematopoiesis can drive relapse. Blood Adv. 2018;2(22):3118-25.
11. Ivey A, Hills RK, Simpson MA, et al. Assessment of Minimal Residual Disease in Standard-Risk AML. N Engl J Med. 2016;374(5):422-33.
12. Krönke J, Bullinger L, Teleanu V, et al. Clonal evolution in relapsed NPM1-mutated acute myeloid leukemia. Blood. 2013;122(1):100-8.
13. van der Lee DI, Reijmers RM, Honders MW, et al. Mutated nucleophosmin 1 as immunotherapy target in acute myeloid leukemia. J Clin Invest. 2019;129(2):774-85.
14. Narayan R, Olsson N, Wagar LE, et al. Acute myeloid leukemia immunopeptidome reveals HLA presentation of mutated nucleophosmin. PLoS One. 2019;14(7):e0219547.
15. Miller G, Shope T, Lisco H, et al. Epstein-Barr virus: transformation, cytopathic changes, and viral antigens in squirrel monkey and marmoset leukocytes. Proc Natl Acad Sci U S A. 1972;69(2):383-7.
16. Kremer AN, van der Meijden ED, Honders MW, et al. Endogenous HLA class II epitopes that are immunogenic in vivo show distinct behavior toward HLA-DM and its natural inhibitor HLA-DO. Blood. 2012;120(16):3246-55.
17. Garboczi DN, Hung DT, Wiley DC. HLA-A2-peptide complexes: refolding and crystallization of molecules expressed in Escherichia coli and complexed with single antigenic peptides. Proc Natl Acad Sci U S A. 1992;89(8):3429-33.
18. Tan TL, Geluk A, Toebes M, et al. A novel, highly efficient peptide-HLA class I binding assay using unfolded heavy chain molecules: identification of HIV-1 derived peptides that bind to HLA-A*0201 and HLA-A*0301. J Immunol Methods. 1997;205(2):201-9.
19. van Bergen CA, van Luxemburg-Heijs SA, de Wreede LC, et al. Selective graft-versus-leukemia depends on magnitude and diversity of the alloreactive T cell response. J Clin Invest. 2017;127(2):517-29.
20. Linnemann C, Heemskerk B, Kvistborg P, et al. High-throughput identification of antigen-specific TCRs by TCR gene capture. Nat Med. 2013;19(11):1534-41.
21. Parham P, Brodsky FM. Partial purification and some properties of BB7.2. A cytotoxic monoclonal antibody with specificity for HLA-A2 and a variant of HLA-A28. Hum Immunol. 1981;3(4):277-99.
22. Dustin ML. The immunological synapse. Cancer Immunol Res. 2014;2(11):1023-33.

23. Brouwer RE, Zwinderman KH, Kluin-Nelemans HC, et al. Expression and induction of costimulatory and adhesion molecules on acute myeloid leukemic cells: implications for adoptive immunotherapy. Exp Hematol. 2000;28(2):161-8.
24. Costello RT, Mallet F, Sainty D, et al. Regulation of CD80/B7-1 and CD86/B7-2 molecule expression in human primary acute myeloid leukemia and their role in allogenic immune recognition. Eur J Immunol. 1998;28(1):90-103.
25. Villalobos IB, Takahashi Y, Akatsuka Y, et al. Relapse of leukemia with loss of mismatched HLA resulting from uniparental disomy after haploidentical hematopoietic stem cell transplantation. Blood. 2010;115(15):3158-61.
26. Vago L, Perna SK, Zanussi M, et al. Loss of mismatched HLA in leukemia after stem-cell transplantation. N Engl J Med. 2009;361(5):478-88.
27. Brouwer RE, van der Heiden P, Schreuder GM, et al. Loss or downregulation of HLA class I expression at the allelic level in acute leukemia is infrequent but functionally relevant, and can be restored by interferon. Hum Immunol. 2002;63(3):200-10.
28. Karpanen T, Olweus J. The Potential of Donor T-Cell Repertoires in Neoantigen-Targeted Cancer Immunotherapy. Front Immunol. 2017;8:1718.
29. Falkenburg JH, Jedema I. Allo-reactive T cells for the treatment of hematological malignancies. Mol Oncol. 2015;9(10):1894-903.
30. Kunert A, Obenaus M, Lamers CHJ, et al. T-cell Receptors for Clinical Therapy: In Vitro Assessment of Toxicity Risk. Clin Cancer Res. 2017;23(20):6012-20.
31. Holler PD, Holman PO, Shusta EV, et al. In vitro evolution of a T cell receptor with high affinity for peptide/MHC. Proc Natl Acad Sci U S A. 2000;97(10):5387-92.
32. Li Y, Moysey R, Molloy PE, et al. Directed evolution of human T-cell receptors with picomolar affinities by phage display. Nat Biotechnol. 2005;23(3):349-54.
33. Chervin AS, Aggen DH, Raseman JM, et al. Engineering higher affinity T cell receptors using a T cell display system. J Immunol Methods. 2008;339(2):175-84.
34. Malecek K, Zhong S, McGary K, et al. Engineering improved T cell receptors using an alanine-scan guided T cell display selection system. J Immunol Methods. 2013;392(1-2):1-11.
35. Haidar JN, Pierce B, Yu Y, et al. Structure-based design of a T-cell receptor leads to nearly 100-fold improvement in binding affinity for pepMHC. Proteins. 2009;74(4):948-60.
36. Malecek K, Grigoryan A, Zhong S, et al. Specific increase in potency via structure-based design of a TCR. J Immunol. 2014;193(5):2587-99.
37. Bassan D, Gozlan YM, Sharbi-Yunger A, et al. Optimizing T-cell receptor avidity with somatic hypermutation. Int J Cancer. 2019;145(10):2816-26.
38. Thomas S, Mohammed F, Reijmers RM, et al. Framework engineering to produce dominant T cell receptors with enhanced antigen-specific function. Nat Commun. 2019;10(1):4451.
39. Parkhurst MR, Yang JC, Langan RC, et al. T cells targeting carcinoembryonic antigen can mediate regression of metastatic colorectal cancer but induce severe transient colitis. Mol Ther. 2011;19(3):620-6.
40. Morgan RA, Chinnasamy N, Abate-Daga D, et al. Cancer regression and neurological toxicity following anti-MAGE-A3 TCR gene therapy. J Immunother. 2013;36(2):133-51.
41. Cameron BJ, Gerry AB, Dukes J, et al. Identification of a Titin-derived HLA-A1-presented peptide as a cross-reactive target for engineered MAGE A3-directed T cells. Sci Transl Med. 2013;5(197):197ra03.
42. Linette GP, Stadtmauer EA, Maus MV, et al. Cardiovascular toxicity and titin cross-reactivity of affinity-enhanced T cells in myeloma and melanoma. Blood. 2013;122(6):863-71.
43. Johnson LA, June CH. Driving gene-engineered T cell immunotherapy of cancer. Cell Res. 2017;27(1):38-58.
44. Schmitt S, Tahk S, Lohner A, et al. Fusion of Bacterial Flagellin to a Dendritic Cell-Targeting αCD40 Antibody Construct Coupled With Viral or Leukemia-Specific Antigens Enhances Dendritic Cell Maturation and Activates Peptide-Responsive T Cells. Front Immunol. 2020;11:602802.

Supplemental information

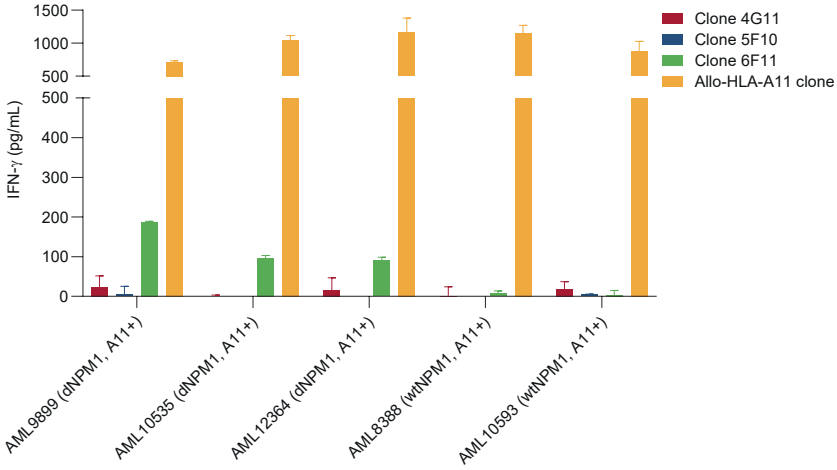

Figure S1. Clone 6F11 recognizes primary AMLs. T-cell clones 4G11 (red bars), 5F10 (blue bars) and 6F11 (green bars) were tested for recognition of 5 HLA-A11+ primary AMLs at an E:S ratio of 1:15. After overnight incubation, IFN-γ production was measured by ELISA. Clone 6F11 reacted against AMLs with dNPM1, while wtNPM1 AMLs were not recognized. Clones 4G11 and 5F10 did not show recognition of primary AMLs. An allo-HLA-A11 clone (orange bars) was included as positive control and reacted against all 5 HLA-A11+ AMLs. Bars represent mean + SD of duplicate wells.

Figure S2. Surface expression of HLA class I, co-stimulation and adhesion molecules on primary AML. Primary AML samples were stained with a mix of anti-CD45 FITC or PE antibody, anti-CD33 Alexa Fluor 700 antibody and either anti-CD40 FITC, anti-CD54 PE, anti-CD58 FITC, anti-CD80 PE, anti-CD86 PE or anti-HLA class I FITC antibodies. Dead cells were excluded using Zombie Aqua. (**A**) Depicted is the gating strategy for measuring surface expression of HLA class I, costimulation and adhesion molecules on AML in a representative staining for AML9899. Using CD45, AML blasts ($CD45^{dim}$) were distinguished from other peripheral blood or bone marrow mononuclear cells ($CD45^{high}$). Next, CD33+ blasts were selected from viable single cells and expression of various adhesion and co-stimulation molecules within CD33+ AML blasts was determined using Fluorescence Minus One (FMO) controls without FITC (top panels) or PE (lower panels). (**B**-**G**) Staining for CD40 (**B**), CD54 (**C**), CD58 (**D**), CD80 (**E**), CD86 (**F**) and HLA-class I (**G**) on AML cells (blue histograms). Expression of CD40, CD54, CD58, CD80, CD86 and HLA class I was absent or low on dNPM1 AML6498, which correlated with absence of T-cell recognition. Black histograms depict FMO controls. *Figure on next page.*

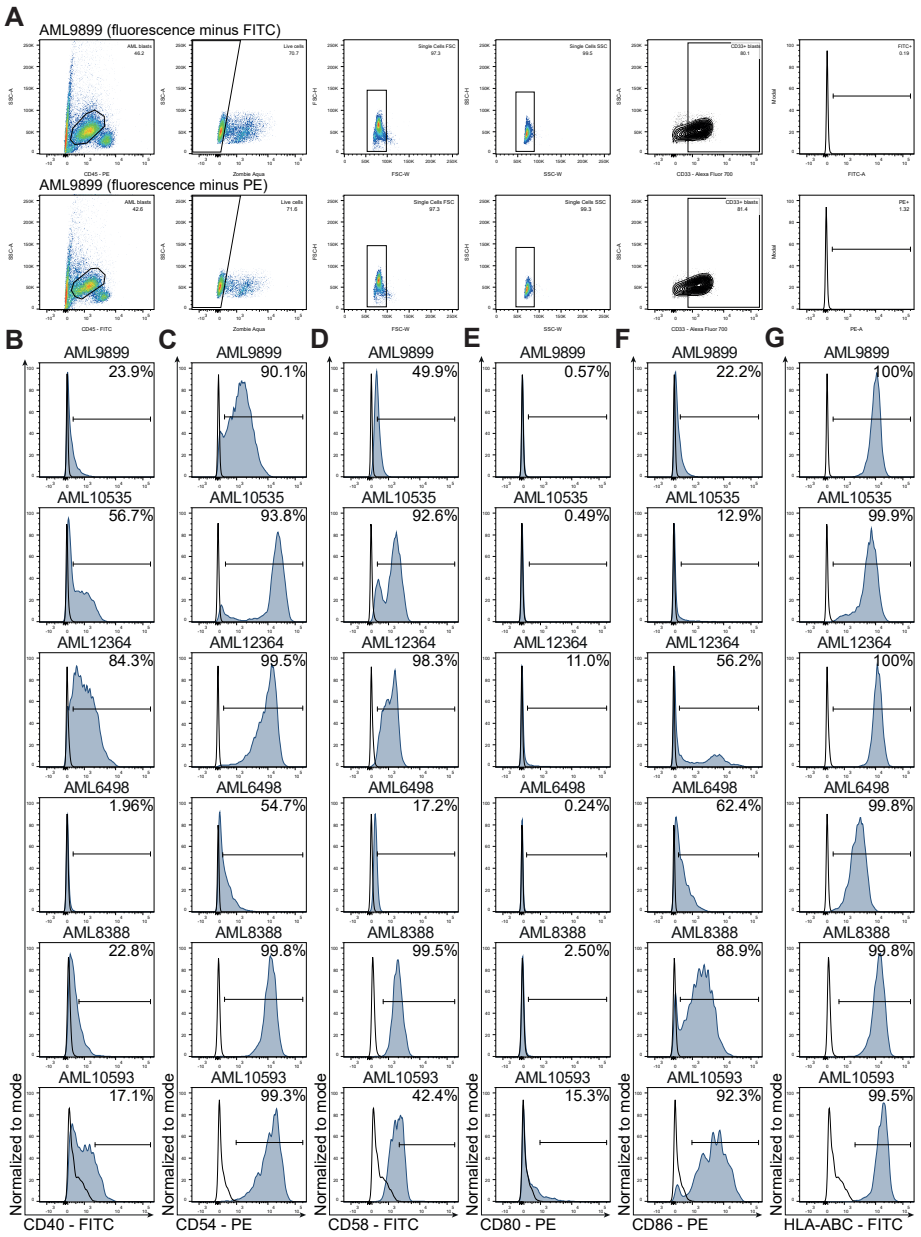
A
AML9899 (fluorescence minus FITC)
AML9899 (fluorescence minus PE)
B
C
D
E
F
G
AML9899
AML10535
AML12364
AML6498
AML8388
AML10593
23.9%
56.7%
84.3%
1.96%
22.8%
17.1%
90.1%
93.8%
99.5%
54.7%
99.8%
99.3%
49.9%
92.6%
98.3%
17.2%
99.5%
42.4%
0.57%
0.49%
11.0%
0.24%
2.50%
15.3%
22.2%
12.9%
56.2%
62.4%
88.9%
92.3%
100%
99.9%
100%
99.8%
99.8%
99.5%
Normalized to mode
CD40 - FITC
CD54 - PE
CD58 - FITC
CD80 - PE
CD86 - PE
HLA-ABC - FITC

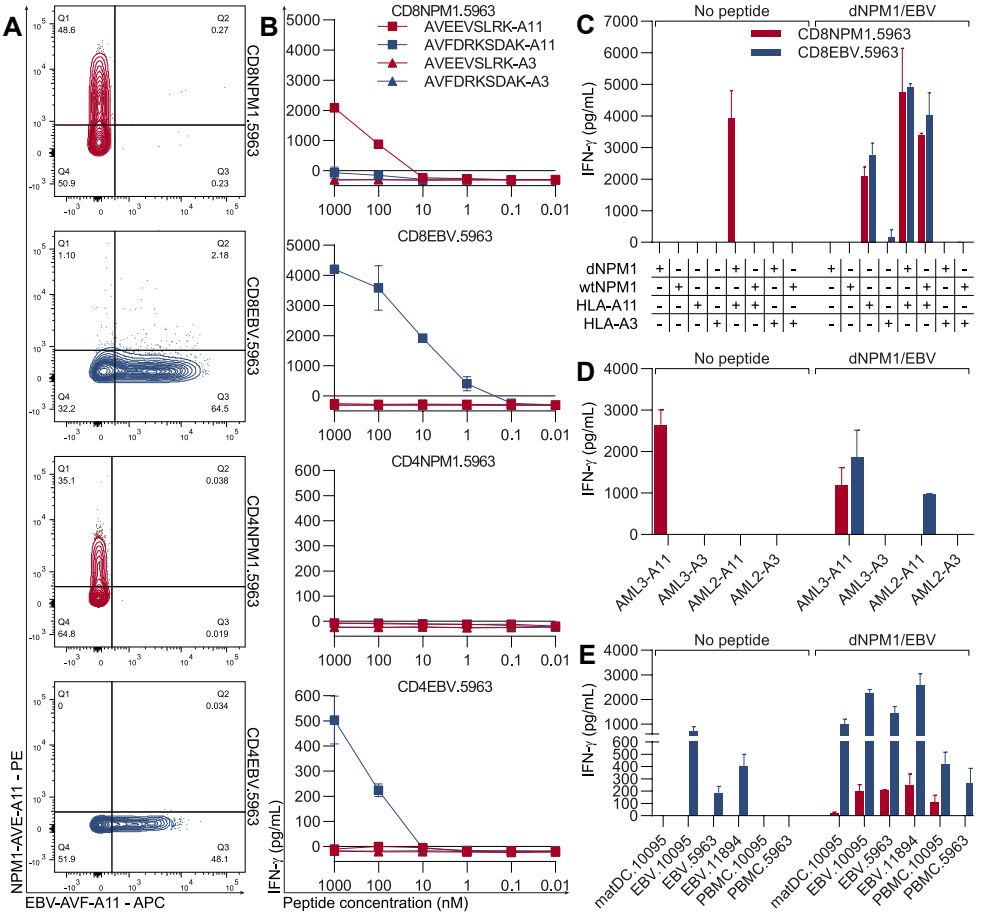

Figure S3. TCR gene transfer targeting dNPM1-derived AVEEVSLRK in HLA-A11. TCR-transduced T-cells were generated from donors 10095 and 5963 and tested as described in Figure 2. Results are shown for donor 5963. (**A**) Tetramer staining was assessed by flow cytometry. Staining with the NPM1-AVE-A11 tetramer was observed for 48.6% of CD8 and 35.1% of CD4 T-cells with the dNPM1 TCR (red) and 64.5% of CD8 and 48.1% of CD4 T-cells with the EBV TCR (blue) stained with the EBV-AVF-A11 tetramer. (**B**) T2 cells transduced with HLA-A11 (squares) or -A3 (triangles) were pulsed with AVEEVSLRK (red) or AVFDRKSDAK (blue) and incubated with T-cells. Recognition of AVEEVSLRK in HLA-A11 was seen for CD8 T-cells with the dNPM1 TCR, but not CD4 T-cells with the dNPM1 TCR. CD8 and CD4 T-cells with the EBV TCR recognized AVFDRKSDAK in HLA-A11. (**C**) K562 cells transduced with dNPM1 or wtNPM1 and HLA-A11 or -A3 were tested for recognition by CD8 T-cells. T-cells with the dNPM1 TCR (red bars) reacted against K562 cells with HLA-A11 and dNPM1. After peptide pulsing, K562 cells with HLA-A11 were recognized by T-cells with the dNPM1 TCR regardless of NPM1 transduction status, as well as by T-cells with the EBV TCR (blue bars). (**D**) CD8 T-cells were tested against OCI-AML3 with dNPM1 and OCI-AML2 with wtNPM1 transduced with HLA-A11 or -A3. T-cells with the dNPM1 TCR (red bars) secreted IFN-γ upon incubation with OCI-AML3 with HLA-A11, but not OCI-AML2. Peptide-pulsed OCI-AML2 with HLA-A11 was only recognized by T-cells with the EBV TCR (blue bars). (**E**) CD8 T-cells were incubated with autologous PBMCs, matDCs and EBV-LCLs from donors 10095 and 5963, and EBV-LCLs from donor 11894 from whom clone 6F11 was isolated. Healthy hematopoietic cells were not recognized by T-cells with the dNPM1 TCR (red bars), whereas T-cells with the EBV TCR (blue bars)

reacted against EBV-LCLs. PBMCs and EBV-LCLs were also recognized by dNPM1 T-cells after peptide loading. Symbols and bars represent mean + SD of duplicate wells.

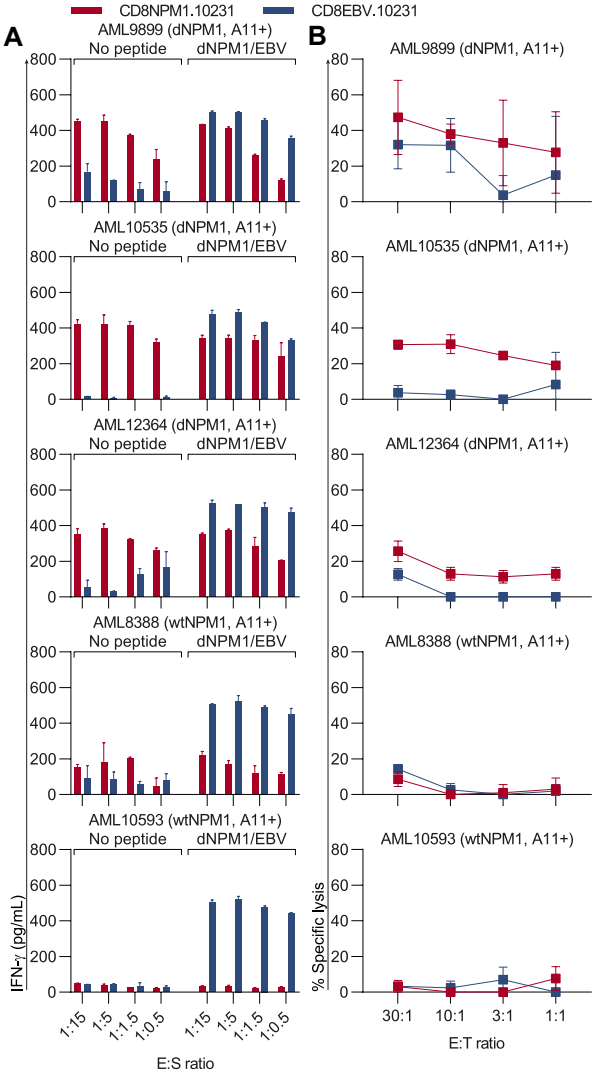

Figure S4. The HLA-A11-restricted dNPM1 TCR targets primary AML. CD8 T-cells transduced with the dNPM1 or EBV TCR were generated from donors 10095 and 10231 and tested as described in Figure 3. Results are shown for donor 10231. (**A**) T-cells were incubated with 5 HLA-A11+ primary AMLs. T-cells with the dNPM1 TCR (red bars) reacted against dNPM1 AMLs, while wtNPM1 AMLs were not recognized. T-cells with the EBV TCR (blue bars) were reactive against all 5 AMLs after peptide loading. Bars represent mean + SD of duplicate wells. (**B**) T-cell cytotoxicity against 5 HLA-A11+ primary AMLs was tested in a 9-h chromium-51 release assay. T-cells with the dNPM1 TCR (red line) lysed dNPM1 AMLs, while wtNPM1 AMLs were not killed. T-cells with the EBV TCR (blue line) did not show specific lysis of AMLs. Symbols represent mean ± SD of triplicate wells.

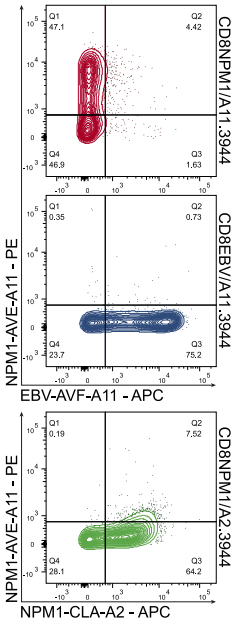

Figure S5. Tetramer staining of TCR-transduced T-cells as used for mouse experiments. CD8 T-cells from donor 3944 were transduced with the HLA-A11 dNPM1 or HLA-A11 EBV TCR or the HLA-A2 dNPM1 TCR. TCR-transduced T-cells were analyzed by FACS one day before injection into mice. T-cells with the HLA-A11 dNPM1 TCR (red), HLA-A11 EBV TCR (blue) and HLA-A2 dNPM1 TCR (green) stained with the NPM1-AVE-A11, EBV-AVF-A11 and NPM1-CLA-A2 tetramer, respectively.

Figure S6. FACS analyses of mouse bone marrow samples. (**A**) Gating strategy for the analysis of T-cell persistence in bone marrow samples. Samples were stained with anti-human CD8 Pacific Blue and anti-mouse TCR β chain APC antibodies. Dead cells were excluded using Zombie Aqua. Depicted is a representative staining for bone marrow from mouse 1 treated with PBS. Within viable single cells, CD8+ mouse TCR β chain+ cells were selected (red rectangle). (**B**) Gating strategy to measure surface expression of HLA class I, co-stimulation and adhesion molecules on bone marrow samples. Samples were stained with anti-CD40 FITC, anti-CD54 APC, anti-CD58 FITC, anti-CD80 FITC, anti-CD86 FITC or anti-PD-L1 Brilliant Violet 421 antibodies. HLA-A11 and HLA-A2 expression were measured by indirect staining with primary human anti-HLA-A11 and mouse anti-HLA-A2 antibodies, followed by secondary rabbit anti-human IgG FITC and goat anti-mouse IgG Alexa Fluor 647 antibodies, respectively. Dead cells were excluded using Zombie Aqua. Depicted is a representative staining of fluorescence minus FITC on bone marrow cells from mouse 1 treated with PBS. Viable single cells were gated and selected for tdTomato Red+ OCI-AML3.bm10 cells. Positive staining for the different markers within tdTomato Red+ OCI-AML3.bm10 cells was determined using FMO controls. (**C**) Bone marrow samples were analyzed for T-cell persistence. No T-cell persistence was observed in any of the treatment groups, with samples from mice receiving HLA-A11 dNPM1 T-cells (*n* = 8, red squares), EBV T-cells (*n* = 5, blue triangles) or HLA-A2 dNPM1 T-cells (*n* = 4, green circles) and mice injected with PBS (*n* = 2, black diamonds) showing similar background staining. (**D**) The frequency of OCI-AML3.bm10 cells in bone marrow samples was analyzed. The percentage of tdTomato Red+ OCI-AML3.bm10 cells was similar in bone marrow samples from mice treated with HLA-A11 dNPM1 T-cells (*n* = 8, red squares) or EBV T-cells (*n* = 5, blue triangles) and mice receiving PBS (*n* = 2, black diamonds), but was lower in mice injected with HLA-A2 dNPM1 T-cells (*n* = 4, green circles). (**E**) Surface expression of HLA class I, co-stimulation and adhesion molecules on bone marrow samples was assessed. AML cells from mice treated with HLA-A2 dNPM1 T-cells (*n* = 4, green circles) showed slightly lower CD86 expression and higher HLA-A11 expression than AML cells from mice treated with HLA-A11 dNPM1 T-cells (*n* = 8, red squares), EBV T-cells (*n* = 5, blue triangles) or mice receiving PBS (*n* = 2, black diamonds). ΔMFI was calculated by subtraction of the MFI of the FMO control for each sample. For HLA-A11 and HLA-A2, ΔMFI was calculated by subtraction of the MFI of the secondary antibody only. Horizontal lines depict mean ± SD. *Figure on next page.*

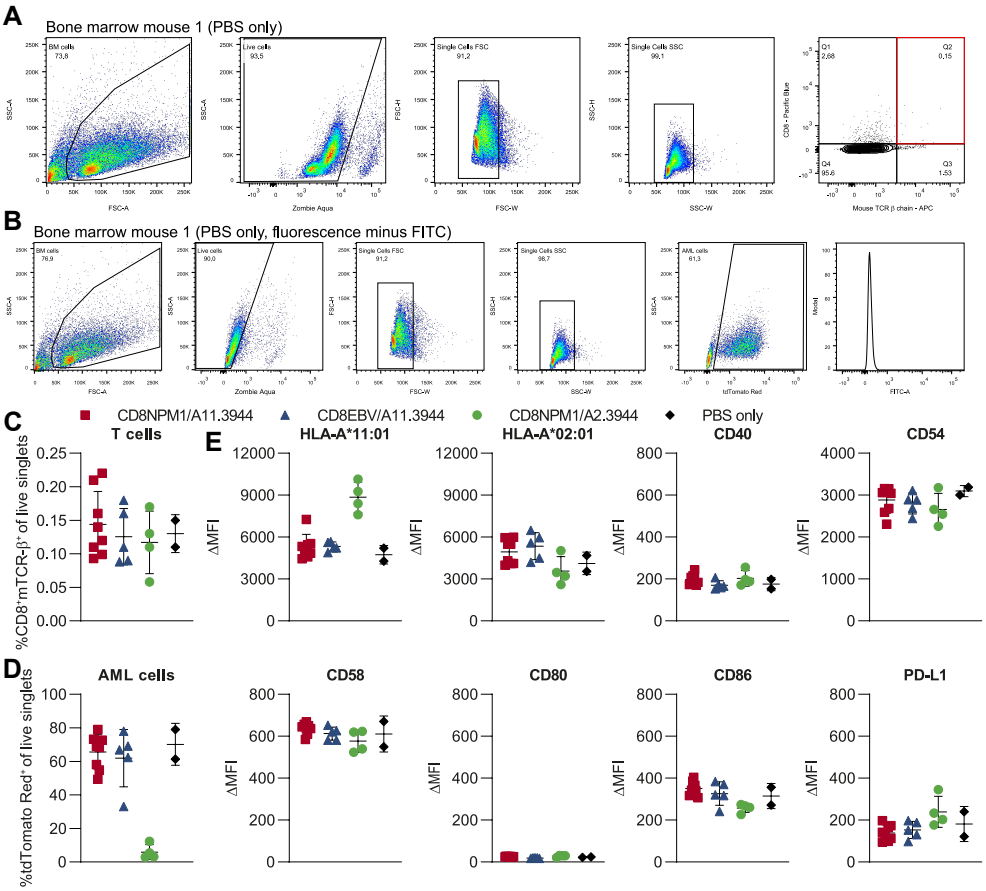
A
Bone marrow mouse 1 (PBS only)
B
Bone marrow mouse 1 (PBS only, fluorescence minus FITC)
C
CD8NPM1/A11.3944
CD8EBV/A11.3944
CD8NPM1/A2.3944
PBS only
T cells
%CD8+mTCR-β+ of live singlets
D
AML cells
%tdTomato Red+ of live singlets
E
HLA-A*11:01
HLA-A*02:01
CD40
CD54
CD58
CD80
CD86
PD-L1
ΔMFI

Table S1. Isolation of tetramer+ CD8 T-cells from healthy individuals

Healthy individual[A]	HLA-allele	PBMC[B] (×10^6)	Sorted T-cells[C]	Growing clones
1	HLA-A11	575	224	122
2	HLA-A11	375	12	6
3	HLA-A11	4906	768	510
4	HLA-A11	340	369	139
5	HLA-A11	710	501	225
6	HLA-A3	520	156	82
7	HLA-A3	435	120	93
8	HLA-A3	605	91	67
9	HLA-A3	645	78	32
10	HLA-A3	440	62	30
11	HLA-A3	420	19	13
12	HLA-A3	225	60	37
13	HLA-A3	695	228	85
14	HLA-A3	475	136	80
15	HLA-A3	730	384	158
16	HLA-A3	450	113	35

[A] PBMCs from individuals 1-5 were stained with an HLA-A11 tetramer for the dNPM1 AVEEVSLRK peptide. For individuals 4 and 5, HLA-A11 tetramers for the dNPM1 CLAVEEVSLRK peptide and UV-exchange HLA-A11 tetramers for CLAVEEVSLRK and its cysteinylated variant C*LAVEEVSLRK were also added to the PBMCs. PBMCs from individuals 6-16 were stained with a mix containing HLA-A3 tetramers for AVEEVSLRK and CLAVEEVSLRK and UV-exchange HLA-A3 tetramers for CLAVEEVSLRK and cysteinylated C*LAVEEVSLRK. [B] Indicated is the amount of PBMCs from each healthy individual as used for T-cell isolation. [C] Indicated are numbers of tetramer+ CD8 T-cells that are sorted by flow cytometry from PBMCs.

Chapter 5

Mutated *DNMT3A* creates a public HLA-DQ-binding neoantigen on acute myeloid leukemia

Dyantha I. van der Lee[1], Eva M. Argiro[1], Sebastiaan N.J. Laan[1], M. Willy Honders[1], Rob C.M. de Jong[1], Nadine E. Struckman[1], J.H. Frederik Falkenburg[1], Marieke Griffioen[1]

[1] Department of Hematology, Leiden University Medical Center, Leiden, The Netherlands

Frontiers in Immunology. 2025 Mar 13;16:1556121
DOI: 10.3389/fimmu.2025.1556121

Abstract

Introduction: Patients with acute myeloid leukemia (AML) often carry the same gene mutations. Neoantigens encoded by these mutations are attractive targets for immunotherapy.

Methods: We searched for public human leukocyte antigen (HLA) class II-restricted neoantigens on AML using an *in vitro* T cell stimulation method. Peptides from 26 recurrent genetic aberrations were assessed for predicted HLA class II binding, and 24 long neopeptides encoded by 10 recurrent mutations were synthesized. Naive CD4 T cells from healthy individuals were cocultured with autologous dendritic cells pulsed with neopeptides.

Results: Multiple CD4 T cell clones were isolated that recognized neopeptides encoded by 5 different genetic aberrations. Two of these peptides, one from the well-known *DNMT3A-R882H* hotspot mutation and one from a long alternative reading frame created by frameshift mutations in *RUNX1*, were recognized by CD4 T cell clones after endogenous processing and presentation on cell lines transduced or CRISPR-Cas9-edited with the mutation of interest. The T cell clone for DNMT3A-R882H was also activated upon stimulation with primary AML samples from HLA-DQB1*06:02 or -DQB1*06:03 positive patients with the mutation.

Conclusion: We here identified a public HLA class II-restricted neoantigen encoded by a driver mutation occurring in 10% of patients with AML that could become an important target for immunotherapy to treat patients with *DNMT3A-R882H*-mutated AML.

Introduction

Acute myeloid leukemia (AML) is a malignancy of the myeloid lineage caused by disrupted maturation and uncontrolled expansion of hematopoietic progenitor cells. Current treatment consists of (combinations of) chemotherapy, hypomethylating agents or targeted small molecule inhibitors, which can be followed by allogeneic hematopoietic stem cell transplantation in patients with high risk AML (1, 2). Although most patients initially enter complete remission, relapses occur in approximately half of the patients (3). To improve overall survival, novel therapies are needed to effectively treat AML.

T cell-based immunotherapies targeting different tumor antigens are actively being explored for the treatment of AML (4). Selecting the right target antigen is crucial to ensure strong anti-tumor effects while minimizing side effects (5). Identifying suitable target antigens on AML, however, remains a major challenge. So far, clinical trials have focused on lineage antigens, which are restricted to myeloid cells, and leukemia-associated antigens, which are overexpressed on AML (4, 6). While these targets often allow treatment of relatively large patient populations, they also carry a significant risk for on-target off-tumor toxicity, where antigen-expressing healthy cells are also attacked (6). For example, patients with AML treated with chimeric antigen receptor-engineered T cells against myeloid lineage antigens such as CD33, CD123 or CLEC12A have experienced myelosuppression due to damage to healthy hematopoietic cells (7). To overcome these challenges, researchers are actively searching for novel antigens that are more AML-specific to enhance therapeutic precision and safety.

Neoantigens are peptides presented on tumor cells by human leukocyte antigens (HLA) that are recognized by T cells. They arise from tumor-specific somatic mutations and are expressed only on malignant cells, making them attractive targets for immunotherapy. However, only a small fraction of tumor-specific mutations generate neoantigens, and these antigens are therefore more common on tumors with a high mutational burden, such as melanoma and lung carcinoma (8). Although AML has a relatively low number of mutations, with an average of 10–13 coding mutations per patient (9, 10), many mutations are recurrent and shared across different patient populations (9, 11). Moreover, many recurrent genetic aberrations in AML are driver mutations that play a key role in tumor development and progression (12). As a result, targeting neoantigens encoded by recurrent mutations presents a promising new approach for immunotherapy of AML.

Various groups have identified HLA class I-restricted neoantigens on AML (13-22). We (15, 16) and others (18-20) have shown that specific T cell receptors (TCRs) for HLA class I neoantigens can be used to target AML *in vitro* and in mice. CD8 T cells release cytotoxic molecules upon recognizing antigens presented by HLA class I molecules, which are expressed on most tumor cells, making them optimal tools for targeting tumors. However, CD4 T cells play an essential and more indirect role in anti-cancer immunity by promoting CD8 T cell priming, stimulating their effector and memory functions and overcoming immunosuppression (23, 24). Some CD4 T cells are also capable of directly killing HLA class II-expressing tumor cells (25). Since AML cells often express HLA class II on their surface, it is worth exploring the potential of CD4 T cells to target HLA class II-restricted neoantigens on AML.

In this study, we aimed to identify HLA class II-restricted neoantigens encoded by recurrent driver mutations in AML. We analyzed 26 recurrent genetic aberrations for encoding peptides with predicted HLA class II binding and synthesized 24 long neopeptides created by 9 recurrent driver mutations in *DNMT3A*, *FLT3*, *IDH1*, *IDH2*, *KIT*, *NRAS*, *RUNX1* and *NPM1* and one recurrent *NUP98::NSD1* gene fusion. Naive CD4 T cells from healthy individuals were stimulated with dendritic cells pulsed with mixes of long neopeptides, and various neopeptide-specific CD4 T cell clones were isolated. Two neopeptides, one encoded by the *DNMT3A-R882H* hotspot mutation and one derived from a long alternative reading frame created by *RUNX1* frameshift mutations, were shown to be endogenously processed and presented on the cell surface. One CD4 T cell clone also reacted against multiple patient-derived *DNMT3A*-mutated AML, thereby confirming that this mutation encodes an HLA class II neoantigen on AML.

Materials and methods

Peptide selection

A total of 26 recurrent genetic aberrations in AML were selected based on mutation frequencies reported in the COSMIC database (26). The genetic aberrations were searched for encoding peptides with predicted HLA class II binding using the algorithm NetMHCIIpan 3.2 (27). Peptide sequences of 12-17 amino acids were entered into the algorithm to predict binding to 23 common HLA class II beta alleles with respective alpha alleles as available in the algorithm. The 23 HLA class II beta alleles are each present at an allele frequency of 10% in at least one population from different world regions as specified in the Allele Frequency Net Database (28). Strong and weak binding peptides as defined by default thresholds of ≤2% and ≤10% rank, respectively, were selected, and partially overlapping length variants were combined *in silico* into 68 unique long sequences. Of these 68 sequences, 16 long

peptides comprising sequences with predicted binding to at least 4 HLA class II beta alleles were synthesized and used for T cell stimulation.

Cell culture

Bone marrow and peripheral blood mononuclear cells (PBMCs) were collected from patients with AML and healthy individuals using density gradient centrifugation with Ficoll-amidotrizoate (pharmacy Leiden University Medical Center) and cryopreserved. Patient-derived AML samples were cultured in Iscove's Modified Dulbecco's Medium (IMDM) (Lonza) with 10% heat-inactivated human serum (HS) (Sanquin Reagents) and 1% penicillin/streptomycin (Lonza). B cells and monocytes were isolated from PBMCs by magnetic-activated cell sorting (MACS) using CD19 MicroBeads and CliniMACS CD14 Reagent (Miltenyi Biotec), respectively. Epstein-Barr virus-transformed lymphoblastoid cell lines (EBV-LCL) were generated from B cells. EBV-LCL and myeloid leukemia cell line K562 (ATCC), which lacks HLA class I and class II surface expression, were cultured in IMDM with 10% heat-inactivated fetal bovine serum (FBS) (Gibco), 1.5% L-glutamine (Lonza) and 1% penicillin/streptomycin. The monocytic leukemia cell line SIG-M5 (DSMZ) was cultured in IMDM with 20% FBS and 1% penicillin/streptomycin. All cell lines were regularly tested for mycoplasma using the MycoAlert Mycoplasma Detection Kit (Lonza).

CRISPR-Cas9 genome editing of cell lines

Frameshift mutations were introduced in *RUNX1* (exon 7 in ENST00000300305.7) in K562 and SIG-M5 by CRISPR-Cas9 genome editing to generate the same alternative reading frame as created by the *c.883dup* mutation. Two CRISPR RNA sequences (crRNA) (iD1: GGCGUUGCUGGGUGCACAGA, iD4: CUGGCACGUCCAGGUGAAAU) were selected using the online tool inDelphi (29), and on- and off-targeting potential of crRNAs was assessed with the CRISPR-Cas9 guide RNA design checker tool from Integrated DNA Technologies (IDT, https://www.idtdna.com/SciTools). Ribonucleoprotein complexes (RNPs) were produced by combining crRNA with trans-activating CRISPR RNA (tracrRNA) and S*treptococcus pyogenes* Cas9 nuclease (all ordered from IDT) as previously described with modifications (30, 31). In short, crRNA and tracrRNA were mixed at a 1:1 ratio, heated for 5 minutes at 95°C and cooled to room temperature. Cas9 nuclease was added at a 1:3 ratio (30 pmol Cas9 to 90 pmol crRNA:tracrRNA duplex per transfection) and incubated for 10-20 minutes at room temperature to form RNPs. Transfection of cells was performed with the Neon Transfection System (Invitrogen). Cas9 Electroporation Enhancer (IDT) was added to RNPs to 11 µM. Per transfection, $1.1x10^6$ cells were resuspended in 110 µl Resuspension Buffer R and added to 4 µl RNPs. Using Neon Tips, 10 or 100 µl of cells and RNPs were transferred to Electroporation Tubes containing 3 ml Electrolytic Buffer E2. K562 was

transfected using 1450 V, 10 ms, 3 pulses and SIG-M5 using 1200 V, 10 ms, 4 pulses. Electroporated cells were single cell cultured and clones were screened for introduced mutations by PCR and Sanger sequencing (Leiden Genome Technology Center, Leiden University Medical Center). Two clones were selected based on their introduced mutations, i.e. K562-E4 containing a homozygous *c.907dup* mutation (p.Ser303Phefs*297, iD1) and SIG-M5-C9 containing a heterozygous *c.906_907insG* mutation (p.Ser303Valfs*297, iD4). Expression of *RUNX1* mutations was confirmed by RNA sequencing as previously described (32).

Retroviral transduction of cell lines

Cell lines K562, K562-E4 and SIG-M5-C9 were retrovirally transduced with two LZRS or MP71.60 constructs, one encoding HLA-DRB1*03:01, -DRB1*04:01, -DRB1*04:04 or -DRB1*15:01 and one encoding HLA-DRA*01:02, one encoding HLA-DQB1*03:02 and one encoding HLA-DQA1*03:01, or single constructs encoding HLA-DQA1*02:01 and -DQB1*03:03, HLA-DQA1*01:02 and -DQB1*06:02, or HLA-DQA1*01:03 and -DQB1*06:03 in which the alpha and beta chains were linked by a T2A protein cleavage site. Cell lines were also transduced with LZRS-IRES-NGFR constructs containing full-length mutated *FLT3* (p.Asp835Tyr), wild-type *FLT3*, mutated *DNMT3A* (p.Arg882His), wild-type *DNMT3A*, mutated *RUNX1* (p.Ser295Phefs*305), wild-type *RUNX1* or the full-length fusion gene *NUP98::NSD1*. Transduced cells were purified by MACS or fluorescence-activated cell sorting (FACS) using PE- (catalog 557196, BD Biosciences) or APC-conjugated NGFR (catalog CL10013APC, Sanbio) and PE-conjugated HLA-DR (catalog 347400, BD Biosciences) or HLA-DQ antibodies (catalog 318106, Biolegend).

Neopeptide-specific CD4 T cell isolation

Naive CD4 T cells were isolated by MACS from PBMCs of healthy female individuals using the Naive CD4+ T Cell Isolation Kit II (Miltenyi Biotec). By selecting naive CD4 T cells, regulatory CD4 T cells, which mainly reside in the memory T cell pool, were largely depleted (33). Moreover, naive T cells have not yet encountered their specific antigen and represent a broad repertoire of potential antigen specificities (34). Autologous mature dendritic cells were generated by culturing monocytes for 5 days in medium with GM-CSF (Novartis Pharma) and IL-4 (Schering-Plough), followed by two days of culture in medium with GM-CSF, TNF-α (CellGenix), IL-1β (Sclavo), IL-6 (Sandoz), PGE_2 (Sigma-Aldrich) and IFN-γ (Boehringer Ingelheim), as previously described (35). Autologous mature dendritic cells were pulsed for 4 hours with peptide pools containing each peptide at 100 nM in IMDM with 2% FBS at a concentration of $10x10^6$ dendritic cells/ml. Dendritic cells were washed and cocultured with naive CD4 T cells at a T cell:dendritic cell ratio of 10:1 in IMDM with 5% HS, 5% FBS, 2% L-glutamine, 1% penicillin/streptomycin, 10 ng/ml IL-12

(Hoffmann-La Roche) and 20 IU/ml IL-2 (Novartis Pharma) at a concentration of $1x10^6$ T cells/ml. On days 3 and 6, 100 IU/ml IL-2 and 10 ng/ml IL-15 (Miltenyi Biotec) were added. After two weeks, autologous PBMCs pulsed with the same peptide pools were irradiated at 40 Gy and added to CD4 T cells at a T cell:PBMC ratio of 2:1 in IMDM with 5% HS, 5% FBS and 10 IU/ml IL-2 at a concentration of $1x10^6$ T cells/ml. Two days after restimulation with peptide-pulsed PBMCs, activated CD137 positive CD4 T cells were bulk sorted by FACS using CD4-Pacific Blue (catalog 558116) and CD137-APC (catalog 550890) antibodies. PE-conjugated antibodies against CD8 (catalog 555367), CD14 (catalog 345785), CD16 (catalog 555407) and CD19 (catalog 345777) (all from BD Biosciences) were used for exclusion. Sorting was performed with a BD FACS Aria II 3L or BD FACS Aria III 4L cell sorter using BD FACSDiva software (BD Biosciences) at the Flow cytometry Core Facility of the Leiden University Medical Center. Sorted T cells were seeded at three cells per well in 384 well flat bottom tissue culture plates (Greiner Bio-One) containing 30 µl T cell medium consisting of IMDM with 5% HS, 5% FBS, 1.5% L-glutamine, 1% penicillin/streptomycin and 100 IU/ml IL-2, with 50,000 irradiated (40 Gy) allogeneic PBMCs as feeder cells and 0.8 µg/ml phytohemagglutinin (PHA, Thermo Scientific). Growing T cell clones were restimulated every 14-21 days with irradiated allogeneic PBMCs at a T cell:feeder cell ratio of 1:5 in T cell medium with 0.8 µg/ml PHA.

TCR Vbeta analysis

TCR Vbeta usage of RUNX1-specific T cell clones was determined by flow cytometry using the Beta Mark TCR Vbeta Repertoire Kit (catalog IM3497, Beckman Coulter).

T cell recognition assays

Assays were performed in 384 well flat or 96 well round bottom (Corning Life Sciences) tissue culture plates. In 384 well plates, 2,000 T cells were incubated with 10,000 stimulator cells in 50-60 µl T cell medium. In 96 well plates, T cells were incubated with stimulator cells in 100 µl T cell medium at two different ratios. For assays with HLA- and gene-transduced K562, 5,000 T cells were incubated with 60,000 stimulator cells. For assays with K562-E4, SIG-M5-C9 and patient-derived AML cells, 50,000 T cells were incubated with 100,000 stimulator cells. Release of IFN-γ or GM-CSF in supernatant was measured after overnight coincubation by enzyme-linked immunosorbent assay (ELISA) (Invitrogen, R&D Systems or Diaclone SAS). Peptide loading of stimulator cells was performed for 4 hours at 37°C in IMDM with 2% FBS. One day before use in assays, AML samples were thawed and dead cells were removed using Ficoll-amidotrizoate. Enrichment of HLA class II-expressing AML cells was performed with MACS using PE-conjugated HLA-DP antibody (catalog H130, Leinco Technologies) and anti-PE MicroBeads (Miltenyi Biotec). HLA-DP was used to avoid possible interference of anti-HLA-DQ antibodies in the interaction between the TCR and peptide-HLA-DQ complex.

Flow cytometry-based cytotoxicity assay

For cytotoxicity assays, 50,000 T cells were incubated with 50,000 AML cells in 100 µl of IMDM without phenol red (Gibco) with 10% HS, 1.5% L-glutamine, 1% penicillin/streptomycin and 100 IU/ml IL-2 in 96 well round bottom tissue culture plates. AML cells were thawed on the day of the assay and dead cells were removed using Ficoll-amidotrizoate. Peptide loading of AML cells was performed for 2 hours at 37°C in IMDM with 2% FBS. After 48 hours of coincubation, samples were stained for 15 minutes at room temperature with viability dye Zombie Red (catalog 423109, Biolegend) and blocked for 15 minutes at room temperature with PBS (Fresenius Kabi) with 2.5% HS. Following blocking, samples were stained for 30 minutes at 4°C with CD33-PE (catalog 303404, Biolegend), CD34-APC (catalog 343510, Biolegend), HLA-DQ-FITC (catalog 318104, Biolegend), CD3-BV421 (catalog 562427, BD Biosciences), CD8-BV421 (catalog 344747, Biolegend) and CD19-BV421 (catalog 302233, Biolegend) antibodies. Samples were fixed with 1% paraformaldehyde (pharmacy Leiden University Medical Center) for 20 minutes at room temperature before acquisition on the Aurora 5L-2 (Cytek Biosciences). Results were analyzed using OMIQ (Dotmatics).

Statistics

Statistical analyses as indicated in figure legends were performed using GraphPad Prism Software version 10.2.3 (GraphPad, Dotmatics). P-values < 0.05 were considered significant ($p < 0.05$ *; $p < 0.01$ **; $p < 0.001$ ***).

Study approval

Peripheral blood and bone marrow samples were collected from patients after informed consent according to the Declaration of Helsinki and stored in the Leiden University Medical Center Biobank for Hematological Diseases. This study was approved by the Institutional Review Board of the Leiden University Medical Center (approval number B16.039) and was conducted in accordance with the local legislation and institutional requirements.

Results

Selection of peptides encoded by recurrent mutations in AML

A total of 26 recurrent genetic aberrations in AML were searched for encoding peptides with predicted binding to 23 common HLA class II alleles using the online tool NetMHCIIpan 3.2 (27). These aberrations included 12 missense mutations in *DNMT3A*, *FLT3*, *IDH1*, *IDH2*, *KIT* and *NRAS*, 5 small insertions or deletions leading to frameshifts in *ASXL1*, *CEBPA*, *NPM1* and *RUNX1* and 9 gene fusions involving the genes *CBFB*, *MYH11*, *KMT2A*, *MLLT3*, *NUP98*, *NSD1*, *PML*, *RARA*, *RUNX1* and *RUNX1T1* (Supplemental Tables S1-2). Based on these results, 16 long peptides each comprising sequences with weak or strong predicted binding to at least 4 HLA class II beta alleles were selected and synthesized (Table 1, Figure 1). These neopeptides are designated by their encoding gene followed by the first three N-terminal amino acids. Of these 16 neopeptides, 7 peptides were encoded by the missense mutations *DNMT3A-R882H*, *DNMT3A-R882C*, *FLT3-D835Y*, *IDH1-R132H*, *IDH2-R140Q*, *KIT-D816V* and *NRAS-G12D*, 8 peptides were derived from a long alternative reading frame generated by frameshift mutations in *RUNX1* and one peptide originated from a gene fusion between exon 12 of *NUP98* and exon 7 of *NSD1*. The median number of HLA class II beta alleles to which the neopeptides were predicted to bind was 9.5 (range 4 – 17), and strong predicted binding to at least one beta allele was observed for 13 of the 16 peptides. Of the 23 common HLA class II beta alleles, all alleles were predicted to bind to at least three neopeptides, and HLA-DQB1*06:02 was predicted to bind to a maximum of 15 neopeptides. Weak binding to at least one neopeptide was predicted for all 23 beta alleles and strong binding to at least one neopeptide for 16 of the 23 alleles. In addition to the 16 neopeptides, 8 overlapping 17-mer peptides spanning the entire alternative reading frame of 11 amino acids created by *NPM1* mutations were included irrespective of predicted HLA class II binding. *NPM1* mutations are 4 base pair insertions occurring in the final exon of the gene in 30-35% of patients with AML. As controls, peptides were synthesized for two H-Y antigens, i.e. LB-ZFY-1 and LB-RPS4Y-1 both binding to HLA-DRB1*03:01, and three minor histocompatibility antigens as well as their allelic variants, i.e. LB-LY75-2R/LB-LY75-2K, LB-MTHFD1-1Q/LB-MTHFD1-1R and LB-PTK2B-1T/LB-PTK2B-1K binding to HLA-DPB1*04:01, -DRB1*03:01 and -DRB3*01:01, respectively. The H-Y and minor histocompatibility antigens have been identified as T cell targets in patients with hematological malignancies after allogeneic hematopoietic stem cell transplantation and have thus been confirmed to be immunogenic *in vivo* (35, 36). In conclusion, 32 peptides, including 8 control antigens, were selected to stimulate CD4 T cells (Table 1).

Table 1. Peptides selected for CD4 T cell stimulation

Peptide sequence[A]	Gene	Origin	Position	Length (AA)
AGRPVPSQLALLPPVLRRLGRLLPV	*RUNX1*	Frameshift	*c.883dup*	25
LALLPPVLRRLGRLLPVLHGGRRALAAA	*RUNX1*	Frameshift	*c.883dup*	28
AAAHPAALHQRLHRLRAAQPQPPE	*RUNX1*	Frameshift	*c.883dup*	24
RAPGGGRVEALLRRQAWPGWAP	*RUNX1*	Frameshift	*c.883dup*	22
QAWPGWAPRAAAFASGRAGLLFATSPP	*RUNX1*	Frameshift	*c.883dup*	27
ASGRAGLLFATSPPGSRALGPATVLG	*RUNX1*	Frameshift	*c.883dup*	26
PRAPDGQDLAVGQARAASCAQKPTPP	*RUNX1*	Frameshift	*c.883dup*	26
CAQKPTPPPSAGAPALAEVSEATHLEGV	*RUNX1*	Frameshift	*c.883dup*	28
FPVHYTDVSNMS**H**LARQRLLGRSWSVP	*DNMT3A*	Missense	*c.2645G>A*	27
FPVHYTDVSNMS**C**LARQRLLGRSWSVP	*DNMT3A*	Missense	*c.2644C>T*	27
GKVVKICDFGLAR**Y**IMSDSNYVVRGNAR	*FLT3*	Missense	*c.2503G>T*	28
PRLVSGWVKPIIIG**H**HAYG	*IDH1*	Missense	*c.395G>A*	19
GTI**Q**NILGGTVFREPIIC	*IDH2*	Missense	*c.419G>A*	18
ITKICDFGLAR**V**IKNDSNYVVKGNAR	*KIT*	Missense	*c.2447A>T*	26
MTEYKLVVVGA**D**GVGKSALTIQLI	*NRAS*	Missense	*c.35G>A*	24
TTTATLGFGAPQAPV**A**VRSEKKRLRKPS	*NUP98::NSD1*	Fusion gene	*NUP98 exon 12-NSD1 exon 7*	28
CFRMTDQEAIQDL**CLAV**	*NPM1*	Frameshift	*c.860_863dup*	17
FRMTDQEAIQDL**CLAVE**	*NPM1*	Frameshift	*c.860_863dup*	17
RMTDQEAIQDL**CLAVEE**	*NPM1*	Frameshift	*c.860_863dup*	17
MTDQEAIQDL**CLAVEEV**	*NPM1*	Frameshift	*c.860_863dup*	17
TDQEAIQDL**CLAVEEVS**	*NPM1*	Frameshift	*c.860_863dup*	17
DQEAIQDL**CLAVEEVSL**	*NPM1*	Frameshift	*c.860_863dup*	17
QEAIQDL**CLAVEEVSLR**	*NPM1*	Frameshift	*c.860_863dup*	17
EAIQDL**CLAVEEVSLRK**	*NPM1*	Frameshift	*c.860_863dup*	17
QIVVEIQEAVFVSNIVDSDI	*ZFY*	Male-specific gene	NA	20
EKTGEHFRLVYDTKGRFAVH (36)	*RPS4Y*	Male-specific gene	NA	20
RPTIKNE**R**FLAGLS (36)	*LY75*	SNP	*c.4040A>G*	14
RPTIKNE**K**FLAGLS (36)	*LY75*	SNP	*c.4040G>A*	14
HGNSSIIAD**Q**IALKLV (35)	*MTHFD1*	SNP	*c.1958G>A*	16
HGNSSIIAD**R**IALKLV (35)	*MTHFD1*	SNP	*c.1958A>G*	16
PMVYMND**T**SPLTPEK (35)	*PTK2B*	SNP	*c.2513A>C*	15
PMVYMND**K**SPLTPEK (35)	*PTK2B*	SNP	*c.2513C>A*	15

[A] Bold type amino acids (AA) represent residues translated in alternative reading frames in neopeptides created by frameshift mutations in *RUNX1* and *NPM1*, a residue indicating the position of fusion between exon 12 of *NUP98* and exon 7 of *NSD1* with both fusion partners translated in the normal reading frame, mutated residues in neopeptides encoded by missense mutations in *DNMT3A*, *FLT3*, *IDH1*, *IDH2*, *KIT*

and *NRAS*, H-Y antigens LB-ZFY-1 and LB-RPS4Y-1 and polymorphic residues in minor histocompatibility antigens (LB-LY75-2R, LB-MTHFD1-1Q, LB-PTK2B-1T) and their allelic variants encoded by single nucleotide polymorphisms (SNPs). NA. Not applicable.

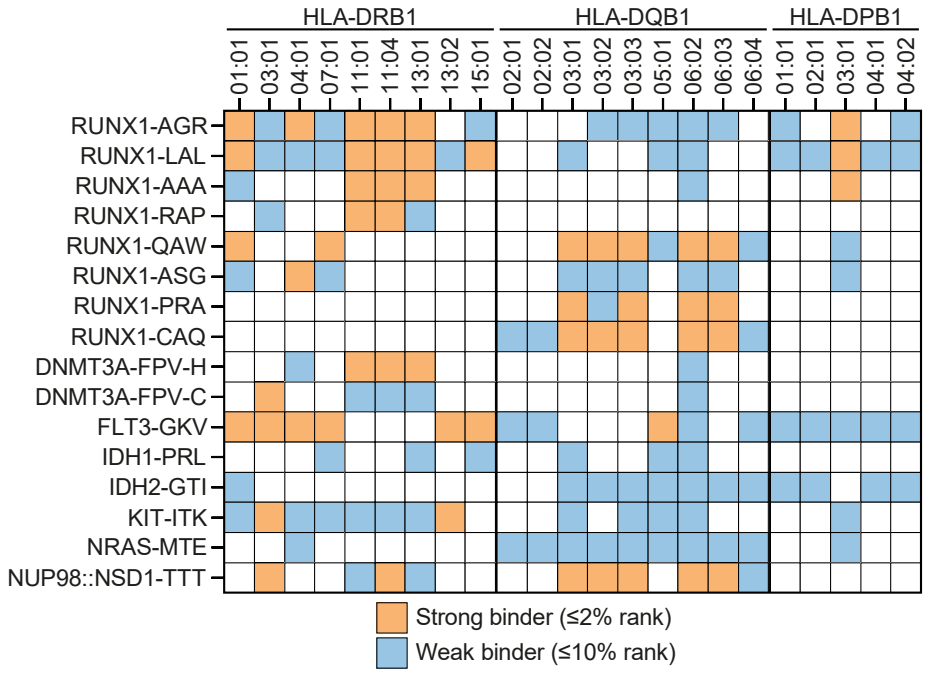

Figure 1. Selection of 16 neopeptides with predicted HLA class II binding. Sequences of 12-17 amino acids encoded by recurrent mutations in AML were analyzed by NetMHCIIpan 3.2 to predict binding affinity to 23 common HLA-DRB1, -DQB1 or -DPB1 alleles paired with respective HLA-DRA, -DQA1 or -DPA1 alleles as available in the algorithm. Peptides with strong or weak predicted binding were identified using default thresholds of ≤2% and ≤10% rank, respectively. A total of 16 neopeptides (18- to 28-mer peptides), annotated by their encoding gene and first three N-terminal amino acids, were synthesized. Depicted is strong (orange squares) or weak (blue squares) predicted binding to 23 HLA-DRB1 (*n* = 9), -DQB1 (*n* = 9) and -DPB1 (*n* = 5) alleles in combination with at least one respective alpha allele. White squares indicate that predicted binding was >10% rank for all alpha-beta allele combinations.

Isolation of neopeptide-specific CD4 T cell clones

CD4 T cells from three healthy female individuals (donors HD1-3) were incubated with autologous mature dendritic cells exogenously pulsed with 27-30 peptides mixed based on predicted binding to the HLA class II alleles of the donors (Figure 2). Donors HD1, HD2 and HD3 expressed 6, 5 and 4 of the 23 common HLA class II beta alleles, respectively. All three donors were positive for HLA-DRB1*03:01 and HLA-DQB1*02:01. Strong binding to at least one HLA class II allele of donor HD1 was predicted for 8 neopeptides and weak binding was predicted for 8 other neopeptides in the mix. For donor HD2, 13 neopeptides were included in the mix, including 8 peptides with strong and 5 peptides with weak predicted HLA class II binding. The peptide mix for donor HD3 contained 13 neopeptides, including 6 peptides with strong and 7 peptides with weak predicted HLA class II binding. Additionally, each peptide mix contained all 8 mutated NPM1 peptides irrespective of predicted HLA class II binding and 6-8 control peptides for polymorphic antigens (H-Y antigens, minor histocompatibility antigens and allelic variants). After two weeks of culture, activated CD137 positive CD4 T cells were sorted by flow cytometry and expanded as single T cell clones. From each donor, 17,280 single T cells were cultured, and 540-936 T cell clones were isolated. Growing T cell clones were tested for reactivity against autologous EBV-LCL pulsed with peptides divided in three mixes containing mutated NPM1 peptides, other neopeptides or polymorphic peptides (Supplemental Figure S1). A total of 16 clones specifically reacted against peptide-pulsed EBV-LCL. Of these T cell clones, 5 clones from donor HD1 and 8 clones from donor HD3 recognized the mix of neopeptides, and one clone from donor HD2 and two clones from donor HD3 reacted against the mix of polymorphic peptides. None of the T cell clones were reactive against EBV-LCL pulsed with mutated NPM1 peptides.

To elucidate which peptides were recognized, CD4 T cell clones were tested against autologous EBV-LCL pulsed with single peptides (Figure 3). Of the 5 neopeptide-specific clones from donor HD1, one clone (1.5.F1^{DNMT3A}) recognized peptide DNMT3A-FPV-H encoded by *DNMT3A-R882H*, one clone (1.7.E7$^{NUP98::NSD1}$) reacted against peptide NUP98::NSD1-TTT created by the *NUP98::NSD1* fusion and three clones (1.5.C8^{FLT3}, 1.8.H4^{FLT3} and 1.9.H7$^{FLT3/KIT}$) were specific for peptide FLT3-GKV encoded by *FLT3-D835Y*. In addition to FLT3-GKV, clone 1.9.H7$^{FLT3/KIT}$ also recognized peptide KIT-ITK encoded by *KIT-D816V*, which shares 20 amino acids with FLT3-GKV. All 8 neopeptide-reactive T cell clones from donor HD3 (1.2.C2^{RUNX1}, 1.2.D2^{RUNX1}, 1.3.E8^{RUNX1}, 1.4.B7^{RUNX1}, 1.4.F6^{RUNX1}, 1.4.G7^{RUNX1}, 1.5.F10^{RUNX1} and 1.5.H7^{RUNX1}) were specific for peptide RUNX1-CAQ derived from the long alternative reading frame created by frameshift mutations in *RUNX1*. TCR Vbeta analysis of RUNX1-reactive T cell clones by flow cytometry identified TRBV20-1 as Vbeta chain for clone 1.3.E8^{RUNX1}, whereas the other 7 clones expressed TCR Vbeta chains that

could not be identified by the antibodies in the TCR Vbeta Repertoire Kit. Lastly, all three T cell clones from donors HD2 (1.1.C3^{RPS4Y}) and HD3 (1.3.D11^{RPS4Y} and 1.4.A3^{RPS4Y}) recognizing the polymorphic peptide mix were specific for H-Y antigen LB-RPS4Y-1 (peptide RPS4Y-EKT) (represented by clone 1.3.D11^{RPS4Y} in Figure 3).

Donor	DRB1	DRB3	DRB4	DRB5	DQB1	DPB1
HD1	03:01 15:01	01:01		01:01:01	02:01:01 06:02:01	02:01 04:01/81:01
HD2	03:01:01 07:01:01	01:01:02	01:03:01:01		02:01:01 02:02:01	03:01/104:01 09:01
HD3	03:01:01 04:04:01	01:01:02	01:03:01:01		02:01:01 03:02:01	04:01:01

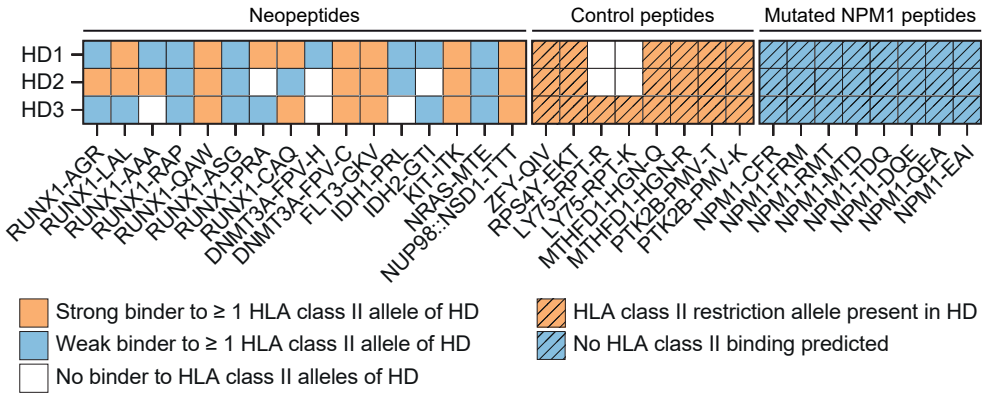

Figure 2. Peptide mixes used for T cell stimulation. CD4 T cells from healthy female individuals (HD1-3) were incubated with autologous dendritic cells pulsed with mixes of 27-30 peptides. Peptide mixes included 13-16 neopeptides with predicted HLA class II binding, 8 overlapping peptides spanning the entire 11 amino acid alternative reading frame of mutated NPM1 and 6-8 peptides for previously identified HLA class II-binding polymorphic antigens, including H-Y antigens, minor histocompatibility antigens and allelic variants. Donors HD1, HD2 and HD3 expressed 6, 5 and 4 of the 23 common HLA class II beta alleles, respectively, with all three donors expressing HLA-DRB1*03:01 and HLA-DQB1*02:01. Neopeptides were mixed according to their predicted binding to the HLA class II alleles of the donors. Peptides with strong (orange squares) or weak (blue squares) predicted binding to at least one HLA class II allele are indicated for each donor, and peptides that were not predicted to bind to any HLA class II allele of the donor were excluded from the mix (white squares). All 8 control peptides (patterned orange squares) were included in mixes for each of the three donors, except for peptide LY75-RPT-R and its allelic variant LY75-RPT-K, which were only used for HD3. NPM1 peptides (patterned blue squares) were included in each peptide mix irrespective of predicted HLA class II binding.

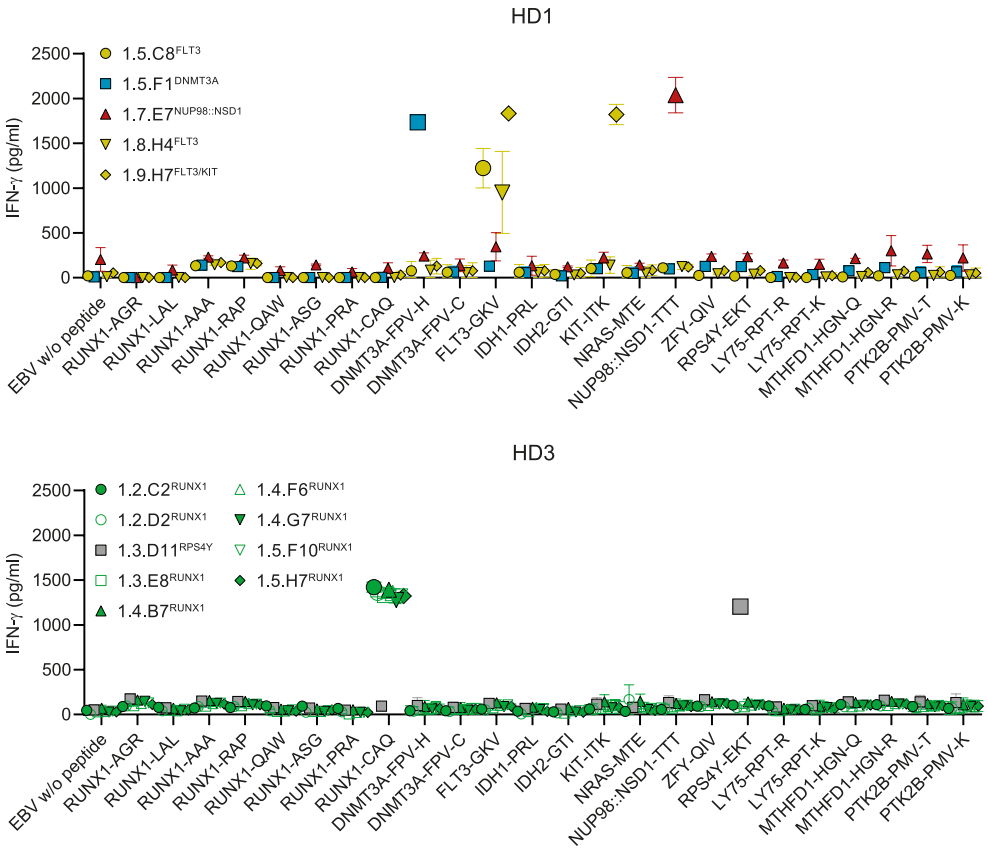

Figure 3. CD4 T cell clones recognize neopeptides encoded by recurrent mutations in AML. CD4 T cells from healthy donors HD1-3 were stimulated with autologous dendritic cells pulsed with mixes of neopeptides and polymorphic peptides as shown in Figure 2. After two weeks of culture, activated CD137 positive CD4 T cells were sorted, and single T cell clones were tested for recognition of peptide pools containing neopeptides, mutated NPM1 peptides or polymorphic peptides as depicted in Supplemental Figure S1. The 16 peptide pool-specific CD4 T cell clones were tested for reactivity against autologous EBV-LCL pulsed with single peptides at 1 µM. After overnight coincubation, IFN-γ release was measured by ELISA. Of the 5 neopeptide pool-specific T cell clones from donor HD1 (upper panel), one clone reacted against peptide DNMT3A-FPV-H (blue symbols), one clone recognized peptide NUP98::NSD1-TTT (red symbols) and three clones were specific for peptide FLT3-GKV (yellow symbols). Clone 1.9.H7$^{FLT3/KIT}$ recognized peptide KIT-ITK in addition to FLT3-GKV. All 8 neopeptide pool-specific T cell clones from donor HD3 (lower panel) reacted against the RUNX1-CAQ peptide (green symbols). The three T cell clones that reacted against the polymorphic peptide pool were specific for H-Y antigen RPS4Y-EKT as represented by clone 1.3.D11^{RPS4Y} (grey symbols). Symbols represent mean ± SD of duplicate wells. Representative data from one of two independent experiments is shown.

Peptide specificity was further confirmed for all 13 neopeptide-specific T cell clones by recognition of EBV-LCL pulsed with titrated concentrations of mutated peptides and, if existing, wild-type peptides as controls. Clones 1.5.C8^{FLT3}, 1.5.F1^{DNMT3A}, 1.7.E7$^{NUP98::NSD1}$, 1.8.H4^{FLT3} and 1.9.H7$^{FLT3/KIT}$ all recognized mutated peptides (Figure 4A). No reactivity was observed against wild-type peptides, except for clones 1.8.H4^{FLT3} and 1.9.H7$^{FLT3/KIT}$, which showed weak or similar reactivity against the wild-type FLT3 peptide. All RUNX1-specific T cell clones, represented by clones 1.3.E8^{RUNX1} and 1.4.B7^{RUNX1} (Figure 4B; other RUNX1-specific clones in Supplemental Figure S2), showed reactivity against the mutated RUNX1-CAQ peptide, but not against the RPS4Y-EKT negative control peptide, whereas clone 1.3.D11^{RPS4Y} was specific for RPS4Y-EKT, but not RUNX1-CAQ. In conclusion, the data showed that CD4 T cell clones 1.5.C8^{FLT3} and 1.5.F1^{DNMT3A} specifically reacted against HLA class II-binding neopeptides encoded by *FLT3-D835Y* and *DNMT3A-R882H* hotspot mutations, respectively, whereas T cell clone 1.7.E7$^{NUP98::NSD1}$ reacted against an HLA class II-binding neopeptide encoded by the *NUP98::NSD1* fusion gene and CD4 T cell clones 1.2.C2^{RUNX1}, 1.2.D2^{RUNX1}, 1.3.E8^{RUNX1}, 1.4.B7^{RUNX1}, 1.4.F6^{RUNX1}, 1.4.G7^{RUNX1}, 1.5.F10^{RUNX1} and 1.5.H7^{RUNX1} against an HLA class II-binding neopeptide created by frameshift mutations in *RUNX1*.

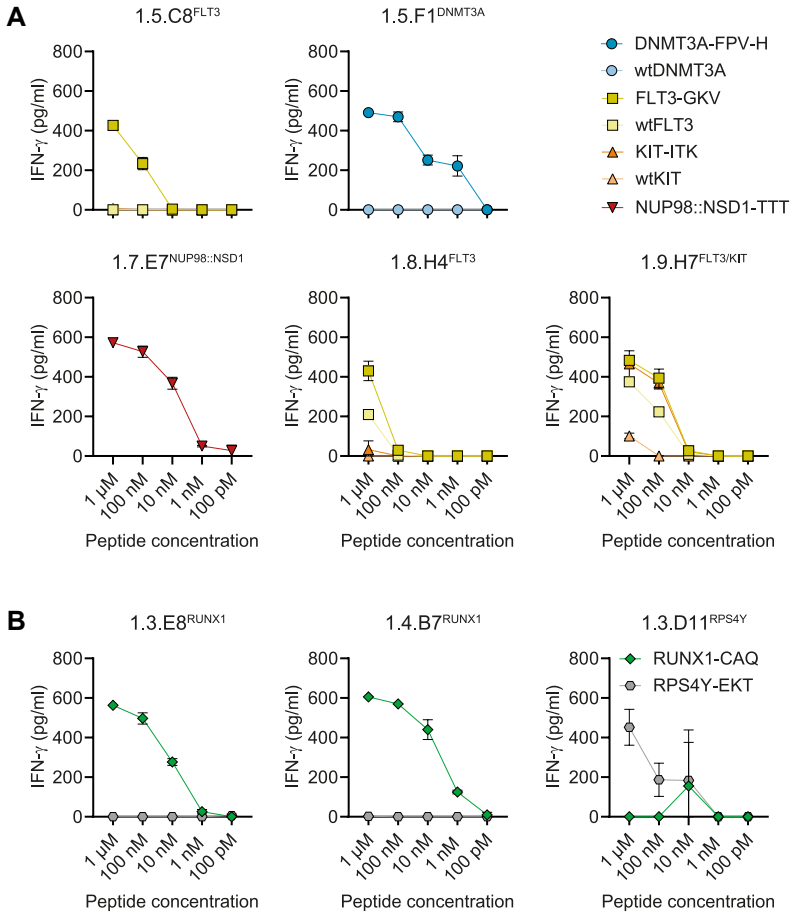

Figure 4. Affinity of CD4 T cell clones for titrated neopeptides. Neopeptide-specific T cell clones from donors HD1 (**A**) and HD3 (**B**) were tested against autologous EBV-LCL pulsed with titrated concentrations of neopeptides (dark symbols) or, if existing, wild-type peptides (wt, light symbols). After overnight coincubation, IFN-γ release was measured by ELISA. Specific recognition of neopeptides (DNMT3A-FPV-H, FLT3-GKV, KIT-ITK, NUP98::NSD1-TTT, RUNX1-CAQ) was observed for T cell clones 1.5.C8^{FLT3}, 1.5.F1^{DNMT3A} and 1.7.E7$^{NUP98::NSD1}$ and all RUNX1-specific clones represented by clones 1.3.E8^{RUNX1} and 1.4.B7^{RUNX1} (results for clones 1.2.C2^{RUNX1}, 1.2.D2^{RUNX1}, 1.4.F6^{RUNX1}, 1.4.G7^{RUNX1}, 1.5.F10^{RUNX1} and 1.5.H7^{RUNX1} are shown in Supplemental Figure S2). T cell clones 1.8.H4^{FLT3} and 1.9.H7$^{FLT3/KIT}$ were also reactive against the wild-type peptide. Symbols represent mean ± SD of duplicate wells. Representative data from one of two independent experiments is shown.

HLA class II restriction of neopeptide-specific T cell clones

To determine HLA class II restriction of T cell clones, reactivity was tested against 20 EBV-LCL each expressing at least three of the 23 HLA class II alleles to which the neopeptides were predicted to bind (Supplemental Table S3). Candidate HLA class II restriction alleles were deduced from T cell recognition patterns of EBV-LCL pulsed with neopeptides (Supplemental Figure S3). T cell clones 1.5.C8^{FLT3}, 1.7.E7$^{NUP98::NSD1}$ and 1.3.D11^{RPS4Y} all reacted against 5 peptide-pulsed EBV-LCL sharing HLA-DRB1*03:01. HLA-DRB1*15:01, -DQB1*06:02 and -DQB1*06:03 were deduced as candidate restriction alleles for clone 1.5.F1^{DNMT3A}, since all EBV-LCL expressing these alleles were recognized. Recognition patterns were less clear for RUNX1-reactive T cell clones, since only 4 out of 6 peptide-loaded EBV-LCL that were recognized expressed HLA-DQB1*03:02.

HLA class II restriction was validated by measuring T cell reactivity against peptide-pulsed K562 transduced with candidate HLA class II alleles (Figure 5). HLA-DRB1*03:01 was confirmed as restriction allele for clones 1.5.C8^{FLT3}, 1.7.E7$^{NUP98::NSD1}$ and 1.3.D11^{RPS4Y}, since these clones reacted against K562 transduced with HLA-DRA*01:02/B1*03:01 when loaded with the respective peptides. HLA-DQB1*06:02 and -DQB1*06:03, but not HLA-DRB1*15:01, were confirmed as restriction elements for clone 1.5.F1^{DNMT3A} as demonstrated by reactivity against peptide-pulsed K562 transduced with the HLA-DQ alleles. Finally, HLA-DQB1*03:02 was validated as restriction allele for RUNX1-specific T cell clones, since all clones were reactive against peptide-pulsed K562 transduced with HLA-DQA1*03:01/B1*03:02 (1.3.E8^{RUNX1} and 1.4.B7^{RUNX1} in Figure 5; other RUNX1-specific clones in Supplemental Figure S4). With the exception of clone 1.3.E8^{RUNX1}, RUNX1-reactive clones also reacted against K562 transduced with HLA-DQA1*02:01/B1*03:03 in the absence of RUNX1-CAQ peptide, indicating cross-reactivity against another peptide in HLA-DQB1*03:03. In summary, the results demonstrated that HLA-DRA*01:02/B1*03:01 is the HLA class II restriction allele for FLT3-D835Y-, NUP98::NSD1- and RPS4Y-specific T cell clones, whereas the DNMT3A-R882H-specific T cell clone was restricted to HLA-DQA1*01:02/B1*06:02 and HLA-DQA1*01:03/B1*06:03 and the RUNX1-specific T cell clones to HLA-DQA1*03:01/B1*03:02.

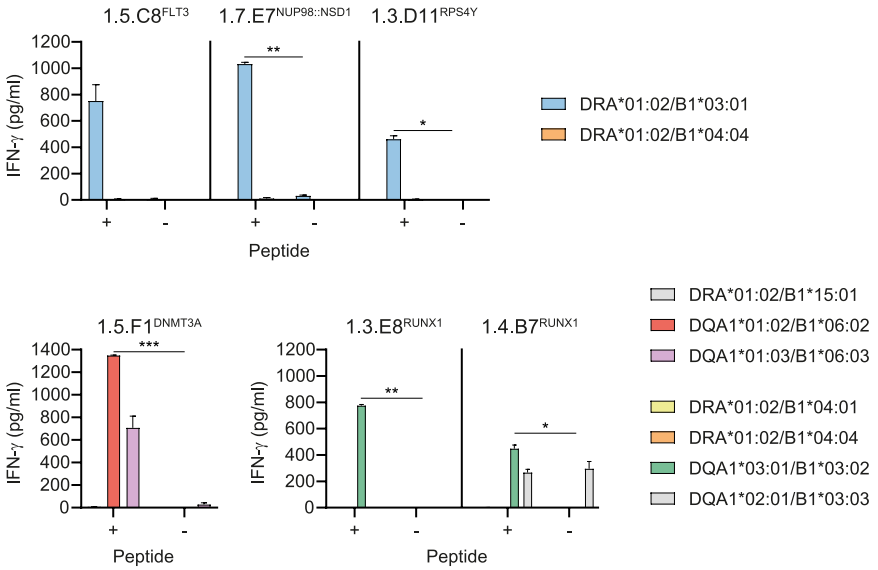

Figure 5. Validation of HLA class II restriction of neopeptide-specific CD4 T cell clones. Candidate HLA class II restriction alleles as deduced from T cell recognition patterns of peptide-loaded EBV-LCL were retrovirally introduced into K562. T cells were tested against K562 transduced with the indicated HLA-DRA, -DRB1, -DQA1 and -DQB1 alleles and pulsed with (+) or without (-) 1000 nM neopeptide. After overnight coincubation, IFN-γ release was measured by ELISA. HLA-DRA*01:02/B1*03:01 (blue bars) was validated as restriction allele for T cell clones 1.5.C8^{FLT3}, 1.7.E7$^{NUP98::NSD1}$ and 1.3.D11^{RPS4Y}. T cell clone 1.5.F1^{DNMT3A} reacted against peptide-pulsed K562 transduced with HLA-DQA1*01:02/B1*06:02 (red bars) and to a lesser extent against peptide-pulsed K562 transduced with HLA-DQA1*01:03/B1*06:03 (purple bars), whereas K562 transduced with HLA-DRA*01:02/B1*15:01 (grey bars) was not recognized, thereby validating HLA-DQB1*06:02 and -DQB1*06:03 as restriction elements for clone 1.5.F1^{DNMT3A}. HLA-DQA1*03:01/B1*03:02 (green bars) was confirmed as restriction element for T cell clones 1.3.E8^{RUNX1} and 1.4.B7^{RUNX1} (results for other RUNX1-specific T cell clones are shown in Supplemental Figure S4). T cell clone 1.4.B7^{RUNX1} also recognized K562 transduced with HLA-DQA1*02:01/B1*03:03 (grey bars) irrespective of peptide loading. A two-sided paired t-test was performed to determine if T cell reactivity against peptide-pulsed HLA-transduced K562 was significantly higher than against HLA-transduced K562 without peptide ($p < 0.05$ *, $p < 0.01$ **, $p < 0.001$ ***). Bars represent mean + SD of duplicate wells in a single experiment.

T cell recognition of endogenously processed HLA class II neopeptides

To investigate whether the neopeptides can be endogenously processed and presented by HLA class II on the cell surface, we tested T cell reactivity against K562 transduced with the relevant HLA class II restriction alleles as well as whole genes encoding full-length mutated or wild-type proteins. Clone 1.5.F1^{DNMT3A} reacted against K562 transduced with HLA-DQA1*01:02/B1*06:02 and mutated *DNMT3A* (K562-mDNMT3A-HLA), but not wild-type *DNMT3A* (K562-wtDNMT3A-HLA) (Figure 6A). T cell clone 1.5.C8^{FLT3} failed to react against K562 transduced with mutated *FLT3* and the relevant HLA allele (K562-mFLT3-HLA), whereas clone

1.7.E7$^{NUP98::NSD1}$ secreted only low levels of IFN-γ upon stimulation with K562 transduced with the *NUP98::NSD1* fusion gene and relevant HLA allele (K562-NUP98::NSD1-HLA). All 8 RUNX1-reactive T cell clones showed stronger reactivity against K562 transduced with HLA-DQA1*03:01/B1*03:02 and mutated *RUNX1* (K562-mRUNX1-HLA) than against K562 transduced with wild-type *RUNX1* (K562-wtRUNX1-HLA) (1.3.E8^{RUNX1} and 1.4.B7^{RUNX1} in Figure 6B; other RUNX1-specific clones in Supplemental Figure S5A). Four of the 8 T cell clones (1.3.E8^{RUNX1}, 1.4.B7^{RUNX1}, 1.4.F6^{RUNX1} and 1.4.G7^{RUNX1}) also reacted against K562-E4 transduced with the relevant HLA-DQ allele (K562-E4-HLA) in which a homozygous *RUNX1* frameshift mutation was introduced by CRISPR-Cas9 (1.3.E8^{RUNX1} and 1.4.B7^{RUNX1} in Figure 6C; other RUNX1-specific clones in Supplemental Figure S5B). In contrast, AML cell line SIG-M5-C9 transduced with the relevant HLA-DQ allele (SIG-M5-C9-HLA) in which a similar heterozygous *RUNX1* frameshift mutation was introduced by CRISPR-Cas9 was not recognized. Altogether, our data showed that DNMT3A-FPV-H and RUNX1-CAQ are two neopeptides that can be endogenously processed and presented by HLA class II on the cell surface.

Recognition of patient-derived AML cells by T cell clone 1.5.F1^{DNMT3A}

Since T cell clone 1.5.F1^{DNMT3A} showed reactivity against K562 transduced with mutated *DNMT3A* and the relevant HLA-DQ restriction allele, we tested reactivity of the clone against HLA-DQB1*06:02 or -DQB1*06:03 positive patient-derived AML samples with *DNMT3A-R882H*. We first tested reactivity against AML cells and, as negative control, EBV-LCL that were obtained from the same patient (Figure 7A). In this test, HLA class II-expressing AML cells were enriched by MACS, and EBV-LCL, generated from PBMCs when entering clinical remission after intensive chemotherapy, expressed high levels of HLA class II and wild-type *DNMT3A*. Clone 1.5.F1^{DNMT3A} specifically secreted IFN-γ upon stimulation with AML cells, but not EBV-LCL. Next, we tested clone 1.5.F1^{DNMT3A} against a larger panel (n = 5) of HLA-DQB1*06:02 or -DQB1*06:03 positive patient-derived AML samples with *DNMT3A-R882H* (Figure 7B). In this experiment, AML cells were not enriched for HLA class II expression. Clone 1.5.F1^{DNMT3A} showed reactivity against all AML samples, albeit to different extents, and all AML samples were also recognized by positive control CD4 T cell clones for minor histocompatibility antigens (37). The only exception was AML24, which was not recognized by clone 1.5.F1^{DNMT3A} and weakly by the positive control T cell clone.

To determine whether T cell clone 1.5.F1^{DNMT3A} was able to kill AML cells with *DNMT3A-R882H*, clone 1.5.F1^{DNMT3A} was coincubated with patient-derived AML samples (n = 4) for 48 hours, and numbers of viable HLA-DQ-expressing AML cells were measured in a flow cytometry-based killing assay (Figure 7C and Supplemental Figure S6). All 4 AML samples were subtyped as HLA-DQB1*06:03, and three AML

carried *DNMT3A-R882H* (AML23, AML24, AML25), whereas one AML was negative for the mutation (AML27). In all AML samples, HLA-DQ expression was variable, with subpopulations expressing high levels and subpopulations expressing no or low HLA-DQ. The proportion of HLA-DQ-expressing cells was higher in AML23 and AML27 as compared to AML24 and AML25. The data showed that clone 1.5.F1^{DNMT3A} failed to induce specific lysis of AML cells with *DNMT3A-R882H* irrespective of HLA-DQ expression. Similarly, no lysis was observed after exogenous pulsing of AML cells with the DNMT3A-FPV-H peptide. In conclusion, we identified a DNMT3A-R882H neoantigen presented on patient-derived AML cells by HLA-DQB1*06:02 and -DQB1*06:03 that is recognized by a CD4 T cell clone, which is not able to kill AML cells.

Figure 6. CD4 T cell recognition of endogenously processed neopeptides. K562 transduced with the relevant HLA class II restriction alleles as well as whole genes encoding mutated or wild-type proteins were coincubated overnight with neopeptide-specific CD4 T cell clones from donors HD1 (**A**) and HD3 (**B**). Autologous EBV-LCL or HLA-transduced K562 (K562-HLA) were pulsed with 1 µM of neopeptide as positive controls. IFN-γ release was measured by ELISA. T cell clone 1.5.F1^{DNMT3A} recognized K562 transduced with HLA-DQA1*01:02/B1*06:02 and mutated *DNMT3A* (K562-mDNMT3A-HLA), but not K562 transduced with wild-type *DNMT3A* (K562-wtDNMT3A-HLA). T cell clone 1.5.C8^{FLT3} failed to react against K562 transduced with the relevant HLA class II allele and mutated gene (K562-mFLT3-HLA), while clone 1.7.E7$^{NUP98::NSD1}$ secreted only low levels of IFN-γ. All RUNX1-specific T cell clones were more reactive against K562 transduced with HLA-DQA1*03:01/B1*03:02 and mutated *RUNX1* (K562-mRUNX1-HLA) than against K562 transduced with wild-type *RUNX1* (K562-wtRUNX1-HLA). Results are shown for clones 1.3.E8^{RUNX1} and 1.4.B7^{RUNX1} (results for the other RUNX1-specific clones are shown in Supplemental Figure S5A). A two-sided paired t-test was performed to determine if T cell reactivity against K562 transduced with HLA and the mutated gene was significantly higher than against K562 transduced with HLA and the wild-type gene ($p < 0.05$ *, $p < 0.01$ **, $p < 0.001$ ***). Bars represent mean + SD of duplicate wells in a single experiment. (**C**) RUNX1-specific T cell clones were tested against CML cell line K562 and AML cell line SIG-M5 in which *RUNX1* frameshift mutations were introduced by CRISPR-Cas9. The resulting genome-edited K562-E4 and SIG-M5-C9 cell lines were transduced with HLA-DQA1*03:01/B1*03:02 (K562-E4-HLA, SIG-M5-C9-HLA) and pulsed with 1 µM RUNX1-CAQ peptide as positive controls. After overnight coincubation, IFN-γ release was measured by ELISA. T cell clones 1.3.E8^{RUNX1}, 1.4.B7^{RUNX1}, 1.4.F6^{RUNX1} and 1.4.G7^{RUNX1} were more reactive against K562-E4-HLA than K562-E4 (clones 1.4.F6^{RUNX1} and 1.4.G7^{RUNX1} are shown in Supplemental Figure S5B). Clones 1.2.C2^{RUNX1}, 1.2.D2^{RUNX1}, 1.5.F10^{RUNX1} and 1.5.H7^{RUNX1} secreted only low levels of IFN-γ or did not react against K562-E4-HLA (Supplemental Figure S5B). None of the T cell clones recognized SIG-M5-C9-HLA. A two-sided paired t-test was performed to determine if T cell reactivity against K562-E4-HLA was significantly higher than against K562-E4, and reactivity against SIG-M5-C9-HLA significantly higher than against SIG-M5-C9 ($p < 0.05$ *, $p < 0.01$ **, $p < 0.001$ ***). Bars represent mean + SD of duplicate wells in a single experiment, except for peptide-pulsed SIG-M5-C9, which was tested in single wells. *Figure on opposite page.*

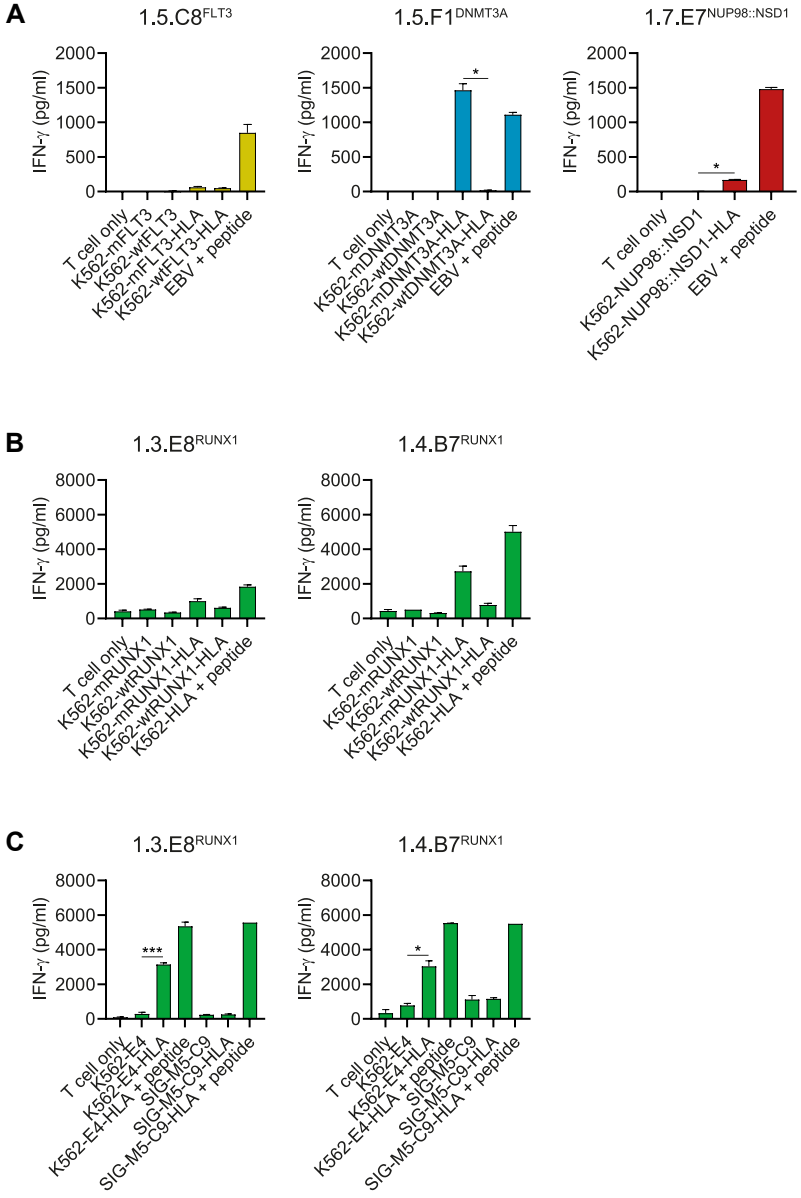
A
1.5.C8FLT3
1.5.F1DNMT3A
1.7.E7NUP98::NSD1
IFN-γ (pg/ml)
2000
1500
1000
500
0
*
T cell only
K562-mFLT3
K562-wtFLT3
K562-mFLT3-HLA
K562-wtFLT3-HLA
EBV + peptide
K562-mDNMT3A
K562-wtDNMT3A
K562-mDNMT3A-HLA
K562-wtDNMT3A-HLA
K562-NUP98::NSD1
K562-NUP98::NSD1-HLA
B
1.3.E8RUNX1
1.4.B7RUNX1
8000
6000
4000
2000
K562-mRUNX1
K562-wtRUNX1
K562-mRUNX1-HLA
K562-wtRUNX1-HLA
K562-HLA + peptide
C
***
K562-E4
K562-E4-HLA
K562-E4-HLA + peptide
SIG-M5-C9
SIG-M5-C9-HLA
SIG-M5-C9-HLA + peptide

Figure 7. Targeting of patient-derived AML cells by T cell clone 1.5.F1^{DNMT3A}. (**A**) T cell clone 1.5.F1^{DNMT3A} was tested for reactivity against HLA-DQB1*06:02 positive patient-derived AML cells with *DNMT3A-R882H*. To select AML cells with high HLA class II expression, cells were isolated by magnetic anti-PE beads after staining with a PE-conjugated antibody against HLA-DP prior to the test. EBV-LCL from the same patient were pulsed in the absence or presence of 1 μM of DNMT3A-FPV-H peptide and included as negative and positive control, respectively. After overnight coincubation, IFN-γ release was measured by ELISA. T cell clone 1.5.F1^{DNMT3A} showed specific recognition of AML cells, but not EBV-LCL. A two-sided paired t-test was performed to determine if T cell reactivity against AML cells was significantly higher than against EBV-LCL ($p < 0.05$ *, $p < 0.01$ **, $p < 0.001$ ***). Bars represent mean + SD of duplicate wells in a single experiment. (**B**) T cell clone 1.5.F1^{DNMT3A} was tested for reactivity against multiple HLA-DQB1*06:02 or -DQB1*06:03 positive patient-derived AML samples with *DNMT3A-R882H* (*n* = 5). HLA-DQB1*06:02-restricted T cell clone 8-10A and HLA-DQB1*06:03-restricted T cell clone ZRZ38 are reactive against minor histocompatibility antigens LB-TNFRSF10D-1S and LB-PI4K2B-1S, respectively, and were included as positive controls. For clone 1.5.F1^{DNMT3A}, EBV22 was used as negative control. For clones 8-10A and ZRZ38, EBV-LCL positive for HLA-DQB1*06:02 and HLA-DQB1*06:03, respectively, but negative for the minor histocompatibility antigens were used as negative controls. After overnight coincubation, IFN-γ release was measured by ELISA. T cell clone 1.5.F1^{DNMT3A} reacted against 4 out of 5 AML, i.e. AML22, AML23, AML25 and AML26, but not against AML24. T cell recognition of AML24 was also low for positive control clone ZRZ38. A two-sided paired t-test was performed to determine if T cell reactivity against AML cells was significantly higher than against EBV-LCL ($p < 0.05$ *, $p < 0.01$ **, $p < 0.001$ ***). Bars represent mean + SD of duplicate wells in a single experiment. (**C**) T cell clone 1.5.F1^{DNMT3A} was tested for lysis of HLA-DQB1*06:03 positive patient-derived AML samples with *DNMT3A-R882H* (AML23, AML24 and AML25) or wild-type *DNMT3A* (AML27) in a flow cytometry-based killing assay. AML samples were also tested for lysis by clone 1.5.F1^{DNMT3A} after pulsing with 1 μM DNMT3A-FPV-H peptide. All AML samples were also positive for HLA-A*02:01 and coincubated with CD8 T cells transduced with an HLA-A*02:01-restricted CMVpp65-specific TCR (CMV-A2 TCR-T cells) or mutated NPM1-specific TCR (mNPM1-A2 TCR-T cells) as negative and positive controls, respectively. After 48 hours of coincubation at a ratio of 1:1, samples were stained with PE-, APC- and FITC-conjugated antibodies against CD33, CD34 and HLA-DQ, respectively, viability dye Zombie Red to exclude dead cells and BV421-conjugated antibodies against CD3, CD8 and CD19 to exclude lymphocytes. Viable AML cells after coincubation with T cell clone 1.5.F1^{DNMT3A} (upper panels) or control CMV-A2 TCR-T cells (lower panels) were clustered by HLA-DQ expression. Each AML sample contained subpopulations with high HLA-DQ expression and subpopulations with no or low HLA-DQ expression. T cell clone 1.5.F1^{DNMT3A} did not kill AML cells with *DNMT3A-R882H* irrespective of HLA-DQ surface expression. Results were similar for negative control CMV-A2 TCR-T cells. Combined data from triplicate wells in a single experiment are visualized. Quantification of absolute numbers of viable AML cells is shown in Supplemental Figure S6C. *Figure on opposite page.*

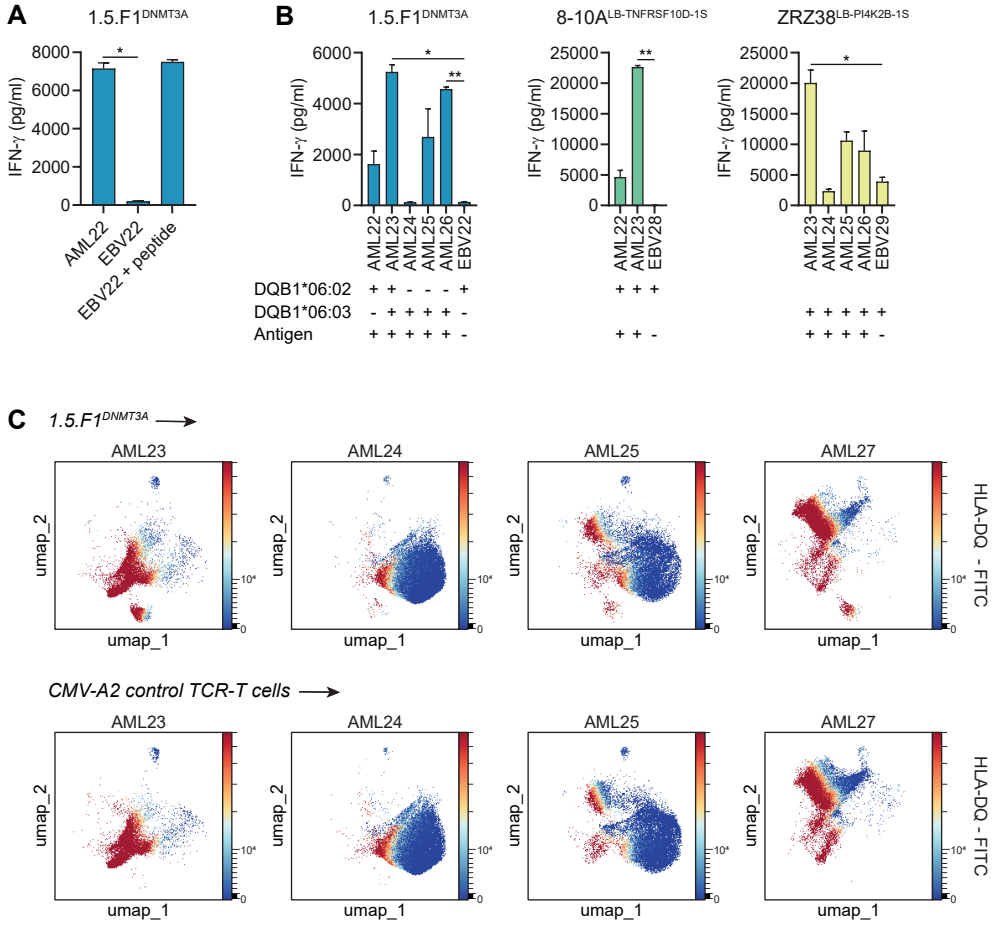
A
1.5.F1DNMT3A
IFN-γ (pg/ml)
AML22
EBV22
EBV22 + peptide
B
1.5.F1DNMT3A
8-10ALB-TNFRSF10D-1S
ZRZ38LB-PI4K2B-1S
AML22
AML23
AML24
AML25
AML26
EBV22
EBV28
EBV29
DQB1*06:02
DQB1*06:03
Antigen
C
1.5.F1DNMT3A
CMV-A2 control TCR-T cells
AML23
AML24
AML25
AML27
umap_1
umap_2
HLA-DQ - FITC

Discussion

In this study, we developed a strategy to isolate neoantigen-specific CD4 T cells after *in vitro* peptide stimulation, since T cell isolation by peptide-HLA class II tetramers is still challenging. Two neopeptides endogenously processed from *DNMT3A-R882H* and a long alternative reading frame created by *RUNX1* frameshift mutations were shown to be recognized by CD4 T cell clones. The DNMT3A-R882H peptide was also presented on patient-derived AML cells, thereby validating this peptide as public HLA class II neoantigen on AML.

RUNX1 is mutated in 10-15% of patients with AML, of which one-third are frameshift mutations creating the same long alternative reading frame (38). We isolated 8 CD4 T cell clones specific for the RUNX1-CAQ peptide, which is located 30 amino acids from the C-terminus of the prolonged protein and shared by most *RUNX1* frameshift mutations. RUNX1-specific T cell clones reacted differently to K562-E4 and SIG-M5-C9, both expressing the same alternative reading frame. Of the 8 T cell clones, 4 clones recognized K562-E4, whereas none of the T cell clones reacted against SIG-M5-C9. Since the 8 T cell clones expressed at least two different TCR clonotypes, this lack of recognition by all T cell clones is unlikely to be caused by the TCRs, but probably attributable to intrinsic differences between the two cell lines. For instance, antigen expression may be lower on SIG-M5-C9 due to differences in HLA class II antigen processing and presentation, which is known to depend partly on the balance between HLA-DM and HLA-DO (39). Analysis of public gene expression data (40) demonstrated that the ratio of HLA-DO to HLA-DM in K562 and SIG-M5 is high, suggesting that both cell lines have the potential to present a broad repertoire of HLA class II peptides on their cell surface. Besides processing and presentation, lower antigen expression on SIG-M5-C9 may be caused by a heterozygous *RUNX1* mutation, whereas homozygous mutations are present in K562-E4. Moreover, T cell recognition could be influenced by differential expression of adhesion, costimulatory or inhibitory molecules on the cell surface of both cell lines. Although the exact reason remains unknown, T cell recognition of K562-E4 demonstrated that the RUNX1-CAQ peptide can be endogenously processed and presented on the cell surface. Whether the peptide is a neoantigen that can be targeted on AML by immunotherapy, for example by T cells engineered with TCRs of our RUNX1-specific clones, requires further testing of T cell clones against HLA-DQB1*03:02 positive patient-derived AML samples carrying *RUNX1* frameshift mutations, which were not available in our biobank and could not be easily collected.

DNMT3A-R882 is a hotspot mutation in exon 23 occurring in approximately 15% of patients with AML. More than half of the mutations are *DNMT3A-R882H* mutations

(32, 41). *DNMT3A* mutations are frequent in elderly people with clonal hematopoiesis of indeterminate potential (CHIP) or clonal cytopenia of undetermined significance (CCUS) who are at increased risk of developing hematological malignancies (42). This indicates that *DNMT3A* mutations are early driver mutations in preleukemic hematopoietic stem cells and that malignant transformation occurs upon accumulation of other cooperating mutations. *DNMT3A-R882H* is also often detectable in patients with AML in complete remission after chemotherapy (43-45), probably due to persistence of preleukemic stem cells after therapy. Our identified DNMT3A-R882H neoantigen may be used to target preleukemic stem cells by immunotherapy. Pre-emptive treatment with DNMT3A-R882H neoantigen-directed immunotherapy may be particularly attractive to prevent disease recurrence in patients with CHIP/CCUS who are in remission after treatment for AML.

Since all neoantigen-specific T cell clones in this study were isolated from healthy individuals, it remains unclear whether DNMT3A-R882H neoantigen-specific CD4 T cells are circulating in patients with AML. If present, neoantigen vaccination may be considered to induce or boost immune responses against *DNMT3A*-mutated AML. Personalized neoantigen vaccines have been shown to increase frequencies of neoantigen-specific T cells, and two recent studies reported clinical benefit of these vaccines (46, 47). Another approach, which is independent of circulating DNMT3A-R882H neoantigen-specific CD4 T cells, are bispecific T cell engagers. These engagers can be composed of a TCR or TCR-like domain that binds to a neoantigen-HLA complex and a domain that binds to CD3, thereby stimulating and redirecting CD8 as well CD4 T cell reactivity towards tumor cells (48). Alternatively, CD4 T cells can be genetically engineered with the DNMT3A-R882H neoantigen-specific TCR of clone 1.5.F1^{DNMT3A} and adoptively transferred to patients after *in vitro* expansion (49). Although these therapies may show clinical benefit, their efficacy can potentially be limited by the immunosuppressive tumor microenvironment in AML. AML cells can employ various mechanisms to suppress anti-tumor responses and have been shown to induce T cell dysfunction, upregulate expression of inhibitory molecules, secrete immunosuppressive soluble factors and downregulate HLA expression (50, 51). Therefore, the above immunotherapies may be more effective when combined with additional treatment targeting the immunosuppressive environment in AML.

Although cytotoxic CD4 T cells exist, T cell clone 1.5.F1^{DNMT3A} was able to release IFN-γ upon stimulation with patient-derived AML cells, but failed to induce lysis of these cells. Based on this lack of killing capacity, the TCR of clone 1.5.F1^{DNMT3A} is not expected to produce T cells with direct anti-tumor potential upon transfer to CD4 T cells. Our data also showed substantial intra- and inter-patient heterogeneity in HLA class II expression on AML cells, suggesting that AML cells with low or negative HLA class II expression may escape direct killing by CD4 T cells. Instead of

mediating direct cytotoxicity, clone 1.5.F1^{DNMT3A} may promote anti-tumor immunity indirectly as T helper cell. CD4 T cells are known to contribute to anti-tumor responses by providing help to induction of cytotoxic CD8 T cells and stimulating their effector and memory functions (23, 24). Recent studies in mice convincingly demonstrated that CD4 T cells transduced with neoantigen-specific TCRs play an important role in eliminating major histocompatibility complex class II negative tumors when combined with CD8 T cells (52, 53). This provides a rationale to combine DNMT3A-R882H neoantigen-specific TCR-engineered CD4 T cells with neoantigen-specific CD8 T cells to treat AML. No HLA class I-restricted TCRs for DNMT3A neoantigens have been identified to date, but we previously isolated an HLA-A*02:01-restricted TCR for a NPM1 neoantigen, which upon transfer to CD8 T cells effectively targets AML *in vitro* and *in vivo* (15). Since *DNMT3A-R882* and *NPM1* mutations often co-occur (11), it is worth exploring whether combined transfer of CD8 T cells with the NPM1-specific TCR and CD4 T cells with the DNMT3A-specific TCR leads to more effective eradication of AML with *DNMT3A* and *NPM1* co-mutations as compared to NPM1-specific CD8 T cells alone.

In conclusion, we here identified an HLA class II neoantigen encoded by the well-known *DNMT3A-R882H* hotspot mutation that may become an important target for immunotherapeutic strategies to treat HLA-DQB1*06:02 or -DQB1*06:03 positive patients with AML.

Acknowledgements

The authors gratefully acknowledge the Flow cytometry Core Facility (FCF) of the Leiden University Medical Center in Leiden, The Netherlands, for cell sorting assistance.

References

1. Döhner H, Wei AH, Appelbaum FR, et al. Diagnosis and management of AML in adults: 2022 recommendations from an international expert panel on behalf of the ELN. Blood. 2022;140(12):1345-77.
2. DiNardo CD, Erba HP, Freeman SD, et al. Acute myeloid leukaemia. Lancet. 2023;401(10393):2073-86.
3. Sasaki K, Ravandi F, Kadia TM, et al. De novo acute myeloid leukemia: A population-based study of outcome in the United States based on the Surveillance, Epidemiology, and End Results (SEER) database, 1980 to 2017. Cancer. 2021;127(12):2049-61.
4. Subklewe M, Bücklein V, Sallman D, et al. Novel immunotherapies in the treatment of AML: is there hope? Hematology Am Soc Hematol Educ Program. 2023;2023(1):691-701.
5. Peri A, Salomon N, Wolf Y, et al. The landscape of T cell antigens for cancer immunotherapy. Nat Cancer. 2023;4(7):937-54.
6. Daver N, Alotaibi AS, Bücklein V, et al. T-cell-based immunotherapy of acute myeloid leukemia: current concepts and future developments. Leukemia. 2021;35(7):1843-63.
7. Haubner S, Subklewe M, Sadelain M. Honing CAR T cells to tackle acute myeloid leukemia. Blood. 2025;145(11):1113-25.
8. Schumacher TN, Schreiber RD. Neoantigens in cancer immunotherapy. Science. 2015;348(6230):69-74.
9. Ley TJ, Miller C, Ding L, et al. Genomic and epigenomic landscapes of adult de novo acute myeloid leukemia. N Engl J Med. 2013;368(22):2059-74.
10. Alexandrov LB, Nik-Zainal S, Wedge DC, et al. Signatures of mutational processes in human cancer. Nature. 2013;500(7463):415-21.
11. Papaemmanuil E, Gerstung M, Bullinger L, et al. Genomic Classification and Prognosis in Acute Myeloid Leukemia. N Engl J Med. 2016;374(23):2209-21.
12. Kishtagari A, Levine RL, Viny AD. Driver mutations in acute myeloid leukemia. Curr Opin Hematol. 2020;27(2):49-57.
13. Graf C, Heidel F, Tenzer S, et al. A neoepitope generated by an FLT3 internal tandem duplication (FLT3-ITD) is recognized by leukemia-reactive autologous CD8+ T cells. Blood. 2007;109(7):2985-8.
14. Greiner J, Ono Y, Hofmann S, et al. Mutated regions of nucleophosmin 1 elicit both CD4(+) and CD8(+) T-cell responses in patients with acute myeloid leukemia. Blood. 2012;120(6):1282-9.
15. van der Lee DI, Reijmers RM, Honders MW, et al. Mutated nucleophosmin 1 as immunotherapy target in acute myeloid leukemia. J Clin Invest. 2019;129(2):774-85.
16. van der Lee DI, Koutsoumpli G, Reijmers RM, et al. An HLA-A*11:01-Binding Neoantigen from Mutated NPM1 as Target for TCR Gene Therapy in AML. Cancers (Basel). 2021;13(21):5390.
17. Forghieri F, Riva G, Lagreca I, et al. Characterization and dynamics of specific T cells against nucleophosmin-1 (NPM1)-mutated peptides in patients with NPM1-mutated acute myeloid leukemia. Oncotarget. 2019;10(8):869-82.
18. Biernacki MA, Foster KA, Woodward KB, et al. CBFB-MYH11 fusion neoantigen enables T cell recognition and killing of acute myeloid leukemia. J Clin Invest. 2020;130(10):5127-41.
19. Giannakopoulou E, Lehander M, Virding Culleton S, et al. A T cell receptor targeting a recurrent driver mutation in FLT3 mediates elimination of primary human acute myeloid leukemia in vivo. Nat Cancer. 2023;4(10):1474-90.
20. Biernacki MA, Lok J, Black RG, et al. Discovery of U2AF1 neoantigens in myeloid neoplasms. J Immunother Cancer. 2023;11(12):e007490.
21. Leung WK, Torres Chavez AG, French-Kim M, et al. Targeting IDH2R140Q and other neoantigens in acute myeloid leukemia. Blood. 2024;143(17):1726-37.

22. Struckman NE, de Jong RCM, Honders MW, et al. Hotspot DNA Methyltransferase 3A (DNMT3A) and Isocitrate Dehydrogenase 1 and 2 (IDH1/2) Mutations in Acute Myeloid Leukemia and Their Relevance as Targets for Immunotherapy. Biomedicines. 2024;12(5):1086.
23. Borst J, Ahrends T, Bąbała N, et al. CD4(+) T cell help in cancer immunology and immunotherapy. Nat Rev Immunol. 2018;18(10):635-47.
24. Speiser DE, Chijioke O, Schaeuble K, et al. CD4(+) T cells in cancer. Nat Cancer. 2023;4(3):317-29.
25. Oh DY, Fong L. Cytotoxic CD4(+) T cells in cancer: Expanding the immune effector toolbox. Immunity. 2021;54(12):2701-11.
26. Sondka Z, Dhir NB, Carvalho-Silva D, et al. COSMIC: a curated database of somatic variants and clinical data for cancer. Nucleic Acids Res. 2024;52(D1):D1210-d7.
27. Jensen KK, Andreatta M, Marcatili P, et al. Improved methods for predicting peptide binding affinity to MHC class II molecules. Immunology. 2018;154(3):394-406.
28. Gonzalez-Galarza FF, McCabe A, Santos E, et al. Allele frequency net database (AFND) 2020 update: gold-standard data classification, open access genotype data and new query tools. Nucleic Acids Res. 2020;48(D1):D783-d8. Available at https://www.allelefrequencies.net/top10freqs.asp.
29. Shen MW, Arbab M, Hsu JY, et al. Predictable and precise template-free CRISPR editing of pathogenic variants. Nature. 2018;563(7733):646-51.
30. Seki A, Rutz S. Optimized RNP transfection for highly efficient CRISPR/Cas9-mediated gene knockout in primary T cells. J Exp Med. 2018;215(3):985-97.
31. Morton LT, Reijmers RM, Wouters AK, et al. Simultaneous Deletion of Endogenous TCRαβ for TCR Gene Therapy Creates an Improved and Safe Cellular Therapeutic. Mol Ther. 2020;28(1):64-74.
32. Arindrarto W, Borràs DM, de Groen RAL, et al. Comprehensive diagnostics of acute myeloid leukemia by whole transcriptome RNA sequencing. Leukemia. 2021;35(1):47-61.
33. Miyara M, Yoshioka Y, Kitoh A, et al. Functional delineation and differentiation dynamics of human CD4+ T cells expressing the FoxP3 transcription factor. Immunity. 2009;30(6):899-911.
34. Qi Q, Liu Y, Cheng Y, et al. Diversity and clonal selection in the human T-cell repertoire. Proc Natl Acad Sci U S A. 2014;111(36):13139-44.
35. Stumpf AN, van der Meijden ED, van Bergen CA, et al. Identification of 4 new HLA-DR-restricted minor histocompatibility antigens as hematopoietic targets in antitumor immunity. Blood. 2009;114(17):3684-92.
36. van Balen P, van Bergen CAM, van Luxemburg-Heijs SAP, et al. CD4 Donor Lymphocyte Infusion Can Cause Conversion of Chimerism Without GVHD by Inducing Immune Responses Targeting Minor Histocompatibility Antigens in HLA Class II. Front Immunol. 2018;9:3016.
37. Griffioen M, van der Meijden ED, Slager EH, et al. Identification of phosphatidylinositol 4-kinase type II beta as HLA class II-restricted target in graft versus leukemia reactivity. Proc Natl Acad Sci U S A. 2008;105(10):3837-42.
38. Tang JL, Hou HA, Chen CY, et al. AML1/RUNX1 mutations in 470 adult patients with de novo acute myeloid leukemia: prognostic implication and interaction with other gene alterations. Blood. 2009;114(26):5352-61.
39. Kremer AN, van der Meijden ED, Honders MW, et al. Endogenous HLA class II epitopes that are immunogenic in vivo show distinct behavior toward HLA-DM and its natural inhibitor HLA-DO. Blood. 2012;120(16):3246-55.
40. Scholtalbers J, Boegel S, Bukur T, et al. TCLP: an online cancer cell line catalogue integrating HLA type, predicted neo-epitopes, virus and gene expression. Genome Med. 2015;7:118.
41. Ley TJ, Ding L, Walter MJ, et al. DNMT3A mutations in acute myeloid leukemia. N Engl J Med. 2010;363(25):2424-33.
42. Weeks LD, Ebert BL. Causes and consequences of clonal hematopoiesis. Blood. 2023;142(26):2235-46.

43. Gaidzik VI, Weber D, Paschka P, et al. DNMT3A mutant transcript levels persist in remission and do not predict outcome in patients with acute myeloid leukemia. Leukemia. 2018;32(1):30-7.
44. Rothenberg-Thurley M, Amler S, Goerlich D, et al. Persistence of pre-leukemic clones during first remission and risk of relapse in acute myeloid leukemia. Leukemia. 2018;32(7):1598-608.
45. Tanaka T, Morita K, Loghavi S, et al. Clonal dynamics and clinical implications of postremission clonal hematopoiesis in acute myeloid leukemia. Blood. 2021;138(18):1733-9.
46. Rojas LA, Sethna Z, Soares KC, et al. Personalized RNA neoantigen vaccines stimulate T cells in pancreatic cancer. Nature. 2023;618(7963):144-50.
47. Katsikis PD, Ishii KJ, Schliehe C. Challenges in developing personalized neoantigen cancer vaccines. Nat Rev Immunol. 2024;24(3):213-27.
48. Fenis A, Demaria O, Gauthier L, et al. New immune cell engagers for cancer immunotherapy. Nat Rev Immunol. 2024;24(7):471-86.
49. Zhou W, Yu J, Li Y, et al. Neoantigen-specific TCR-T cell-based immunotherapy for acute myeloid leukemia. Exp Hematol Oncol. 2022;11(1):100.
50. Vadakekolathu J, Rutella S. Escape from T-cell-targeting immunotherapies in acute myeloid leukemia. Blood. 2024;143(26):2689-700.
51. Restelli C, Ruella M, Paruzzo L, et al. Recent Advances in Immune-Based Therapies for Acute Myeloid Leukemia. Blood Cancer Discov. 2024;5(4):234-48.
52. Brightman SE, Becker A, Thota RR, et al. Neoantigen-specific stem cell memory-like CD4(+) T cells mediate CD8(+) T cell-dependent immunotherapy of MHC class II-negative solid tumors. Nat Immunol. 2023;24(8):1345-57.
53. Wolf SP, Anastasopoulou V, Drousch K, et al. One CD4+TCR and One CD8+TCR Targeting Autochthonous Neoantigens Are Essential and Sufficient for Tumor Eradication. Clin Cancer Res. 2024;30(8):1642-54.

Supplemental information

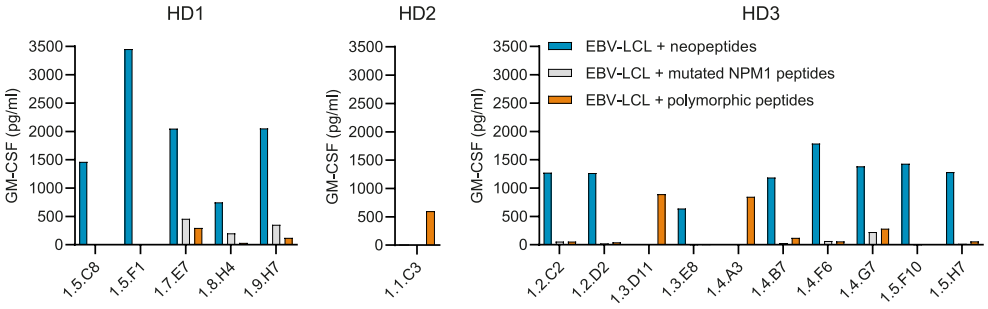

Figure S1. CD4 T cell clones recognizing neopeptide pools. CD4 T cells from healthy female donors HD1-3 were stimulated with peptides *in vitro*, and activated CD4 T cells were sorted and single cell expanded as described in Figure 3. T cell clones were tested for reactivity against autologous EBV-LCL pulsed with three peptide mixes containing 13-16 neopeptides (blue bars), 8 mutated NPM1 peptides (grey bars) or 6-8 polymorphic peptides (orange bars) each at 100 nM. After overnight coincubation, GM-CSF release was measured by ELISA. Results are shown for 16 T cell clones that specifically reacted against peptide pools. The neopeptide pool was recognized by 5 T cell clones from donor HD1 and 8 clones from donor HD3. The polymorphic peptide pool was recognized by one T cell clone from donor HD2 and two clones from donor HD3. No T cell clones reacted against EBV-LCL loaded with mutated NPM1 peptides. Bars represent results from single wells in a single experiment.

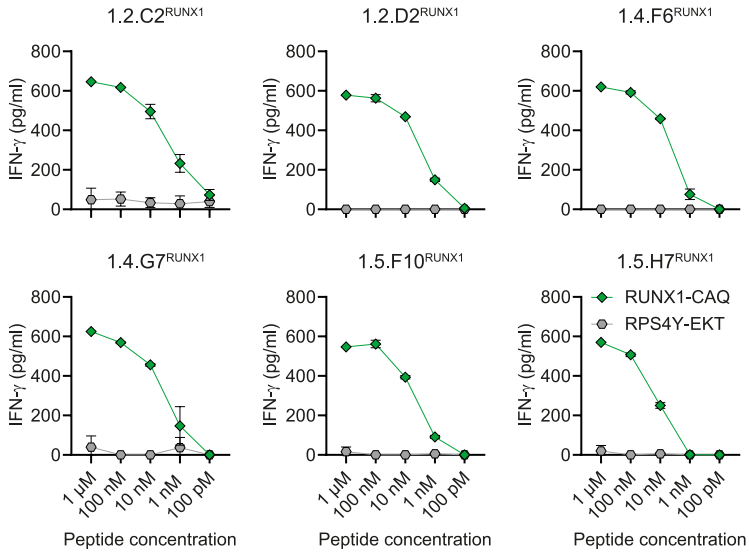

Figure S2. Affinity of CD4 T cell clones for titrated RUNX1-CAQ neopeptide. T cell clones 1.2.C2^{RUNX1}, 1.2.D2^{RUNX1}, 1.4.F6^{RUNX1}, 1.4.G7^{RUNX1}, 1.5.F10^{RUNX1} and 1.5.H7^{RUNX1} from donor HD3 were tested against autologous EBV-LCL pulsed with titrated concentrations of RUNX1-CAQ neopeptide (green diamonds) as described in Figure 4. Specific recognition of RUNX1-CAQ was observed for all clones. Symbols represent mean ± SD of duplicate wells. Representative data from one of two independent experiments is shown.

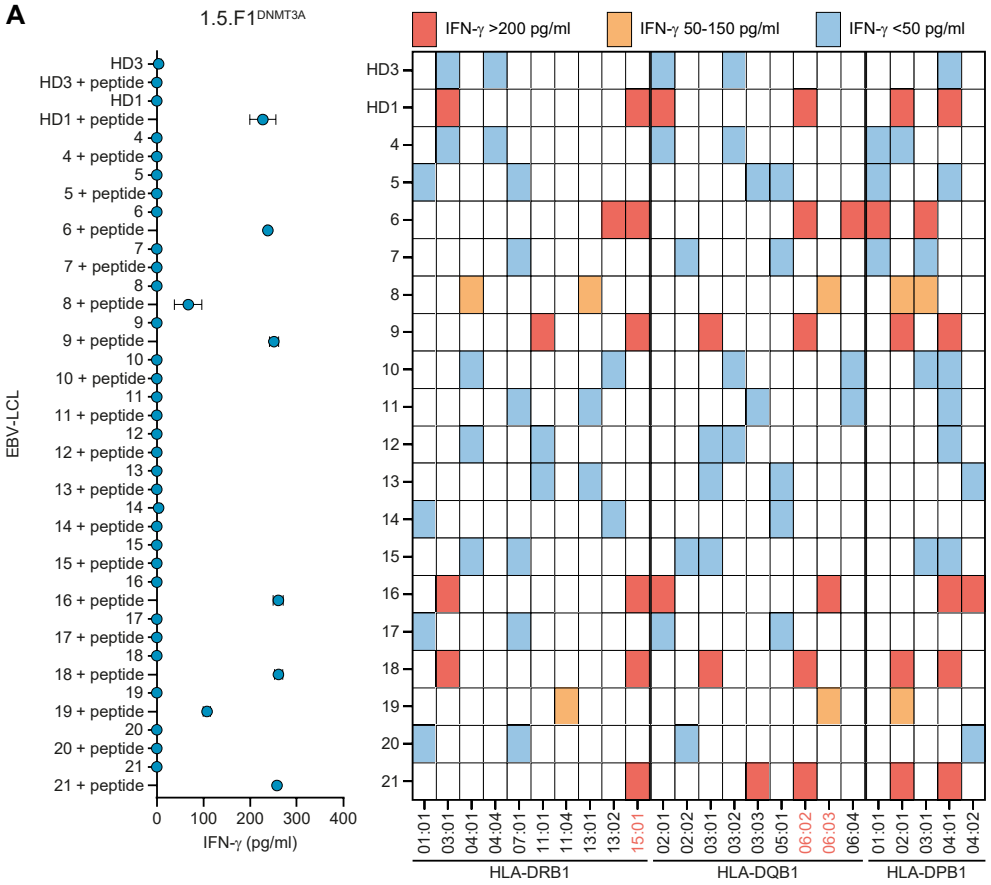

Figure S3. Determination of candidate HLA class II restriction alleles of neopeptide-specific CD4 T cell clones. To determine HLA class II restriction, neopeptide-specific T cell clones were tested against a panel of 20 EBV-LCL pulsed in the absence or presence of 1 µM neopeptide. Positive EBV-LCL were included for each of the 23 common HLA-DRB1, -DQB1 and -DPB1 alleles as used for peptide selection as well as for HLA-DRB1*04:04, which is expressed by donor HD3. After overnight coincubation, IFN-γ release was measured by ELISA. Symbols represent mean ± SD of duplicate wells. Representative data from one of three independent experiments is shown. (**A**) T cell clone 1.5.F1^{DNMT3A} showed >200 pg/ml IFN-γ release upon stimulation with peptide-loaded EBV-LCL from donors HD1, 6, 9, 16, 18 and 21, whereas low levels of IFN-γ of 50-150 pg/ml were released upon stimulation with peptide-loaded EBV-LCL from donors 8 and 19 (left panel). The right panel depicts typing for the 24 HLA class II beta alleles in the panel of 20 EBV-LCL. Colored rectangles represent peptide-loaded EBV-LCL inducing IFN-γ release by clone 1.5.F1^{DNMT3A} of >200 pg/ml (red), 50-150 pg/ml (orange) or <50 pg/ml (blue). All 6 peptide-loaded EBV-LCL that were strongly recognized were positive for HLA-DRB1*15:01, whereas this allele was absent on EBV-LCL that were not recognized. HLA-DQB1*06:02 was shared between 5 out of 6 EBV-LCL and was absent on EBV-LCL that were not recognized. EBV-LCL from donors 8 and 19, which induced low levels of IFN-γ, were negative for HLA-DRB1*15:01 and -DQB1*06:02, but positive for HLA-DQB1*06:03. Based on these data, HLA-DRB1*15:01, -DQB1*06:02 and -DQB1*06:03 were candidate restriction alleles for clone 1.5.F1^{DNMT3A}.

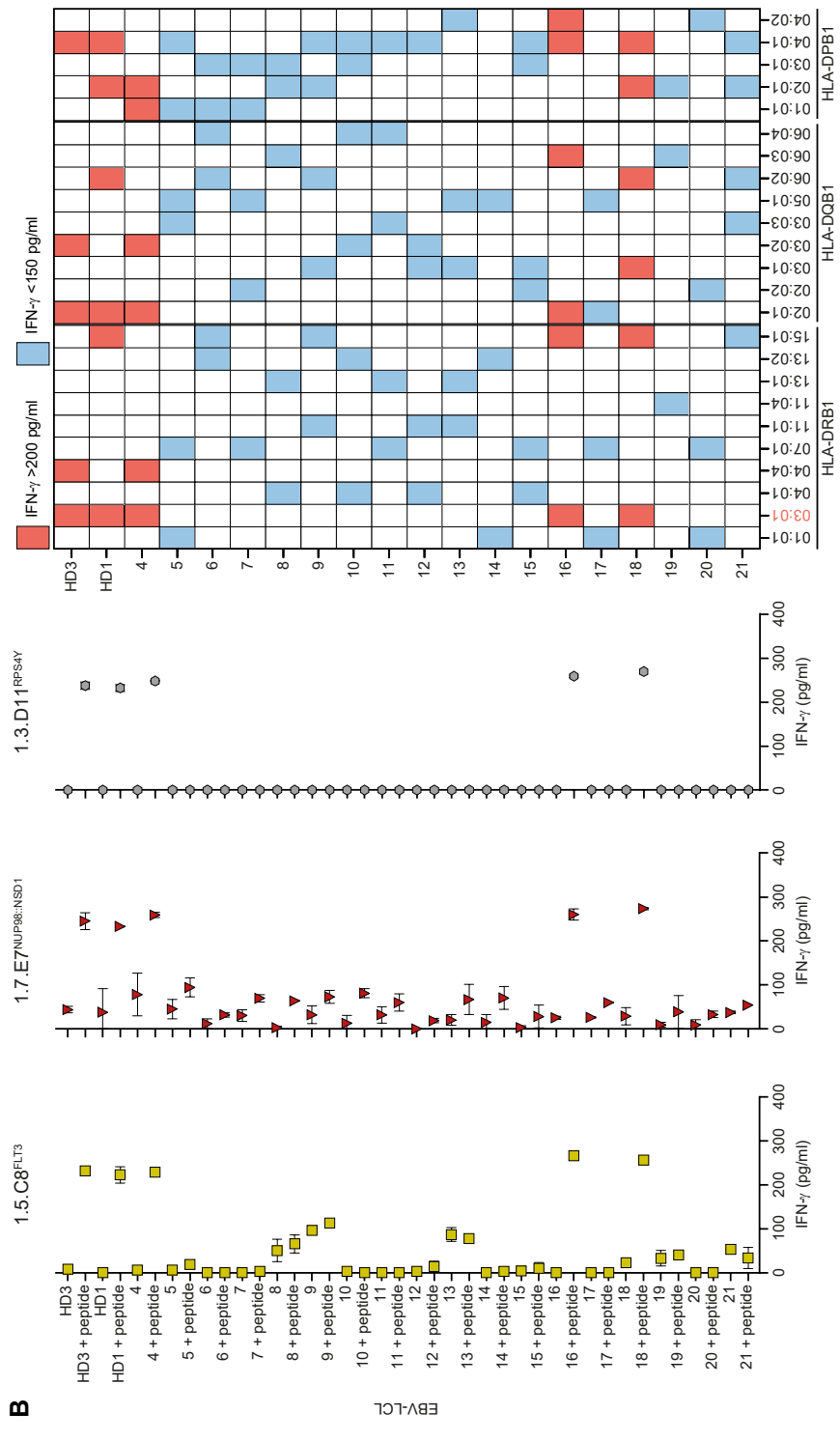

(**B**) T cell clones 1.5.C8^{FLT3}, 1.7.E7$^{NUP98::NSD1}$ and 1.3.D11^{RPS4Y} showed strong IFN-γ release (>200 pg/ml, red rectangles) upon stimulation with peptide-loaded EBV-LCL from donors HD3, HD1, 4, 16 and 18. These 5 EBV-LCL all expressed HLA-DRB1*03:01, whereas this allele was absent on EBV-LCL that were not recognized, suggesting that these T cell clones were HLA-DRB1*03:01-restricted.

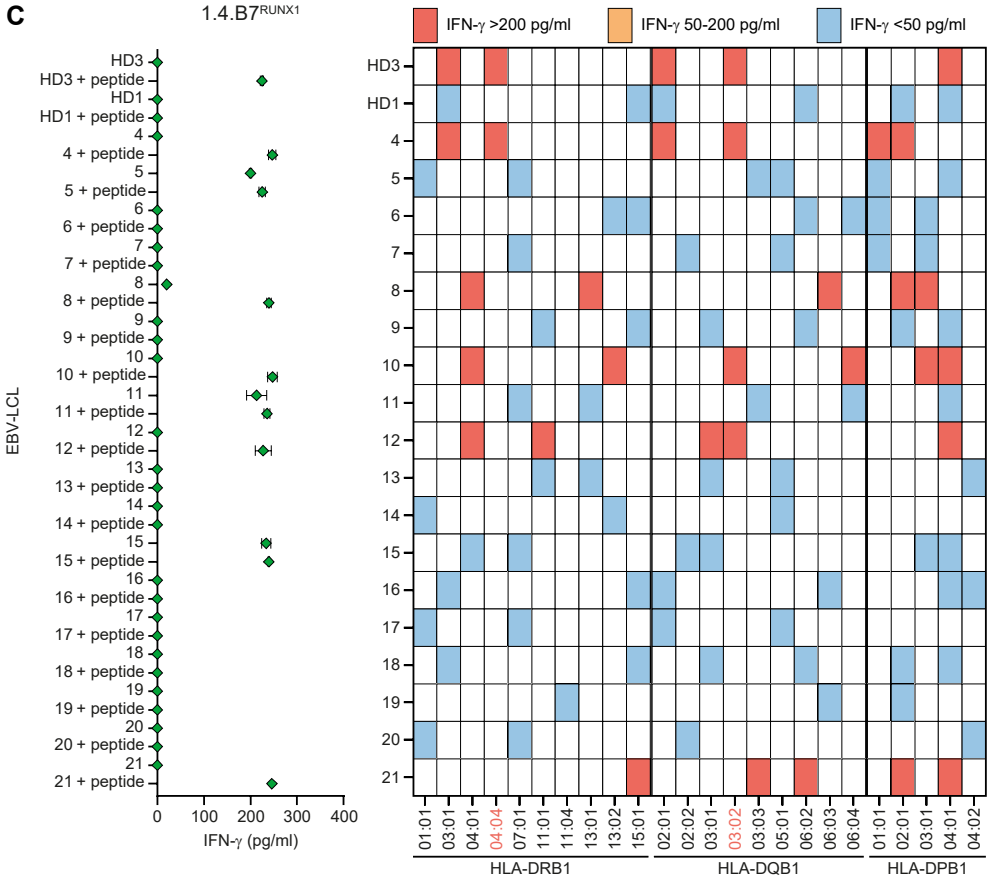

(**C**) All RUNX1-specific T cell clones, with the exception of clone 1.3.E8^{RUNX1}, showed similar recognition patterns as represented by T cell clone 1.4.B7^{RUNX1}. The T cell clones were strongly reactive against peptide-pulsed EBV-LCL from donors HD3, 4, 8, 10, 12 and 21. Of these 6 EBV-LCL, 4 shared HLA-DQB1*03:02 and two shared HLA-DRB1*04:04, while these alleles were absent on EBV-LCL that were not recognized. Based on these data, HLA-DQB1*03:02 was the candidate restriction element of RUNX1-specific T cell clones. All RUNX1-specific T cell clones, except for clone 1.3.E8^{RUNX1}, reacted against EBV-LCL from donors 5, 11 and 15 irrespective of peptide pulsing.

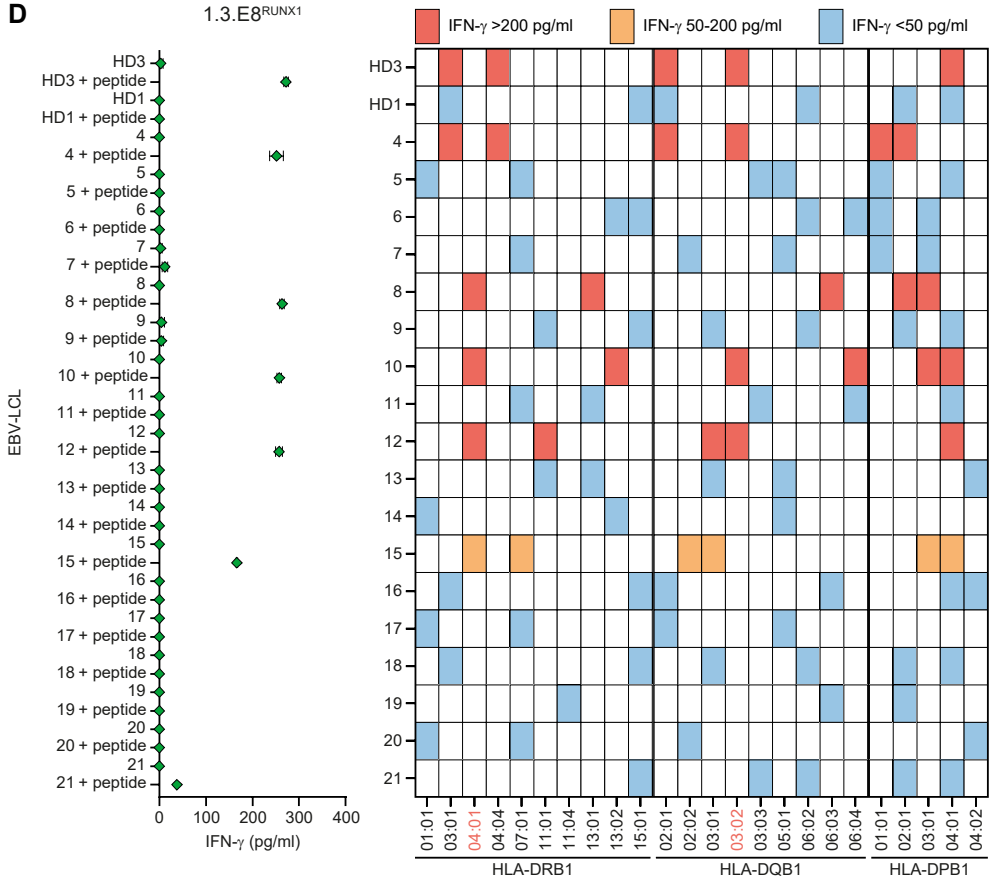

(**D**) T cell clone 1.3.E8^{RUNX1} showed a recognition pattern that was slightly different from other RUNX1-specific T cell clones, with strong recognition of peptide-loaded EBV-LCL from donors HD3, 4, 8, 10 and 12, whereas peptide-pulsed EBV-LCL from donor 15 was weakly recognized with IFN-γ release of 50-200 pg/ml. HLA-DQB1*03:02 and HLA-DRB1*04:01 were expressed by 4 and three of 5 strongly recognized EBV-LCL, respectively, suggesting that HLA-DQB1*03:02 was the candidate restriction allele for clone 1.3.E8^{RUNX1}.

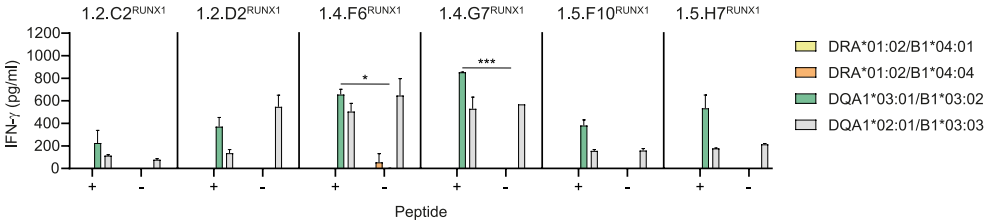

Figure S4. Validation of HLA class II restriction alleles for RUNX1-reactive T cell clones. Based on T cell recognition patterns of peptide-loaded EBV-LCL as shown in Supplemental Figure S3, K562 cells were transduced with HLA-DRA*01:02/B1*04:01 (yellow bars), -DRA*01:02/B1*04:04 (orange bars), -DQA1*03:01/B1*03:02 (green bars) or -DQA1*02:01/B1*03:03 (grey bars) and used to stimulate RUNX1-specific T cell clones as described in Figure 5. HLA-DQA1*03:01/B1*03:02 was confirmed as restriction element for T cell clones 1.2.C2^{RUNX1}, 1.2.D2^{RUNX1}, 1.4.F6^{RUNX1}, 1.4.G7^{RUNX1}, 1.5.F10^{RUNX1} and 1.5.H7^{RUNX1}. RUNX1-specific clones were cross-reactive against K562 transduced with HLA-DQA1*02:01/B1*03:03 irrespective of the RUNX1 neopeptide. A two-sided paired t-test was performed to determine if T cell reactivity against peptide-pulsed HLA-transduced K562 was significantly higher than against HLA-transduced K562 without peptide ($p < 0.05$ *, $p < 0.01$ **, $p < 0.001$ ***). Bars represent mean + SD of duplicate wells in a single experiment.

5

Figure S5. Recognition of cell lines with endogenous *RUNX1* mutations by CD4 T cell clones. (**A**) T cell clones 1.2.C2^{RUNX1}, 1.2.D2^{RUNX1}, 1.4.F6^{RUNX1}, 1.4.G7^{RUNX1}, 1.5.F10^{RUNX1} and 1.5.H7^{RUNX1} were tested for recognition of K562 transduced with HLA-DQA1*03:01/B1*03:02 as well as whole genes encoding mutated or wild-type RUNX1 proteins as described in Figure 6A and B. All T cell clones were more reactive against K562 transduced with HLA-DQ and mutated *RUNX1* (K562-mRUNX1-HLA) than against K562 transduced with wild-type *RUNX1* (K562-wtRUNX1-HLA). A two-sided paired t-test was performed to determine if T cell reactivity against K562-mRUNX1-HLA was significantly higher than against K562-wtRUNX1-HLA ($p < 0.05$ *, $p < 0.01$ **, $p < 0.001$ ***). Bars represent mean + SD of duplicate wells in a single experiment. (**B**) T cell clones 1.2.C2^{RUNX1}, 1.2.D2^{RUNX1}, 1.4.F6^{RUNX1}, 1.4.G7^{RUNX1}, 1.5.F10^{RUNX1} and 1.5.H7^{RUNX1} were tested against K562-E4 and SIG-M5-C9 cell lines in which *RUNX1* frameshift mutations were introduced by CRISPR-Cas9 as described in Figure 6C. T cell clones 1.4.F6^{RUNX1} and 1.4.G7^{RUNX1} were more reactive against K562-E4 transduced with HLA-DQA1*03:01/B1*03:02 (K562-E4-HLA) than K562-E4, whereas clones 1.2.C2^{RUNX1}, 1.2.D2^{RUNX1}, 1.5.F10^{RUNX1} and 1.5.H7^{RUNX1} showed low or no recognition of K562-E4-HLA. None of the RUNX1-specific T cell clones reacted against SIG-M5-C9 transduced with HLA-DQA1*03:01/B1*03:02 (SIG-M5-C9-HLA). A two-sided paired t-test was performed to determine if T cell reactivity against K562-E4-HLA was significantly higher than against K562-E4, and reactivity against SIG-M5-C9-HLA significantly higher than against SIG-M5-C9 ($p < 0.05$ *, $p < 0.01$ **, $p < 0.001$ ***). Bars represent mean + SD of duplicate wells in a single experiment, except for peptide-pulsed SIG-M5-C9, which was tested in single wells. *Figure on opposite page.*

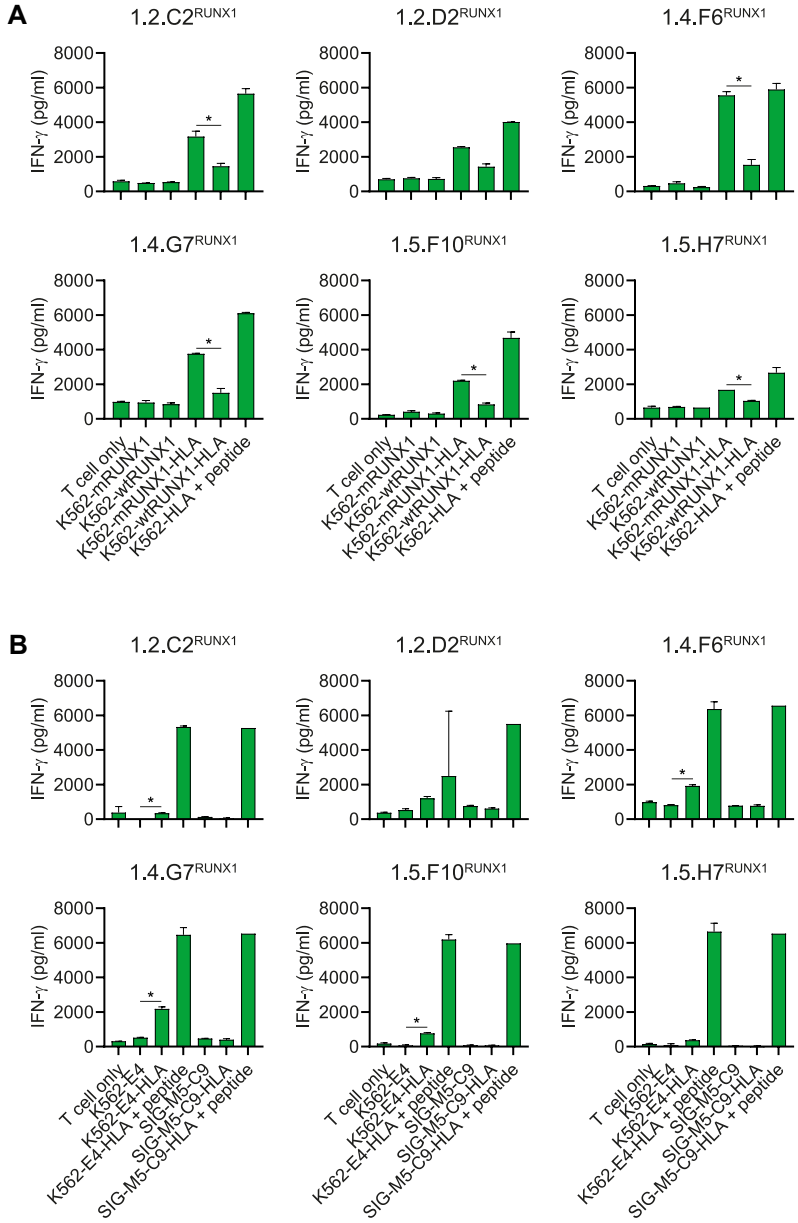
A
1.2.C2RUNX1
1.2.D2RUNX1
1.4.F6RUNX1
1.4.G7RUNX1
1.5.F10RUNX1
1.5.H7RUNX1
IFN-γ (pg/ml)
8000
6000
4000
2000
0
*
T cell only
K562-mRUNX1
K562-wtRUNX1
K562-mRUNX1-HLA
K562-wtRUNX1-HLA
K562-HLA + peptide
B
1.2.C2RUNX1
1.2.D2RUNX1
1.4.F6RUNX1
1.4.G7RUNX1
1.5.F10RUNX1
1.5.H7RUNX1
IFN-γ (pg/ml)
T cell only
K562-E4
K562-E4-HLA
K562-E4-HLA + peptide
SIG-M5-C9
SIG-M5-C9-HLA
SIG-M5-C9-HLA + peptide

Figure S6. Flow cytometry-based killing assay of patient-derived AML cells. T cell clone 1.5.F1^{DNMT3A} was tested for lysis of patient-derived AML cells (n = 4) in a flow cytometry-based killing assay as described in Figure 7C. After 48 hours of coincubation, samples were stained with viability dye Zombie Red and antibodies against CD3, CD8, CD19, CD33, CD34 and HLA-DQ. (**A**) Depicted is the gating strategy for measuring HLA-DQ expression on viable AML cells for representative AML23. Debris and doublets were excluded using FSC and SSC, dead cells were excluded using Zombie Red viability dye and lymphocytes were excluded using antibodies against CD3, CD8 and CD19. AML cells were gated using antibodies against CD33 and CD34, and HLA-DQ expression was measured on viable AML cells. (**B**) Viable AML cells after coincubation with T cells were clustered by HLA-DQ expression as described in Figure 7C. Clustering of viable AML cells after pulsing with DNMT3A-FPV-H peptide and coincubation with T cell clone 1.5.F1^{DNMT3A} (upper panels) and clustering of viable AML cells after coincubation with positive control mNPM1-A2 TCR-T cells (lower panels) are shown. HLA-DQ expression was heterogenous within AML samples. (**C**) Absolute numbers of total viable AML cells (blue bars) and HLA-DQ positive viable AML cells (orange bars) pulsed in the absence or presence of DNMT3A-FPV-H peptide are shown after coincubation with T cell clone 1.5.F1^{DNMT3A}. Clone 1.5.F1^{DNMT3A} did not mediate specific lysis of AML cells with *DNMT3A-R882H* irrespective of HLA-DQ expression and exogenous peptide pulsing. Results were similar for CMV-A2 TCR-T cells, whereas all AML cells were killed by mNPM1-A2 TCR-T cells. A two-sided unpaired t-test was performed to determine if lysis of absolute numbers of total AML cells was higher for clone 1.5.F1^{DNMT3A} (with and without peptide pulsing of target cells) and mNPM1-A2 TCR-T cells than for CMV-A2 TCR-T cells ($p < 0.05$ *, $p < 0.01$ **, $p < 0.001$ ***). Bars represent mean + SD of triplicate wells in a single experiment. *Figure on opposite page*.

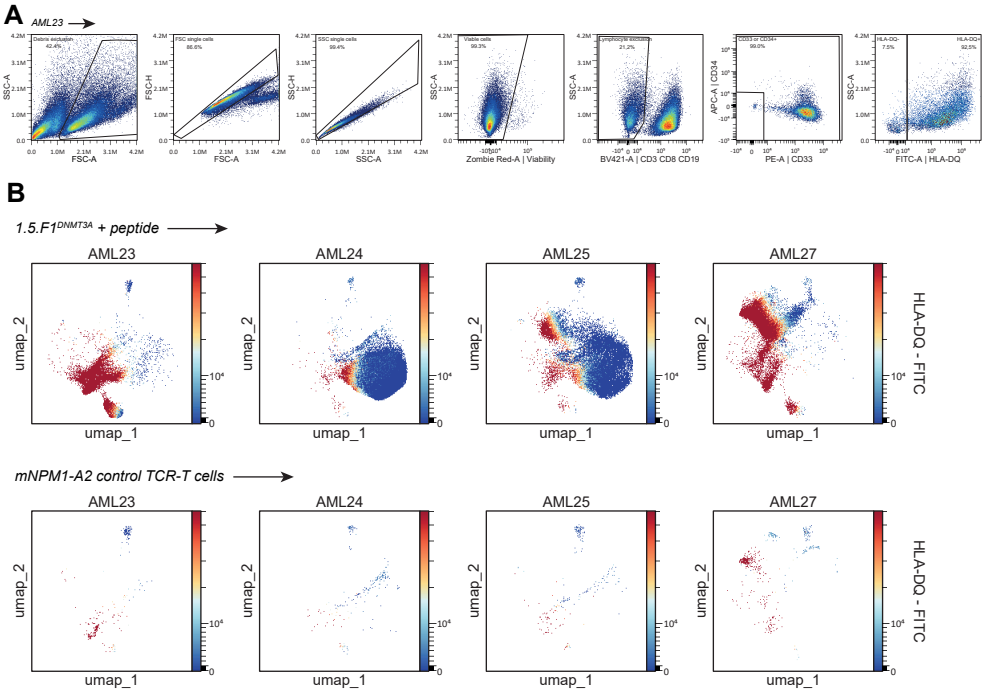
A
AML23
SSC-A
FSC-A
FSC-H
SSC-H
Zombie Red-A | Viability
BV421-A | CD3 CD8 CD19
APC-A | CD34
PE-A | CD33
HLA-DQ
FITC-A | HLA-DQ
B
1.5.F1DNMT3A + peptide
AML23
AML24
AML25
AML27
umap_2
umap_1
HLA-DQ - FITC
mNPM1-A2 control TCR-T cells
C
AML23 (DNMT3A-R882H)
AML24 (DNMT3A-R882H)
AML25 (DNMT3A-R882H)
AML27 (wtDNMT3A)
Absolute cell count
***
Total AML cells
HLA-DQ+ cells
AML only
1.5.F1DNMT3A + peptide
CMV-A2 TCR-T cells
mNPM1-A2 TCR-T cells

Table S1. Recurrent mutations in AML analyzed to encode neopeptides

Gene	Mutation type	Position	Protein consequence
DNMT3A	Missense	*c.2645G>A* *c.2644C>T*	p.Arg882His p.Arg882Cys
FLT3	Missense	*c.2503G>T*	p.Asp835Tyr
IDH1	Missense	*c.395G>A* *c.394C>T* *c.394C>G* *c.394C>A*	p.Arg132His p.Arg132Cys p.Arg132Gly p.Arg132Ser
IDH2	Missense	*c.419G>A* *c.515G>A*	p.Arg140Gln p.Arg172Lys
KIT	Missense	*c.2447A>T*	p.Asp816Val
NRAS	Missense	*c.35G>A* *c.38G>A*	p.Gly12Asp p.Gly13Asp
ASXL1	1 bp insertion	*c.1934dup*	p.Gly646Trpfs*12
CEBPA[A]	1 bp insertion 1 bp deletion	*c.68dup* *c.247del*	p.His24Alafs*84 p.Gln83Serfs*77
NPM1	4 bp insertion	*c.860_863dup*	p.Trp288Cysfs*12
RUNX1[A]	1 bp insertion	*c.883dup*	p.Ser295Phefs*305

[A] Insertions or deletions at different positions within specific regions of *CEBPA* and *RUNX1* create different lengths of the same alternative reading frame. The indicated mutations create long reading frames between 76 and 83 amino acids for *CEBPA* and 304 amino acids for *RUNX1*. bp. Base pair.

Table S2. Recurrent gene fusions in AML analyzed to encode neopeptides[A]

5' Gene	Exon	3' Gene	Exon
CBFB	*5*	*MYH11*	*34*
KMT2A	*9*	*MLLT3*	*2*
KMT2A	*9*	*MLLT3*	*6*
KMT2A	*10*	*MLLT3*	*6*
NUP98	*11*	*NSD1*	*7*
NUP98	*12*	*NSD1*	*7*
PML	*3*	*RARA*	*3*
RUNX1	*3*	*RUNX1T1*	*2*
RUNX1	*3*	*RUNX1T1*	*3*

[A] The exon fusions of the two partner genes in known fusion transcripts were recurrently measured in 100 AML by whole transcriptome RNA-Seq (32).

Table S3. HLA class II typing of 20 EBV-LCL

EBV-LCL	DRB1	DRB3	DRB4	DRB5	DQB1	DPB1
HD3	03:01:01 04:04:01	01:01:02	01:03:01:01		02:01:01 03:02:01	04:01:01
HD1	03:01 15:01	01:01		01:01:01	02:01:01 06:02:01	02:01 04:01/81:01
4	04:04 03:01	01:01	01:03		03:02 02:01	02:01 01:01
5	01:01:01 07:01:01		01:03:01:02		03:03:02 05:01:01	01:01/89:01 04:01/278:01/377:01
6	13:02 15:01	03:01		01:01	06:02 06:04	01:01 03:01
7	07:01:01 10:01:01		01:03:01:01		02:02:01 05:01:01	01:01:01 03:01/104:01
8	04:01 13:01	01:01	01:03		03:04 06:03	02:01 03:01
9	11:01 15:01	02:02		01:01	03:01 06:02	02:01:02 04:01
10	04:01:01 13:02:01	03:01:01	01:03:01:01		03:02/03:251 06:04/06:39	03:01/104:01/124:01 04:01/350:01
11	07 13:01/13:02/13:06	03	01/02/03		03:03 06:04/06:08/06:17	04:01 14:01
12	04:01/04:03/04:07 11:01/11:04/11:12	01/02/03	01/02/03		03:01/03:02/03:03 03:02/03:19/03:04	04:01:01
13	11:01 13:01	02:02 03:01			03:01 05:01	04:02 40:01
14	01:01:01 13:02:01	03:01:01			05:01:01 06:09	05:01:01 10:01
15	04 07		01/02/03		02:02 03:01	03:01 04:01
16	15:01 03:01	01:01:01		01:01:01	06:03 02:01	04:02 04:01
17	01:01/01:07/01:04 07:01/07:03/07:04		01/02/03		02:01/02:02/02:04 05:01/05:07	11:01:01 14:01
18	03:01/03:04/03:05 15	02		01	03:01 06:02/06:11/06:14	02:01:02 04:01
19	11:04:01 15:02:01	02:02:01		01:02	06:01:01 06:03:01	02:01:02
20	07:01:01 01:01/01:04/01:05		01:01:01:01 01/02/03		05:04 02:02	11:01:01 04:02
21	09 15		01/02/03	01	03:03 06:02/06:11/06:14	02:01:02 04:01

Chapter 6

Summary and general discussion

Summary

Acute myeloid leukemia (AML) is an aggressive disease that, despite initial complete responses to current standard therapies in most patients, frequently relapses (1, 2). Relapsed AML is difficult to treat and has a very poor prognosis (3). To improve the outcome of patients with AML, novel potent and safe therapies are required to treat and prevent relapsed disease.

Immunotherapy directed against neoantigens forms a promising new treatment option for patients with AML. Neoantigens are created by tumor-specific mutations and their expression is thus restricted to malignant cells (4, 5). Neoantigens are not presented during negative selection in the thymus and, therefore, T cells with high-affinity T-cell receptors (TCRs) for these antigens are expected to be present in the T-cell repertoire. As such, T-cell-based immunotherapies targeting neoantigens could potentially induce effective anti-leukemic responses without on-target off-tumor toxicity against healthy tissues.

Although AML generally contains few somatic mutations (6, 7), many patients carry driver mutations that are recurrently mutated in AML (8, 9). AML may therefore be particularly suitable for TCR-engineered T-cell therapy in which one or a few neoantigens are targeted. Especially neoantigens encoded by common recurrent driver mutations are relevant targets for TCR-engineered T-cell therapy, since these antigens are shared between patients and carry a low risk of being lost during immune escape (10).

In this thesis, we aimed to identify human leukocyte antigen (HLA) class I- as well as HLA class II-binding neoantigens encoded by frequent recurrent driver mutations in AML. We employed different strategies to select candidate neoantigens and isolate neoantigen-specific CD8 or CD4 T cells. For selected T cells that demonstrated superior reactivity against leukemic cells *in vitro*, TCRs were sequenced. After introduction into T cells from healthy individuals, anti-leukemic reactivity of these TCRs was evaluated *in vitro* and in a preclinical mouse model to assess their suitability for TCR-engineered T-cell therapy to treat patients with AML.

Most strategies that are followed for neoantigen discovery start with large sets of candidate neoantigens that all need to be screened for T-cell recognition. To improve the efficiency of neoantigen discovery, candidate neoantigens can be filtered based on immunobiological features as predicted by *in silico* algorithms (11, 12). In **chapter 2**, we explored the potential of various online available prediction tools to identify T-cell antigens, such as neoantigens and minor histocompatibility antigens (MiHAs).

Using these prediction tools, we determined the *in silico* characteristics for 68 autosomal HLA class I-binding MiHAs that have been identified as T-cell targets in patients who developed immune responses after allogeneic hematopoietic stem cell transplantation. These MiHAs by definition fulfill all requirements for endogenous processing, HLA presentation and T-cell recognition. To allow accurate evaluation of the predictive performance of the online algorithms, we also composed a set of reference peptides that have not been identified as T-cell antigens. The reference set consisted of peptides with predicted binding to HLA-A*02:01 or HLA-B*07:02 that are encoded by the same genes for which MiHAs in these HLA alleles have been identified. By comparing the *in silico* characteristics of MiHAs and reference peptides, we found that only the prediction algorithm for HLA class I binding substantially contributed to MiHA characterization (Figure 1). Using this algorithm, 87% of MiHAs were correctly predicted as HLA class I ligands, with most MiHAs being predicted as strong HLA binders. We observed that the default threshold for strong HLA binding has a high specificity, but low sensitivity, whereas the default threshold for weak HLA binding has a low specificity, but high sensitivity. This implies that applying the strong binding threshold will exclude many true ligands from the list of candidate T-cell antigens, whereas the weak binding threshold will result in many false-positives. We also compared and demonstrated similar *in silico* characteristics for most MiHAs and their allelic variants, supporting the suggestion that allelic variants can also be endogenously processed, presented by HLA and recognized by T cells. The reason why many allelic variants have not (yet) been identified as MiHAs may be their low mismatch frequencies in patient-donor pairs.

Amongst the most frequent mutations in AML are 4 base pair insertions in nucleophosmin 1 (*NPM1*), which occur in 30-35% of adult patients with AML (6, 8, 13). The mutations produce an 11 amino acid alternative reading frame (most often CLAVEEVSLRK) at the C-terminus of the mutated protein, resulting in elongation of the mutated protein by 4 amino acids compared to the wild-type (wt) protein (13, 14). The alternative reading frame could potentially give rise to neoantigens. These neoantigens are desirable targets for T-cell-based immunotherapies, since mutated NPM1 is an early driver mutation that is essential for AML development (9, 15). The mutation is also clonally expressed and retained upon relapse in most patients (16-18). In **chapter 3**, we identified a neoantigen that could efficiently be targeted on *NPM1*-mutated AML *in vitro* and *in vivo* by TCR-engineered T cells. We first searched for NPM1 neopeptides in the HLA class I ligandome of patient-derived AML samples and identified 5 neopeptides in the ligandome of *NPM1*-mutated AML, confirming that peptides derived from the alternative reading frame of mutated NPM1 are naturally processed and presented by HLA on AML. For one of these neopeptides, HLA-A*02:01-binding CLAVEEVSL, we searched for specific CD8 T cells using peptide-HLA class I tetramers. We first screened HLA-A*02:01 positive

patients with *NPM1*-mutated AML who were in remission after chemotherapy, but were unable to detect CLAVEEVSL-specific CD8 T cells. We then screened HLA-A*02:01 positive healthy individuals and isolated multiple tetramer positive CD8 T-cell clones. Two of these clones showed specific recognition of *NPM1*-mutated AML. The TCR from the T-cell clone with superior anti-leukemic reactivity was sequenced and introduced into CD8 and CD4 T cells from HLA-A*02:01 positive healthy individuals. NPM1-A2-specific TCR-transduced CD8 as well as CD4 T cells showed clear and specific recognition and killing of *NPM1*-mutated AML, while no reactivity against AML with wt *NPM1* was seen. TCR-transduced T cells also reduced tumor growth and improved survival in immunodeficient mice engrafted with the HLA-A*02:01 positive *NPM1*-mutated OCI-AML3 cell line. We concluded that CLAVEEVSL is an HLA-A*02:01-binding neoantigen on *NPM1*-mutated AML that could be a relevant target for T-cell-based immunotherapy and demonstrated that our NPM1-A2-specific TCR is a promising candidate for TCR-engineered T-cell therapy to treat patients with *NPM1*-mutated AML.

To broaden the applicability of T-cell-based immunotherapies for patients with *NPM1*-mutated AML, we examined in **chapter 4** whether AVEEVSLRK, another neopeptide detected in the HLA class I ligandome of *NPM1*-mutated AML, is a neoantigen on AML that can be targeted by TCR-engineered T-cell therapy. Predicted binding of AVEEVSLRK to HLA-A*03:01 and HLA-A*11:01 was confirmed in a competition-based peptide-HLA class I binding assay. Using peptide-HLA class I tetramers, we screened HLA-A*03:01 or HLA-A*11:01 positive healthy individuals for specific CD8 T cells. Three HLA-A*11:01-restricted CD8 T-cell clones were isolated that reacted against the AVEEVSLRK peptide and one of these clones selectively recognized *NPM1*-mutated AML. The TCR from this T cell was cloned and tested after transfer into CD8 and CD4 T cells from HLA-A*11:01 positive healthy individuals. The results showed that this TCR conferred peptide reactivity in CD8 T cells, but not in CD4 T cells, indicating that CD8 is required as coreceptor for the function of the NPM1-A11-specific TCR. NPM1-A11-specific TCR-transduced CD8 T cells demonstrated recognition and lysis of *NPM1*-mutated AML. In contrast to the NPM1-A2-specific TCR, CD8 T cells transduced with the NPM1-A11-specific TCR did not induce an anti-tumor effect in immunodeficient mice engrafted with HLA-A*11:01-transduced *NPM1*-mutated OCI-AML3 cells. These *in vivo* results were supported by lower levels of IFN-γ released by NPM1-A11-specific TCR-transduced T cells as compared to NPM1-A2-specific TCR-transduced T cells upon incubation with HLA-A*11:01-transduced OCI-AML3 cells *in vitro*. We concluded that AVEEVSLRK is an HLA-A*11:01-binding neoantigen on *NPM1*-mutated AML. Whether this neoantigen can be efficiently targeted in patients treated with our NPM1-A11-specific TCR after transfer to autologous T cells is unclear and requires additional preclinical testing.

CD4 T cells are often essential as helper T cells in efficient anti-tumor immune responses (19-21) and can also have the potential to directly kill HLA class II positive tumor cells (22). Since AML blasts frequently express HLA class II, we investigated in **chapter 5** whether neoantigens are presented by HLA class II and recognized by specific CD4 T cells. We first used the Catalogue Of Somatic Mutations In Cancer (COSMIC) database (23) to select 26 recurrent genetic aberrations in AML, which were subsequently analyzed for encoding neopeptides with predicted binding to common HLA class II molecules. A total of 24 long neopeptides derived from 10 recurrent genetic aberrations were synthesized. These neopeptides included 8 overlapping peptides spanning the entire alternative reading frame of mutated NPM1, which were added to the set of neopeptides irrespective of predicted HLA class II binding. Mixes of the long neopeptides were loaded onto dendritic cells (DCs), which were used to stimulate autologous CD4 T cells from healthy individuals. Numerous neopeptide-specific CD4 T-cell clones were isolated and tested for their potency and specificity. For two neopeptides, one created by the *DNMT3A-R882H* hotspot mutation and one derived from a long alternative reading frame created by *RUNX1* frameshift mutations, T-cell clones were isolated with reactivity against cell lines that were transduced or CRISPR-Cas9-edited with the relevant driver mutation, indicating that these neopeptides can be endogenously processed and presented by HLA class II on the cell surface. The DNMT3A neopeptide was also recognized by a CD4 T-cell clone on *DNMT3A*-mutated AML cells that were positive for HLA-DQB1*06:02 or HLA-DQB1*06:03. Despite clear recognition in IFN-γ ELISA, the CD4 T-cell clone failed to directly kill AML cells, demonstrating that the CD4 T-cell clone lacked cytotoxic capacity. We concluded that the *DNMT3A-R882H* hotspot mutation encodes an HLA class II-binding neoantigen on AML that could potentially become a relevant target for CD4 T-cell-based immunotherapy.

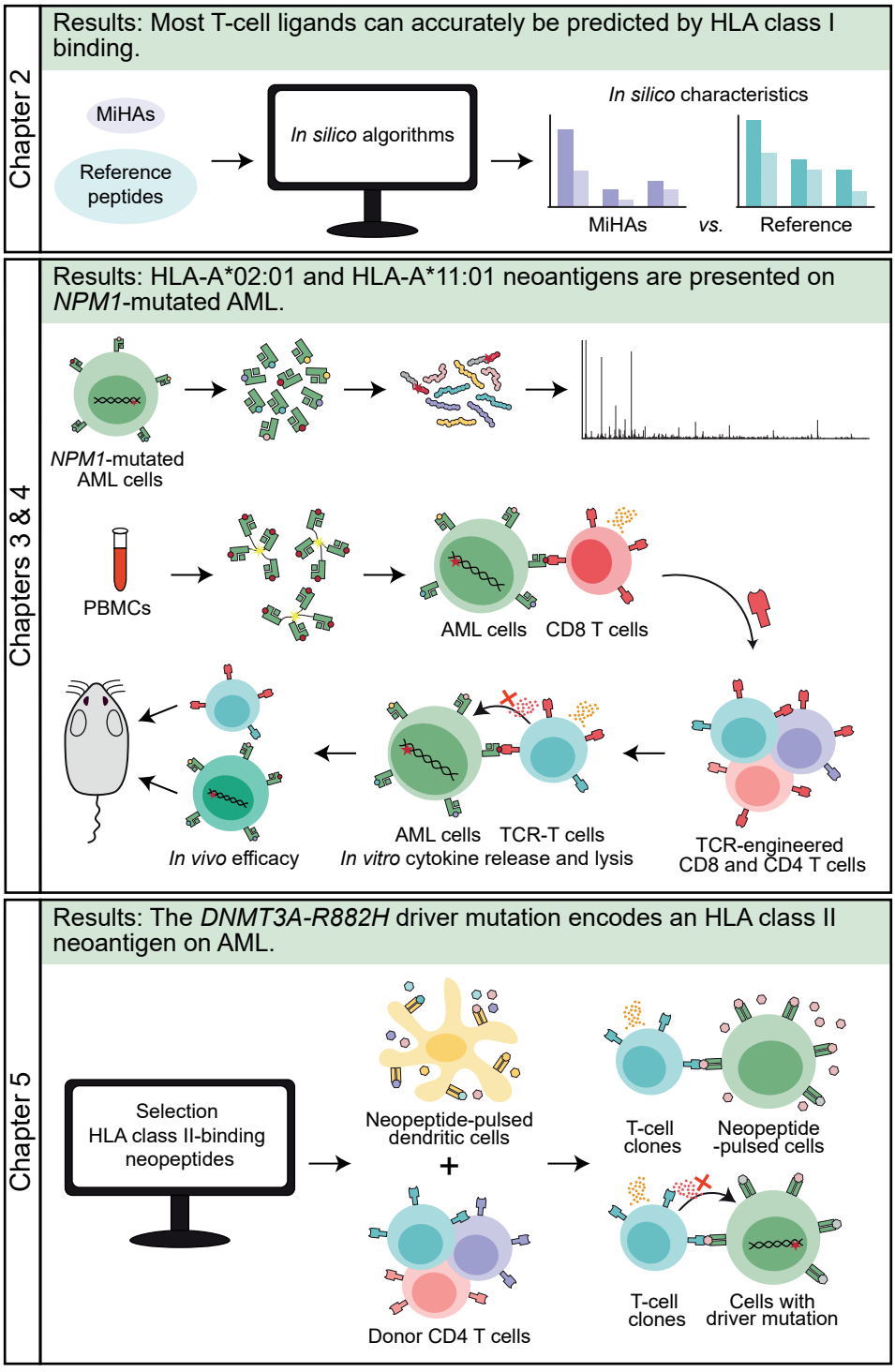

Figure 1. Summary of the thesis.

General discussion

Mutated NPM1 as target for TCR-engineered T-cell therapy

The frequent occurrence of *NPM1* hotspot mutations in adult patients with AML points to an important role of these mutations as drivers in leukemogenesis. Wt *NPM1* encodes a protein that functions as nucleocytoplasmic shuttle and nucleolar chaperone (15, 24). Although wt NPM1 shuttles between the nucleolus and cytoplasm, it primarily resides in the nucleolus. Wt NPM1 plays a role in various cellular processes, including nucleolus formation, ribosome biogenesis and transport, inhibition of centrosome duplication and DNA repair (24). It is also involved in the tumor suppressive p14ARF-MDM2-p53 pathway. The preferential nucleolar localization of wt NPM1 is promoted by a nucleolar localization signal at the C-terminus of the protein (15, 24). In mutated NPM1, the new alternative reading frame disrupts this nucleolar localization signal and creates a novel nuclear export signal. As a result, mutated NPM1 is delocalized from the nucleus to the cytoplasm. This cytoplasmic relocation seems to be required for tumorigenesis, since all hotspot mutations in exon 12 of *NPM1*, as well as rare mutations outside the hotspot region and rare *NPM1* gene fusions, result in displacement of the mutated protein to the cytoplasm. How cytoplasmic displacement of mutated NPM1 leads to leukemia is not yet understood (24). Disruption of essential processes in the nucleus due to haploinsufficiency of wt NPM1 or new interactions of mutated NPM1 with cytoplasmic proteins or, as a small fraction of the mutated protein is not exported to the cytoplasm, new interactions with nuclear proteins are all possible explanations. Mutated NPM1 may also associate with nuclear proteins and disrupt their function by transporting these proteins from the nucleus into the cytoplasm. Besides the observation that all *NPM1* mutations share a final common outcome of cytoplasmic delocalization of the mutated protein (15, 24), the importance of *NPM1* hotspot mutations for the development of AML is further supported by their early acquisition during malignant transformation (9, 15) and the finding that these mutations are only occasionally lost upon relapse (16-18). Since *NPM1* mutations are essential for leukemogenesis, AML blasts are not expected to escape from NPM1 neoantigen-targeted TCR-engineered T-cell therapy by losing these essential driver mutations.

We successfully isolated a CD8 T-cell clone that is specific for the HLA-A*02:01-binding neoantigen CLAVEEVSL on *NPM1*-mutated AML in **chapter 3**. Analysis of the HLA class I ligandome of 8 *NPM1*-mutated AML samples revealed that neopeptides derived from mutated NPM1 could be detected in 7 out of 8 samples, with CLAVEEVSL in two out of three HLA-A*02:01 positive samples, indicating that mutated NPM1 is processed and presented by AML cells. Despite surface presentation of NPM1 neopeptides, no CLAVEEVSL-specific CD8 T cells could be

isolated from a total number of 80 x 10^6 peripheral blood mononuclear cells (PBMCs) from 6 patients with *NPM1*-mutated AML who were in remission after chemotherapy. The failure to isolate CLAVEEVSL-specific CD8 T cells from patients with *NPM1*-mutated AML indicates that these cells were not present at high frequencies in the memory T-cell repertoire, and were either completely absent or present at frequencies in the naive T-cell repertoire that are too low to detect in limited numbers of available PBMCs from these patients. We therefore searched for CLAVEEVSL-specific CD8 T cells in 6 healthy individuals. By screening a total number of 5 x 10^9 PBMCs, two T-cell clones were isolated that were reactive against patient-derived *NPM1*-mutated AML. Of these two clones, one T-cell clone demonstrated reactivity against all *NPM1*-mutated AML samples tested. Two other research groups have also searched for CLAVEEVSL-specific CD8 T cells in patients with *NPM1*-mutated AML or healthy individuals. Forghieri et al. (25) analyzed PBMCs or bone marrow mononuclear cells from patients in IFN-γ ELISPOT assays after stimulation with NPM1 neopeptides, while Greiner et al. (26) stimulated CD8 T cells from patients or healthy individuals *in vitro* with NPM1 neopeptide-pulsed autologous PBMCs for 8 days before analyzing their reactivity against neopeptide-pulsed T2 cells in IFN-γ and granzyme B ELISPOT assays. Both groups failed to detect CD8 T cells specific for CLAVEEVSL, but successfully identified T cells for other NPM1 neopeptides. These results collectively suggest that CLAVEEVSL-specific CD8 T cells are rare and that these T cells are absent in the T-cell repertoire of most HLA-A*02:01 positive patients and healthy individuals.

The neoantigen CLAVEEVSL is not expected to be presented on healthy cells, since the peptide is derived from an alternative reading frame that is created by a tumor-specific frameshift mutation. However, it is known that out-of-frame translation can also occur in healthy cells. This has, for instance, been demonstrated for MiHAs that are translated from wt genes in alternative open reading frames (27, 28). It can therefore be hypothesized that wt *NPM1* may also produce peptides in alternative reading frames. If alternative translation occurs, wt *NPM1* encodes SLAVEEVSL, which differs from CLAVEEVSL by only one amino acid. Although SLAVEEVSL is predicted to bind to HLA-A*02:01, the peptide could not be identified in the HLA class I ligandome of 7 HLA-A*02:01 positive AML samples carrying no (*n* = 4) or heterozygous (*n* = 3) *NPM1* mutations. Furthermore, as demonstrated in **chapter 3**, T cells expressing the NPM1-A2-specific TCR showed no reactivity against HLA-A*02:01 positive autologous mature monocyte-derived DCs and allogeneic Epstein-Barr virus-transformed lymphoblastoid cell lines (EBV-LCL), suggesting that SLAVEEVSL is not produced in these cells. Restricted expression of SLAVEEVSL as a result of alternative translation of wt *NPM1* in specific healthy tissues, however, cannot be entirely excluded. It is interesting to speculate that SLAVEEVSL may be produced in medullary thymic epithelial cells or other antigen-presenting cell (APC)

subsets in the thymus during negative selection. Since SLAVEEVSL is highly similar to CLAVEEVSL, presentation of SLAVEEVSL as self-peptide during negative selection may result in clonal deletion of T cells with TCRs that can interact with both peptides. This could explain the low frequency of CLAVEEVSL-specific T cells in the T-cell repertoire, since only T cells expressing a TCR that interacts with abundant expression of CLAVEEVSL on *NPM1*-mutated AML, but not with low expression of SLAVEEVSL on healthy tissues would survive negative selection.

Besides CLAVEEVSL, mutated *NPM1* also encodes the neoantigen AVEEVSLRK. In **chapter 3**, CD8 as well as CD4 T cells transduced with the NPM1-A2-specific TCR for CLAVEEVSL were shown to bind to peptide-HLA class I tetramers and strongly react against patient-derived *NPM1*-mutated AML. In **chapter 4**, we isolated an HLA-A*11:01-restricted T-cell clone specific for AVEEVSLRK and tested the TCR from this clone similarly after introduction into CD8 and CD4 T cells. In contrast to the NPM1-A2-specific TCR, CD4 T cells transduced with the NPM1-A11-specific TCR were poorly stained with tetramers and failed to recognize neoantigen peptide-pulsed T2 cells. Furthermore, when introduced into CD8 T cells from the same individual, T cells with the NPM1-A2-specific TCR induced an anti-tumor effect in immunodeficient mice engrafted with an *NPM1*-mutated AML cell line, whereas no effect was observed for T cells with the NPM1-A11-specific TCR. Altogether, these results indicate that the NPM1-A11-specific TCR has a lower avidity for *NPM1*-mutated AML than the NPM1-A2-specific TCR. *In vitro*, however, CD8 T cells transduced with the NPM1-A11-specific TCR showed clear recognition and killing of patient-derived *NPM1*-mutated AML. This raises the question whether the NPM1-A11-specific TCR may still be useful for clinical application. T cells with high-avidity TCRs can achieve potent tumor control (29-33) and are generally favored for clinical application. Furthermore, T cells with high-avidity TCRs are expected to mediate anti-tumor reactivity even in the context of low antigen expression on tumor cells. However, this can also increase the risk of substantial on-target off-tumor toxicity if other antigens than neoantigens are targeted that are not exclusively presented on malignant cells, but also expressed at low levels on healthy cells (34-36). Besides high-avidity T cells, T cells with lower avidity can also play an important role in anti-tumor immunity (37-39). For instance, a recent study in mice demonstrated that adoptive transfer of relatively low-avidity T cells specific for a neoepitope controlled tumor growth and improved survival in mice bearing palpable tumors of a murine sarcoma cell line, whereas high-avidity T cells failed to induce tumor control (39). The lack of anti-tumor immunity by high-avidity T cells could be explained by their increased expression of exhaustion markers. In addition to reduced susceptibility to T-cell exhaustion (32, 37-39), T cells with relatively low avidity may also carry a decreased risk of on-target off-tumor toxicity, as low antigen expression on healthy cells is insufficient to activate these T cells (40). T cells with high- and relatively low-

avidity TCRs may thus both contribute to anti-tumor immune responses. Although high-avidity TCRs specific for AVEEVSLRK in HLA-A*11:01 are still preferable for clinical application, a relatively low-avidity NPM1-A11-specific TCR may also be used for immunotherapy, particularly considering that high-avidity TCRs for AVEEVSLRK are absent or extremely rare in the T-cell repertoire, as evidenced by our failure to isolate any high-avidity TCRs from 7 x 10^9 screened PBMCs. An optimal immunotherapeutic strategy may be to treat patients with *NPM1*-mutated AML with a mixture of T cells in which high- and relatively low-avidity TCRs have been introduced (40). In **chapter 3**, we also isolated a CLAVEEVSL-specific T-cell clone with weak reactivity against AML that may express a relatively low-avidity TCR. Further preclinical characterization and clinical development of the TCR from this T-cell clone would allow targeting of HLA-A*02:01-binding CLAVEEVSL on *NPM1*-mutated AML with this relatively low-avidity TCR as well as the high-avidity NPM1-A2-specific TCR.

The possible roles of neoantigen-specific CD4 T cells in anti-leukemic immunity

In **chapters 3**, **4** and **5** of this thesis, we have identified two HLA class I-binding neoantigens derived from the hotspot frameshift mutation in *NPM1* as well as one HLA class II-binding neoantigen derived from the *R882H* hotspot mutation in *DNMT3A*. Interestingly, *DNMT3A-R882H* mutations are frequently found in patients with *NPM1*-mutated AML (8), thereby potentially allowing concurrent targeting of AML blasts using neoantigen-specific CD8 and CD4 T cells. Many studies have reported that effective anti-tumor immunity relies on CD8 as well as CD4 T-cell responses (19-21). CD8 T cells are the main mediators of direct tumor cell killing. CD4 T cells can also induce direct cytolysis (22), but most often promote anti-tumor immunity by helping other immune cells (19-21). In contrast to aiding anti-tumor immunity, CD4 T cells can also have pro-tumorigenic functions that enable tumor progression (20, 21). Understanding the different roles that CD4 T cells can play in cancer immunity is crucial for employing their functions to stimulate anti-tumor immunity while suppressing their pro-tumorigenic functions in T-cell-based immunotherapies.

Direct lysis of tumor cells by CD4 T cells requires efficient processing of neoantigens from intracellular mutated proteins encoded by somatic mutations in tumor cells and presentation by HLA class II on the tumor cell surface. In **chapter 5**, we confirmed that AML blasts can process and present the HLA class II-binding DNMT3A neoantigen by showing that HLA-DQB1*06:02 or HLA-DQB1*06:03 positive patient-derived AML cells that naturally carry the *DNMT3A-R882H* mutation are recognized

by a CD4 T-cell clone. However, despite efficient recognition, the isolated CD4 T-cell clone did not kill AML cells. It is unknown why this T-cell clone lacks cytolytic capacity. Although we observed intra- and inter-patient heterogeneity in HLA class II expression, AML cells with high HLA class II expression could also not be killed by the T-cell clone. The observed heterogeneity in HLA class II expression also suggests that AML cells with no or low HLA class II expression may resist and escape direct cytolysis by CD4 T cells. Since AML cells were not killed despite high HLA class II expression, the lack of direct cytolytic capacity of the CD4 T-cell clone may be attributable to the T-cell phenotype or to TCR avidity (22). For example, the T-cell clone may lack granules with cytotoxic mediators, such as granzyme B and perforins, or the avidity of the HLA class II-restricted TCR may be sufficiently high to induce cytokine release, but too low for release of cytotoxic mediators. Nevertheless, our data showed that CD4 T cells specific for the HLA class II-binding DNMT3A neoantigen exist in the T-cell repertoire, offering the possibility to leverage their role as helper T cells to induce indirect anti-tumor effects, for instance by promoting tumor-specific CD8 T-cell responses.

CD4 T cells can stimulate CD8 T-cell responses in the priming phase as well as in the effector phase (19-21). During priming, CD4 T cells provide help to CD8 T cells via licensing of DCs (19). DC licensing requires direct CD4 T-cell-DC interaction that is mediated by binding of the TCR and CD40 ligand on CD4 T cells to peptide-HLA class II complexes and CD40 on DCs, respectively. This interaction stimulates DCs to upregulate costimulatory receptors and release cytokines, such as IL-12 and IL-15. In a mouse model of therapeutic cancer vaccination, effector CD8 T cells that were primed by licensed DCs showed enhanced clonal expansion, higher expression of cytotoxic effector molecules, including TNF, IFN-γ and granzyme B, and lower expression of coinhibitory receptors as compared to CD8 T cells primed without CD4 T-cell help (41). Furthermore, helped CD8 T cells demonstrated increased migratory and invasive potential and superior cytotoxicity. CD8 T-cell priming by licensed DCs is also essential for the differentiation, survival and function of memory CD8 T cells (19, 42-45). The value of CD4 help during T-cell priming is particularly important when designing cancer vaccines, since vaccination is often used for inducing *de novo* CD8 and CD4 T-cell responses. Neoantigen vaccines should therefore preferably include HLA class I as well as HLA class II neoantigens (46).

The NPM1 and DNMT3A neoantigens could potentially be used in neoantigen vaccination to stimulate combined DNMT3A neoantigen-specific CD4 T-cell responses and NPM1 neoantigen-specific CD8 T-cell responses *in vivo*. However, as evidenced by our results in **chapter 3** and **chapter 4**, CD8 T cells with high-avidity TCRs specific for HLA-A*02:01-binding CLAVEEVSL and HLA-A*11:01-binding

AVEEVSLRK NPM1 neoantigens are rare or even absent in most individuals. Vaccination with these NPM1 neoantigens to induce *de novo* CD8 T-cell responses is therefore not expected to be successful. Vaccination with NPM1 and DNMT3A neoantigens may, however, be used to boost TCR-engineered CD8 and CD4 T-cell responses (47). In particular in the setting of low tumor burden, for instance in patients who are in disease remission with measurable residual disease (MRD), vaccination may support robust activation and persistence of TCR-engineered T cells, thereby reducing the risk of relapse. When, for instance, synthetic peptide vaccines are used, the DNMT3A as well as NPM1 neoantigen peptides need to be presented by DCs. For the HLA-A*11:01-binding AVEEVSLRK neoantigen, we demonstrated in **chapter 4** that mature monocyte-derived DCs exogenously loaded with the synthetic neoantigen peptide were not recognized by NPM1-A11-specific TCR-transduced CD8 T cells. However, exogenous loading of the neoantigen peptide on other cell types, including the OCI-AML2 cell line, PBMCs and patient-derived AML blasts also resulted in low to no T-cell recognition. In a peptide-HLA class I binding assay, the affinity of the neoantigen peptide for HLA-A*11:01 was similar to a positive control peptide. These results suggest that the HLA-A*11:01-binding NPM1 neoantigen peptide is poorly presented upon exogenous loading, suggesting that neoantigen vaccination should not be performed with synthetic peptides, but rather with mRNA vaccines, for example. As described in **chapter 5**, the CD4 T-cell clone specific for the HLA-DQ-binding DNMT3A neoantigen has been isolated by stimulating CD4 T cells *in vitro* with mature monocyte-derived DCs that were exogenously pulsed with synthetic long peptides, indicating that the HLA class II-binding DNMT3A neoantigen peptide can be efficiently processed and presented by DCs. Whether the results as observed for monocyte-derived DCs are also applicable to DCs involved in CD4 T-cell help, which are primarily conventional type 1 DCs, still remains unclear (19, 48).

Besides help in the priming phase, CD4 T cells can also provide help to CD8 T cells in the effector phase (20, 21). In the tumor microenvironment (TME), intra-tumoral CD4 T cells may secrete cytokines upon recognition of their cognate antigen on APCs or tumor cells. Tumor cells can be positive for HLA class II or become positive in the presence of cytokines released by innate immune cells or CD4 T cells interacting with APCs. These cytokines may also create an inflammatory TME, thereby promoting recruitment, infiltration, local expansion and effector function of anti-tumor CD8 T cells (20, 21). For instance, in a mouse model, IFN-γ secretion by intra-tumoral CD4 T cells resulted in the production of chemokines within the TME, which led to improved recruitment of tumor-specific cytotoxic T cells, while IL-2 production by CD4 T cells enhanced cytotoxic T cells by stimulating their proliferation and granzyme B production (49). The inflammatory environment created by CD4 T cells may also affect antigen processing and presentation by tumor cells and other

cells in the TME. IFN-γ is known to increase expression of HLA, costimulatory and adhesion molecules (50). Furthermore, IFN-γ enhances intracellular antigen processing, for instance by converting the constitutive proteasome into the immunoproteasome or by stimulating transport of peptides into the endoplasmic reticulum by the transporter associated with antigen processing (TAP). Due to improved antigen processing and presentation, tumor cells in an inflammatory environment can become more susceptible to CD8 T-cell attack.

Cellular therapy with CD8 and CD4 T cells engineered with the HLA class I-restricted NPM1 TCR and HLA class II-restricted DNMT3A TCR, respectively, in combination with cancer vaccination with HLA class I-binding NPM1 and HLA class II-binding DNMT3A neoantigens may induce effective anti-tumor immunity by eliciting cytotoxic CD8 as well as helper CD4 T-cell responses. It is appealing to speculate about the added value of combining TCR-engineered T-cell therapy and cancer vaccination directed against HLA class I and class II neoantigens in general. CD4 T-cell help during priming can be delivered by endogenous CD4 T cells, which can be induced by vaccination, but perhaps also by TCR-engineered CD4 T cells. In the effector phase, help in the TME can also be provided by vaccine-stimulated endogenous CD4 T cells or by TCR-engineered CD4 T cells. In both situations, help can boost cytotoxic T-cell responses either by stimulating endogenous CD8 T cells, provided that these T cells are naturally present in the T-cell repertoire, or TCR-engineered CD8 T cells. Especially in tumors with an immunosuppressive environment in which endogenous T cells may fail to infiltrate the tumor in sufficient numbers, administration of large numbers of TCR-engineered CD4 T cells may convert the cold TME into a hot inflammatory TME, thereby promoting the accumulation and effector function of tumor-specific endogenous and TCR-engineered CD8 and CD4 T cells within the tumor, ultimately leading to efficient tumor destruction.

Equipping CD4 and CD8 T cells with identical neoantigen-specific TCRs

Identifying HLA class II neoantigens and their cognate TCRs for TCR-engineered T-cell therapy requires considerable effort and time. To bypass this laborious process while retaining the beneficial anti-tumor effects of CD4 T cells, CD4 T cells can be redirected towards tumor cells by introducing an HLA class I-restricted TCR derived from neoantigen-specific CD8 T cells. This is supported by our own observations in **chapter 3**, in which we demonstrated that, similar to CD8 T cells, CD4 T cells transduced with the HLA class I-restricted NPM1-A2-specific TCR were capable of recognizing and killing *NPM1*-mutated AML. Whereas CD4 T cells redirected to HLA class I-binding neoantigens have not yet been administered in clinical trials, the

administration of CD8 and CD4 T cells engineered to express identical HLA class I-restricted TCRs specific for a tissue differentiation antigen, cancer germline antigen, viral antigen or MiHA has been investigated in patients with hematological or solid tumors (51-58). Clinical responses have been observed in these trials and several trials also reported persistence of TCR-engineered CD8 as well as CD4 T cells in the peripheral blood (51-55, 58). Apart from eliminating the need for HLA class II neoantigen discovery and TCR identification, another benefit of HLA class I TCR-redirected CD4 T cells is the more ubiquitous expression of HLA class I on tumors (59), which is expected to stimulate CD4 T-cell-mediated cytotoxicity and help. While many solid tumors do not express HLA class II (59, 60), HLA class I is present on most hematological and solid tumor types and is often more uniformly expressed on malignant cells within the tumor as compared to HLA class II (60). Another advantage of introducing the same HLA class I-restricted TCR into CD8 and CD4 T cells is that only one viral vector or non-viral delivery system needs to be produced under Good Manufacturing Practice conditions, and that CD8 and CD4 T cells do not need to be separated and processed individually, as would be necessary when introducing different TCRs (61). Despite these advantages, some disadvantages can also be envisioned. CD8 and CD4 T cells may differ in their cytolytic potential, expansion rate and capacity to integrate the transgenic TCR into their genome. This increases the risk that suboptimal T-cell products will be generated in which strongly cytolytic CD8 T cells are outcompeted by CD4 T cells with no or inferior cytolytic function (61). CD4 T cells could also potentially possess higher copy number integrations of the introduced TCR (61), which may increase the risk of insertional mutagenesis and could possibly result in malignant transformation. It may therefore still be preferred to process CD8 and CD4 T cells individually to create well-defined T-cell products.

In most clinical trials, HLA class I-restricted tumor-reactive TCRs have been introduced into CD8 and CD4 T cells without the CD8 coreceptor (51-57), except for one trial in which a MiHA-specific TCR was co-transferred with CD8 (58). For the NPM1-A2-specific TCR, we demonstrated peptide-HLA class I tetramer binding as well as anti-AML efficacy for CD4 T cells transduced with the TCR in the absence of CD8. CD8 interacts with the non-polymorphic region of the HLA class I heavy chain, a site that is distinct from the peptide-binding groove that interacts with the TCR (62). Binding of CD8 to HLA class I stabilizes the TCR:peptide-HLA interaction and promotes TCR signaling, thereby increasing antigen sensitivity of the T cell and enhancing T-cell activation. The importance of the CD8:HLA interaction for T-cell activation and function is dependent on the affinity of the TCR for its cognate peptide-HLA ligand (63, 64). While T cells with relatively low- or intermediate-affinity TCRs require CD8 for their activation, T cells with high-affinity TCRs can function in a CD8 independent manner. The (partial) CD8 coreceptor independence of the NPM1-A2-specific TCR may indicate that the TCR has a relatively high affinity for its peptide-

HLA ligand. In contrast, the NPM1-A11-specific TCR has a lower affinity and CD4 T cells transduced with this TCR showed poor binding to tetramers and failed to recognize cells exogenously pulsed with the NPM1 neoantigen peptide. It may be interesting to investigate whether the efficacy of CD4 T cells transduced with the NPM1-A11-specific TCR can be stimulated by introducing CD8, either the wt coreceptor or a modified version with enhanced affinity for HLA, as recently demonstrated *in vitro* for CD4 T cells engineered with other HLA class I-restricted tumor-targeting TCRs (65).

Analogous to HLA class I TCR-redirected CD4 T cells, CD8 T cells can be engineered to express a tumor-reactive HLA class II-restricted TCR. These TCR-redirected CD8 T cells can potentially be used to target HLA class II positive tumor cells, including AML blasts. HLA class II TCR-redirected CD8 T cells may also be safe, since HLA class II expression on healthy cells is mainly restricted to specialized APCs of hematopoietic origin. However, HLA class II can be broadly induced on hematopoietic and non-hematopoietic healthy cells under inflammatory conditions, for example during infection. This may increase the risk of toxicity, especially when tumor antigens are targeted that are not exclusively expressed on malignant cells (66). The anti-tumor potential of HLA class II TCR-redirected CD8 T cells has been reported in a preclinical study in which an HLA-DP-restricted TCR against an overexpressed tumor antigen was introduced into CD4 and CD8 T cells (67). The authors investigated combined TCR-engineered CD4 and CD8 T cells, and demonstrated killing of melanoma cell lines endogenously expressing the tumor antigen as well as autologous malignant ascites cells, while no reactivity was observed against healthy hematopoietic cells. The TCR-engineered CD4 and CD8 T cells also reduced tumor growth and improved survival in a xenograft mouse model. The TCR from the CD4 T-cell clone specific for the HLA-DQ-binding DNMT3A neoantigen as isolated in **chapter 5**, may, in future studies, be sequenced, cloned and used to redirect CD8 T cells in a similar way as described above. However, as discussed previously, it should be noted that HLA class II expression on AML is often heterogeneous, suggesting that complete clearance of tumor cells may not be possible. Furthermore, no clinical studies have been reported yet that demonstrate that CD8 T cells can acquire strong antigen-specific cytolytic potential upon transfer of an HLA class II-restricted TCR.

Future perspective on treatment of patients with the NPM1-A2-specific TCR

The safety and efficacy of the NPM1-A2-specific TCR are currently being investigated in a phase I/II clinical trial (registered at https://clinicaltrials.gov/ as

NCT06424340). In this trial, HLA-A*02:01 positive patients with *NPM1*-mutated AML who have refractory, relapsed, or MRD positive disease are treated with autologous T cells that are engineered to express the NPM1-A2-specific TCR. If proven safe and effective in clinical studies, NPM1-A2 TCR-engineered T-cell therapy could become available as a highly needed new treatment option for these patients. Ultimately, NPM1-A2 TCR-engineered T-cell therapy may be approved as treatment for patients with newly diagnosed *NPM1*-mutated AML and, if effective, it may even eliminate the need for allogeneic hematopoietic stem cell transplantation. Following induction therapy, patients could be treated preemptively or prophylactically with NPM1-A2 TCR-engineered T-cell therapy as consolidation treatment. Preemptive treatment may be guided by detection of mutated *NPM1* in MRD analyses (68) for optimal timing of NPM1-A2 TCR-engineered T-cell therapy and prevent unnecessary intervention in patients who have achieved durable complete remissions. Since AML is an aggressive disease and leukemic blasts can rapidly expand to life-threatening numbers, MRD analyses should be regularly performed at short time intervals to ensure timely administration of NPM1-A2-specific TCR-engineered T cells. However, frequent MRD evaluations can place a substantial psychological and logistical burden on patients and the risk remains that leukemic progression outpaces production of the T-cell product. Prophylactic administration of NPM1-A2 TCR-engineered T-cell therapy provides an attractive alternative, but is presently hindered by its feasibility. Since *ex vivo* production of TCR-engineered T cells is a laborious and logistically complex procedure, expanding the application of NPM1-A2 TCR-engineered T-cell therapy to large patient numbers will be challenging (69). However, novel cell engineering methods are currently being explored, which could potentially overcome these capacity issues in the future (70, 71). For example, various strategies are under development to selectively deliver an antigen receptor into autologous T cells and produce receptor-engineered T cells *in vivo* (70). If these novel methods prove safe, effective and feasible, they could make NPM1-A2 TCR-engineered T-cell therapy more widely available as treatment option for HLA-A*02:01 positive patients with *NPM1*-mutated AML.

References

1. Döhner H, Weisdorf DJ, Bloomfield CD. Acute Myeloid Leukemia. N Engl J Med. 2015;373(12):1136-52.
2. Döhner H, Estey E, Grimwade D, et al. Diagnosis and management of AML in adults: 2017 ELN recommendations from an international expert panel. Blood. 2017;129(4):424-47.
3. Thol F, Ganser A. Treatment of Relapsed Acute Myeloid Leukemia. Curr Treat Options Oncol. 2020;21(8):66.
4. Schumacher TN, Schreiber RD. Neoantigens in cancer immunotherapy. Science. 2015;348(6230):69-74.
5. Schumacher TN, Scheper W, Kvistborg P. Cancer Neoantigens. Annu Rev Immunol. 2019;37:173-200.
6. Ley TJ, Miller C, Ding L, et al. Genomic and epigenomic landscapes of adult de novo acute myeloid leukemia. N Engl J Med. 2013;368(22):2059-74.
7. Alexandrov LB, Nik-Zainal S, Wedge DC, et al. Signatures of mutational processes in human cancer. Nature. 2013;500(7463):415-21.
8. Papaemmanuil E, Gerstung M, Bullinger L, et al. Genomic Classification and Prognosis in Acute Myeloid Leukemia. N Engl J Med. 2016;374(23):2209-21.
9. Kishtagari A, Levine RL, Viny AD. Driver mutations in acute myeloid leukemia. Curr Opin Hematol. 2020;27(2):49-57.
10. Pearlman AH, Hwang MS, Konig MF, et al. Targeting public neoantigens for cancer immunotherapy. Nat Cancer. 2021;2(5):487-97.
11. Garcia-Garijo A, Fajardo CA, Gros A. Determinants for Neoantigen Identification. Front Immunol. 2019;10:1392.
12. Lang F, Schrörs B, Löwer M, et al. Identification of neoantigens for individualized therapeutic cancer vaccines. Nat Rev Drug Discov. 2022;21(4):261-82.
13. Falini B, Mecucci C, Tiacci E, et al. Cytoplasmic nucleophosmin in acute myelogenous leukemia with a normal karyotype. N Engl J Med. 2005;352(3):254-66.
14. Thiede C, Koch S, Creutzig E, et al. Prevalence and prognostic impact of NPM1 mutations in 1485 adult patients with acute myeloid leukemia (AML). Blood. 2006;107(10):4011-20.
15. Falini B, Brunetti L, Sportoletti P, et al. NPM1-mutated acute myeloid leukemia: from bench to bedside. Blood. 2020;136(15):1707-21.
16. Krönke J, Bullinger L, Teleanu V, et al. Clonal evolution in relapsed NPM1-mutated acute myeloid leukemia. Blood. 2013;122(1):100-8.
17. Höllein A, Meggendorfer M, Dicker F, et al. NPM1 mutated AML can relapse with wild-type NPM1: persistent clonal hematopoiesis can drive relapse. Blood Adv. 2018;2(22):3118-25.
18. Cocciardi S, Dolnik A, Kapp-Schwoerer S, et al. Clonal evolution patterns in acute myeloid leukemia with NPM1 mutation. Nat Commun. 2019;10(1):2031.
19. Borst J, Ahrends T, Bąbała N, et al. CD4(+) T cell help in cancer immunology and immunotherapy. Nat Rev Immunol. 2018;18(10):635-47.
20. Speiser DE, Chijioke O, Schaeuble K, et al. CD4(+) T cells in cancer. Nat Cancer. 2023;4(3):317-29.
21. Montauti E, Oh DY, Fong L. CD4(+) T cells in antitumor immunity. Trends Cancer. 2024;10(10):969-85.
22. van Wandeloo IMB, Bol K, van Herpen C, et al. Cytotoxic CD4+ T cells in cancer: an emerging target for next-generation anticancer immunotherapy? J Immunother Cancer. 2025;13(12):e013461.
23. Sondka Z, Dhir NB, Carvalho-Silva D, et al. COSMIC: a curated database of somatic variants and clinical data for cancer. Nucleic Acids Res. 2024;52(D1):D1210-d7.

24. Falini B, Sorcini D, Perriello VM, et al. Functions of the native NPM1 protein and its leukemic mutant. Leukemia. 2025;39(2):276-90.
25. Forghieri F, Riva G, Lagreca I, et al. Characterization and dynamics of specific T cells against nucleophosmin-1 (NPM1)-mutated peptides in patients with NPM1-mutated acute myeloid leukemia. Oncotarget. 2019;10(8):869-82.
26. Greiner J, Ono Y, Hofmann S, et al. Mutated regions of nucleophosmin 1 elicit both CD4(+) and CD8(+) T-cell responses in patients with acute myeloid leukemia. Blood. 2012;120(6):1282-9.
27. Griffioen M, van Bergen CA, Falkenburg JH. Autosomal Minor Histocompatibility Antigens: How Genetic Variants Create Diversity in Immune Targets. Front Immunol. 2016;7:100.
28. Fuchs KJ, van de Meent M, Honders MW, et al. Expanding the repertoire reveals recurrent, cryptic, and hematopoietic HLA class I minor histocompatibility antigens. Blood. 2024;143(18):1856-72.
29. Chapuis AG, Egan DN, Bar M, et al. T cell receptor gene therapy targeting WT1 prevents acute myeloid leukemia relapse post-transplant. Nat Med. 2019;25(7):1064-72.
30. Sim MJW, Lu J, Spencer M, et al. High-affinity oligoclonal TCRs define effective adoptive T cell therapy targeting mutant KRAS-G12D. Proc Natl Acad Sci U S A. 2020;117(23):12826-35.
31. Purcarea A, Jarosch S, Barton J, et al. Signatures of recent activation identify a circulating T cell compartment containing tumor-specific antigen receptors with high avidity. Sci Immunol. 2022;7(74):eabm2077.
32. Hay ZLZ, Knapp JR, Magallon RE, et al. Low TCR Binding Strength Results in Increased Progenitor-like CD8+ Tumor-Infiltrating Lymphocytes. Cancer Immunol Res. 2023;11(5):570-82.
33. Schmidt J, Chiffelle J, Perez MAS, et al. Neoantigen-specific CD8 T cells with high structural avidity preferentially reside in and eliminate tumors. Nat Commun. 2023;14(1):3188.
34. Johnson LA, Morgan RA, Dudley ME, et al. Gene therapy with human and mouse T-cell receptors mediates cancer regression and targets normal tissues expressing cognate antigen. Blood. 2009;114(3):535-46.
35. Parkhurst MR, Yang JC, Langan RC, et al. T cells targeting carcinoembryonic antigen can mediate regression of metastatic colorectal cancer but induce severe transient colitis. Mol Ther. 2011;19(3):620-6.
36. Zhong S, Malecek K, Johnson LA, et al. T-cell receptor affinity and avidity defines antitumor response and autoimmunity in T-cell immunotherapy. Proc Natl Acad Sci U S A. 2013;110(17):6973-8.
37. Shakiba M, Zumbo P, Espinosa-Carrasco G, et al. TCR signal strength defines distinct mechanisms of T cell dysfunction and cancer evasion. J Exp Med. 2022;219(2):e20201966.
38. Sugiyarto G, Lau D, Hill SL, et al. Reactivation of low avidity tumor-specific CD8(+) T cells associates with immunotherapeutic efficacy of anti-PD-1. J Immunother Cancer. 2023;11(8):e007114.
39. Singhaviranon S, Dempsey JP, Hagymasi AT, et al. Low-avidity T cells drive endogenous tumor immunity in mice and humans. Nat Immunol. 2025;26(2):240-51.
40. D'Ippolito E, Schober K, Nauerth M, et al. T cell engineering for adoptive T cell therapy: safety and receptor avidity. Cancer Immunol Immunother. 2019;68(10):1701-12.
41. Ahrends T, Spanjaard A, Pilzecker B, et al. CD4(+) T Cell Help Confers a Cytotoxic T Cell Effector Program Including Coinhibitory Receptor Downregulation and Increased Tissue Invasiveness. Immunity. 2017;47(5):848-61.e5.
42. Janssen EM, Lemmens EE, Wolfe T, et al. CD4+ T cells are required for secondary expansion and memory in CD8+ T lymphocytes. Nature. 2003;421(6925):852-6.
43. Shedlock DJ, Shen H. Requirement for CD4 T cell help in generating functional CD8 T cell memory. Science. 2003;300(5617):337-9.
44. Sun JC, Bevan MJ. Defective CD8 T cell memory following acute infection without CD4 T cell help. Science. 2003;300(5617):339-42.

45. Ahrends T, Busselaar J, Severson TM, et al. CD4(+) T cell help creates memory CD8(+) T cells with innate and help-independent recall capacities. Nat Commun. 2019;10(1):5531.
46. Alspach E, Lussier DM, Miceli AP, et al. MHC-II neoantigens shape tumour immunity and response to immunotherapy. Nature. 2019;574(7780):696-701.
47. Drakes DJ, Abbas AM, Shields J, et al. Lymph Node-Targeted Vaccine Boosting of TCR T-cell Therapy Enhances Antitumor Function and Eradicates Solid Tumors. Cancer Immunol Res. 2024;12(2):214-31.
48. Ferris ST, Durai V, Wu R, et al. cDC1 prime and are licensed by CD4(+) T cells to induce anti-tumour immunity. Nature. 2020;584(7822):624-9.
49. Bos R, Sherman LA. CD4+ T-cell help in the tumor milieu is required for recruitment and cytolytic function of CD8+ T lymphocytes. Cancer Res. 2010;70(21):8368-77.
50. Alspach E, Lussier DM, Schreiber RD. Interferon γ and Its Important Roles in Promoting and Inhibiting Spontaneous and Therapeutic Cancer Immunity. Cold Spring Harb Perspect Biol. 2019;11(3).
51. Moore T, Wagner CR, Scurti GM, et al. Clinical and immunologic evaluation of three metastatic melanoma patients treated with autologous melanoma-reactive TCR-transduced T cells. Cancer Immunol Immunother. 2018;67(2):311-25.
52. D'Angelo SP, Melchiori L, Merchant MS, et al. Antitumor Activity Associated with Prolonged Persistence of Adoptively Transferred NY-ESO-1 (c259)T Cells in Synovial Sarcoma. Cancer Discov. 2018;8(8):944-57.
53. Stadtmauer EA, Faitg TH, Lowther DE, et al. Long-term safety and activity of NY-ESO-1 SPEAR T cells after autologous stem cell transplant for myeloma. Blood Adv. 2019;3(13):2022-34.
54. Nagarsheth NB, Norberg SM, Sinkoe AL, et al. TCR-engineered T cells targeting E7 for patients with metastatic HPV-associated epithelial cancers. Nat Med. 2021;27(3):419-25.
55. Hong DS, Van Tine BA, Biswas S, et al. Autologous T cell therapy for MAGE-A4(+) solid cancers in HLA-A*02(+) patients: a phase 1 trial. Nat Med. 2023;29(1):104-14.
56. D'Angelo SP, Araujo DM, Abdul Razak AR, et al. Afamitresgene autoleucel for advanced synovial sarcoma and myxoid round cell liposarcoma (SPEARHEAD-1): an international, open-label, phase 2 trial. Lancet. 2024;403(10435):1460-71.
57. Wermke M, Araujo DM, Chatterjee M, et al. Autologous T cell therapy for PRAME(+) advanced solid tumors in HLA-A*02(+) patients: a phase 1 trial. Nat Med. 2025;31(7):2365-74.
58. Krakow EF, Brault M, Summers C, et al. HA-1-targeted T-cell receptor T-cell therapy for recurrent leukemia after hematopoietic stem cell transplantation. Blood. 2024;144(10):1069-82.
59. Axelrod ML, Cook RS, Johnson DB, et al. Biological Consequences of MHC-II Expression by Tumor Cells in Cancer. Clin Cancer Res. 2019;25(8):2392-402.
60. Macy AM, Herrmann LM, Adams AC, et al. Major histocompatibility complex class II in the tumor microenvironment: functions of nonprofessional antigen-presenting cells. Curr Opin Immunol. 2023;83:102330.
61. Yonezawa Ogusuku IE, Herbel V, Lennartz S, et al. Automated manufacture of ΔNPM1 TCR-engineered T cells for AML therapy. Mol Ther Methods Clin Dev. 2024;32(2):101224.
62. Cole DK, Laugel B, Clement M, et al. The molecular determinants of CD8 co-receptor function. Immunology. 2012;137(2):139-48.
63. Holler PD, Kranz DM. Quantitative analysis of the contribution of TCR/pepMHC affinity and CD8 to T cell activation. Immunity. 2003;18(2):255-64.
64. Laugel B, van den Berg HA, Gostick E, et al. Different T cell receptor affinity thresholds and CD8 coreceptor dependence govern cytotoxic T lymphocyte activation and tetramer binding properties. J Biol Chem. 2007;282(33):23799-810.
65. Knezevic L, Wachsmann TLA, Francis O, et al. High-affinity CD8 variants enhance the sensitivity of pMHCI antigen recognition via low-affinity TCRs. J Biol Chem. 2023;299(8):104981.

66. Stevanovic S, van Bergen CA, van Luxemburg-Heijs SA, et al. HLA class II upregulation during viral infection leads to HLA-DP-directed graft-versus-host disease after CD4+ donor lymphocyte infusion. Blood. 2013;122(11):1963-73.
67. Dillard P, Köksal H, Maggadottir SM, et al. Targeting Telomerase with an HLA Class II-Restricted TCR for Cancer Immunotherapy. Mol Ther. 2021;29(3):1199-213.
68. Ivey A, Hills RK, Simpson MA, et al. Assessment of Minimal Residual Disease in Standard-Risk AML. N Engl J Med. 2016;374(5):422-33.
69. Shafer P, Kelly LM, Hoyos V. Cancer Therapy With TCR-Engineered T Cells: Current Strategies, Challenges, and Prospects. Front Immunol. 2022;13:835762.
70. Bot A, Scharenberg A, Friedman K, et al. In vivo chimeric antigen receptor (CAR)-T cell therapy. Nat Rev Drug Discov. 2026;25(2):116-37.
71. Diorio C, Teachey DT, Grupp SA. Allogeneic chimeric antigen receptor cell therapies for cancer: progress made and remaining roadblocks. Nat Rev Clin Oncol. 2025;22(1):10-27.

Appendices

Nederlandse samenvatting

PhD portfolio

List of publications

Curriculum vitae

Dankwoord

Nederlandse samenvatting

Publieke neoantigenen voor immuuntherapie tegen acute myeloïde leukemie

T-cellen zijn specifieke immuuncellen

T-cellen zijn immuuncellen die essentieel zijn voor de afweer tegen ziekteverwekkers. Ziekteverwekkers produceren lichaamsvreemde peptiden, kleine eiwitfragmenten, die op het celoppervlak kunnen worden gepresenteerd door humane leukocyten antigenen (HLA). Deze HLA-gebonden peptiden kunnen vervolgens worden herkend door T-cellen via hun specifieke T-celreceptor (TCR). Een HLA-gebonden peptide dat door een T-cel wordt herkend, heet een antigeen. Wanneer een T-cel zijn doelwitantigeen herkent, kan de T-cel worden geactiveerd om zijn functies uit te voeren. T-cellen worden onderverdeeld in CD8 en CD4 T-cellen. De primaire functie van CD8 T-cellen is het direct vernietigen van cellen. Sommige CD4 T-cellen kunnen dit ook, maar de meeste fungeren als helpercellen die andere immuuncellen ondersteunen en zo de immuunrespons bevorderen. CD8 en CD4 T-cellen herkennen peptiden die door verschillende HLA-moleculen worden gepresenteerd. HLA-klasse-I-moleculen zijn aanwezig op bijna alle lichaamscellen en presenteren peptiden van intracellulaire eiwitten aan CD8 T-cellen. HLA-klasse-II-moleculen komen vooral voor op antigeen-presenterende cellen (APC's) en presenteren met name peptiden van extracellulaire of membraangebonden eiwitten aan CD4 T-cellen, alhoewel ook intracellulaire peptiden kunnen worden gepresenteerd. Er zijn drie soorten HLA-klasse-I-moleculen (HLA-A, HLA-B en HLA-C) en drie soorten HLA-klasse-II-moleculen (HLA-DR, HLA-DP en HLA-DQ). Van elke soort bestaan vele varianten met elk een eigen verdeling in de bevolking. Iedere HLA-variant kan een groot repertoire aan peptiden binden. Elke T-cel heeft een unieke TCR die specifiek is voor één of enkele peptide:HLA-complexen. Ieder individu bezit zo een omvangrijk T-celrepertoire met miljoenen verschillende TCR's.

Tumorcellen kunnen neoantigenen produceren

Een belangrijke oorzaak voor het ontstaan van tumoren is de ophoping van mutaties in het DNA. Deze tumor-specifieke mutaties kunnen neoantigenen produceren: afwijkende peptiden die door HLA-moleculen op tumorcellen worden gepresenteerd en door T-cellen worden herkend. Omdat neoantigenen worden gecodeerd door mutaties die afwezig zijn in gezonde cellen, zijn neoantigenen aantrekkelijke doelwitten voor T-cel immuuntherapieën. Tumoren kunnen echter ontsnappen aan T-celimmuniteit door mutaties die voor neoantigenen coderen te verliezen. Sommige mutaties, zogenaamde driver-mutaties, zijn essentieel voor het voortbestaan van de tumor en kunnen daarom niet makkelijk worden kwijtgeraakt. Voor het ontstaan van neoantigenen moeten mutaties aanwezig zijn in genen die tot expressie komen. De

afwijkende eiwitten dienen in de cel afgebroken te worden tot gemuteerde peptiden, die vervolgens moeten binden aan de HLA-moleculen van de patiënt om op het celoppervlak te worden gepresenteerd. Tenslotte moeten deze HLA-gebonden neopeptiden worden herkend door T-cellen. Vaak wordt niet aan al deze voorwaarden voldaan, waardoor de meeste mutaties geen neoantigenen genereren. De kans op neoantigeen vorming is afhankelijk van het aantal aanwezige mutaties en neemt toe met het aantal mutaties in een tumor. Het is lastig te voorspellen welke mutaties uiteindelijk neoantigenen zullen creëren. Dit bemoeilijkt het identificeren van neoantigenen. De meeste identificatie strategieën starten met het bepalen van mutaties in het tumorweefsel van de patiënt, wat vaak een groot aantal mutaties oplevert. Dit aantal kan worden gefilterd met online predictietools die voorspellen of de neopeptiden die door deze mutaties worden gecodeerd, voldoen aan de voorwaarden voor neoantigeen vorming. De geselecteerde neopeptiden moeten vervolgens worden gevalideerd als neoantigenen, wat inhoudt dat moet worden aangetoond dat zij op tumorcellen worden gepresenteerd en door T-cellen worden herkend.

Minor histocompatibiliteitsantigenen (MiHA's)

Net zoals neoantigenen zijn MiHA's peptiden die ontstaan door variaties in het DNA en die worden herkend door T-cellen. MiHA's kunnen door T-cellen worden herkend na allogene stamceltransplantatie (alloSCT), een mogelijk genezende behandeling voor patiënten met bloedkanker. Voorafgaand aan alloSCT wordt de patiënt behandeld met chemotherapie, eventueel gecombineerd met radiotherapie, om het zieke bloedvormende systeem te vernietigen. Vervolgens ontvangt de patiënt stamcellen van een donor die uitgroeien tot een nieuw, gezond bloedvormend systeem. Na een succesvolle alloSCT is het bloedvormende systeem in de patiënt dus van donor oorsprong, oftewel allogeen. Donor T-cellen kunnen na alloSCT zowel tumorcellen als gezonde cellen van de patiënt aanvallen. Wanneer patiënt en donor identieke HLA-moleculen hebben, kunnen afweerreacties worden veroorzaakt door donor T-cellen die MiHA's herkennen op cellen van de patiënt. MiHA's ontstaan door natuurlijk voorkomende genetische variaties tussen patiënt en donor, waardoor peptiden ontstaan die tussen beiden verschillen. Het peptide dat op cellen van de patiënt wordt gepresenteerd en herkend, wordt een MiHA genoemd. Het corresponderende peptide in de donor is de allelische variant.

Publieke neoantigenen als doelwit op acute myeloïde leukemie (AML)

AML is een type bloedkanker waarbij de myeloïde cellen zijn aangedaan. De behandeling is gericht op het vernietigen van deze kwaadaardige cellen en het verkleinen van de kans op terugkeer van de ziekte. AML is echter een agressieve aandoening en, ondanks intensieve therapie, krijgt een aanzienlijk deel van de patiënten een recidief. De behandeling van recidief AML is lastig en het ziektebeloop

is doorgaans ongunstig. Nieuwe, effectieve behandelstrategieën zijn daarom dringend nodig. T-cel immuuntherapie gericht tegen neoantigenen is een veelbelovende optie. In AML komen relatief weinig mutaties voor, waardoor de kans op neoantigeen vorming klein is. De meeste patiënten hebben echter tenminste één driver-mutatie, en deze mutaties zijn vaak identiek tussen patiënten. Veelvoorkomende mutaties kunnen daardoor publieke neoantigenen creëren, wat AML geschikt maakt voor TCR-T-celtherapie waarbij één of enkele publieke neoantigenen worden aangevallen. Bij deze therapie worden T-cellen uit het bloed van de patiënt verzameld en buiten het lichaam uitgerust met een tumor-specifieke TCR. Deze TCR-T-cellen worden vervolgens vermeerderd en teruggegeven aan de patiënt, zodat zij tumorcellen kunnen opsporen en elimineren. Door genetische modificatie kunnen grote aantallen TCR-T-cellen worden geproduceerd die zich specifiek richten tegen zorgvuldig geselecteerde neoantigenen. Bovendien kunnen de T-cellen worden voorzien van TCR's die uitvoerig zijn getest op effectiviteit en veiligheid.

Dit proefschrift

TCR-T-celtherapie gericht tegen publieke neoantigenen die worden gecodeerd door driver-mutaties in AML, kan bij meerdere patiënten worden toegepast en heeft een relatief laag risico op ontsnapping van AML-cellen door verlies van neoantigeen-coderende mutaties. Het onderzoek in dit proefschrift richtte zich op het identificeren van publieke neoantigenen afkomstig van veelvoorkomende driver-mutaties in AML die worden gepresenteerd door HLA-klasse-I- of HLA-klasse-II-moleculen. Daarnaast zijn TCR's geïsoleerd die gericht zijn tegen deze neoantigenen en kunnen worden ingezet voor TCR-T-celtherapie.

Om efficiënt neoantigenen te identificeren, worden neopeptiden vaak gefilterd met online predictietools. Deze tools verschillen in hun vermogen om het aantal fout-positieve neopeptiden te verminderen, terwijl daadwerkelijke neoantigenen behouden blijven. In **hoofdstuk 2** onderzochten we diverse predictietools op hun vermogen om T-celantigenen te identificeren. Deze predictietools voorspelden verschillende biologische kenmerken die van belang zijn voor antigeen vorming, zoals de efficiëntie waarmee het peptide in de cel wordt geproduceerd en het vermogen om te binden aan HLA-klasse-I-moleculen. We voorspelden deze kenmerken voor 68 HLA-klasse-I-bindende MiHA's. Deze waren in eerdere onderzoeken geïdentificeerd als T-celantigenen en voldeden dus per definitie aan de voorwaarden voor antigeen vorming. Om het voorspellend vermogen van de tools te beoordelen, stelden we ook een referentiegroep samen van peptiden met voorspelde binding aan HLA-A*02:01 of HLA-B*07:02 die niet waren geïdentificeerd als T-celantigenen. We vergeleken de voorspelde kenmerken tussen de MiHA's en de referentiegroep, en concludeerden dat alleen de tool die HLA-binding voorspelt

substantieel bijdraagt aan de karakterisering van MiHA's. Met deze tool werd 87% van de MiHA's correct voorspeld te binden aan HLA, vaak met sterke binding. Daarnaast vergeleken we de voorspelde kenmerken tussen MiHA's en hun allelische varianten, en vonden dat deze vaak vergelijkbaar waren. Dit suggereert dat allelische varianten mogelijk ook kunnen worden geproduceerd in de cel, gepresenteerd in HLA en herkend door T-cellen.

Onder de meest voorkomende driver-mutaties in AML vallen mutaties in het *NPM1* gen, die aanwezig zijn in 30-35% van de volwassen patiënten. Door deze mutaties, waarbij 4 nieuwe basenparen worden ingebouwd, ontstaat een gemuteerd eiwit met een afwijkende aminozuurvolgorde. Ten opzichte van het normale eiwit is het gemuteerde NPM1 eiwit 4 aminozuren langer en zijn de laatste 11 aminozuren afwijkend. Deze afwijkende aminozuren kunnen mogelijk neoantigenen creëren. Omdat deze worden gecodeerd door een veelvoorkomende driver-mutatie die essentieel is voor de ontwikkeling en het voortbestaan van AML, vormen zij aantrekkelijke doelwitten voor T-cel immuuntherapie. In **hoofdstuk 3** beschrijven we de identificatie van een HLA-klasse-I-bindend publiek neoantigeen afkomstig van gemuteerd NPM1. We onderzochten eerst of NPM1 neopeptiden worden gepresenteerd in HLA-klasse-I-moleculen op AML-cellen. Hiervoor isoleerden we peptide:HLA-complexen van het celoppervlak van 12 AML-monsters, scheidden de peptiden van de HLA-moleculen en bepaalden hun aminozuurvolgorde met massaspectrometrie. We detecteerden 5 verschillende NPM1 neopeptiden op *NPM1*-gemuteerde AML, wat bevestigt dat het afwijkende eiwit in de cel wordt afgebroken tot neopeptiden die daarna in HLA worden gepresenteerd op AML. Om deze neopeptiden te valideren als neoantigenen, moet herkenning door T-cellen worden aangetoond. Voor één van de 5 neopeptiden, het peptide CLAVEEVSL dat bindt aan de veelvoorkomende HLA-klasse-I-variant HLA-A*02:01, zochten we naar specifieke CD8 T-cellen met peptide:HLA-klasse-I-tetrameren. Hiermee kunnen antigeen-specifieke T-cellen worden geïsoleerd. In HLA-A*02:01-positieve patiënten met *NPM1*-gemuteerde AML vonden we geen CLAVEEVSL-specifieke CD8 T-cellen. Daarom onderzochten we HLA-A*02:01-positieve gezonde individuen en isoleerden meerdere tetrameer-positieve CD8 T-celklonen. Twee hiervan herkenden *NPM1*-gemuteerde AML-cellen. Voor de T-celkloon met de sterkste reactiviteit bepaalden we de DNA-sequentie van de TCR, kloonden deze en introduceerden de TCR in CD8 en CD4 T-cellen van HLA-A*02:01-positieve gezonde individuen. Zowel CD8 als CD4 T-cellen met deze NPM1-A2-specifieke TCR konden *NPM1*-gemuteerde AML-cellen herkennen en doden, terwijl zij AML-cellen met het normale NPM1 eiwit spaarden. Bovendien remden NPM1-A2-specifieke TCR-T-cellen de groei van een *NPM1*-gemuteerde AML-cellijn in muizen, wat leidde tot een betere overleving. Deze resultaten tonen aan dat CLAVEEVSL een publiek neoantigeen is dat wordt gepresenteerd door HLA-A*02:01 op *NPM1*-gemuteerde AML, en dat de

NPM1-A2-specifieke TCR kan worden ingezet voor TCR-T-celtherapie om patiënten met *NPM1*-gemuteerde AML te behandelen.

Het aantal patiënten met *NPM1*-gemuteerde AML dat kan worden behandeld met T-cel immuuntherapie, kan worden uitgebreid door NPM1 neoantigenen in verschillende HLA-varianten te identificeren. In **hoofdstuk 4** onderzochten we daarom of AVEEVSLRK ook een neoantigeen is op AML. Dit peptide werd, net als CLAVEEVSL, met massaspectrometrie gedetecteerd op *NPM1*-gemuteerde AML. Een online predictietool voorspelde binding van AVEEVSLRK aan de HLA-klasse-I-varianten HLA-A*03:01 en HLA-A*11:01, wat we bevestigden met een peptide:HLA-klasse-I-bindingstest. Met tetrameren zochten we naar AVEEVSLRK-specifieke CD8 T-cellen in HLA-A*03:01- of HLA-A*11:01-positieve gezonde individuen. We isoleerden drie T-celklonen die het peptide in HLA-A*11:01 herkenden, waarvan één kloon ook *NPM1*-gemuteerde AML-cellen kon herkennen. De DNA-sequentie van de TCR van deze kloon werd bepaald, waarna de TCR werd geïntroduceerd in CD8 en CD4 T-cellen van HLA-A*11:01-positieve gezonde individuen. Alleen CD8 T-cellen met de NPM1-A11-specifieke TCR waren in staat *NPM1*-gemuteerde AML-cellen te herkennen en te vernietigen. Deze T-cellen slaagden er echter niet in de groei van een *NPM1*-gemuteerde AML-cellijn in muizen te remmen. Deze resultaten tonen aan dat AVEEVSLRK een publiek HLA-A*11:01-bindend neoantigeen is op *NPM1*-gemuteerde AML. Er is echter aanvullend onderzoek nodig om te bepalen of de NPM1-A11-specifieke TCR geschikt is voor toepassing in TCR-T-celtherapie voor patiënten met AML.

CD4 T-cellen zijn vaak cruciaal als helpercellen voor een efficiënte anti-tumor immuunrespons. Daarnaast kunnen zij in sommige gevallen HLA-klasse-II-positieve tumorcellen direct doden. AML-cellen brengen vaak HLA-klasse-II-moleculen tot expressie. In **hoofdstuk 5** richtten we ons daarom op het identificeren van neoantigenen die worden gepresenteerd door HLA-klasse-II-moleculen. Met behulp van een publieke database waarin mutaties in verschillende kankersoorten zijn gecatalogiseerd, selecteerden we 26 mutaties die vaak voorkomen in AML. Met een online predictietool onderzochten we of deze mutaties coderen voor neopeptiden met voorspelde binding aan frequent voorkomende HLA-klasse-II-varianten. Dit leidde tot de selectie en synthese van 24 lange neopeptiden afkomstig van 10 mutaties. Hieronder vielen 8 overlappende neopeptiden van het gemuteerde NPM1 eiwit die onafhankelijk van voorspelde HLA-binding waren geselecteerd. De synthetische peptiden werden van buitenaf beladen op HLA-klasse-II-positieve dendritische cellen, een bekend type APC, om CD4 T-cellen van gezonde individuen te stimuleren. Na stimulatie isoleerden we meerdere CD4 T-celklonen die neopeptiden afkomstig van verschillende mutaties herkenden wanneer deze waren beladen op HLA-klasse-II-positieve cellen. Voor twee neopeptiden, gecodeerd door

mutaties in *DNMT3A* en *RUNX1*, werden CD4 T-celklonen geïsoleerd die cellijnen herkenden waarin zowel de mutatie als de relevante HLA-klasse-II-varianten waren geïntroduceerd. Dit toont aan dat deze neopeptiden in de cel worden geproduceerd en in HLA-klasse-II-moleculen op het celoppervlak worden gepresenteerd. Het DNMT3A neopeptide, afkomstig van een driver-mutatie die voorkomt in circa 10% van de volwassen patiënten met AML en leidt tot één enkele aminozuur verandering, werd ook herkend door een CD4 T-celkloon op AML-cellen waarin zowel de mutatie als de relevante HLA-DQB1*06:02- of HLA-DQB1*06:03-moleculen natuurlijk aanwezig waren. Hoewel deze CD4 T-celkloon AML-cellen kon herkennen, was hij niet in staat de tumorcellen direct te doden. We concludeerden dat de driver-mutatie in *DNMT3A* een publiek HLA-klasse-II-bindend neoantigeen op AML voortbrengt dat een relevant doelwit zou kunnen vormen voor CD4 T-cel immuuntherapie.

In dit proefschrift worden drie publieke neoantigenen geïdentificeerd die worden gecodeerd door veelvoorkomende driver-mutaties in het *NPM1* of *DNMT3A* gen en worden gepresenteerd door frequente HLA-klasse-I- of HLA-klasse-II-varianten op AML. Deze neoantigenen kunnen mogelijk dienen als doelwitten voor immuuntherapieën waarin neoantigeen-specifieke CD8 of CD4 T-cellen, of een combinatie daarvan, worden ingezet. Onze geïsoleerde NPM1-A2-specifieke TCR tegen het NPM1 neoantigeen CLAVEEVSL in HLA-A*02:01 is bovendien geschikt voor TCR-T-celtherapie. Immuuntherapieën gericht tegen publieke neoantigenen kunnen in de toekomst mogelijk worden ingezet als therapie voor patiënten met AML om recidief van de ziekte te behandelen of zelfs te voorkomen.

PhD portfolio

The PhD trajectory – an overview

Dyantha van der Lee began conducting research in the spring of 2014 during her bachelor's programme in Medicine as part of the MD/PhD-track of the Honours College. She combined her medical studies with part-time research at the Department of Hematology under the supervision of Dr. Marieke Griffioen and Prof. dr. Fred Falkenburg. Her project was focused on the identification of minor histocompatibility antigens that play a role in immune responses after allogeneic hematopoietic stem cell transplantation in adult patients with hematological malignancies. After she obtained her bachelor's degree in 2015, she continued this project during the research internship that formed part of her master's programme. Besides identifying minor histocompatibility antigens, Dyantha also investigated the potential of various online available prediction algorithms for the discovery of T-cell antigens. This work resulted in a publication and **chapter 2** of this thesis. She has shared this work in an oral presentation at the Dutch Tumor Immunology Meeting and in a poster presentation at the Joint British Society for Immunology (BSI) and Dutch Society for Immunology (NVVI) Congress.

In May 2016, Dyantha was awarded a two-year research grant from the LUMC by the selection committee of the MD/PhD-track. This prompted her to temporarily suspend her master's programme to continue working on her research full-time from June 2016. At this stage, she began exploring whether neoantigens are expressed on acute myeloid leukemia. After successfully identifying an NPM1 neoantigen and a T-cell receptor specific for this antigen, her research focus shifted toward the identification of public neoantigens encoded by driver mutations in adult patients with acute myeloid leukemia.

Dyantha's research efforts were concentrated on the discovery of HLA class I-binding neoantigens derived from mutated NPM1. In collaboration with the research group of Dr. Peter van Veelen from the Center for Proteomics and Metabolomics at the LUMC, several NPM1 neopeptides were successfully identified in the HLA class I ligandome of acute myeloid leukemia. With support from the research group of Prof. dr. Mirjam Heemskerk at the Department of Hematology, and with assistance from the Flow cytometry Core Facility and the Central Animal Facility of the LUMC, she validated one of the identified NPM1 neopeptides as neoantigen on acute myeloid leukemia, and isolated a T-cell receptor directed against this neoantigen that mediated anti-leukemic reactivity *in vitro* and in a murine model. This work has been published along with a commentary and is outlined in **chapter 3** of this thesis.

Dyantha has presented this research at various national and international scientific conferences, including an oral presentation at the American Society of Hematology (ASH) Annual Meeting and Exposition, and at the International Cellular Therapy Symposium. This work also led to interview invitations for the website Oncologie.nu, and for HemaTalks of the Dutch Journal of Haematology (NTvH). Concerning public outreach, Dyantha has presented this work at a meeting for charity fundraisers of the Dutch Cancer Society and at a meeting for people interested in research at the Department of Hematology to recruit benefactors for the Doelfonds Leukemie.

The identified NPM1 neoantigen and T-cell receptor have been used by other research groups at the LUMC and in Germany for research on the immunotherapy of cancer. Moreover, based on the research in **chapter 3**, a patent has been granted for the identified NPM1 neoantigen and T-cell receptor. This work formed the basis for a collaboration with biopharmaceutical company Miltenyi Biotec & Biomedicine, in which Dyantha was involved in the initial stages. This collaboration ultimately led to the initiation of a phase I/II clinical trial in which T cells engineered with the identified T-cell receptor are investigated as treatment for patients with relapsed or refractory acute myeloid leukemia.

The collaborations described for the research in **chapter 3** also contributed to the work described in **chapter 4**. In this chapter, Dyantha applied the theoretical knowledge and experimental skills that she acquired to another NPM1 neopeptide that had been identified in the HLA class I ligandome of acute myeloid leukemia. Additionally, in collaboration with the research group of Dr. Jan Wouter Drijfhout from the Department of Immunology at the LUMC, peptide-HLA class I binding assays were performed to confirm HLA-binding of this neopeptide. The work presented in **chapter 4** also reflects the efforts of master's students Karl Harber, Lisanne Roelofsen and Annemiek Schouten, who were supervised by Dyantha.

Dyantha's final research project focused on the identification of neoantigens presented on acute myeloid leukemia by HLA class II. During this project, she supervised master's student Bas Laan, whose work has contributed to the research described in **chapter 5**.

In addition to the supervision of four master's students, Dyantha has strengthened her teaching and communication skills by giving a lecture on targeting neoantigens on acute myeloid leukemia in the FOS course Allogeneic Stem cell Transplantation and Immunotherapy in 2017, 2018 and 2019, and in the half minor Immunotherapy of Cancer in 2018 and 2019. Furthermore, she complemented her experimental research development with several courses to improve her theoretical knowledge on

statistics, data analysis, immunology, oncology, and the regulations and organization of clinical research.

After 3.5 years of full-time research, Dyantha returned to her master's programme in 2020 and graduated in 2023. Since 2020, she has worked part-time on her research, which resulted in scientific publications describing the research of **chapters 4** and **5**.

CRediT table

CRediT table for the thesis of Dyantha I. van der Lee

Ch.	Type*	Short Title	Conceptualization	Data Curation	Formal Analysis	Funding Acquisition	Investigation	Methodology	Project Administration	Resources	Software	Supervision	Validation	Visualization	Writing – Original Draft	Writing – Review & Editing	Preregistered	Preprinted	Published with Peer Review
1	Introduction	General introduction	■													■	☐	☐	☐
2	PhD project chapter	Value of online algorithms	■	■	■		■	■	■						■	■	☐	☐	☑
3	PhD project chapter	An HLA-A*02:01 NPM1 neoantigen	■	■	■		■	■	■						■	■	☐	☐	☑
4	PhD project chapter	An HLA-A*11:01 NPM1 neoantigen	■	■	■		■	■	■			■			■	■	☐	☐	☑
5	PhD project chapter	An HLA-DQ DNMT3A neoantigen	■	■	■		■	■	■			■			■	■	☐	☐	☑
6	Discussion	Summary and general discussion	■													■	☐	☐	☐

**PhD project chapters are the direct result of the PhD project of the PhD candidate.*
Some theses also include Collaboration Chapters, to which the PhD candidate has contributed but fall outside the PhD project.

Dissemination table

The value of online algorithms to predict T-cell ligands created by genetic variants Van der Lee DI, Pont MJ, Falkenburg JHF, Griffioen M PLoS One. 2016;11(9):e0162808	
Chapter in this thesis	2
Publication in peer-reviewed journal	DOI: 10.1371/journal.pone.0162808
Conference contributions of the PhD candidate	*Oral presentation at:* Dutch Tumor Immunology Meeting *Poster presentation at:* Joint BSI and NVVI Congress
Mutated nucleophosmin 1 as immunotherapy target in acute myeloid leukemia Van der Lee DI, Reijmers RM, Honders MW, Hagedoorn RS, de Jong RCM, Kester MGD, van der Steen DM, de Ru AH, Kweekel C, Bijen HM, Jedema I, Veelken H, van Veelen PA, Heemskerk MHM, Falkenburg JHF, Griffioen M J Clin Invest. 2019;129(2):774-785	
Chapter in this thesis	3
Publication in peer-reviewed journal	DOI: 10.1172/JCI97482
Conference contributions of the PhD candidate	*Oral presentation at:* ASH Annual Meeting and Exposition NVVI Annual Meeting Dutch Hematology Congress Dutch Tumor Immunology Meeting European Congress of Immunology International Cellular Therapy Symposium *Laptop presentation at:* Dutch Tumor Immunology Meeting *Poster presentation at:* CRI – CIMT – EATI – AACR International Cancer Immunotherapy Conference
Other forms of dissemination	*Presentation at:* Meeting for charity fundraisers of the Dutch Cancer Society Meeting for benefactors of Doelfonds Leukemie *Interview for:* Website Oncologie.nu HemaTalks of the NTvH
An HLA-A*11:01-binding neoantigen from mutated NPM1 as target for TCR gene therapy in AML Van der Lee DI, Koutsoumpli G, Reijmers RM, Honders MW, de Jong RCM, Remst DFG, Wachsmann TLA, Hagedoorn RS, Franken KLMC, Kester MGD, Harber KJ, Roelofsen LM, Schouten AM, Mulder A, Drijfhout JW, Veelken H, van Veelen PA, Heemskerk MHM, Falkenburg JHF, Griffioen M Cancers (Basel). 2021;13(21):5390	
Chapter in this thesis	4
Publication in peer-reviewed journal	DOI: 10.3390/cancers13215390
Mutated *DNMT3A* creates a public HLA-DQ-binding neoantigen on acute myeloid leukemia Van der Lee DI, Argiro EM, Laan SNJ, Honders MW, de Jong RCM, Struckman NE, Falkenburg JHF, Griffioen M Front Immunol. 2025;16:1556121	
Chapter in this thesis	5
Publication in peer-reviewed journal	DOI: 10.3389/fimmu.2025.1556121

Overview of completed courses and other training

	Mandatory activities	
Year	*Title*	*Hours*
2016	Leiden University Onboarding Programme	5
2017	Responsible Research: BROK Certification	42
2018	Basic Methods and Reasoning in Biostatistics	42
	Scientific courses	
Year	*Title*	*Hours*
2016	Leiden Institute for Immunology Course in Immunology	80
2018	Course Basic and Translational Oncology	50
2019	Course Statistical Aspects of Clinical Trials	20
2019	Course Using R for Data Analysis	32
2021 2024	BROK Recertification	5 17

Other relevant scientific activities related to this thesis

Year	Presentations at scientific conferences Description	Linked to chapter
2016	Dutch Tumor Immunology Meeting Breukelen, the Netherlands *Oral presentation*	2
2016	Joint BSI and NVVI Congress Liverpool, the United Kingdom *Poster presentation*	2
2017	Dutch Tumor Immunology Meeting Breukelen, the Netherlands *Laptop presentation*	3
2017	ASH Annual Meeting and Exposition Atlanta, GA, the United States of America *Oral presentation*	3
2017	NVVI Annual Meeting Noordwijkerhout, the Netherlands *Oral presentation*	3
2018	Dutch Hematology Congress Papendal, the Netherlands *Oral presentation*	3
2018	Dutch Tumor Immunology Meeting Breukelen, the Netherlands *Oral presentation*	3
2018	European Congress of Immunology Amsterdam, the Netherlands *Oral presentation*	3
2018	CRI – CIMT – EATI - AACR International Cancer Immunotherapy Conference New York City, NY, the United States of America *Poster presentation*	3
2019	International Cellular Therapy Symposium Erlangen, Germany *Oral presentation*	3

Year	Other presentations Description	Linked to chapter
2017	Presentation at a meeting for charity fundraisers of the Dutch Cancer Society	3
2017	Presentation at a meeting for benefactors of Doelfonds Leukemie (part of the Bontius Stichting)	3
2017	Interview for website Oncologie.nu	3
2017	Interview for HemaTalks of the NTvH	3

List of publications

Struckman N.E., Koutsoumpli G., de Jong R.C.M., **van der Lee D.I.**, Remst D.F.G., Smith S.I., Honders M.W., Hagedoorn R.S., de Ru A.H., Matsuda M., Ishikawa F., Tak T., Valk P.J.M., Heemskerk M.H.M., van Veelen P.A., Falkenburg J.H.F., Griffioen M. *A T-cell receptor targeting RUNX1 frameshift mutations in acute myeloid leukemia.* Leukemia. 2026 Feb;40(2):265-278.

Van der Lee D.I., Argiro E.M., Laan S.N.J., Honders M.W., de Jong R.C.M., Struckman N.E., Falkenburg J.H.F., Griffioen M. *Mutated DNMT3A creates a public HLA-DQ-binding neoantigen on acute myeloid leukemia.* Front Immunol. 2025;16:1556121.

Struckman N.E., de Jong R.C.M., Honders M.W., Smith S.I., **van der Lee D.I.**, Koutsoumpli G., de Ru A.H., Mikesch J.H., van Veelen P.A., Falkenburg J.H.F., Griffioen M. *Hotspot DNA methyltransferase 3A (DNMT3A) and isocitrate dehydrogenase 1 and 2 (IDH1/2) mutations in acute myeloid leukemia and their relevance as targets for immunotherapy.* Biomedicines. 2024;12(5):1086.

Van der Lee D.I., Koutsoumpli G., Reijmers R.M., Honders M.W., de Jong R.C.M., Remst D.F.G., Wachsmann T.L.A., Hagedoorn R.S., Franken K.L.M.C., Kester M.G.D., Harber K.J., Roelofsen L.M., Schouten A.M., Mulder A., Drijfhout J.W., Veelken H., van Veelen P.A., Heemskerk M.H.M., Falkenburg J.H.F., Griffioen M. *An HLA-A*11:01-binding neoantigen from mutated NPM1 as target for TCR gene therapy in AML.* Cancers (Basel). 2021;13(21):5390.

Fuchs K.J., Honders M.W., van der Meijden E.D., Adriaans A.E., **van der Lee D.I.**, Pont M.J., Monajemi R., Kielbasa S.M., 't Hoen P.A.C., van Bergen C.A.M., Falkenburg J.H.F., Griffioen M. *Optimized whole genome association scanning for discovery of HLA class I-restricted minor histocompatibility antigens.* Front Immunol. 2020;11:659.

Van der Lee D.I., Reijmers R.M., Honders M.W., Hagedoorn R.S., de Jong R.C.M., Kester M.G.D., van der Steen D.M., de Ru A.H., Kweekel C., Bijen H.M., Jedema I., Veelken H., van Veelen P.A., Heemskerk M.H.M., Falkenburg J.H.F., Griffioen M. *Mutated nucleophosmin 1 as immunotherapy target in acute myeloid leukemia.* J Clin Invest. 2019;129(2):774-785.

Van der Lee D.I., Pont M.J., Falkenburg J.H.F., Griffioen M. *The value of online algorithms to predict T-cell ligands created by genetic variants.* PLoS One. 2016;11(9):e0162808.

Pont M.J., **van der Lee D.I.**, van der Meijden E.D., van Bergen C.A.M., Kester M.G.D., Honders M.W., Vermaat M., Eefting M., Marijt E.W.A., Kielbasa S.M., 't Hoen P.A.C., Falkenburg J.H.F., Griffioen M. *Integrated whole genome and transcriptome analysis identified a therapeutic minor histocompatibility antigen in a splice variant of ITGB2.* Clin Cancer Res. 2016;22(16):4185-96.

Struckman N.E., Honders M.W., Koutsoumpli G., de Jong R.C.M., **van der Lee D.I.**, Kester M.G.D., van de Meent M., Hagedoorn R.S., de Ru A.H., van der Reijden B.A., Valk P.J.M., Mak G.W.Y., Verhoef J.J.F., Heemskerk M.H.M., van Veelen P.A., Falkenburg J.H.F., Griffioen M. *T-cell receptors targeting distinct FLT3-D835Y neoantigens exhibit variable reactivity against acute myeloid leukemia*. Under review at Blood Immunology & Cellular Therapy.

Dankwoord

De inzet, expertise, hulp en steun van oud-collega's, vrienden en familie waren essentieel voor het tot stand komen van dit proefschrift. Ik ben iedereen die heeft bijgedragen dan ook immens dankbaar.

Mijn promotor Fred Falkenburg en copromotor Marieke Griffioen, jullie hebben mij de kans gegeven om aan dit promotietraject te werken en dankzij jullie fantastische begeleiding heb ik me niet alleen kunnen ontwikkelen als onderzoeker, maar ook als persoon. Fred, dankjewel voor je scherpe blik en behulpzame commentaar, altijd gebracht met humor. Marieke, jij was niet alleen onmisbaar voor mijn onderzoek, maar jouw deur stond ook open om persoonlijkere dingen te bespreken. Dit is voor mij onvoorstelbaar waardevol geweest.

Mijn oud-collega's van het Laboratorium voor Experimentele Hematologie, bij jullie kon ik altijd terecht voor hulp, advies, vragen en gezelligheid. Jullie hebben een warme en vertrouwde sfeer op de afdeling gecreëerd, waardoor ik me heel erg op mijn plek heb gevoeld. Ik heb mooie herinneringen aan de tijd die ik in het lab heb doorgebracht. Ik wil jullie vanuit de grond van mijn hart hiervoor bedanken.

Edith en Margot, bedankt dat jullie mij de weg hebben gewezen in het lab toen ik als student op de afdeling begon. Edith, je was er aan het begin van mijn promotietraject en ook weer aan het einde en stond altijd klaar om me aan te moedigen. Rob en Willy, ik waardeer de ongelooflijke hoeveelheid werk die jullie voor dit proefschrift hebben verzet enorm. Ook kon ik tijdens grote experimenten altijd op jullie rekenen. Ik kijk met veel plezier en dankbaarheid terug op onze samenwerking. Willy, ik wil jou in het bijzonder bedanken voor alle proeven die je hebt uitgevoerd toen ik weer verder ging met mijn opleiding. Edith en Willy, wat een voorrecht dat jullie mijn paranimfen zijn. Eva Argiro, Georgia, Kyra en Nadine, enorm bedankt voor jullie inbreng tijdens werkbesprekingen, voor de experimenten die jullie hebben uitgevoerd en voor jullie gezelligheid. Marian, met jou kon ik altijd lachen, zowel tijdens het werk als daarbuiten.

Daarnaast wil ik mijn waardering extra uitspreken voor Chris, Dennis, Dirk, Ilona, Michel, Renate, Rogier en Tassilo. Jullie diverse werkzaamheden in het lab zijn van onschatbaar belang geweest voor dit onderzoek. Ditzelfde geldt voor Guido, Sabrina en de medewerkers van de FCF. Bedankt voor jullie hulp en advies bij het FACSen en sorteren. Mijn oud-kamergenoten op C2, Janneke, Julieta, Kees en Ruben, bij jullie kon ik terecht voor discussies, vragen en leuke gesprekken. Esther en Nelleke, dankzij jullie was het lab piekfijn georganiseerd en liep het als een goed geoliede

machine. Gerrie, wat fijn dat ik altijd op jou kon rekenen als organisatorische duizendpoot. Henk, zonder jou geen goede IT, dankjewel. Bas en Hanny, jullie zorgden ervoor dat de bevoorrading van het lab op-en-top in orde was en dat ik tijdens mijn proeven nooit misgreep. Jullie werk maakte het verschil. Hanny, ik maak nog steeds gebruik van je hardlooptips. Alle (oud-)PhD-studenten en postdocs, jullie hebben mij enorm geholpen met jullie inbreng tijdens seminars en daarbuiten, en met jullie bemoedigende woorden, humor en afleiding. Vooral wil ik hier ook Ana, Cilia, Emma, Eva Koster, Marije, Marthe, Rosa, Sietse en Wesley noemen. Aicha, Laura, Lois, Miranda en Tassilo, jullie hebben mijn promotietraject en mijn leven daarnaast met jullie vriendschap verrijkt. Ik ben heel dankbaar dat ik mijn tijd binnen en buiten het onderzoek met jullie heb mogen delen.

Annemiek, Bas, Karl, en Lisanne, als studenten hebben jullie een belangrijke bijdrage geleverd aan dit onderzoek. Ik heb met veel plezier met jullie samengewerkt, genoten van jullie gezelligheid en humor, en ook veel van jullie geleerd.

Mijn oud-collega's van de afdeling Neurologie van het Groene Hart Ziekenhuis in Gouda, ik ben jullie zeer dankbaar voor jullie begeleiding, hulp en de fijne samenwerking toen ik bij jullie als ANIOS aan de slag ging na het afronden van mijn studie. Ik heb ontzettend veel geleerd van jullie.

Sophie en Maxime, ik ben heel blij dat wij tijdens ons jaar LST bevriend zijn geraakt. Bedankt voor de balans die jullie de afgelopen jaren hebben aangebracht tussen ontspanning en een luisterend oor. Maxime, ik heb vreselijk veel gehad aan je kennis en raadgevingen over het proces van promoveren.

Mijn familie, jullie zijn mijn steun en toeverlaat. Jullie kennen mij door en door. Op jullie kan ik terugvallen en jullie herinneren mij eraan dat dingen ook gevierd moeten worden. Lieve papa, mama, Yenta en Aranxtha, bedankt voor jullie support, de rust en ontspanning die jullie boden, en het hart onder de riem dat ik soms nodig had. Peter en Thomas, jullie brachten altijd gezelligheid en een helpende hand. Oma en opa, jullie betrokkenheid bij mijn onderzoek en opleiding, en jullie onvoorwaardelijke steun hieraan waren mij ongelooflijk dierbaar.